

Decomposition Methods for Nonlinear Optimization and Data Mining

By

BRANDON EMMANUEL DUTRA

B.S. (University of California, Davis) 2012

M.S. (University of California, Davis) 2015

DISSERTATION

Submitted in partial satisfaction of the requirements for the degree of

DOCTOR OF PHILOSOPHY

in

Applied Mathematics

in the

OFFICE OF GRADUATE STUDIES

of the

UNIVERSITY OF CALIFORNIA

DAVIS

Approved:

Jesus De Loera

Matthias Köppe

David Woodruff

Committee in Charge

2016

Contents

Acknowledgments	vii
Chapter 1. Introduction	1
1.1. Polyhedra and their representation	2
1.1.1. Polyhedral cones	4
1.2. Generating functions for integration and summation	5
1.2.1. Working with generating functions: an example	5
1.2.2. Indicator functions	7
1.2.3. Generating functions of simple cones	8
1.2.4. Generating function for non-simple cones	13
1.2.5. Generating functions for full-dimensional polytopes	17
1.2.6. A power of a linear form	18
1.3. Handelman's Theorem and polynomial optimization	19
1.3.1. Handelman and moment methods	22
1.3.2. Complexity of the problem	23
1.4. Ehrhart Polynomials	24
1.4.1. Two classic theorems	24
1.4.2. Special case: knapsack polytopes	26
1.5. MILP Heuristics	27
1.6. Using computational geometry in neuro-immune communication	29
1.6.1. Spleen	30
1.6.2. The data science question	31
Chapter 2. Integration	33
2.1. Integrand: powers of linear forms	34

2.1.1.	Domain: cone decomposition	34
2.1.2.	Domain: a full dimensional simplex	38
2.1.3.	Examples	40
2.1.4.	How the software works: burst tries	43
2.1.5.	Should one triangulate or cone decompose?	46
2.2.	Integrand: products of affine functions	50
2.2.1.	Domain: cone decomposition	53
2.2.2.	Domain: a full dimensional simplex	55
2.2.3.	Benefits of Handelman decomposition	56
Chapter 3. Polynomial Optimization		61
3.1.	Prior work: integer optimization of polynomials	62
3.2.	Continuous Optimization	69
3.2.1.	An example	77
3.2.2.	Summary of the algorithm	78
Chapter 4. Top coefficients of the Ehrhart polynomial for knapsack polytopes		80
4.1.	The residue formula for $E(\boldsymbol{\alpha}; t)$	83
4.1.1.	Poles of high and low order	84
4.2.	Using the poset structure of the α_i	85
4.2.1.	Partial summary so far	88
4.3.	Polyhedral reinterpretation of the generating function $E(\boldsymbol{\alpha}, f; t)$	89
4.3.1.	Review of exponential summation with real shift \mathbf{s}	89
4.3.2.	Rewriting $E(\boldsymbol{\alpha}, f; t)$	92
4.3.3.	$\mathcal{S}(\boldsymbol{\alpha}, f, T; x)$ as the generating function of a cone in fixed dimension	94
4.3.4.	Unimodular decomposition in the dual space	96
4.3.5.	The periodic dependence in \mathbf{T}	98
4.4.	Periodicity of coefficients	99
4.5.	Summary of the algorithm to compute top coefficients	103
4.6.	Experiments	106

4.6.1.	<i>M-Knapsack vs.LattE Knapsack vs.LattE Top-Ehrhart</i>	107
4.6.2.	Other examples	108
Chapter 5. MILP heuristic for finding feasible solutions		115
5.1.	Motivation	115
5.1.1.	Example	115
5.1.2.	MIPLIB	117
5.2.	Dancing Links	117
5.3.	How to use dancing links	124
5.4.	Results	125
Chapter 6. Application in distance geometry for neuro-immune communication		126
6.1.	Cleaning the data	127
6.1.1.	Step 1: the boundary	127
6.1.2.	Step 2: making Imaris spots from voxel data	130
6.1.3.	Step 3: making Imaris filament surfaces from voxel data	132
6.2.	Cluster analysis	134
6.2.1.	Step 1: computing nearest neighbour	135
6.2.2.	Step 2: dimensionality reduction	137
Appendix A. Computer source code		141
A.1.	Codes for integrating a polynomial over a polytope and for computing the top coefficients of the Ehrhart polynomial	141
A.2.	Codes for cleaning and processing the spleen data	141
A.2.1.	Code for processing the boundary of the spleen	141
A.2.2.	Code for processing the filament surfaces	146
A.2.3.	Code for computing nearest neighbors	158
Bibliography		160

Abstract

We focus on two central themes in this dissertation. The first one is on decomposing polytopes and polynomials in ways that allow us to perform nonlinear optimization. We start off by explaining important results on decomposing a polytope into special polyhedra. We use these decompositions and develop methods for computing a special class of integrals exactly. Namely, we are interested in computing the exact value of integrals of polynomial functions over convex polyhedra. We present prior work and new extensions of the integration algorithms. Every integration method we present requires that the polynomial has a special form. We explore two special polynomial decomposition algorithms that are useful for integrating polynomial functions. Both polynomial decompositions have strengths and weaknesses, and we experiment with how to practically use them.

After developing practical algorithms and efficient software tools for integrating a polynomial over a polytope, we focus on the problem of maximizing a polynomial function over the continuous domain of a polytope. This maximization problem is NP-hard, but we develop approximation methods that run in polynomial time when the dimension is fixed. Moreover, our algorithm for approximating the maximum of a polynomial over a polytope is related to integrating the polynomial over the polytope. We show how the integration methods can be used for optimization.

We then change topics slightly and consider a problem in combinatorics. Specifically, we seek to compute the function $E(t)$ that counts the number of nonnegative integer solutions to the equation $\alpha_1 x_1 + \dots + \alpha_n x_n = t$ where the α_i are given positive integers. It is known that this function is a quasi-polynomial function, and computing every term is $\#P$ -hard. Instead of computing every term, we compute the top k terms of this function in polynomial time in varying dimension when k is fixed. We review some applications and places where this counting function appears in mathematics. Our new algorithm for computing the largest order terms of $E(t)$ is based on the polyhedral decomposition methods we used in integration and optimization. We also use an additional polyhedral decomposition: Barvinok's fast decomposition of a polyhedral cone into unimodular cones.

The second central topic in this dissertation is on problems in data science. We first consider a heuristic for mixed-integer linear optimization. We show how many practical mixed-integer linear

have a special substructure containing set partition constraints. We then describe a nice data structure for finding feasible zero-one integer solutions to systems of set partition constraints.

Finally, we end with an applied project using data science methods in medical research. The focus is on identifying how T-cells and nervous-system cells interact in the spleen during inflammation. To study this problem, we apply topics in data science and computational geometry to clean data and model the problem. We then use clustering algorithms and develop models for identifying when a spleen sample is responding to inflammation. This project's lifetime surpasses the author's involvement in it. Nevertheless, we focus on the author's contributions, and on the future steps.

Acknowledgments

My advisers: Jesus De Loera and Matthias Köppe. These two people have played a big role during my time at UC Davis. I appreciated working with two experts with diverse backgrounds. They greatly enriched my experience in graduate school. My advisers have also been supportive of my career development. As I went through graduate school, my career and research goals changed a few times, but my advisers have been agile and supportive. Some of the most important career development experiences I had were from my three summer internships, and I'm grateful for their support in getting and participating in these opportunities.

Through undergraduate and graduate school at UC Davis, I have spent about 7 years working on the `LattE` project. I am very grateful for this enriching experience. I have enjoyed every aspect of working within the intersection of mathematical theory and mathematical software. `LattE` was my first experience with the software life cycle and with real software development tools like GNU Autotools, version control, unit testing, et cetera. I have grown to love software development through this work, and how it has enriched my graduate experience. I also want to acknowledge the `LattE` users. I am thankful they find our work interesting, useful, and care enough to tell us how they use it and how to improve it. I hope that future graduate students get the experience of working on this great project.

Professors. I wish to thank David Woodruff for being in my dissertation and qualifying exam committees. I also thank Dan Gusfield and Angela Cheer for also taking part in my qualifying exam committee. I also owe a thank you to Janko Gravner and Ben Morris for their support and letters of recommendation.

Co-authors. I wish to thank Velleda Baldoni (University of Rome Tor Vergata, Rome, Italy), Nicole Berline (École Polytechnique, Palaiseau, France), and Michèle Vergne (The Mathematical Institute of Jussieu, Paris Rive Gauche, Paris, France) for their work in Chapter 4. I also thank my collaborators from the UC Davis School of Veterinary Medicine who contributed to Chapter 6: Colin Reardon and Ingrid Brust-Mascher.

Life. I am also very lucky to have found my wife in graduate school. I am very happy, and I look forward to our life together. She is an amazing person, and my best friend.

Money. I am thankful for the funding I received from my advisers and the mathematics department. I am especially thankful for the funding I received over my first year and summer, which allowed me to focus on passing the preliminary examinations. I also owe a big thank you to my friend Swati Patel who played a monumental role in editing my NSF Graduate Research Fellowship Program application, which resulted in me obtaining the award! The financial support I received over the years greatly reduced stress and made the experience great. Money makes all the difference. I also wish to thank some organizations for their financial support for conferences: American Institute of Mathematics, Institute for Mathematics and Its Applications, and the Rocky Mountain Mathematics Consortium at the University of Wyoming. I was partially supported by NSF award number 0914107, and a significant amount of this dissertation was supported by NSF grant number DGE-1148897.

Internships. I am grateful for three great summer internships: two at SAS Institute (in 2013 and 2014 under Manoj Chari and Yan Xu, respectively), and one at Google, Inc. (in 2015 under Nicolas Mayoraz). All three showed me how diverse the software industry can be.

People. All family members alive and dead. Angel Castro. Lorenzo Medina. Andy Tan. Greg Webb. Anne Carey. Julia Mack. Tom Brounstein. Travis Scrimshaw. Gordon Freeman. Jim Raynor. Sarah Kerrigan. Dan Gusfield. Sean Davis. Mohamed Omar. Yvonne Kemper. Robert Hildebrand. Mark Junod.

I would like to end with a quote that perfectly captures why I like mathematics,

Despite some instances where physical application may not exist, mathematics has historically been the primary tool of the social, life, and physical sciences. It is remarkable that a study, so potentially pure, can be so applicable to everyday life. Albert Einstein questions, “How can it be that mathematics, being after all a product of human thought which is independent of experience, is so admirably appropriate to the objects of reality?” This striking duality gives mathematics both power and charm. [154, p. 171]

CHAPTER 1

Introduction

The first three chapters of this thesis are focused on the optimization of a polynomial function where the domain is a polytope. That is, we focus on the continuous optimization problem

$$\begin{aligned} \max f(x) \\ x \in P, \end{aligned}$$

where P is a polytope and $f(x)$ is a polynomial. As we review in Section 1.3.2, exactly computing the maximum of a polynomial over a polytopal domain is hard, and even approximating the maximum is still hard. However, this has not damped research in this area, and many of the popular methods for approximating the optimum depend on decomposing the polynomial function, approximating the polynomial function with similar functions, or decomposing the domain. References are numerous in the literature [9, 50, 106, 103, 104, 105, 107, 120, 129]. A common characteristic between these methods is their reliance on ideas in real semialgebraic geometry and semidefinite programming. A key contribution of this thesis is another algorithm for approximating the maximum of a polynomial function over P . Unlike previous methods, our method is based on combinatorial results. When convenient, to help develop our tools for the continuous optimization problem, we also state analogous results for the discrete optimization problem

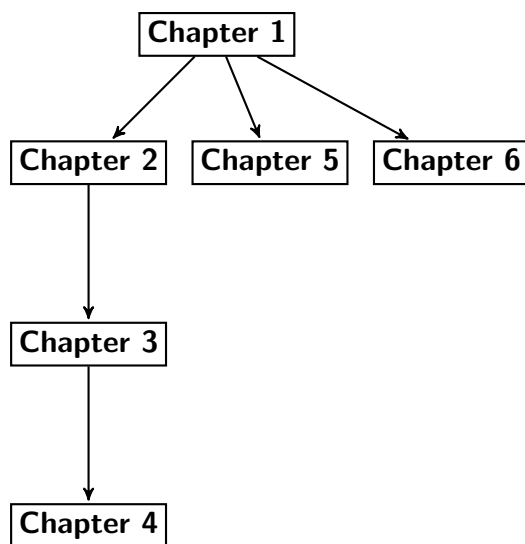
$$\begin{aligned} \max f(x) \\ x \in P \cap \mathbb{Z}^d. \end{aligned}$$

One key step of our method for approximating the polynomial optimization problem requires computing the integral $\int_P (f(x))^k dx$ where k is some integer power. Chapter 2 is devoted to this step. Then Chapter 3 connects the pieces together and culminates in an efficient algorithm for the continuous polynomial optimization problem. Some of the tools developed, namely the way we apply polyhedral decompositions and generating functions, can also be applied to a different type

of problem: computing the Ehrhart polynomial of a knapsack polytope. Chapter 4 addresses this idea.

The remaining chapters cover the second part of this thesis: topics in data science. In particular, Chapter 5 develops a useful heuristic for finding solutions to set partition constraints, which are a common constraint type in linear integer programming. Then Chapter 6 applies tools from distance geometry and cluster analysis to identify disease in spleens.

In this chapter, we review the background material used in all the other chapters. In the figure below, we suggest possible reading orders and identify which chapters builds upon topics in other chapters.



1.1. Polyhedra and their representation

Polytopes and polyhedra appear as a central object in this thesis. We state just the basic definitions and results that we need. For a complete review, see [19, 58, 143, 157].

DEFINITION 1.1.1. Let $x_1, \dots, x_k \in \mathbb{R}^d$, then the combination $a_1x_1 + \dots + a_kx_k$ with $a_i \in \mathbb{R}$ is called

- *linear* with no restrictions on the a_i
- *affine* if $\sum_{i=1}^k a_i = 1$
- *conical* if $a_i \geq 0$
- *convex* if it is affine and conical.

1.1. POLYHEDRA AND THEIR REPRESENTATION

We can define a polytope as a special kind of convex set.

DEFINITION 1.1.2. A set $C \in \mathbb{R}^d$ is *convex* if $\forall x, y \in C \Rightarrow tx + (1-t)y \in C, \forall 0 \leq t \leq 1$. This means, the line segment between x and y is in C .

DEFINITION 1.1.3. Let $C \in \mathbb{R}^d$, the *convex hull* of C is

$$\text{Conv}(C) = \{t_1x_1 + \cdots + t_kx_k \mid x_i \in C \text{ and } t_i \geq 0 \text{ and } \sum_{i=1}^k t_i = 1\}$$

DEFINITION 1.1.4. Let $V \in \mathbb{R}^d$, be a finite point set, then a *polytope* P is $P = \text{Conv}(V)$.

Polytopes are the convex hull of finite point sets. But there are other ways to represent a polytope. Instead of looking at convex combinations, we can look at halfspaces:

DEFINITION 1.1.5. Let $a \in \mathbb{R}^d$, then $H = \{x \in \mathbb{R}^d \mid a^T x \leq b\}$ is a *halfspace*. A halfspace is “one side” of a linear function.

DEFINITION 1.1.6. Let $P = \{x \in \mathbb{R}^d \mid Ax \leq b\}$ be a finite intersection of halfspaces, then P is called a *polyhedron*.

EXAMPLE 1.1.7. Take the unit square with vertices $(0,0)$, $(1,0)$, $(0,1)$, and $(1,1)$ in \mathbb{R}^2 . The interior of the square is given by all convex combinations of the vertices. It is also given by all $x, y \in \mathbb{R}$ such that

$$0 \leq x \leq 1$$

$$0 \leq y \leq 1$$

but this can be rewritten as

$$x \leq 1$$

$$-x \leq 0$$

$$y \leq 1$$

$$-y \leq 0$$

or in matrix form $Ax \leq b$ as in

$$\begin{pmatrix} 1 & 0 \\ -1 & 0 \\ 0 & 1 \\ 0 & -1 \end{pmatrix} \begin{pmatrix} x \\ y \end{pmatrix} \leq \begin{pmatrix} 1 \\ 0 \\ 1 \\ 0 \end{pmatrix}.$$

The unit square can be described by two different objects: as convex combinations of a point set, and the bounded intersection of finitely many half spaces. By the next theorem, these descriptions are equivalent as every polytope has these two representations.

THEOREM 1.1.8 (Finite basis theorem for polytopes, Minkowski-Steinitz-Weyl, see Corollary 7.1c in [143]). *A set P is a polytope if and only if it is a bounded polyhedron.*

Because both polytope representations are very important, there are many ways or algorithms to convert one to the other. Instead of describing convex hull algorithms and others, we will consider them a technology and seek an appropriate software tool when needed. For more details about transferring from one representation to another, see [1, 10, 72, 76].

1.1.1. Polyhedral cones. A special type of unbounded polyhedra that will appear often is a polyhedral cone. Generally, a *cone* is a set that is closed under taking nonnegative scalar multiplication, and a *convex cone* is also closed under addition. For example the set $D = \{(x, 0) : x \geq 0\} \cup \{(0, y) : y \geq 0\}$ is closed under nonnegative scalar multiplication because if $z \in C$ then $az \in C$ for any $a \in \mathbb{R}_{\geq 0}$, but D is not closed under addition. But if $K = \text{Conv}(C)$, then K is $\mathbb{R}_{\geq 0}^d$ and K is a convex cone. We will always want cones to be convex, and we will use cone to mean convex cone.

DEFINITION 1.1.9. A *finitely generated cone* C has the form

$$C = \left\{ \sum_{j=1}^m a_j x_j \mid a_j \geq 0, j = 1, \dots, m \right\},$$

for some finite collections of points $x_j \in \mathbb{R}^d$.

DEFINITION 1.1.10. A *polyhedral cone* is a cone of the form $\{x \in \mathbb{R}^d \mid Ax \leq 0\}$. Therefore, a polyhedral cone is a finite set of homogeneous linear inequalities.

Just as bounded polyhedra and polytopes are the same object, a polyhedral cone and a finitely generated cone are two descriptions of the same object.

THEOREM 1.1.11 (Farkas-Minkowski-Weyl, see Corollary 7.1a in [143]). *A convex cone is polyhedral if and only if it is finitely generated.*

DEFINITION 1.1.12. Let K be a convex set, then the *polar cone* K is $K^\circ = \{y \in \mathbb{R}^d \mid y^T x \leq 0, \forall x \in K\}$.

The polar of a finitely generated cone is easy to compute.

THEOREM 1.1.13. (Polar of a finitely generated cone) *Let $K = \text{cone}(\{c_1, \dots, c_m\})$, then the polar cone is the interception of a finite number of halfspaces: $K^\circ = \{y \in \mathbb{R}^d : c_j^T y \leq 0, \forall j = 1, \dots, m\}$. Likewise, if K is given by $Cy \leq 0$, then K° is generated by the rows of C .*

1.2. Generating functions for integration and summation

Chapters 2, 3, and 4 make great use of encoding values in generating functions. This section gives a general introduction to how they are used in the later chapters. For a more complete description of the topics in this section, see [19, 20].

1.2.1. Working with generating functions: an example. Let us start with an easy example. Consider the one dimensional polyhedra in \mathbb{R} given by $P = [0, n]$. We encode the lattice points of $P \cap \mathbb{Z}$ by placing each integer point as the power of a monomial, thereby obtaining the polynomial $S(P; z) := z^0 + z + z^2 + z^3 + \dots + z^n$. The polynomial $S(P; z)$ is called the *generating function of P* . Notice that counting $P \cap \mathbb{Z}$ is equivalent to evaluating $S(P, 1)$.

In terms of the computational complexity, listing each monomial in the polynomial $S(P, z)$ results in a polynomial with exponential length in the bit length of n . However, we can rewrite the summation with one term:

$$S(P, z) = 1 + z^1 + \dots + z^n = \frac{1 - z^{n+1}}{1 - z}.$$

Counting the number of points in $|P \cap \mathbb{Z}|$ is no longer as simple as evaluating $\frac{1-z^{n+1}}{1-z}$ at $z = 1$ because this is a singularity. However, this singularity is removable. One could perform long-polynomial division, but this would result in a exponentially long polynomial in the bit length of n . Another option that yields a polynomial time algorithm would be to apply L'Hospital's rule:

$$\lim_{z \rightarrow 1} S(P, z) = \lim_{z \rightarrow 1} \frac{-(n+1)z^n}{1} = n + 1.$$

Notice that $S(P, z)$ can be written in two ways:

$$S(P, z) = \frac{1}{1-z} - \frac{z^{n+1}}{1-z} = \frac{1}{1-z} + \frac{z^n}{1-z^{-1}}.$$

The first two rational expressions have a nice description in terms of their series expansion:

$$1 + z + \dots + z^n = (1 + z^1 + \dots) - (z^{n+1} + z^{n+2} + \dots).$$

For the second two rational functions, we have to be careful about the domain of convergence when computing the series expansion. Notice that in the series expansion,

$$\frac{1}{1-z} = \begin{cases} 1 + z^1 + z^2 \dots & \text{if } |z| < 1 \\ -z^{-1} - z^{-2} - z^{-3} - \dots & \text{if } |z| > 1 \end{cases}$$

$$\frac{z^n}{1-z^{-1}} = \begin{cases} -z^{n+1} - z^{n+2} - z^{n+3} - \dots & \text{if } |z| < 1 \\ z^n + z^{n-1} + z^{n-2} + \dots & \text{if } |z| > 1 \end{cases}$$

adding the terms when $|z| < 1$ or $|z| > 1$ results in the desired polynomial: $1 + z^1 + \dots + z^n$. But we can also get the correct polynomial by adding the series that correspond to different domains of convergence. However, to do this we must now add the series $\dots + z^{-2} + z^{-1} + 1 + z + z^2 + \dots$

which corresponds to the polyhedra that is the entire real line:

$$\begin{aligned} 1 + z + \cdots z^n &= (1 + z + z^2 + \cdots) \\ &\quad + (z^n + z^{n-1} + \cdots) \\ &\quad - (\cdots + z^{-2} + z^{-1} + 1 + z + z^2 + \cdots) \end{aligned}$$

and

$$\begin{aligned} 1 + z + \cdots z^n &= (-z^{-1} - z^{-2} - z^{-3} - \cdots) \\ &\quad + (-z^{n+1} - z^{n+2} - z^{n+3} - \cdots) \\ &\quad + (\cdots + z^{-2} + z^{-1} + 1 + z + z^2 + \cdots) \end{aligned}$$

Hence by including the series $\cdots + z^{-2} + z^{-1} + 1 + z + z^2 + \cdots$, we can perform the series expansion of $\frac{1}{1-z} + \frac{z^n}{1-z^{-1}}$ by computing the series expansion of each term on potentially different domains of convergence.

In the next sections, we will develop a rigorous justification for adding the series $\cdots + z^{-2} + z^{-1} + 1 + z + z^2 + \cdots$.

1.2.2. Indicator functions.

DEFINITION 1.2.1. The indicator function, $[A] : \mathbb{R}^d \rightarrow \mathbb{R}$, of a set $A \subseteq \mathbb{R}^d$ takes two values: $[A](x) = 1$ if $x \in A$ and $[A](x) = 0$ otherwise.

The set of indicator functions on \mathbb{R}^d spans a vector space with point-wise additions and scalar multiplication. The set also has an algebra structure where $[A] \cdot [B] = [A \cap B]$, and $[A] + [B] = [A \cup B] + [A \cap B]$.

Recall the *cone* of a set $A \subseteq \mathbb{R}^d$ is all conic combinations of the points from A :

$$\text{Cone}(A) := \left\{ \sum_i \alpha_i a_i \mid a_i \in A, \alpha_i \in \mathbb{R}_{\geq 0} \right\}.$$

DEFINITION 1.2.2. Let P be a polyhedron and $x \in P$. Then the *tangent cone*, of P at x is the polyhedral cone

$$\text{TCone}(P, x) := x + \text{Cone}(P - x)$$

DEFINITION 1.2.3. Let P be a polyhedron and $x \in P$. Then the *cone of feasible directions*, of P at x is the polyhedral cone $\text{Cone}(P - x)$.

Note that if x is a vertex of P , and P is given by an inequality description, then the tangent cone $\text{TCone}(P, x)$ is the intersection of inequalities that are tight at x . Also, $\text{TCone}(P, x)$ includes the affine hull of the smallest face that x is in, so the tangent cone is pointed only if x is a vertex. The difference between a tangent cone and a cone of feasible directions is that the latter is shifted to the origin.

When F is a face of P , we will also use the notation $\text{TCone}(P, F)$ to denote $\text{TCone}(P, x)$ where x is any interior point of F .

THEOREM 1.2.4 ([32], [79]). *Let P be a polyhedron, then*

$$[P] = \sum_F (-1)^{\dim(F)} [\text{TCone}(P, F)]$$

where the sum ranges over all faces F of P including $F = P$ but excluding $F = \emptyset$

This theorem is saying that if the generating function of a polytope is desired, it is sufficient to just find the generating function for every face of P . The next corollary takes this a step further and says it is sufficient to just construct the generating functions associated at each vertex. This is because, as we will see, the generating functions for non-pointed polyhedra can be ignored.

COROLLARY 1.2.5. *Let P be a polyhedron, then*

$$[P] \equiv \sum_{v \in V} [\text{TCone}(P, v)] \pmod{\text{indicator functions of non-pointed polyhedra}},$$

where V is the vertex set of P .

1.2.3. Generating functions of simple cones. In this section, we quickly review the generating function for summation and integration when the polyhedron is a cone.

And there's still confusion regarding multiplication: To make a vector space, you need addition of two elements and multiplication of an element by a scalar (field element). The multiplication of two indicator functions is NOT a multiplication by a scalar. Instead, multiplication by a scalar is really just scaling a function: Take indicator function of positive real numbers: $f(x) = 1$ if $x_i = 0$;

0 if $x \leq 0$. Take a real number, say 7. Then $(7 \cdot f)(x) = 7$ if $x \geq 0$; 0 if $x \leq 0$. This makes the "algebra of polyhedra" a real vector space. But the algebra of polyhedra is also an "algebra". For that you need another multiplication, namely the multiplication of two elements; and that is the multiplication that you describe (actually it's the bilinear extension of what you describe – because the multiplication needs to be defined not only for two indicator functions, but for two \mathbb{R} -linear combinations of indicator functions).

DEFINITION 1.2.6. Let V and W be vector spaces. Let \mathcal{P} be the real vector space spanned by the indicator functions of all polyhedra in V where scalar multiplication is with a real number and an indicator function, and the addition operator is addition of indicator functions. When \mathcal{P} is equipped with the additional binary operation from $\mathcal{P} \times \mathcal{P}$ to \mathcal{P} representing multiplication of indicator functions, then \mathcal{P} is called the *algebra of polyhedra*. A *valuation* T is a linear transformation $T : \mathcal{P} \rightarrow W$.

The next Proposition serves as a basis for all the summation algorithms we will discuss. Its history can be traced to Lawrence in [111], and Khovanskii and Pukhlikov in [133]. It is well described as Theorem 13.8 in [19].

PROPOSITION 1.2.7. *There exists a unique valuation $S(\cdot, \ell)$ which associates to every rational polyhedron $P \subset \mathbb{R}^d$ a meromorphic function in ℓ so that the following properties hold*

- If $\ell \in \mathbb{R}^d$ such that $e^{\langle \ell, x \rangle}$ is summable over the lattice points of P , then

$$S(P, \ell) = \sum_{P \cap \mathbb{Z}^d} e^{\langle \ell, x \rangle}.$$

- For every point $s \in \mathbb{Z}^d$, one has

$$S(s + P, \ell) = e^{\langle \ell, s \rangle} S(P, \ell).$$

- If P contains a straight line, then $S(P, \ell) = 0$.

A consequence of the valuation property is the following fundamental theorem. It follows from the Brion–Lasserre–Lawrence–Varchenko decomposition theory of a polyhedron into the supporting cones at its vertices [19, 23, 33, 102].

LEMMA 1.2.8. *Let P be a polyhedron with set of vertices $V(P)$. For each vertex s , let $C_s(P)$ be the cone of feasible directions at vertex s . Then*

$$S(P, \ell) = \sum_{s \in V(P)} S(s + C_s(P), \ell).$$

This last lemma can be identified as the natural result of combining Corollary 1.2.5 and Proposition 1.2.7 part (3). A non-pointed polyhedron is another characterization of a polyhedron that contains a line.

Note that the cone $C_s(P)$ in Lemma 1.2.8 may not be simplicial, but for simplicial cones there are explicit rational function formulas. As we will see in Proposition 1.2.12, one can derive an explicit formula for the rational function $S(s + C_s(P), \ell)$ in terms of the geometry of the cones.

PROPOSITION 1.2.9. *For a simplicial full-dimensional pointed cone C generated by rays u_1, u_2, \dots, u_d (with vertex 0) where $u_i \in \mathbb{Z}^d$ and for any point s*

$$S(s + C, \ell) = \sum_{a \in (s + \Pi_C) \cap \mathbb{Z}^d} e^{\langle \ell, a \rangle} \prod_{i=1}^d \frac{1}{1 - e^{\langle \ell, u_i \rangle}}$$

where $\Pi_C := \{\sum_{i=1}^d \alpha_i u_i \mid 0 \leq \alpha_i < 1\}$ This identity holds as a meromorphic function of ℓ and pointwise for every ℓ such that $\langle \ell, u_i \rangle \neq 0$ for all u_i .

The set Π_C is often called the *half-open fundamental parallelepiped* of C . It is also common to force each ray u_i to be *primitive*, meaning that the greatest common divisor of the elements in u_i is one, and this can be accomplished by scaling each ray.

The continuous generating function for P almost mirrors the discrete case. It can again be attributed to Lawrence, Khovanskii, and Pukhlikov, and appears as Theorem 8.4 in [19].

PROPOSITION 1.2.10. *There exists a unique valuation $I(\cdot, \ell)$ which associates to every polyhedron $P \subset \mathbb{R}^d$ a meromorphic function so that the following properties hold*

- (1) *If ℓ is a linear form such that $e^{\langle \ell, x \rangle}$ is integrable over P with the standard Lebesgue measure on \mathbb{R}^d , then*

$$I(P, \ell) = \int_P e^{\langle \ell, x \rangle} dx$$

(2) For every point $s \in \mathbb{R}^d$, one has

$$I(s + P, \ell) = e^{\langle \ell, s \rangle} I(P, \ell).$$

(3) If P contains a line, then $I(P, \ell) = 0$.

LEMMA 1.2.11. Let P be a polyhedron with set of vertices $V(P)$. For each vertex s , let $C_s(P)$ be the cone of feasible directions at vertex s . Then

$$I(P, \ell) = \sum_{s \in V(P)} I(s + C_s(P), \ell).$$

Again, this last lemma can be identified as the natural result of combining Corollary 1.2.5 and Proposition 1.2.10 part (3).

PROPOSITION 1.2.12. For a simplicial full-dimensional pointed cone C generated by rays u_1, u_2, \dots, u_d (with vertex 0) and for any point s

$$I(s + C, \ell) = \text{vol}(\Pi_C) e^{\langle \ell, s \rangle} \prod_{i=1}^d \frac{1}{-\langle \ell, u_i \rangle}.$$

These identities holds as a meromorphic function of ℓ and pointwise for every ℓ such that $\langle \ell, u_i \rangle \neq 0$ for all u_i .

1.2.3.1. *Integration example.* Let $a < b < c < d$, then it is a well known fact from calculus that

$$\int_a^c e^{\ell_1 x_1} dx_1 = \int_a^b e^{\ell_1 x_1} dx_1 + \int_b^c e^{\ell_1 x_1} dx_1 = \int_a^d e^{\ell_1 x_1} dx_1 - \int_c^d e^{\ell_1 x_1} dx_1.$$

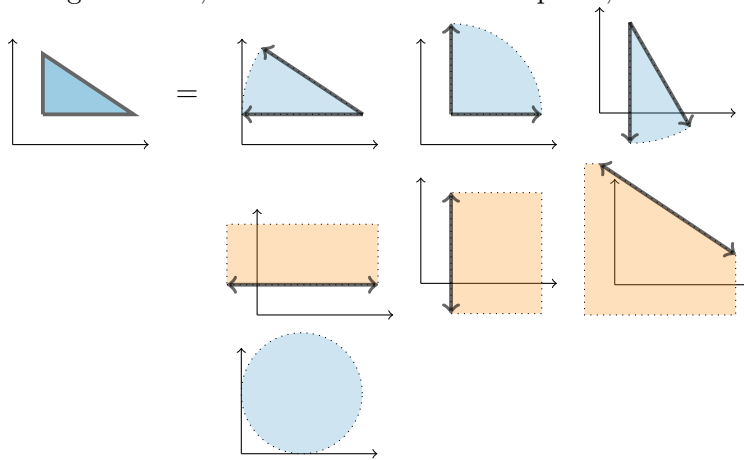
However, the domain $[a, c]$ cannot be decomposed in every way. For example

$$\int_a^c e^{\ell_1 x_1} dx_1 \neq \int_a^\infty e^{\ell_1 x_1} dx_1 + \int_{-\infty}^c e^{\ell_1 x_1} dx_1 - \int_{-\infty}^\infty e^{\ell_1 x_1} dx_1.$$

Notice that not only is the expression on the right hand side of the equation not equal to the left hand side, but there is no value for ℓ_1 that makes the three integrals finite. However, results in this section allow us to assign numbers (or meromorphic functions) to the integrals that do not converge!

1.2. GENERATING FUNCTIONS FOR INTEGRATION AND SUMMATION

We now consider an example in dimension two. Consider the triangle below with coordinates at $(1, 1)$, $(1, 3)$, and $(4, 1)$. This domain can be written as the sum of 7 polyhedrons: addition of three tangent cones, subtraction of three halfspaces, and the addition of one copy of \mathbb{R}^2 .



For example, the point $(1, 1)$ is part of the triangle, so it is counted once. In the decomposition, the point $(1, 1)$ is counted positively four times (once in each tangent cone and once in \mathbb{R}^2), and is counted negatively three times (once in each halfspace), resulting in being counted exactly once. A similar calculation shows that $(0, 0)$ is counted negatively in one of the halfspaces, and positively in \mathbb{R}^2 , resulting in a total count of zero, meaning $(0, 0)$ is not part of the triangle.

The integral of $e^{\ell_1 x + \ell_2 y}$ over the triangle clearly exist because the function is continuous and the domain is compact. As the triangle can be written as the sum of 7 other polyhedrons, we want to integrate $e^{\ell_1 x + \ell_2 y}$ over each of the 7 polyhedrons. However, the integral of $e^{\ell_1 x + \ell_2 y}$ over some of them does not converge! Instead, we map each domain to a meromorphic function using Propositions 1.2.10 and 1.2.12. Because $I(\cdot, \ell)$ is a valuation, we can apply $I(\cdot, \ell)$ to each domain. The fact that $I(P, \ell) = 0$ if P contains a line, simplifies the calculation to just the three tangent cones: $s_1 + C_1$, $s_2 + C_2$, and $s_3 + C_3$.

The diagram shows the triangle being equated to the sum of three tangent cones (top row). Below this, the corresponding equation is written:

$$I(\Delta, \ell) = I(s_1 + C_1, \ell) + I(s_2 + C_2, \ell) + I(s_3 + C_3, \ell)$$

$$\begin{aligned} \int_1^4 \int_1^{\frac{-2}{3}x + \frac{11}{3}} e^{\ell_1 x + \ell_2 y} dy dx &= 2e^{4\ell_1 + \ell_2} \frac{1}{(-3\ell_1 + 2\ell_2)} \frac{1}{(-\ell_1)} \\ &+ 1e^{\ell_1 + \ell_2} \frac{1}{\ell_1} \frac{1}{\ell_2} \\ &+ 3e^{1\ell_1 + 3\ell_2} \frac{1}{(-\ell_2)} \frac{1}{(3\ell_1 - 2\ell_2)} \end{aligned}$$

Propositions 1.2.10 and 1.2.12 say that the meromorphic function associated with the triangle is equal to the sum of the three meromorphic functions associated at each tangent cone. Moreover, because the integral over the triangle exist, the meromorphic function associated with the triangle gives the integral. For example, evaluating the meromorphic function at $\ell_1 = 2, \ell_2 = 1$ results in 1924.503881, which is the integral of e^{2x+y} over the triangle.

There is one problem. The integral of $e^{\ell_1 x + \ell_2 y}$ over the triangle is a holomorphic function, and we have written it as the sum of three meromorphic functions, so this means the poles of the meromorphic functions must cancel in the sum. Consider evaluating at $\ell_1 = 2, \ell_2 = 3$. This would produce division by zero, and so $\ell_1 = 2, \ell_2 = 3$ is among the poles. A common approach is to instead evaluate ℓ at $\ell_1 = 2 + \epsilon, \ell_2 = 3 + \epsilon$ and take the limit as $\epsilon \rightarrow 0$. Hence

$$\int_1^4 \int_1^{\frac{-2}{3}x + \frac{11}{3}} e^{2x+3y} dy dx = \lim_{\epsilon \rightarrow 0} \sum_{i=1}^3 I(s_i + C_i, (2, 3) + \epsilon(1, 1)).$$

Notice that for each i , $I(s_i + C_i, (2, 3) + \epsilon(1, 1))$ is a meromorphic in ϵ , but $\sum_{i=1}^3 I(s_i + C_i, (2, 3) + \epsilon(1, 1))$ is a holomorphic function (as it is the integral of $e^{(2+\epsilon)x+(3+\epsilon)y}$ over the triangle). This means that in the Laurent series expansion of $I(s_i + C_i, (2, 3) + \epsilon(1, 1))$, any terms where ϵ has a negative exponent will cancel out in the sum. Thus the limit can be computed by finding the Laurent series expansion at $\epsilon = 0$ for each $I(s_i + C_i, (2, 3) + \epsilon(1, 1))$ and summing the coefficient of ϵ^0 in each Laurent series. Chapter 2 will show that computing the Laurent series is easy in this case.

This is a common technique, and we will see it used many times in this manuscript.

1.2.4. Generating function for non-simple cones. Lemma 1.2.8 and Proposition 1.2.9 (or Lemma 1.2.11 and Proposition 1.2.12) can be used for computing the summation (or integral) over

a polytope only if the polytope is a *simple* polytope. Meaning, for a d -dimensional polytope, every vertex of the polytope is adjacent to exactly d edges.

In this section, we review the generating function of $\sum_{x \in P \cap \mathbb{Z}^d} e^{\langle \ell, x \rangle}$ and $\int_P e^{\langle \ell, x \rangle} dx$ for a general polytope P . When P is not simple, the solution is to triangulate it the tangent cones.

DEFINITION 1.2.13. A triangulation of a cone C is the set Γ of simplicial cones C_i of the same dimension as the affine hull of C such that

- (1) the union of all the simplicial cones in Γ is C ,
- (2) the intersection of any pair of simplicial cones in Γ is a common face of both simplicial cones,
- (3) and every ray of every simplicial cone is also a ray of C .

There are many references and software tools for computing a triangulation of a polytope or polyhedral cone, see [1, 10, 62, 72, 76, 112, 135].

Let C be a full-dimensional pointed polyhedral cone, and $\Gamma_1 = \{C_i \mid i \in I_1\}$ be a triangulation into simplicial cones C_i where I_1 is a finite index set. It is true that $C = \bigcup_{i \in I_1} C_i$, but $[C] = \sum_{i \in I_1} [C_i]$ is false as points on the boundary of two adjacent simplicial cones are counted multiple times. The correct approach is to use the inclusion-exclusion formula:

$$[C] = \sum_{\emptyset \neq J \subseteq I_1} (-1)^{|J|-1} [\bigcap_{j \in J} C_j]$$

Also, note that this still holds true when C (and the C_i) is shifted by a point s . When $|J| \geq 2$, $I(\bigcap_{j \in J} C_j, \ell) = 0$ as $\bigcap_{j \in J} C_j$ is not full-dimensional, and the integration is done with respect to the Lebesgue measure on \mathbb{R}^d . This leads us to the next lemma.

LEMMA 1.2.14. *For any triangulation Γ_s of the feasible cone at each of the vertices s of the polytope P we have $I(P, \ell) = \sum_{s \in V(P)} \sum_{C \in \Gamma_s} I(s + C, \ell)$*

Lemma 1.2.14 states that we can triangulate a polytope's feasible cones and apply the integration formulas on each simplicial cone without worrying about shared boundaries among the cones. Note that there is no restriction on how the triangulation is performed.

More care is needed for the discrete case as $S(\cap_{j \in J} C_j, \ell) \neq 0$ when $|J| \geq 2$. We want to avoid using the inclusion-exclusion formula as it contains exponentially many terms (in size of $|I_1|$).

The discrete case has another complication. Looking at Proposition 1.2.9, we see that the sum

$$\sum_{a \in (s + \Pi_C) \cap \mathbb{Z}^d} e^{\langle \ell, a \rangle}$$

has to be enumerated. However, there could be an exponential number of points in $(s + \Pi_C) \cap \mathbb{Z}^d$ in terms of the bit length of the simplicial cone C .

We will illustrate one method for solving these problems called the *Dual Barvinok Algorithm*.

1.2.4.1. *Triangulation*. Recall that the *polar* of a set $A \subset \mathbb{R}^d$ is the set $A^\circ = \{x \in \mathbb{R}^d \mid \langle x, a \rangle \leq 1 \text{ for every } a \in A\}$. Cones enjoy many properties under the polar operation. If C is a finitely generated cone in \mathbb{R}^d , then

- (1) $C^\circ = \{x \in \mathbb{R}^d \mid \langle x, c \rangle \leq 0, \forall c \in C\}$,
- (2) C° is also a cone,
- (3) $(C^\circ)^\circ = C$, and
- (4) if $C = \{x \mid A^T x \leq 0\}$, then C° is generated by the columns of A .

The next lemma is core to Brion's "polarization trick" [33] for dealing with the inclusion-exclusion terms.

LEMMA 1.2.15 (Theorem 5.3 in [19]). *Let \mathcal{C} be the vector space spanned by the indicator functions of all closed convex sets in \mathbb{R}^d . Then there is a unique linear transformation \mathcal{D} from \mathcal{C} to itself such that $\mathcal{D}([A]) = [A^\circ]$ for all non-empty closed convex sets A .*

Instead of taking the non-simplicial cone C and triangulating it, we first compute C° and triangulate it to $\Gamma' = \{C_i^\circ \mid i \in I_2\}$. Then

$$[C^\circ] = \sum_{i \in I_2} [C_i^\circ] + \sum_{\emptyset \neq J \subseteq I_2, |J| > 1} (-1)^{|J|-1} [\cap_{j \in J} C_j^\circ].$$

Applying the fact that $(C^\circ)^\circ = C$ we get

$$[C] = \sum_{i \in I_2} [C_i] + \sum_{\emptyset \neq J \subseteq I_2, |J| > 1} (-1)^{|J|-1} [(\cap_{j \in J} C_j^\circ)^\circ].$$

Notice that the polar of a full-dimensional pointed cone is another full-dimensional pointed cone. For each J with $|J| \geq 2$, $\cap_{j \in J} C_j^\circ$ is not a full-dimensional cone. The polar of a cone that is not full dimensional is a cone that contains a line. Hence $S((\cap_{j \in J} C_j^\circ)^\circ, \ell) = 0$. By polarizing a cone, triangulating in the dual space, and polarizing back, the boundary terms from the triangulation can be ignored.

1.2.4.2. *Unimodular cones.* Next, we address the issue that for a simplicial cone C , the set $\Pi_C \cap \mathbb{Z}^d$ contains too many terms for an enumeration to be efficient. The approach then is to decompose C into cones that only have one lattice point in the fundamental parallelepiped. Such cones are called *unimodular cones*. Barvinok in [17] first developed such a decomposition and showed that it can be done in polynomial time when the dimension is fixed. We next give an outline of Barvinok's decomposition algorithm.

Given a pointed simplicial full-dimensional cone C , Barvinok's decomposition method will produce new simplicial cones C_i such that $|\Pi_{C_i} \cap \mathbb{Z}^d| \leq |\Pi_C \cap \mathbb{Z}^d|$ and values $\epsilon_i \in \{1, -1\}$ such that

$$[C] \equiv \sum_{i \in I} \epsilon_i [C_i] \quad (\text{mod indicator functions of lower dimensional cones}).$$

Let C be generated by the rays u_1, \dots, u_d . The algorithm first constructs a vector w such that

$$w = \alpha_1 u_1 + \dots + \alpha_d u_d \text{ and } |\alpha_i| \leq |\det(U)|^{-1/d} \leq 1,$$

where the columns of U are the u_i . This is done with integer programming or using a lattice basis reduction method [61]. Let $K_i = \text{Cone}(u_1, \dots, u_{i-1}, w, u_{i+1}, \dots, u_d)$, then it can be shown that $|\Pi_{K_i} \cap \mathbb{Z}^d| \leq |\Pi_C \cap \mathbb{Z}^d|^{\frac{d-1}{d}}$, meaning that these new cones have less integer points in the fundamental parallelepiped than the old cone. This process can be recursively repeated until unimodular cones are obtained.

THEOREM 1.2.16 (Barvinok [17]). *Let C be a simplicial full-dimensional cone generated by rays u_1, \dots, u_d . Collect the rays into the columns of a matrix $U \in \mathbb{Z}^{d \times d}$. Then the depth of the recursive decomposition tree is at most*

$$\left\lceil 1 + \frac{\log_2 \log_2 |\det(U)|}{\log_2 \frac{n}{n-1}} \right\rceil.$$

Because at each node in the recursion tree has at most n children, and the depth of the tree is doubly logarithmic in $\det(U)$, only polynomial many unimodular cones are constructed.

In [17], the inclusion-exclusion formula was applied to boundaries between the unimodular cones in the primal space. However, like in triangulation, the decomposition can be applied in the dual space where the lower dimensional cones can be ignored. For the full details of Barvinok's decomposition algorithm, see [61], especially Algorithm 5 therein. This variant of Barvinok's algorithm has efficient implementations in `LatTe` [57] and the library `barvinok` [153].

1.2.5. Generating functions for full-dimensional polytopes. In this section, we explicitly combine the results from the last two sections and write down the polynomial time algorithms for computing the discrete and continuous generating function for a polytope P .

Algorithm 1 Barvinok's Dual Algorithm

Output: the rational generating function for $S(P, \ell) = \sum_{x \in P \cap \mathbb{Z}^d} e^{\langle \ell, x \rangle}$ in the form

$$S(P, \ell) = \sum_{i \in I} \epsilon_i \frac{e^{\langle \ell, v_i \rangle}}{\prod_{j=1}^d (1 - e^{\langle \ell, u_{ij} \rangle})}$$

where $\epsilon_i \in \{-1, 1\}$, $v_i \in \mathbb{Z}^d$, $u_{ij} \in \mathbb{Z}^d$, and $|I|$ is polynomially bounded in the input size of P when d is fixed. Each $i \in I$ corresponds to a simplicial unimodular cone $v_i + C_i$ where u_{i1}, \dots, u_{id} are the d rays of the cone C_i .

- (1) Compute all vertices v_i and corresponding supporting cones C_i of P
- (2) Polarize the supporting cones C_i to obtain C_i°
- (3) Triangulate C_i° into simplicial cones C_{ij}° , discarding lower-dimensional cones
- (4) Apply Barvinok's signed decomposition (see [61]) to the cones C_{ij}° to obtain cones C_{ijk}° , which results in the identity

$$[C_{ij}^\circ] \equiv \sum_k \epsilon_{ijk} [C_{ijk}^\circ] \pmod{\text{indicator functions of lower dimensional cones}}.$$

Stop the recursive decomposition when unimodular cones are obtained. Discard all lower-dimensional cones

- (5) Polarize back C_{ijk}° to obtain cones C_{ijk}
 - (6) v_i is the unique integer point in the fundamental parallelepiped of every resulting cone $v_i + C_{ijk}$
 - (7) Write down the above formula
-

The key part of this variant of Barvinok's algorithm is that computations with rational generating are simplified when non-pointed cones are used. The reason is that the rational generating function of every non-pointed cone is zero. By operating in the dual space, when computing the

polar cones, lower-dimensional cones can be safely discarded because this is equivalent to discarding non-pointed cones in the primal space.

Triangulating a non-simplicial cone in the dual space was done to avoid the many lower-dimensional terms that arise from using the inclusion-exclusion formula for the indicator function of the cone. Other ways to get around this exist. In [23, 25, 97], irrational decompositions were developed which are decompositions of polyhedra whose proper faces do not contain any lattice points. Counting formulas for lattice points that are constructed with irrational decompositions do not need the inclusion-exclusion principle. The implementation of this idea [98] was the first practically efficient variant of Barvinok's algorithm that works in the primal space.

For an extremely well written discussion on other practical algorithms to solve these problems using slightly different decompositions, see [97]. For completeness, we end with the algorithmic description for the continuous generating function.

Algorithm 2 Continuous generating function

Output: the rational generating function for $I(P, \ell) = \int_P e^{\langle \ell, x \rangle} dx$ in the form

$$I(P, \ell) = \sum_{s \in V(P)} \sum_{C \in \Gamma_s} \text{vol}(\Pi_C) e^{\langle \ell, s \rangle} \prod_{i=1}^d \frac{1}{-\langle \ell, u_i \rangle}.$$

where u_1, \dots, u_d are the rays of cone C .

- (1) Compute all vertices $V(P)$ and corresponding supporting cones $\text{Cone}(P - s)$
 - (2) Triangulate $\text{Cone}(P - s)$ into a collection of simplicial cones Γ_s using any method
 - (3) Write down the above
-

Note that in fixed dimension, the above algorithms compute the generating functions in polynomial time. We will repeatedly use the next lemma to multiply series in polynomial time in fixed dimension. The idea is to multiply each factor, one at a time, truncating after total degree M .

1.2.6. A power of a linear form. Above, we developed an expression for $\sum_{x \in P \cap \mathbb{Z}^d} e^{\langle \ell, x \rangle}$, and $I(P, \ell) = \int_P e^{\langle \ell, x \rangle} dx$. Later in Chapters 2 and 3, we will compute similar sums and integrals where instead of an exponential function, the summand or integrand is a power of a linear form, or more generally, a product of affine functions. The common trick will be to introduce a new variable t and compute $S(P, \ell \cdot t)$ or $I(P, \ell \cdot t)$. If the series expansion in t about $t = 0$ is computed, we get a series in t where the coefficient of t^m is $\sum_{x \in P \cap \mathbb{Z}^d} \langle \ell, x \rangle^m$ or $\int_P \langle \ell, x \rangle^m dx$. To compute these series

expansions, many polynomials will be multiplied together while deleting monomials whose degree is larger than some value M . The next lemma shows that this process is efficient when the number of variables is fixed, and we repeatedly apply it in Chapters 2 and 3.

LEMMA 1.2.17 (Lemma 4 in [13]). *For k polynomials $h_1, \dots, h_k \in \mathbb{Q}[x]$ in d variables, the product $h_1 \cdots h_k$ can be truncated at total degree M by performing $O(kM^{2d})$ elementary rational operations.*

1.3. Handelman's Theorem and polynomial optimization

In this section, we comment on the problem

$$\begin{aligned} \max f(x) \\ x \in P, \end{aligned}$$

where $f(x)$ is a polynomial and P is a polytope. Handelman's Theorem is used in Chapters 2 and 3 as a tool for rewriting a polynomial in a special way. This section introduces Handelman's theorem along with how it can directly be used for polynomial optimization. Section 1.3.1 briefly illustrates how Handelman's theorem can be used instead of sum of squares polynomials. Then finally in Section 1.3.2, we review the computational complexity of the polynomial optimization problem.

In Chapter 3, Handelman's theorem is *not* used to perform optimization. It is used as a tool to decompose the polynomial $f(x)$ into a form that makes integrating $f(x)^k$ more practical. These integrals are then used to produce bounds on the optimal value. With this view, we are using Handelman's theorem in a novel way.

THEOREM 1.3.1 (Handelman [82]). *Assume that $g_1, \dots, g_n \in \mathbb{R}[x_1, \dots, x_d]$ are linear polynomials and that the semialgebraic set*

$$(1.1) \quad S = \{x \in \mathbb{R}^d \mid g_1(x) \geq 0, \dots, g_n(x) \geq 0\}$$

is compact and has a non-empty interior. Then any polynomial $f \in \mathbb{R}[x_1, \dots, x_d]$ strictly positive on S can be written as $f(x) = \sum_{\alpha \in \mathbb{N}^n} c_\alpha g_1^{\alpha_1} \cdots g_n^{\alpha_n}$ for some nonnegative scalars c_α .

We define the *degree* of a Handelman decomposition be $\max |\alpha|$, where the maximum is taken over all the exponent vectors α of $g_i(x)$ that appear in a decomposition.

Note that this theorem is true when S is a polytope P , and the polynomials $g_i(x)$ correspond to the rows in the constraint matrix $b - Ax \geq 0$. See [40, 50, 110] for a nice introduction to the Handelman decomposition. The Handelman decomposition is only guaranteed to exist if the polynomial is strictly greater than zero on P , and the required degree of the Handelman decomposition can grow as the minimum of the polynomial approaches zero [140]. The next three examples are taken from Section 3.1 of [140].

EXAMPLE 1.3.2. Consider the polynomial $f(x) \in \mathbb{Q}[x]$ given by $f(x) = x^2 - 3x + 2 = (x-2)(x-1)$ on $[-1, 1]$. Because $f(1) = 0$, Handelman's theorem does not say that $f(x)$ must have a Handelman decomposition. However,

$$f(x) = (1-x)^2 + (1-x) = 1 \cdot g_1^2 g_2^0 + 1 \cdot g_2^1 g_2^0$$

where $g_1 := 1 - x$ and $g_2 := x + 1$, so $f(x)$ has a Handelman decomposition.

To apply Handelman's theorem, we must have that $f(x) > 0$ on P .

EXAMPLE 1.3.3. Consider the polynomial $f(x) \in \mathbb{Q}[x]$ given by $f(x) = x^2$ on $[-1, 1]$. Because $f(0) = 0$, Handelman's theorem does not say that $f(x)$ must have a Handelman decomposition. If $f(x)$ had a decomposition, then there would be numbers $c_\alpha > 0$ and integers $\alpha_i \in \mathbb{Z}_{\geq 0}$ such that

$$x^2 = \sum_{\alpha \in J} c_\alpha (1-x)^{\alpha_1} (x+1)^{\alpha_2},$$

with J being a finite subset of $\mathbb{Z}_{\geq 0}^2$. Evaluating both sides at zero produces the contradiction $0 = \sum_{\alpha \in J} c_\alpha > 0$. Hence $f(x) = x^2$ does not have a Handelman decomposition on $[-1, 1]$.

EXAMPLE 1.3.4. For every fixed $\epsilon > 0$, $p(x) = x^2 + \epsilon$ must have a Handelman decomposition on $[-1, 1]$. Let $t = \max\{\alpha_1 + \alpha_2 \mid \alpha \in J\}$ be the total degree of a Handelman representation. Then the next table lists what is the smallest ϵ value for which $x^2 + \epsilon$ has a degree t decomposition.

t	2	3	4	5	6	7
ϵ	1	1/3	1/3	1/5	1/5	1/7

There are many questions relating to Handelman's theorem. For instance, answers to these questions are not well known or completely unknown.

- Given a nonnegative polynomial $f(x)$ on a polytope P , how large does the Handelman degree have to be?
- By adding a positive shift s to $f(x)$, how can the Handelman degree change for $f(x) + s$?
- Fix t . Can a large enough shift be added to $f(x)$ so that $f(x) + s$ has a degree t Handelman decomposition?
- How can redundant inequalities in P 's description lower the Handelman degree or reduce the number of Handelman terms?

However, these questions do not prevent us from using Handelman's theorem as an effective tool for polynomial optimization. We now present a hierarchy of linear relaxations as described in [110] for maximizing a polynomial over a polytope. This is the most traditional way Handelman's theorem can directly be applied for optimization. Let g denote the set of polynomials g_1, \dots, g_n . For an integer $t \geq 1$, define the *Handelman set of order t* as

$$\mathcal{H}_t(g) := \left\{ \sum_{\alpha \in \mathbb{Z}_{\geq 0}^n : |\alpha| \leq t} c_\alpha g^\alpha : c_\alpha \geq 0 \right\}$$

and the corresponding *Handelman bound of order t* as

$$f_{\text{han}}^{(t)} := \inf \{ \lambda : \lambda - f(x) \in \mathcal{H}_t(g) \}.$$

Clearly, any polynomial in $\mathcal{H}_t(g)$ is nonnegative on P and one has the following chain of inclusions:

$$\mathcal{H}_1(g) \subseteq \dots \subseteq \mathcal{H}_t(g) \subseteq \mathcal{H}_{t+1}(g) \subseteq \dots$$

giving the chain of inequalities: $f_{\text{max}} \leq f_{\text{han}}^{(t+1)} \leq f_{\text{han}}^{(t)} \leq \dots \leq f_{\text{han}}^{(1)}$ for $t \geq 1$. When P is a polytope with non-empty interior, the asymptotic convergence of the bounds $f_{\text{han}}^{(t)}$ to f_{max} as the order t increases is guaranteed by Handelman's theorem.

Some results have been proved on the convergence rate in the case when P is the standard simplex or the hypercube $[0, 1]^d$.

THEOREM 1.3.5. [52] *Let P be the standard simplex $P = \{x \in \mathbb{R}^d \mid x_i \geq 0, \sum_{i=1}^d x_i = 1\}$, and let f be a polynomial of total degree D . Let f_{\max} and f_{\min} be the maximum and minimum value f takes on P , respectively. Then*

$$f_{\text{han}}^{(t)} - f_{\max} \leq D^D \binom{2D-1}{D} \frac{\binom{D}{2}}{t - \binom{D}{2}} (f_{\max} - f_{\min}).$$

THEOREM 1.3.6. [51] *Let $K = [0, 1]^d$ be the hypercube. If f is a polynomial of degree D and $r \geq 1$ is an integer then the Handelman bound of order $t = rk$ satisfies:*

$$f_{\text{han}}^{(rk)} - f_{\max} \leq \frac{L(f)}{r} \binom{D+1}{3} d^D,$$

with $L(f) := \max_{\alpha} \frac{\alpha!}{|\alpha|!} |f_{\alpha}|$.

1.3.1. Handelman and moment methods. Lasserre [104] introduced the observation that optimizing a polynomial over a polytope can be done by integrating over all probability measures that are absolutely continuous with respect to the Lebesgue measure:

$$f_{\max} = \sup_{\sigma} \int_P f(x) \sigma(x) dx,$$

where the supremum is taken over all absolutely continuous functions $\sigma(x)$ such that $\sigma(x) \geq 0$ on P and $\int_P \sigma(x) dx = 1$.

A common relaxation is to just integrate over some subset of measures. Such methods are generally called *moment methods*. One such method, the *Lasserre hierarchy* [104], is given by

$$f_t^{\text{sos}} := \max_{\sigma \in \text{SOS}_t} \left\{ \int_P f(x) \sigma(x) dx \mid \int_P \sigma(x) dx = 1 \right\},$$

where SOS_t is the set of all polynomials which are sums of squares (and hence nonnegative on P) of degree at most t . Moreover, it is known that $f_{\max} \geq f_t^{\text{sos}} \geq f_{t+1}^{\text{sos}}$ and $\lim_{t \rightarrow \infty} f_t^{\text{sos}} = f_{\max}$ [107].

The authors of [50] extended this idea using Handelman's theorem. They defined

$$f_t^{\text{han}} := \max_{\sigma \in \mathcal{H}_t} \left\{ \int_P f(x) \sigma(x) dx \mid \int_P \sigma(x) dx = 1 \right\},$$

where \mathcal{H}_t is the set of Handelman polynomials on P of degree at most t . They also show f_t^{han} converges to f_{\max} as $t \rightarrow \infty$.

The roles played by sums of squares polynomials and Handelman polynomials in polynomial optimization are very similar. Our approach to Handelman's theorem is not focused on using it for optimization, but rather as a decomposition of a nonnegative polynomial function. For more information on sum of squares type optimization techniques, see [50, 106, 104, 105, 107, 103].

1.3.2. Complexity of the problem. In Chapter 3, the main results are presented with precise statements on an algorithm's complexity. In this section, we review the complexity of polynomial optimization and explain why we always fix the dimension in complexity statements. First we review the complexity of maximizing a polynomial $f(x) \in \mathbb{R}[x_1, \dots, x_d]$ over a polytope $P \subset \mathbb{R}^d$. That is, consider the complexity of the problems

$$\begin{array}{ccc} \max f(x) & & \max f(x) \\ & \text{and} & \\ x \in P. & & x \in P \cap \mathbb{Z}^d. \end{array}$$

Both exact optimization problems are NP-hard, as they include two well known NP-complete problems: the max-cut problem, and the maximum stable set problem. The max-cut problem can be reduced to a quadratic optimization problem over the integer points of the 0-1 hypercube: $[0, 1]^d \cap \mathbb{Z}^d$ [83]. The maximum stable set problem can be reduced to a quadratic optimization problem over the standard simplex $\Delta_n = \{x \in \mathbb{R}^d \mid \sum x_i = 1, x \geq 0\}$ [125]. Furthermore, problems in fixed dimension can still be hard. For example, the problem of minimizing a degree-4 polynomial over the lattice points of a convex polytope in dimension two is NP-hard. See [99] for a nice survey on the complexity of optimization problems.

Because the exact optimization problems are difficult, even when the domain is a cube or simplex, practical algorithms instead approximate the maximum. However, this too can be hard without some further restrictions. When the dimension is allowed to vary, approximating the optimal objective value of polynomial programming problems is still hard. For instance, Bellare and Rogaway [28] proved that if $P \neq NP$ and $\epsilon \in (0, \frac{1}{3})$ is fixed, there does not exist an algorithm \mathcal{A} for continuous quadratic programming over polytopes that produces an approximation $f_{\mathcal{A}}$ in polynomial time where $|f_{\mathcal{A}} - f_{\max}| < \epsilon |f_{\max} - f_{\min}|$.

Next we give three definitions of approximation algorithm common within combinatorial optimization for nonnegative objective functions $f(x)$.

DEFINITION 1.3.7.

- (1) An algorithm \mathcal{A} is an ϵ -approximation algorithm for a maximization problem with optimal cost f_{\max} , if for each instance of the problem of encoding length n , \mathcal{A} runs in polynomial time in n and returns a feasible solution with cost $f_{\mathcal{A}}$ such that $f_{\mathcal{A}} \geq (1 - \epsilon)f_{\max}$. Note that epsilon in this case is fixed, and is not considered an input to the algorithm.
- (2) A family of algorithms \mathcal{A}_{ϵ} is a *polynomial time approximation scheme (PTAS)* if for every error parameter $\epsilon > 0$, \mathcal{A}_{ϵ} is an ϵ -approximation algorithm and its running time is polynomial in the size of the instance for every fixed ϵ . Here, the algorithms are parameterized by ϵ , but \mathcal{A}_{ϵ} is still efficient when ϵ is fixed.
- (3) A family of ϵ -approximation algorithms \mathcal{A}_{ϵ} is a *fully polynomial time approximation scheme (FPTAS)* if the running time of \mathcal{A}_{ϵ} is polynomial in the encoding size of the instance and $1/\epsilon$. In this case, ϵ is an input to the algorithm, and its complexity term is polynomial in $1/\epsilon$.

In light of these complexity results and definitions, Chapter 3 describes a FPTAS algorithm for polynomial optimization over a polytope, when the dimension d is fixed. Note that we use the usual input size where everything is measured in the binary encoding. However exponents, such as a polynomial's degree or the integer k in $f(x)^k$, must be encoded in unary, otherwise their values cannot be computed in polynomial time. To see this, consider the problem of computing 2^x . The encoding length of this number is x in binary, which is a polynomial size when x is measured in unary. If x is encoded in binary, then its length is $\log_2(x)$, and so the length of 2^x is exponential in the binary encoding size of x .

1.4. Ehrhart Polynomials

This section introduces Chapter 4. In Section 1.4.1, we review the two most important theorems in Ehrhart theory. Then in Section 1.4.2 we set up the main question Chapter 4 addresses.

1.4.1. Two classic theorems. Let P be a rational polytope, meaning each vertex is in \mathbb{Q}^d . The Ehrhart function counts the number of integer points in P as P is scaled by a *nonnegative integer* number t :

$$L(P, t) := |\{x \in \mathbb{Z}^d \mid x \in t \cdot P\}|.$$

If P is given by a vertex representation, $t \cdot P$ is given by multiplying each vertex by the scalar t . If P has the description $Ax \leq b$, then $t \cdot P$ is $Ax \leq tb$. The next theorem states that $L(P, t)$ has remarkable structure, and is the cornerstone to an area of combinatorics called Ehrhart Theory.

THEOREM 1.4.1 (Ehrhart [64]). *For any polytope P with integer vertices, $L(P, t)$ is a polynomial in t , where the degree is equal to the dimension of P , the leading term in the polynomial is equal to the volume of P , and the constant term is 1.*

EXAMPLE 1.4.2. Consider the polytope that is a square in \mathbb{R}^2 given as the convex hull of the vertices $(0, 0)$, $(0, 1)$, $(1, 0)$, and $(1, 1)$. Computing a few values gives $L(P, 0) = 1$, $L(P, 1) = 4$, $L(P, 2) = 9$. The Ehrhart polynomial is $L(P, t) = (t + 1)^2$.

When the polytope has rational vertices, the Ehrhart polynomial can still be defined, but now the coefficients may no longer be constants, they may be periodic functions.

DEFINITION 1.4.3. A *quasi-polynomial* of degree k is a polynomial that has the form $q(t) = c_d(t)t^d + c_{d-1}(t)t^{d-1} + \cdots + c_0(t)$, where $c_i(t)$ is a periodic function with integral period. Quasi-polynomials can be written in many ways. For instance given a collection of polynomials $\{p_i(t)\}$ and a period s , $q(t) = p_i(t)$ where $i = t \bmod s$ is a quasi-polynomial. In Chapter 4, we use another representation: *step functions*.

The other well-known theorem in Ehrhart theory applies to rational polytopes.

THEOREM 1.4.4 (Ehrhart [65]). *For any polytope P with rational vertices, $L(P, t)$ is a quasi-polynomial in t , where the degree is equal to the dimension of P , the leading term in the polynomial is equal to the volume of P , and the constant term is 1.*

There are a few software packages for computing the Ehrhart polynomial. One of the best has to be `LattE`¹ [54]. `LattE` can also be used within some other popular software tools such as `Polymake` [76] and `Sage` [139]. Another good package is `barvinok` [153].

¹Available under the GNU General Public License at <https://www.math.ucdavis.edu/~latte/>.

For introductions to Ehrhart Theory, see [19, 24, 65, 146]. For generalizations when the dilation factor t is real, see [16, 114]. `LattE` can also compute the quasi-polynomial of rational polytopes when t is a real number.

1.4.2. Special case: knapsack polytopes. Given sequence $\alpha = [\alpha_1, \alpha_2, \dots, \alpha_{N+1}]$ of $N + 1$ positive integers, Chapter 4 seeks to compute the the combinatorial function $E(\alpha; t)$ that counts the non-negative integer solutions of the equation $\alpha_1 x_1 + \alpha_2 x_2 + \dots + \alpha_N x_N + \alpha_{N+1} x_{N+1} = t$, where the right-hand side t is a varying non-negative integer. This is precisely the Ehrhart quasi-polynomial of the polytope

$$P = \left\{ x \in \mathbb{R}^{N+1} \mid \sum_{i=1}^{N+1} x_i = 1, x_i \geq 0 \right\}.$$

And so $E(\alpha; t)$ is a quasi-polynomial function in the variable t of degree N . The polytope P can be called by a few different names such as a knapsack polytope and N -dimensional simplex.

The Ehrhart function over this polytope also has a few names and computing it as a close formula or evaluating it for specific t is relevant in several other areas of mathematics. For example, in combinatorial number theory, this function is known as Sylvester's *denumerant*. In the combinatorics literature the denumerant has been studied extensively (see e.g., [3, 22, 45, 115, 137]). The denumerant plays an important role in integer optimization too [93, 122], where the problem is called an *equality-constrained knapsack*. In combinatorial number theory and the theory of partitions, the problem appears in relation to the *Frobenius problem* or the *coin-change problem* of finding the largest value of t with $E(\alpha; t) = 0$ (see [66, 91, 136] for details and algorithms). Authors in the theory of numerical semigroups have also investigated the so called *gaps* or *holes* of the function (see [84] and references therein), which are values of t for which $E(\alpha; t) = 0$, i.e., those positive integers t which cannot be represented by the α_i . For $N = 1$ the number of gaps is $(\alpha_1 - 1)(\alpha_2 - 1)/2$ but for larger N the problem is quite difficult.

Unfortunately, computing $E(\alpha; t)$ or evaluating it are very challenging computational problems. Even deciding whether $E(\alpha; t) > 0$ for a given t , is a well-known (weakly) NP-hard problem. Computing $E(\alpha; t)$ for a given t , is $\#P$ -hard. Computing the Frobenius number is also known to be NP-hard [136]. Despite this, when the dimension N is fixed (the number of variables is fixed), the Frobenius number can be computed in polynomial time [21, 91]. Also, when $N + 1$ is fixed,

the entire quasi-polynomial $E(\alpha; t)$ can be computed in polynomial time as a special case of a well-known result of Barvinok [17]. There are several papers exploring the practical computation of the Frobenius numbers (see e.g., [66] and the many references therein).

One main result in Chapter 4 is a polynomial time algorithm for approximating the Ehrhart polynomial by computing the highest-degree $k + 1$ terms of the Ehrhart quasi-polynomial. Unlike methods for computing the entire polynomial $E(\alpha; t)$ in polynomial time, our method allows the dimension to vary; however, we fix k to obtain a polynomial time algorithm. The algorithm takes advantage of three key things: the simple structure of the knapsack polytope, a geometric reinterpretation of some rational generating functions in terms of lattice points in polyhedral cones, and Barvinok's [17] fast decomposition of a polyhedral cone into unimodular cones.

Chapter 4 is also closely related to some other works. In [14], the authors presented a polynomial-time algorithm to compute the first $k + 1$ coefficients of $L(P, t)$ for any *simple polytope* (a d -dimensional polytope where each vertex is adjacent to exactly d edges) given by its rational vertices. In [18], the entire quasi-polynomial over a simplex is computed for a fixed periodicity value. These two papers use the geometry of the problem very strongly, while the methods of Chapter 4 are based the number-theoretic structure of the knapsack.

1.5. MILP Heuristics

A mixed integer linear program (MILP) is a problem in the form

$$\begin{aligned} \min \quad & c^T x \\ \text{such that} \quad & Ax \leq b \\ & x_i \in \mathbb{Z} \text{ for } i \in I \end{aligned}$$

where $c \in \mathbb{R}^d$, $A \in \mathbb{R}^{m \times d}$, $b \in \mathbb{R}^m$, and I is an index set for the integer variables. The problem is to find values for the d variables x_i that satisfy the linear constraints $Ax \leq b$ and the integer constraints $x_i \in \mathbb{Z}$ for $i \in I$ while minimizing the objective function $c^T x$. The A , b , and c are given as constants and x is the only vector of variables. If $I = \emptyset$, meaning that the problem contains no integer variables, this problem reduces to a linear program. Linear programs are some of the best

understood mathematical objects in optimization, and there exist a large collection of commercial-grade software to solve these problems. Furthermore, linear programs can be solved in polynomial time.

Once some of the variables in a linear program are forced to be integer, the optimization problem becomes a mixed integer problem. MILP have extremely useful modeling power and have been successfully used to solve problems in mining and refinery, air transport, telecommunications, finance, water supply management, chip design and verification, network design—basically all scheduling and planning problems, see for instance [81].

The success of solving MILP problems despite being NP-Hard [142] can be attributed to tricks and techniques that transform the MILP problem into smaller linear programming problems. The common tools include pre-solvers, branch-and-bound, cutting planes, and heuristics [70, 80]. A MILP heuristic is any algorithm that attempts to find a MILP solution, or somehow speeds the process up. A heuristic does not have to have any mathematical logic to why it is a good idea. For example, one simple heuristic for solving MILP problems is to compute the linear programming relaxation. Let x^* be a solution to

$$\begin{aligned} \min \quad & c^T x \\ \text{such that} \quad & Ax \leq b \\ & x_i \in \mathbb{R} \text{ for every } i. \end{aligned}$$

Some of the integer variables $x_i \in I$ might have non-integer-valued solutions in the relaxation. A candidate feasible solution can be obtained by rounding the fractional values to integer values: $\lfloor x_i^* \rfloor$ for $i \in I$. The rounded linear relaxation solution may or may not satisfy $Ax \leq b$. If it does, then this rounding heuristic just produced a feasible point to the MILP problem.

Heuristics themselves come in many types and can appear in every stage of the solving process. There are heuristics for finding an initial feasible point, producing better feasible points, and for directing the search of the optimizer. See [29] for a nice short summary of the different classes of MILP heuristics. Chapter 5 develops a special heuristic for problems with *set partitioning constraints*.

1.6. Using computational geometry in neuro-immune communication

Chapter 6 is based on a collaboration between the author and researchers at the University of California, Davis, School of Veterinary Medicine. The focus is on using tools from data science, image processing, and computational geometry to help identify diseases in the spleen. In this section, we give the medical background of the project.

Imagine a scenario where someone is sick and they visit the doctor. Instead of getting a pill to take, they are connected to a machine that sends electrical current to their body. The electricity is targeted to specific organs or parts of the nervous or lymphatic systems connected to their immune system. Under the electric current, their body's immune system is improved, and the disease is cured! Imagine a world where we can regulate neural impulses to repair the body. Such techniques could be used, for example, to treat diabetes by restoring insulin producing cells. Weight loss could be achieved by regulating food intake by making the body think it is full or by removing cravings for junk food. Imagine treating diseases ranging from hypertension to pulmonary diseases with electricity.

This is not electroshock therapy or something out of Frankenstein, but an area of medical research called electroceuticals [68]. The body's neurons make a great system for delivering medical treatment. First, almost all organs and biological functions are regulated through circuits of neurons which function through electrical charges. In addition, the neural network is discrete; it is composed of nerve bundles and fiber tracts which interconnect individual cells. Hence an electrical current could be precisely applied to an area of the body.

Some electroceuticals have already been developed. Pacemakers and defibrillators already use the body's nervous system to save lives. Sacral-nerve stimulation can restore bladder control in people with paraplegia, and vagus-nerve stimulation can be applied to epilepsy and rheumatoid arthritis. What separates these technologies from future techniques is that they do not target specific areas of the nervous system. It is easy to send a signal to 100,000 nerve fibers, but not to just one. Electroceuticals of the future could be applied on precise areas for targeted results.

Many advances must be made before the full power of electroceuticals can be used. For instance, we must be able to map the body's network of nerve cells, we must know how to excite only a few nerve fibers at a time, and we must understand how the frequency of the electrical current should

change over the course of treatment. For much more detailed description of what electroceuticals can cure and what are the problems we must first solve, see [68, 124, 131].

1.6.1. Spleen. In the spleen and other secondary lymph organs, it has been suggested that $CD4^+ChAT^+$ T-cells (henceforth referred to as just T-cells) directly synapse with neurons; however, there is little data to support or refute this idea [69, 149]. My collaborators in the School of Veterinary Medicine at the University of California, Davis have started addressing this knowledge gap by defining the mechanisms of communication and rigorously mapping the nature of the interaction between T-cells, neurons, and target effector cells in mice during various stages of intestinal inflammation. The functional ramifications of how T-cells and nerve cells interact are vast. A synaptic model could imply that T-cells communicate with neurons, forming intimate associations with these cells, ceasing their surveying of the spleen. In addition, this tight association would suggest that unless released from such synapses, T-cells would have limited mobility and would exert a highly localized regulatory effect. This lymphocyte-neuron synapse notion has led to the hypothesis that immune cells can be innervated and controlled by specific neurons to reduce morbidity in patients suffering from immunopathologies, including inflammatory bowel disease [7, 68]. On the other hand, it could be that the T-cells do not form tight bonds with neurons and are always free to move. This is called the *diffusion model*, and its implications mean the nervous system cannot be easily used to program their function or activation.

My collaborators at the UC Davis School of Veterinary Medicine, Colin Reardon and Ingrid Brust-Mascher, have used an advanced imaging technique [42, 43] to generate detailed mappings of neuro-immune interfaces with subcellular resolution. They have the capability to image the entire lymph node or spleen volume. Mapping these interactions and defining how neural stimulation influences a response from lymphocytes in mice is vital in understanding how cellular communication occurs in mice, and eventually humans. The T-cells form a critical component of the inflammatory reflex by significantly inhibiting morbidity and mortality in septic shock. These cells were proposed to interface directly with sympathetic neurons, and were shown to be in close proximity to these neurons in the spleen. It has been suggested that a complete neuro-immune circuit not only requires input from neurons [138], but that this communication occurs in a classical synapse [69, 149]. A dissenting view has emerged in neurobiology showing that a classical synapse is not

always required for neural signaling [4, 126, 128, 141, 150]. Despite these high profile studies demonstrating neural regulation of innate immune function, a functional circuit tracing in the spleen with and without inflammation has not been performed.

Preliminary data suggests that most T-cells are not in intimate contact with sympathetic neurons. Although we observed T-cells within $5\mu\text{m}$ of sympathetic neurons, the majority of these cells do not appear to be intimately associated, as would be required in a synapse. Our data set also demonstrates the advantage of 3D image reconstruction to assess localization. While T-cells and fibers appear to be co-localized in some orientations, rotation along the axis of the neuron reveals no intimate association. Our data does not directly refute the possibility of synaptic transmission, but it suggests that most T-cells communicate with sympathetic neurons through another mechanism.

However, we still want to study how strongly the T-cells and neurons connect. It may be true that most T-cells are not located near the sympathetic neurons, and hence do not form synaptic connections to them, but there are still clusters of T-cells that seem to connect to the neurons. It might be the case that the distribution of where the T-cells are located changes as the spleen responds to intestinal inflammation. For example, maybe T-cells are more likely to form synaptic bonds with the neurons during inflammation, and then diffuse when the inflammation is over. The advanced imaging techniques allow us to see how the physical relationships between the cells changes as the spleen responds to the inflammation. Images showing the location of T-cells and neurons do not show a clear distinction between healthy and sick spleens. This can be due to a few factors: our data sets are large and hard to visualize, imaging is not perfect and so our data contains noise, and it is possible that there is little relationship between T-cell location and spleen inflammation. Just because it is hard to visualize how the location of T-cells and neurons change with inflammation does not mean we cannot detect a difference. This is where the project leaves the sphere of biology and enters the world of data science.

1.6.2. The data science question. My collaborators have mapped the location of T-cells and nerve cells in the spleen, forming two sets of points in \mathbb{R}^3 . The two main questions now are:

- (1) How does the distance between these two sets of points change during inflammation?
- (2) Can we use the distribution of these point sets to predict inflammation?

Our approach is to compute the distance from each T-cell to a nervous cell. Looking at the distribution of these distance values should reveal if T-cells are closer to nervous cells or not. Hence the problem is to perform a classical supervised clustering analysis on the distance distributions across different spleen samples. How we did this is one of the main topics in Chapter 6.

Before we can compute the distance distributions, the T-cells and nerve cells must first be identified. As it turns out, this is a hard problem. While it is true that we have sophisticated imaging tools and software, our data is still extremely noisy. To accurately extract the location of these cells, we use the software tool Imaris [30]. Despite being the best tool for the job, it cannot process the entire spleen at once without identifying T-cells and nerve cells at locations that are physically impossible! Instead, the spleen data must be divided into many small regions, and correct parameters to Imaris functions must be picked for each region. The result is that it is an extremely labor- and time-intensive process to clean up the image data in Imaris. Hence a major problem is how to automate some of the data cleaning within Imaris. This problem leads us into using topics in distance geometry for data cleaning. Chapter 6 also explores some of the tools we used and developed to significantly reduce this project's time to completion.

CHAPTER 2

Integration

The theory of integrating a polynomial over a polytope by using continuous generating functions has been developed over a series of papers [13, 55, 53]. These papers develop different generating functions and algorithms depending on the form the integrand takes. All the methods are based on the continuous generating function for $\int_P e^{\langle x, \ell \rangle} dx$ (see Section 1.2 for an introduction). In this section, we seek to organize the results by the integrand type.

For this chapter, P will be a d -dimensional rational polytope given by an inequality description $Ax \leq b$ where $A \in \mathbb{Q}^{n \times d}$ and $b \in \mathbb{Q}^n$. Let $f(x) \in \mathbb{Q}[x_1, \dots, x_d]$ be a polynomial. Our goal is to compute $\int_P f(x) dx$. In [13], the focus is on the case when the polytope P is a simplex and the integrand is a power of a linear form (e.g., $(x_1 + 2x_2 - x_3)^5$), or a product of linear forms (e.g., $(x_1 + 2x_2)^2(3x_1 + x_3)^4$). Then in [55], the case when P is an arbitrary full-dimensional polytope and the integrand is a power of a linear form is developed. Most recently in [53], integration of products of affine functions (e.g., $(x_1 + 2x_2 + 3)^2(3x_1 + x_3 - 1)^4$) was developed. The difference between products of linear forms and products of affine functions is that the latter is allowed to have constant terms in the factors.

Section 2.1 covers the discussion on integrating a polynomial $f(x)$ by decomposing it into a sum of powers of linear forms. This section contains highlights from [55], except Section 2.1.2 which contains results from [13].

Section 2.2 covers integrating a product of affine functions. It is a partial summary of [53], except Section 2.2.2 which contains slightly generalized results from [13].

The integration methods we focus on will depend on decomposing the polyhedral domain P in two different ways: triangulating P or triangulating the tangent cones of P . This chapter describes the integration algorithms on both domain types.

Polyhedral triangulation plays a role in every method we develop for integration. For general background in triangulations, see [62, 112, 132, 135] and the software packages [1, 72, 76, 134, 139].

2.1. Integrand: powers of linear forms

In this section, we focus on computing $\int_P f(x) dx$ by decomposing $f(x)$ into a sum of power of linear forms:

$$f(x) = \sum_{\ell} c_{\ell} \langle x, \ell \rangle^{m_{\ell}}$$

where $\ell \in \mathbb{Q}^d$, $c_{\ell} \in \mathbb{Q}$ and $m_{\ell} \in \mathbb{N}$.

This has been done in [55] by using the following formula on each monomial of h . If $x^m = x_1^{m_1} x_2^{m_2} \cdots x_d^{m_d}$, then

$$(2.1) \quad x^m = \frac{1}{|m|!} \sum_{0 \leq p_i \leq m_i} (-1)^{|m| - (p_1 + \cdots + p_d)} \binom{m_1}{p_1} \cdots \binom{m_d}{p_d} (p_1 x_1 + \cdots + p_d x_d)^{|m|},$$

where $|m| = m_1 + \cdots + m_d$. Using this formula on a degree D polynomial in fixed dimension d results in at most $O(D^{2d})$ linear forms.

It is worth noting that Equation (2.1) does *not* yield an optimal decomposition. The problem of finding a decomposition with the smallest possible number of summands is known as the *polynomial Waring problem* [6, 31, 39]. A key benefit of Equation (2.1) is that it is explicit, is computable over \mathbb{Q} , and is sufficient for generating a polynomial-time algorithm on when the dimension is fixed [13]. However, Equation (2.1) has a major problem: it can produce many terms. For example, a monomial in 10 variables and total degree 40 can have more than 4 million terms. See Table 2.1. Nevertheless, in the next two sections we will develop polynomial time algorithms for integrating a power of a linear form over a polytope.

2.1.1. Domain: cone decomposition. We now consider powers of linear forms instead of exponentials. Similar to $I(P, \ell)$ in Section 1.2, we now let $L^M(P, \ell)$ be the meromorphic extension

2.1. INTEGRAND: POWERS OF LINEAR FORMS

TABLE 2.1. Average number of powers of linear forms plus or minus one standard deviation necessary to express one monomial in d variables, averaged over 50 monomials of the same degree

d	Monomial Degree					
	5	10	20	30	40	50
3	14 ± 3	$(6.6 \pm 1.2) \cdot 10^1$	$(4.0 \pm 0.5) \cdot 10^2$	$(1.2 \pm 0.1) \cdot 10^3$	$(2.7 \pm 0.2) \cdot 10^3$	$(5.2 \pm 0.2) \cdot 10^3$
4	16 ± 5	$(1.1 \pm 0.2) \cdot 10^2$	$(1.1 \pm 0.2) \cdot 10^3$	$(4.5 \pm 0.6) \cdot 10^3$	$(1.3 \pm 0.2) \cdot 10^4$	$(3.0 \pm 0.2) \cdot 10^4$
5	19 ± 4	$(1.5 \pm 0.4) \cdot 10^2$	$(2.2 \pm 0.6) \cdot 10^3$	$(1.2 \pm 0.3) \cdot 10^4$	$(4.7 \pm 0.7) \cdot 10^4$	$(1.4 \pm 0.2) \cdot 10^5$
6	20 ± 5	$(2.0 \pm 0.6) \cdot 10^2$	$(4.1 \pm 1.2) \cdot 10^3$	$(3.2 \pm 0.8) \cdot 10^4$	$(1.5 \pm 0.3) \cdot 10^5$	$(5.2 \pm 0.6) \cdot 10^5$
7	21 ± 5	$(2.4 \pm 0.9) \cdot 10^2$	$(6.7 \pm 2.4) \cdot 10^3$	$(7.1 \pm 2.1) \cdot 10^4$	$(4.0 \pm 1.0) \cdot 10^5$	$(1.7 \pm 0.3) \cdot 10^6$
8	21 ± 5	$(2.9 \pm 0.9) \cdot 10^2$	$(1.1 \pm 0.5) \cdot 10^4$	$(1.4 \pm 0.5) \cdot 10^5$	$(9.8 \pm 2.7) \cdot 10^5$	$(4.8 \pm 1.1) \cdot 10^6$
10	24 ± 5	$(3.5 \pm 1.1) \cdot 10^2$	$(2.1 \pm 0.9) \cdot 10^4$	$(4.1 \pm 1.6) \cdot 10^5$	$(4.5 \pm 1.7) \cdot 10^6$	$(3.1 \pm 1.0) \cdot 10^7$

of the function defined by

$$L^M(P, \ell) = \int_P \langle \ell, x \rangle^M dx$$

for those ℓ such that the integral exists. To transfer what we know about integrals of exponentials to those of powers of linear forms, we can consider the formula of Proposition 1.2.12 as a function of the auxiliary parameter t :

$$(2.2) \quad \int_{s+C} e^{\langle t\ell, x \rangle} dx = \text{vol}(\Pi_C) e^{\langle t\ell, s \rangle} \prod_{i=1}^d \frac{1}{\langle -t\ell, u_i \rangle}.$$

Using the series expansion of the left in the variable t , we wish to recover the value of the integral of $\langle \ell, x \rangle^M$ over the cone (by value, we mean a real number or a meromorphic function as explained in Section 1.2). This is the coefficient of t^M in the expansion; to compute it, we equate it to the Laurent series expansion around $t = 0$ of the right-hand-side expression, which is a meromorphic function of t . Clearly

$$\text{vol}(\Pi_C) e^{\langle t\ell, s \rangle} \prod_{i=1}^d \frac{1}{\langle -t\ell, u_i \rangle} = \sum_{n=0}^{\infty} t^{n-d} \frac{\langle \ell, s \rangle^n}{n!} \cdot \text{vol}(\Pi_C) \prod_{i=1}^d \frac{1}{\langle -\ell, u_i \rangle}.$$

COROLLARY 2.1.1. *For a linear form ℓ and a simplicial cone C generated by rays u_1, u_2, \dots, u_d with vertex s and $\langle \ell, u_i \rangle \neq 0$,*

$$(2.3) \quad L^M(s + C, \ell) = \frac{M!}{(M+d)!} \text{vol}(\Pi_C) \frac{(\langle \ell, s \rangle)^{M+d}}{\prod_{i=1}^d \langle -\ell, u_i \rangle}.$$

COROLLARY 2.1.2. *For any triangulation \mathcal{D}_s of the tangent cone C_s at each of the vertices s of the polytope P we have*

$$(2.4) \quad L^M(P, \ell) = \sum_{s \in V(P)} \sum_{C \in \mathcal{D}_s} L^M(s + C)(\ell).$$

Notice that when P is a polytope, $L^M(P, \ell)$ is holomorphic in ℓ , while each summand in the last corollary is meromorphic in ℓ . Hence the singularities in $L^M(s + C, \ell)$ cancel out in the sum.

We say that ℓ is *regular* if $\langle \ell, u_i \rangle \neq 0$ for every ray u_i of a cone C . So if ℓ is not orthogonal to any ray of every simplicial cone in \mathcal{D}_s , then Corollary 2.1.2 gives an explicit formula for evaluating the exact value of $\int_P \langle \ell, x \rangle^M dx$. We will also say that ℓ is *regular on P* , if it is regular for every tangent cone of P , which implies it is regular on every cone $C \in \mathcal{D}_s$ at each vertex $s \in V(P)$.

Otherwise when ℓ is not regular, there is a nearby perturbation which is regular. To obtain it, we use $\ell + \hat{\epsilon}$ where $\hat{\epsilon} = \epsilon a$ is any linear form with $a \in \mathbb{R}^n$ such that $\langle -\ell - \hat{\epsilon}, u_i \rangle \neq 0$ for all u_i . Notice that $L^M(P, \ell + \hat{\epsilon})$ is holomorphic in $\hat{\epsilon}$ when P is a polytope, but for some cones C , $L^M(s + C, \ell + \hat{\epsilon})$ is meromorphic in ϵ ; hence, the singularities cancel out in the sum in Corollary (2.1.2), so taking the limit as ϵ goes to zero is possible. This means when ℓ is not regular, we can just collect the coefficient of ϵ^0 in the series expansion of $L^M(s + C, \ell + \hat{\epsilon})$ and compute $L^M(s + C, \ell)$ as

$$(2.5) \quad \frac{M!}{(M + d)!} \text{vol}(\Pi_C) \text{Res}_{\epsilon=0} \frac{(\langle \ell + \hat{\epsilon}, s \rangle)^{M+d}}{\epsilon \prod_{i=1}^d \langle -\ell - \hat{\epsilon}, u_i \rangle}.$$

We use the residue operator Res as a shorthand to mean to the coefficient of ϵ^0 in the series expansion of

$$\frac{(\langle \ell + \hat{\epsilon}, s \rangle)^{M+d}}{\prod_{i=1}^d \langle -\ell - \hat{\epsilon}, u_i \rangle}.$$

about $\epsilon = 0$.

Next we recall some useful facts on complex analysis (see, e.g., [85] for details). As we observed, there is a pole at $\epsilon = 0$ for our univariate rational function given in Formula (2.5) of Corollary 2.1.1. Recall that if a univariate rational function $f(\epsilon) = p(\epsilon)/q(\epsilon)$ has Laurent series expansion $f(\epsilon) = \sum_{k=-m}^{\infty} a_k \epsilon^k$, the residue is defined as a_{-1} . Given a rational function $f(\epsilon)$ with a pole at $\epsilon = 0$ there are a variety of well-known techniques to extract the value of the residue. For example, if $\epsilon = 0$ is a simple pole ($m = 1$), then $\text{Res}_{\epsilon=0}(f) = \frac{p(0)}{q'(0)}$. Otherwise, when $\epsilon = 0$ is a

pole of order $m > 1$, we can write $f(\epsilon) = \frac{p(\epsilon)}{\epsilon^m q_1(\epsilon)}$. Then expand p, q_1 in powers of ϵ with $p(\epsilon) = a_0 + a_1\epsilon + a_2\epsilon^2 + \dots$ and $q_1(\epsilon) = b_0 + b_1\epsilon + b_2\epsilon^2 + \dots$. This way the Taylor expansion of $p(\epsilon)/q_1(\epsilon)$ at ϵ_0 is $c_0 + c_1\epsilon + c_2\epsilon^2 + c_3\epsilon^3 + \dots$, where $c_0 = \frac{a_0}{b_0}$, and $c_k = \frac{1}{b_0}(a_k - b_1c_{k-1} - b_2c_{k-2} - \dots - b_kc_0)$. Thus we recover the residue $\text{Res}_{\epsilon=0}(f) = c_{m-1}$. We must stress that the special structure of the rational functions in Corollary 2.1.1 can be exploited to speed up computation further rather than using this general methodology. Summarizing the above discussion results in the next theorem.

THEOREM 2.1.3. *Let P be a full dimensional polytope with vertex set $V(P)$, and C_s be the cone of feasible directions at vertex s . Let \mathcal{D}_s be a triangulation of C_s . Then*

- (1) *if ℓ is regular, meaning for every vertex s of P and every ray u in \mathcal{D}_s we have $\langle \ell, u \rangle \neq 0$, then*

$$\int_P \langle \ell, x \rangle^M dx = \sum_{s \in V(P)} \sum_{C \in \mathcal{D}_s} \frac{M!}{(M+d)!} \text{vol}(\Pi_C) \frac{(\langle \ell, s \rangle)^{M+d}}{\prod_{i=1}^d \langle -\ell, u_i \rangle},$$

- (2) *otherwise, pick an $a \in \mathbb{R}^d$ that is regular on P and then*

$$\int_P \langle \ell, x \rangle^M dx = \sum_{s \in V(P)} \sum_{C \in \mathcal{D}_s} \frac{M!}{(M+d)!} \text{vol}(\Pi_C) \text{Res}_{\epsilon=0} \frac{(\langle \ell + \epsilon \cdot a, s \rangle)^{M+d}}{\epsilon \prod_{i=1}^d \langle -\ell - \epsilon \cdot a, u_i \rangle}.$$

In both cases, when the dimension d is fixed, the integral can be computed in polynomial time in the usual binary encoding of P , ℓ , and unary encoding of M .

PROOF. The only thing left to show is the statement about the complexity. Because the dimension is fixed, there are polynomial many cones C_s and simplicial cones \mathcal{D}_s . Hence the only thing that has to be shown is that the residue can be computed in polynomial time. We will do this by multiplying truncated power series. For a fixed cone $C \in \mathcal{D}_s$ with rays $\{u_1, \dots, u_d\}$, let $I_1 := \{i \mid \langle \ell, u_i \rangle = 0\}$ and $I_2 := \{i \mid \langle \ell, u_i \rangle \neq 0\}$. Then

$$\text{Res}_{\epsilon=0} \frac{(\langle \ell + \epsilon \cdot a, s \rangle)^{M+d}}{\epsilon \prod_{i=1}^d \langle -\ell - \epsilon \cdot a, u_i \rangle} = \frac{(\langle \ell + \epsilon \cdot a, s \rangle)^{M+d}}{\epsilon} \cdot \frac{1}{\prod_{i \in I_1} -\epsilon \langle a, u_i \rangle} \cdot \frac{1}{\prod_{i \in I_2} \langle -\ell, u_i \rangle + \epsilon \langle -a, u_i \rangle}$$

2.1. INTEGRAND: POWERS OF LINEAR FORMS

Let $h_i(\epsilon)$ be the series expansion of $\frac{1}{\langle -\ell, u_i \rangle + \epsilon \langle -a, u_i \rangle}$ about $\epsilon = 0$ up to degree $|I_1|$ for each $i \in I_2$, which can be done via the generalized binomial theorem:

$$h_i(\epsilon) := \sum_{j=0}^{|I_1|} (-1)^j (\epsilon \langle -a, u_i \rangle)^j (\langle -\ell, u_i \rangle)^{-1-j}.$$

Let $h_0(\epsilon)$ be the expansion of $(\langle \ell + \epsilon \cdot a, s \rangle)^{M+d}$. Let $H := h_0(\epsilon) \cdot \prod_{i \in I_2} h_i(\epsilon)$ be the resulting polynomial product in ϵ truncated at degree $|I_1|$. This can be done in polynomial time by Lemma 1.2.17. Then the desired residue is simply the coefficient of $\epsilon^{|I_1|}$ in H times the coefficient $\prod_{i \in I_1} \frac{1}{-\langle a, u_i \rangle}$. \square

Algorithm 3 explicitly states the polynomial time algorithm for integrating a polynomial over a polytope by decomposing the polynomial into powers of linear forms, and by decomposing the polytope into simplicial cones. Each main step—decomposing a polynomial into a sum of powers of linear forms, decomposing P into simple cones, and computing the integral over each cone—is done in polynomial time when d is fixed.

2.1.2. Domain: a full dimensional simplex. Suppose now that $\Delta \subset \mathbb{R}^d$ is a d -dimensional simplex with vertices s_1, s_2, \dots, s_{d+1} and $\ell \in \mathbb{R}^d$. We say that ℓ is *regular* for the simplex Δ if it is not orthogonal to any of the edges of the simplex, meaning $\langle \ell, s_i - s_j \rangle \neq 0$ for every $i \neq j$.

THEOREM 2.1.4 (Corollary 12 and 13 in [13]). *Let $\Delta \subset \mathbb{R}^d$ be a d -simplex with vertices s_1, \dots, s_{d+1} , and let $\ell \in \mathbb{R}^d$.*

(1) *If ℓ is regular on Δ , i.e., $\langle \ell, s_i \rangle \neq \langle \ell, s_j \rangle$ for any pair $i \neq j$, then we have the following relation.*

$$L^M(\Delta, \ell) = \int_{\Delta} \langle \ell, x \rangle^M dx = d! \text{vol}(\Delta, dm) \frac{M!}{(M+d)!} \left(\sum_{i=1}^{d+1} \frac{\langle \ell, s_i \rangle^{M+d}}{\prod_{j \neq i} \langle \ell, s_i - s_j \rangle} \right).$$

(2) *If ℓ is not regular on Δ , let $K \subseteq \{1, \dots, d+1\}$ be an index set of the different poles $\langle \ell, s_k \rangle$, and for $k \in K$ let m_k denote the order of the pole, i.e.,*

$$m_k = \#\{i \in \{1, \dots, d+1\} : \langle \ell, s_i \rangle = \langle \ell, s_k \rangle\}.$$

Algorithm 3 Integrate by decomposing a polynomial into a sum of powers of linear forms and by triangulating a polytope's tangent cones

Input: $f(x) \in \mathbb{Q}[x_1, \dots, x_d]$, d -dimensional polytope $P \subset \mathbb{R}^d$

Output: $\int_P f(x) dx$

Use Equation (2.1) to decompose each monomial in f into a sum of powers of linear forms.

Let F be the resulting collection of linear forms.

Let $T = \emptyset$

for all $s \in V(P)$ **do**

Let \mathcal{D}_s be a triangulation of C_s

for all $C \in \mathcal{D}_s$ **do**

$T \leftarrow T \cup \{s + C\}$

end for

end for

Pick $a \in \mathbb{R}^d$ so that for each $s + C \in T$, $\langle a, u_i \rangle \neq 0$, where the u_i are the rays of cone C

sum $\leftarrow 0$

for all linear forms $c\langle \ell, x \rangle^M$ in F **do**

for all $s + C \in T$ **do**

if ℓ is regular on C **then**

sum \leftarrow sum $+ c \cdot L^M(s + C, \ell)$, computed using Corollary 2.1.1

else

sum \leftarrow sum $+ c \cdot L^M(s + C, \ell)$, by computing a residue as outlined in Theorem 2.1.3

end if

end for

end for

return sum

Then we have the following relation.

$$\int_{\Delta} \langle \ell, x \rangle^M dx = d! \text{vol}(\Delta, dm) \frac{M!}{(M+d)!} \sum_{k \in K} \text{Res}_{\epsilon=0} \frac{(\epsilon + \langle \ell, s_k \rangle)^{M+d}}{\epsilon^{m_k} \prod_{\substack{i \in K \\ i \neq k}} (\epsilon + \langle \ell, s_k - s_i \rangle)^{m_i}}.$$

These evaluations of $L^M(\Delta, \ell)$ allows us to show that integrating a power of a linear form over a simplex can be done efficiently. The next theorem is a simplified statement of Theorem 2 in [13] and the alternative proof immediately gives itself to an algorithmic implementation.

THEOREM 2.1.5. *Fix the dimension d . Then there is a polynomial time algorithm for computing $L^M(\Delta, \ell)$ when both Δ and ℓ are encoded in binary and $M \in \mathbb{N}$ is encoded in unary.*

PROOF. When ℓ is regular on Δ , Theorem 2.1.4 makes this clear.

When ℓ is not regular, at most $|K| < d$ residues must be computed. Each residue can be computed by multiplying univariate polynomials and truncating. For $k \in K$, the coefficient of ϵ^{m_k-1} needs to be computed in the series expansion of

$$\frac{(\epsilon + \langle \ell, s_k \rangle)^{M+d}}{\prod_{\substack{i \in K \\ i \neq k}} (\epsilon + \langle \ell, s_k - s_i \rangle)^{m_i}} \text{ for each } k \in K.$$

This can be done in polynomial time by applying Lemma 1.2.17. For a fixed k , let $h_i(\epsilon)$ be the series expansion of $1/(\epsilon + \langle \ell, s_k - s_i \rangle)^{m_i}$ about $\epsilon = 0$ up to degree $m_k - 1$ in ϵ for each $i \in K$ and $i \neq k$. This can be done using the generalized binomial theorem. Also let $h_0(\epsilon)$ be the polynomial expansion of $(\epsilon + \langle \ell, s_k \rangle)^{M+d}$. The product

$$h_0(\epsilon) \prod_{\substack{i \in K \\ i \neq k}} h_i(\epsilon)$$

truncated at degree $m_k - 1$ in ϵ can be computed in polynomial time using Lemma 1.2.17. The residue is then the coefficient of ϵ^{m_k-1} in the truncated product. \square

Algorithm 4 summarizes how to integrate a polynomial via decomposing it into a sum of powers of linear forms and by using integration formulas for simplices. Notice that the algorithm runs in polynomial time when the dimension is fixed. This is because for a polynomial of degree D , Equation (2.1) produces at most $\binom{D+d}{d} \binom{D+d}{d} = O(D^{2d})$ linear forms, and each linear form can be integrated in polynomial time in D . Also, the number of simplices in a triangulation of a polytope is polynomial in fixed dimension.

2.1.3. Examples. Before continuing, let's highlight the power of encoding integral values by rational function identities. For regular linear forms the integration formulas are given by sums of rational functions which we read from the geometry at vertices and possibly a cone decomposition method. Consider a pentagon P with vertices $(0, 0)$, $(2, 0)$, $(0, 2)$, $(3, 1)$, and $(1, 3)$ as in Figure 2.1.

Then the rational function giving the value of $\int_P (c_1 x + c_2 y)^M dx dy$ by using the cone decomposition method is

$$\frac{M!}{(M+2)!} \left(\frac{(2c_1)^{M+2}}{c_1(-c_1-c_2)} + 4 \frac{(3c_1+c_2)^{M+2}}{(c_1+c_2)(2c_1-2c_2)} + 4 \frac{(c_1+3c_2)^{M+2}}{(c_1+c_2)(-2c_1+2c_2)} + \frac{(2c_2)^{M+2}}{(-c_1-c_2)c_2} \right).$$

2.1. INTEGRAND: POWERS OF LINEAR FORMS

Algorithm 4 Integrate by decomposing a polynomial into a sum of powers of linear forms and by triangulating a polytope

Input: $f(x) \in \mathbb{Q}[x_1, \dots, x_d]$, d -dimensional polytope $P \subset \mathbb{R}^d$

Output: $\int_P f(x) dx$

Use Equation (2.1) to decompose each monomial in f into a sum of powers of linear forms.

Let F be the resulting collection of linear forms.

Let T be a list of simplices in a triangulation of P

sum = 0

for all simplices Δ in T **do**

for all linear forms $c\langle \ell, x \rangle^M$ in F **do**

$\alpha \leftarrow c \cdot \int_{\Delta} \langle \ell, x \rangle^M dx$, computed by using the method outlined in Theorem 2.1.5

 sum \leftarrow sum + α

end for

end for

return sum

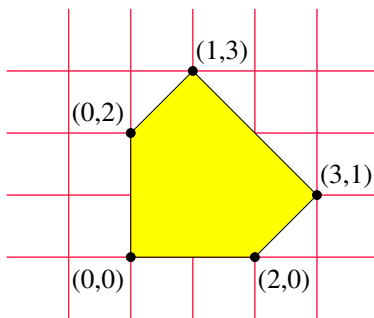


FIGURE 2.1. A pentagon

This rational function expression encodes *every integral* of the form $\int_P (c_1 x + c_2 y)^M dx dy$. For example, if we let $M = 0$, then the integral is equal to the area of the pentagon, and the rational function simplifies to a number by simple high-school algebra:

$$\frac{1}{2} \left(4 \frac{c_1}{-c_1 - c_2} + 4 \frac{(3c_1 + c_2)^2}{(c_1 + c_2)(2c_1 - 2c_2)} + 4 \frac{(c_1 + 3c_2)^2}{(c_1 + c_2)(-2c_1 + 2c_2)} + 4 \frac{c_2}{-c_1 - c_2} \right) = 6.$$

Hence the area is 6. When M and (c_1, c_2) are given and (c_1, c_2) is not perpendicular to any of the edge directions we can simply plug in numbers to the rational function. For instance, when $M = 100$ and $(c_1 = 3, c_2 = 5)$ the answer is a fraction with numerator equal to

227276369386899663893588867403220233833167842959382265474194585

3115019517044815807828554973991981183769557979672803164125396992

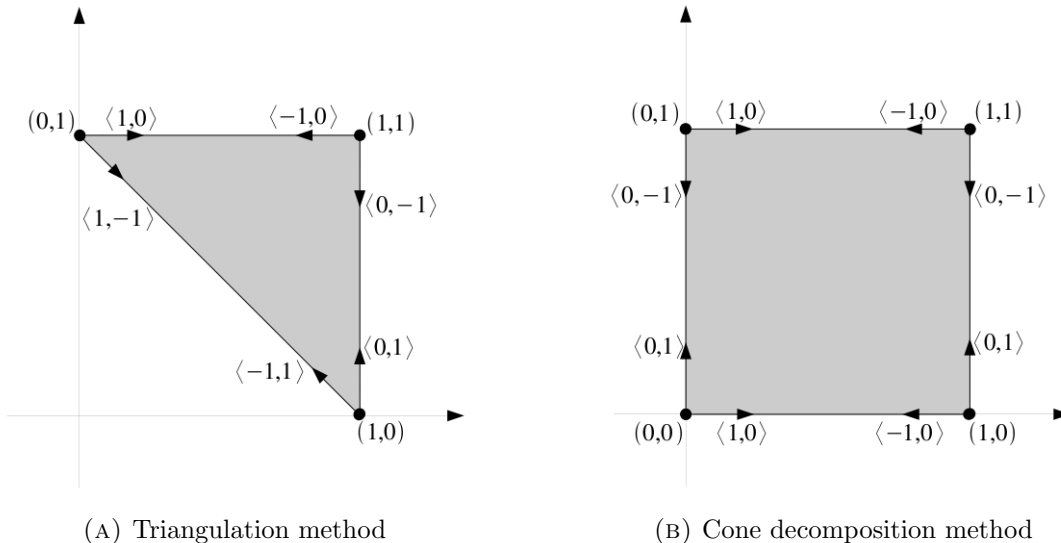


FIGURE 2.2. Example polytopes

and denominator equal to 1717. When (c_1, c_2) is perpendicular to an edge direction, we encounter (removable) singularities in the rational functions, thus using complex residues we can do the evaluation. Note that those linear forms that are perpendicular to some edge direction form a measure zero set inside a hyperplane arrangement.

Now we give an example of each method.

2.1.3.1. *Using the triangulation method.* Take the problem of integrating the polynomial $x + y$ over the triangle Δ with vertices $s_1 = (1, 1)$, $s_2 = (0, 1)$, and $s_3 = (1, 0)$ in Figure 2.2a.

The polynomial is already a power of a linear form, and the polytope is a simplex. Because $\ell = (1, 1)$ is not regular (it is perpendicular to the edge spanned by s_2 and s_3), we have to build the index set K . Note $\langle \ell, s_1 \rangle = 2$, $\langle \ell, s_2 \rangle = 1$, and $\langle \ell, s_3 \rangle = 1$; pick $K = \{1, 2\}$ with $m_1 = 1, m_2 = 2$. We proceed below with this choice, but note that we have a choice in picking the indices and we could have instead $K = \{1, 3\}$. This would yield a different decomposition of the generating function. Note also that the decomposition of the power of a linear form is not necessarily unique either. We now need to compute two values:

Vertex s_1 : We are not dividing by zero, we can simply plug vectors into Corollary 2.1.1,

$$\frac{\langle \ell, s_1 \rangle^3}{\langle \ell, s_1 - s_2 \rangle^2} = 8.$$

Vertex s_2 : Here, we need to compute a residue.

$$\operatorname{Res}_{\epsilon=0} \frac{(\epsilon + \langle \ell, s_2 \rangle)^{1+2}}{\epsilon^2(\epsilon + \langle \ell, s_2 - s_1 \rangle)} = \operatorname{Res}_{\epsilon=0} \frac{(\epsilon + 1)^{1+2}}{\epsilon^2(\epsilon - 1)} = -4.$$

Finally, $\int_{\Delta} (x + y) \, dx \, dy = 2! \times \frac{1}{2} \times \frac{1!}{3!}(8 - 4) = 2/3$.

2.1.3.2. *Using the cone decomposition method.* Next, integrate the polynomial x over the unit square in Figure 2.2b using the cone decomposition algorithm. Let $s_1 = (0, 1)$, $s_2 = (0, 0)$, $s_3 = (1, 0)$, and $s_4 = (1, 1)$. The polynomial is already a power of a linear form, so $\ell = (1, 0)$. The polytope has four vertices that we need to consider, and each tangent cone is already simplicial. The linear form ℓ is not regular at any vertex. We let the reader verify that the residue-based calculation gives the value zero for the integrals on the corresponding cones at vertex s_1 and s_2 . We only do in detail the calculation for vertex $s_3 = (1, 0)$. At this vertex, the rays are $u_1 = (0, 1)$, $u_2 = (-1, 0)$. Because $\langle \ell, u_1 \rangle = 0$, we need a perturbation vector $\hat{\epsilon}$ so that when $\ell := \ell + \hat{\epsilon}$, we do not divide by zero on any cone (we have to check this cone and the next one). Pick $\hat{\epsilon} = (\epsilon, \epsilon)$. Then the integral on this cone is

$$\frac{M!}{(M+d)!} \operatorname{vol}(\Pi_C) \operatorname{Res}_{\epsilon=0} \frac{(1+\epsilon)^{1+2}}{\epsilon(-\epsilon)(1+\epsilon)} = \frac{1!}{(1+2)!} \times 1 \times -2 = -2/6.$$

Vertex $s_4 = (1, 1)$: The rays are $u_1 = (-1, 0)$, $u_2 = (0, -1)$. Again, we divide by zero, so we perturb ℓ by the same $\hat{\epsilon}$. The integral on this cone is

$$\frac{M!}{(M+d)!} \operatorname{vol}(\Pi_C) \operatorname{Res}_{\epsilon=0} \frac{(1+2\epsilon)^{1+2}}{\epsilon(\epsilon)(1+\epsilon)} = \frac{1!}{(1+2)!} \times 1 \times 5 = 5/6.$$

The integral $\int_P x \, dx \, dy = 0 + 0 - 2/6 + 5/6 = 1/2$ as it should be.

2.1.4. How the software works: burst tries. We implemented the two algorithms for integrating a polynomial (via a decomposition into powers of linear forms) over a polytope in C++ as part of the software package `LattE integrale` [54]. Originally `LattE` was developed in 2001 as software to study lattice points of convex polytopes [61]. The algorithms used combinations of geometric and symbolic computation. Two key data structures are rational generating functions and cone decompositions, and it was the first ever implementation of Barvinok’s algorithm. `LattE` was improved in 2007 with various software and theoretical modifications, which increased speed

dramatically. This version was released under the name `LatTE macchiato`; see [97]. In 2011, `LatTE integrale` was released which included the computation of exact integrals of polynomial functions over convex polyhedra. The new integration functions are C++ implementations of the algorithms provided in [13] with additional technical improvements. A key distinction between `LatTE integrale` and other software tools is that the exact value of the integrals are computed since the implementation uses exact rational arithmetic. The code of this software is freely available at [54] under the GNU license.

As we see from the algorithmic descriptions above, one big step is performing manipulation of truncated power series. In this section, we discuss a data structure that improved our running time for multiplying polynomials. We focus here on how to store and multiply polynomials. For more on how we implemented the integration algorithms for powers of linear forms, see [55] and the user manual from the website [54].

Our initial implementation used a pair of linked lists for polynomials and sums of powers of linear forms. For polynomials, each node in the lists contained a monomial. The problem with this data structure was that it was too slow because it lacked any sort of ordering, meaning we had to traverse over every term in the list to find out if there was a duplicate. Hence when multiplying two polynomials, each resulting monomial in the product required a full list transversal in the inner for-loop of Algorithm 5. In [13], the integration over simplices was first implemented in `Maple`, and so there was no control over the data structures used to store the data.

Algorithm 5 Multiplying two polynomials

Input: $p_1, p_2 \in \mathbb{Q}[x_1, \dots, x_d]$

Output: $p_1 \cdot p_2$

$p \leftarrow 0$

for all monomials m_1 of p_1 **do**

for all monomials m_2 of p_2 **do**

 INSERT($p, m_1 \cdot m_2$)

end for

end for

return p

We then switched to using *burst tries*, a data structure designed to have *cache-efficient storage and search*, due to the fact that they are prefix trees with sorted arrays of stored elements as leaves [75]. Such a data structure is performance-critical when computing residues, as a comparison

with a linked-list implementation showed. In our implementation, each node corresponds to a particular dimension or variable and contains the maximal and minimal values of the exponent on this dimension. The node either points to another node a level deeper in the tree or to a list of sorted elements.

Figure 2.3 presents a simplified example from [75] on how burst tries work. We want to save polynomials in the form $x^i y^j z^k$, let R be the root of the tree. R contains a list of ranges for the power on the x term and points to monomials with an x term that has a power in this range. For example, the 2nd column of R points to all monomials with the degree of the x term greater or equal to 1 and less than 2. Thus R_1 contains all monomials in the form $x^1 y^j z^k$. R_1 contains one list per monomial where only the powers of y and z are saved with trailing zeros removed and the coefficient is at the end of the list. In this example, R_1 contains $5x^1 y^1 z^0 + 6x^1 y^1 z^1$.

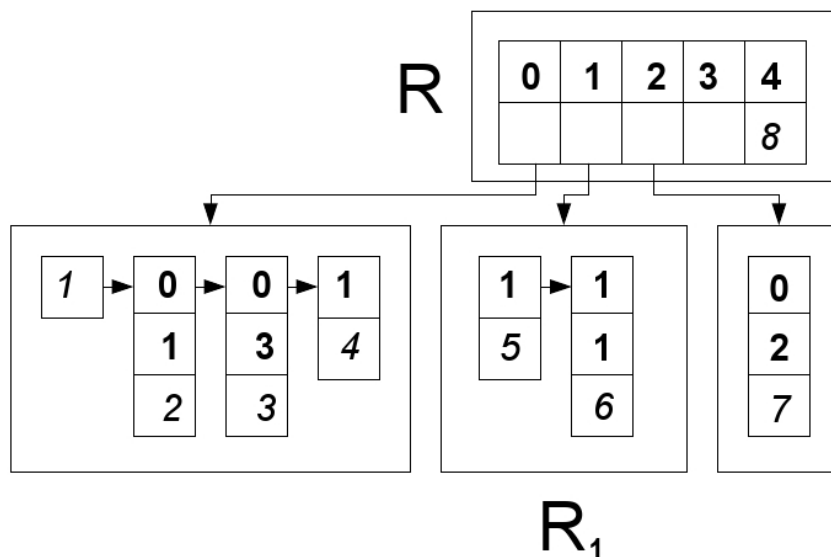


FIGURE 2.3. Burst trie holding $1 + 2z + 3z^3 + 4y + 5xy + 6xyz + 7x^2z^2 + 8x^4$ with a threshold of 5

Whenever a list becomes too large (we imposed a limit of 10 elements per list), it splits on the first variable where the maximal and minimal exponents differ. This process is called “bursting” and doing so ensures that finding potential duplicates is a very fast procedure, while making traversal of the entire tree take negligibly more time. For example, add $9x + 10xy^4 + 11xy^3z$ to the burst trie in Figure 2.3. All of these new elements are added to R_1 . Now add $12xy^3$. This element is added

to R_1 , which now has 6 elements, but the threshold is 5 and so R_1 is bursted to \tilde{R}_1 , see Figure 2.4. We must find the first variable in the list y, z that has different exponents in R_1 . This turns out to be y . Then \tilde{R}_1 now contains the exponents of y from 0 to 5. R_2 now contains all monomials in the form xyz^k and R_3 contains all the monomials in the form xy^3z^k . See [75] for a complete introduction.

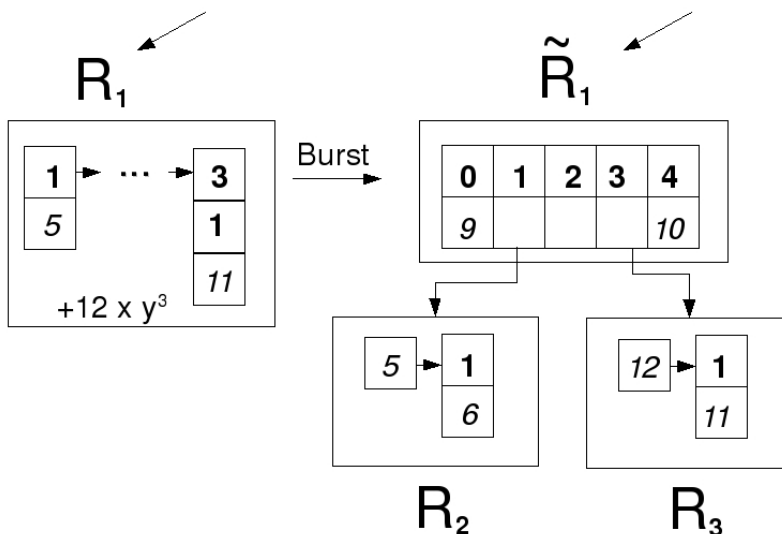


FIGURE 2.4. R_1 is bursted after adding 6 elements. \tilde{R}_1 holds $5xy + 6xyz + 9x + 10xy^4 + 11xy^3z + 12xy^3$

2.1.5. Should one triangulate or cone decompose? We have developed two polynomial time algorithms in Sections 2.1.1 and 2.1.2 for integrating a polynomial over a polytope. The two methods differ on how the domain P is decomposed. One could triangulate the whole polytope, or integrate over each tangent cone. However, each cone must be decomposed into simplicial cones. This is the trade-off: do one (large and possible costly) polytope triangulation, or many smaller cone triangulations. The number of simplices in a triangulation and the number of simplicial cones in a polytope decomposition can significantly differ. Depending on the polytope, choosing the right method can determine its practicality.

We highlight here a fraction of experiments performed in [55, 56]. We describe two experiments. First, we compare the two integration algorithms on random polynomials and random polytopes, and second we compare the algorithms on other numerical software.

Our experimental results agree with [37] in showing that triangulating the polytope is better for polytopes that are “almost simplicial” while cone decomposition is faster for simple polytopes.

2.1.5.1. *Integration over random polytopes.* For each $v \in \{9, 10, 11, 12, 17, 22, 27, 32\}$, we created 50 random polytopes in dimension 7 by taking the convex hull of random points using `Polymake` [76] and ensuring the resulting polytope had v vertices. We call these the primal polytopes. When zero is not in the interior of the polytope, we translated the centroid to the origin before constructing the dual polytope. Because of the construction method, most primal polytopes are simplicial and the duals are mostly simple polytopes. For each degree $D \in \{1, 2, 5, 10, 20, 30, 40, 50\}$, we also constructed a set of 50 random monomials in 7 variables of degree D . Then each polytope was integrated over by one random monomial in degree D . Meaning, for each polytope class with v vertices, and for each D , 50 integration tests were performed. The same test was then performed with the dual polytopes.

We only report those tests where both the triangulation and cone-decomposition method finished under 600 seconds. We define the *relative time difference* as the time taken by the triangulation method *minus* the time taken by the cone-decomposition method, all divided by the time of the triangulation method. Note that when the triangulation method is faster we obtain a negative number. We will use this quantity throughout.

Figure 2.5 displays a histogram on three axes. The first horizontal axis is the relative time difference between the two integration methods. The second horizontal axis shows the degrees of monomials and finally the vertical axis presents the number of random polytopes in dimension 7. The height of a particular solid bar in position (a_k, b^*) tallies the number of random polytopes for which the relative time difference between the two algorithms, when integrating a monomial of degree b^* , was between a_{k-1} and a_k with a_k included in that bar. Thus, the bars with negative relative time difference should be counted as experiments where triangulation is faster.

There is one histogram for the primal polytopes and one for the dual polytopes. The row color corresponds to a degree class. Note that for the primal polytopes, which are simplicial,

the triangulation method is faster than the cone decomposition method. In contrast, the cone decomposition method is slightly better for the simple polytopes. More tables are available in [55, 56].

Our experiments on integrating monomials have the same qualitative behavior as those of [37] for volume computation (polynomial of degree zero): the triangulation method is faster for simplicial polytopes (mass on histograms is highly concentrated on negative relative time differences) while the cone decomposition is faster for simple polytopes (mass on histograms is concentrated on positive relative time differences).

2.1.5.2. *Numerical methods.* There are two general classes of algorithms for finding integrals over polytopes: numerical and exact. Numerical algorithms approximate the valuation on the polytope and involve error bounds, whereas exact algorithms do not contain a theoretical error term. However, exact algorithms may contain errors when they use finite digit integers or use floating-point arithmetic. In order to sidestep this problem, `LattE integrale` uses NTL's arbitrary length integer and rational arithmetic [144] compiled with the GNU Multiple Precision Arithmetic Library [77]. The obvious downside to exact arithmetic is speed, but this cost is necessary to obtain exact answers. In this section, we compare our exact algorithms with `CUBPACK`, a Fortran 90 library which estimates the integral of a function (or vector of functions) over a collection of d -dimensional hyper-rectangles and simplices [47]. This comparison is very interesting because `CUBPACK` uses an adaptive grid to seek better performance and accuracy.

All integration tests with `CUBPACK` in dimension d were done with a product of linear forms with a constant term over a random d -dimensional simplex where the absolute value of any coordinate in any vertex does not exceed 10. For example, we integrated a product of inhomogeneous linear forms such as $(\frac{1}{5} + 2x - \frac{37}{100}y)(2 - 5x)$ over the simplex with vertices $(10, 0)$, $(9, 9)$, $(1, 1)$ and $(0, 0)$. In Table 2.2, `LattE` was run 100 times to get the average running time, while `CUBPACK` was run 1000 times due to variance. Both the dimension and number of linear forms multiplied to construct the integrand were varied.

As shown in Table 2.2, `LattE integrale` tends to take less time, especially when the number of forms and dimension increases. The table does not show the high variance that `CUBPACK` has in its run times. For example, the 5-dimensional test case with 6 linear forms had a maximum

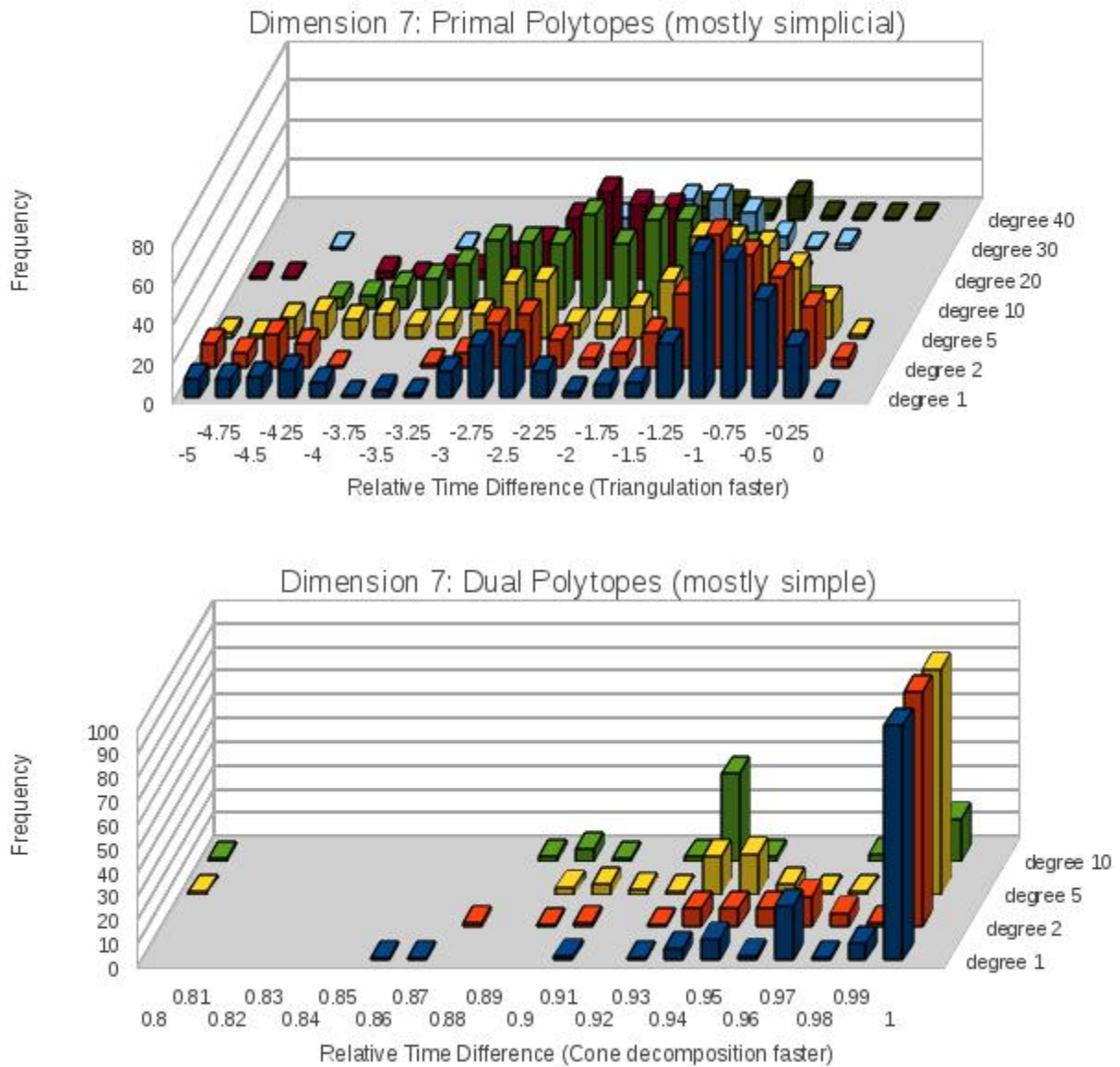


FIGURE 2.5. Histogram of the relative time difference between the triangulation and cone-decomposition methods for integrating over random polytopes in dimension 7

running time of 2874.48 seconds, while the minimum running time was 0.05 seconds on a different random simplex. This contrasted starkly with `LattE integrale`, which had every test be within 0.01 (the minimum time discrepancy recognized by its timer) of every other test case.

`CUBPACK` differs from `LattE integrale` in that since it is based on numerical approximations, one can ask for different levels of precision. Table 2.3 illustrates how `CUBPACK` scales with requested

2.2. INTEGRAND: PRODUCTS OF AFFINE FUNCTIONS

TABLE 2.2. Average Time for `LattE integrale` and `CUBPACK` for integrating products of inhomogeneous linear forms over simplices.

d	Tool	Number of linear factors									
		1	2	3	4	5	6	7	8	9	10
2	<code>LattE</code>	0.0001	0.0002	0.0005	0.0008	0.0009	0.0019	0.0038	0.0048	0.0058	0.0089
	<code>CUBPACK</code>	0.0027	0.0014	0.0016	0.0022	0.0064	0.0052	0.0014	0.0002	0.0026	0.0213
3	<code>LattE</code>	0.0002	0.0005	0.0009	0.0016	0.0043	0.0073	0.0144	0.0266	0.0453	0.0748
	<code>CUBPACK</code>	0.0134	0.0145	0.0018	0.0054	0.0234	0.0219	0.0445	0.0699	0.1170	0.2420
4	<code>LattE</code>	0.0003	0.0012	0.0018	0.0044	0.0121	0.0274	0.0569	0.1094	0.2247	0.4171
	<code>CUBPACK</code>	0.0042	0.0134	0.0028	0.0019	0.0076	0.5788	4.7837	4.3778	22.3530	54.3878
5	<code>LattE</code>	0.0005	0.0008	0.0048	0.0108	0.0305	0.0780	0.0800	–	–	–
	<code>CUBPACK</code>	0.0013	0.0145	0.0048	0.0217	0.0027	37.0252	128.2242	–	–	–

TABLE 2.3. `CUBPACK` scaling with increased relative accuracy. “Relative Error” is a user-specified parameter of `CUBPACK`; “Expected Error” is an estimate of the absolute error, produced by `CUBPACK`’s error estimators. Finally, the “Actual Error” is the difference of `CUBPACK`’s result to the exact integral computed with `LattE integrale`.

Relative Error	Result	Expected Error	Actual Error	# Evaluations	Time (s)
10^{-2}	1260422511.762	9185366.414	94536.015	4467	0.00
10^{-3}	1260507955.807	1173478.333	9091.974	9820	0.01
10^{-4}	1260516650.281	123541.490	397.496	34411	0.04
10^{-5}	1260517042.311	12588.455	5.466	104330	0.10
10^{-6}	1260517047.653	1257.553	0.124	357917	0.31
10^{-7}	1260517047.691	126.042	0.086	1344826	1.16
10^{-8}	1260517047.775	12.601	0.002	4707078	4.15
10^{-9}	1260517047.777	1.260	$< 10^{-3}$	16224509	14.09
10^{-10}	1260517047.777	0.126	$< 10^{-3}$	55598639	48.73

precision on a single, 4-dimensional, 10 linear form test case. It seems that `CUBPACK` scales linearly with the inverse of the requested precision—10 times the precision requires about 3 times the work. All reported tests were done by expanding the multiplication of linear forms, and coding a Fortran 90 function to read in the resulting polynomial and evaluate it for specific points.

2.2. Integrand: products of affine functions

In Section 2.1, polynomial time algorithms for integrating a polynomial over a polytope was developed, when the dimension is fixed. The key step was using Equation (2.1) to decompose a polynomial into a sum of powers of linear forms. That equation has a big problem: it can produce

millions of linear forms for polynomials with modest degree, see Table 2.1. The large number of summands is our motivation for exploring an alternative decomposition.

In this section we focus on decomposing a polynomial into a sum of products of affine functions and develop polynomial time algorithms for integrating over products of affine functions, similar to the last section.

To build such a polynomial decomposition, we seek an application of the next theorem.

THEOREM 2.2.1 (Handelman [82]). *Assume that $g_1, \dots, g_n \in \mathbb{R}[x_1, \dots, x_d]$ are linear polynomials and that the semialgebraic set*

$$(2.6) \quad S = \{x \in \mathbb{R}^d \mid g_1(x) \geq 0, \dots, g_n(x) \geq 0\}$$

is compact and has a non-empty interior. Then any polynomial $f \in \mathbb{R}[x_1, \dots, x_d]$ strictly positive on S can be written as $f(x) = \sum_{\alpha \in \mathbb{N}^n} c_\alpha g_1^{\alpha_1} \cdots g_n^{\alpha_n}$ for some nonnegative scalars c_α .

Note that this theorem is true when S is a polytope P , and the polynomials $g_i(x)$ correspond to the rows in the constraint matrix $b - Ax \geq 0$. In the case of the hypercube $P = [0, 1]^d$, this result was shown earlier by Krivine [101]. See [40, 50, 110] for a nice introduction to the Handelman decomposition. The Handelman decomposition is only guaranteed to exist if the polynomial is strictly greater than zero on P , and the required degree of the Handelman decomposition can grow as the minimum of the polynomial approaches zero [140]. Not much is known if redundant inequalities in P 's description can help.

Let the *degree* of a Handelman decomposition be $\max |\alpha|$, where the maximum is taken over all the exponent vectors α of $g_i(x)$ that appear in a decomposition. For a degree t decomposition, the goal is to find $c_\alpha \geq 0$ and a $s \in \mathbb{R}$ such that

$$f(x) + s = \sum_{\alpha \in \mathbb{Z}_{\geq 0}^n : |\alpha| \leq t} c_\alpha g^\alpha.$$

Adding the unknown constant shift s to $f(x)$ has three important consequences.

- (1) $-s$ will be a lower bound for f_{\min} . So if f is negative on P , $f(x) + s$ will be positive on P , allowing us to use Theorem 2.2.1.

- (2) If the minimum value of f is zero, f might not have a Handelman decomposition for any t . By adding a shift, a decomposition is guaranteed to exist for some t .
- (3) If the minimum value of f is positive, but small, $f(x)$ might only have Handelman decompositions for large degree t . By adding a shift, we can find a Handelman decomposition of smaller size.

If one uses a large shift s so that $f(x)+s$ is positive on its domain, there no known general bound for how large the Handelman degree t has to be for $f(x) + s$ to have a Handelman decomposition. Likewise, it is not known that by fixing the Handelman degree t , a shift s can always be found so that $f(x) + s$ has a Handelman decomposition, but we have not run into this problem in our experiments. For a nice review of known Handelman degree bounds for some special cases see [110].

If we expand the right hand side of $f(x) + s = \sum_{|\alpha| \leq t} c_\alpha g^\alpha$ into monomials, and force the coefficients of monomials on both sides of the equality to be equal, the results would be a linear system in the c_α and s . Hence we seek a solution to the *linear program*

$$\begin{aligned}
 (2.7) \quad & \min s + \sum_{\alpha} c_{\alpha} \\
 & A_H c_{\alpha} = b \\
 & a_0^T c_{\alpha} - s = 0 \\
 & s \text{ free}, c_{\alpha} \geq 0,
 \end{aligned}$$

where the objective has been chosen so that $-s$ is close to f_{\min} and to force a sparse Handelman decomposition of order t . It is common practice to use $\|\cdot\|_1$ as a proxy for sparse solutions [67]. Notice that A_H has $\binom{t+n}{n} = O(t^n)$ columns if the number of facts n of P is bounded, and A_H has $\binom{t+d}{d} = O(t^d)$ rows if the dimension d is fixed. Therefore, if a polynomial had a degree t Handelman decomposition, then the decomposition can be found in polynomial time in t when d and n are fixed by solving a linear program.

Consider the example $f(x) = x^2 - x$ on $[-1, 1] \subset \mathbb{R}$, which cannot have a Handelman decomposition as it takes negative values. We seek a solution to

$$f(x) + s = c_{2,0}(x + 1)^2 + c_{1,1}(1 - x)(x + 1) + c_{0,2}(1 - x)^2 + c_{1,0}(x + 1) + c_{0,1}(1 - x).$$

2.2. INTEGRAND: PRODUCTS OF AFFINE FUNCTIONS

Solving the linear program results in $c_{0,2} = 3/4$, $c_{2,0} = 1/4$, and $s = 1$.

Algorithm 6 illustrates how the Handelman decomposition can be used to integrate $f(x)$.

Algorithm 6 Integrate $f(x)$ by Handelman decomposition

Input: A polynomial $f(x) \in \mathbb{Q}[x_1, \dots, x_d]$ of degree D that has a degree D Handelman representation, and d -dimensional polytope $P \subset \mathbb{R}^d$

Output: $\int_P f(x) dx$

Solve the linear program (2.7) and obtain

$$f(x) + s = \sum_{\alpha_1 + \dots + \alpha_n \leq D} c_\alpha g^\alpha$$

sum $\leftarrow \int_P \sum_\alpha c_\alpha g^\alpha dx$, by methods in Section 2.2.1 or 2.2.2

vol $\leftarrow \text{vol}(P)$, using any integration method where the power of the integrand is zero

return **sum** $- s \cdot \text{vol}$

With a method of decomposing a polynomial into a sum of products of affine functions possible, we describe polynomial time algorithms for integrating such integrands in the next two sections.

2.2.1. Domain: cone decomposition. The next proposition outlines a method for integrating a product of affine functions over a polytope, where the polytope is decomposed into cones like the method in Section 2.1.1.

THEOREM 2.2.2 (proposition 5.6 in [53]). *When the dimension d and number of factors n is fixed, the value of*

$$\int_P \frac{(\langle \ell_1, x \rangle + r_1)^{m_1} \dots (\langle \ell_n, x \rangle + r_n)^{m_n}}{m_1! \dots m_n!} dx$$

can be computed in polynomial time in $M := \sum_{i=1}^n m_i$ and the size of the input data.

PROOF. We will compute the polynomial

$$\sum_{p_1 + \dots + p_n \leq M} \left(\int_P \frac{(\langle \ell_1, x \rangle + r_1)^{p_1} \dots (\langle \ell_n, x \rangle + r_n)^{p_n}}{p_1! \dots p_n!} dx \right) t_1^{p_1} \dots t_n^{p_n}.$$

in polynomial time in M and the input data, which contains the desired value as a coefficient of a polynomial in t_1, \dots, t_n .

We start with the exponential integral in the indeterminate ℓ from Section 1.2:

$$\int_P e^{\langle \ell, x \rangle} dx = \sum_{s \in V(P)} \sum_{C \in D_s} \text{vol}(\Pi_C) e^{\langle \ell, s \rangle} \prod_{i=1}^d \frac{1}{-\langle \ell, u_i \rangle}.$$

Note that because the dimension is fixed, the number of vertices and the number of simplicial cones at each feasible cone of P is polynomial in the input size of P .

First pick $\ell_{n+1} \in \mathbb{Q}^d$ so that $\langle \ell_{n+1}, u \rangle \neq 0$ for every ray u in the simplicial cones D_s at each vertex s . The set of points ℓ_{n+1} that fail this condition have measure zero, so ℓ_{n+1} can be picked randomly. Next, replace ℓ with $\ell_1 t_1 + \dots + \ell_{n+1} t_{n+1}$. To simplify notation, let $\mathbf{t} = (t_1, \dots, t_n)$, $\mathbf{a}_s = (\langle \ell_1, s \rangle, \dots, \langle \ell_n, s \rangle)$, $\mathbf{r} := (r_1, \dots, r_n)$, $\mathbf{b}_i := (\langle \ell_1, u_i \rangle, \dots, \langle \ell_n, u_i \rangle)$, $\beta_i := \langle \ell_{n+1}, u_i \rangle$, and $\ell_x = (\langle \ell_1, x \rangle, \dots, \langle \ell_n, x \rangle)$. Then

$$\int_P e^{\langle \ell_x, \mathbf{t} \rangle + \langle \mathbf{r}, \mathbf{t} \rangle + \langle \ell_{n+1}, x \rangle t_{n+1}} dx = \sum_{s \in V(P)} \sum_{C \in D_s} \text{vol}(\Pi_C) \prod_{i=1}^d \frac{e^{\langle \mathbf{a}_s, \mathbf{t} \rangle} e^{\langle \mathbf{r}, \mathbf{t} \rangle} e^{\langle \ell_{n+1}, s \rangle t_{n+1}}}{-\langle \mathbf{b}_i, \mathbf{t} \rangle - \beta_i t_{n+1}}.$$

Note that the integrand of the left hand side is $e^{\langle \ell_{n+1}, x \rangle t_{n+1}} \prod_{i=1}^n e^{(\langle \ell_i, x \rangle + r_i) t_i}$, which when expanded in series form contains the desired result. We will compute the series expansion of each summand in the right hand side of the above equation in t_1, \dots, t_n up to total degree M where the power of t_{n+1} is zero, and do this in polynomial time in M .

Let h_i be the series expansion of $e^{(\langle \ell_i, s \rangle + r_i) t_i}$ up to degree M in t_i for $1 \leq i \leq n$. Let h_{n+i} be the series expansion of

$$\frac{1}{-\langle \mathbf{b}_i, \mathbf{t} \rangle - \beta_i t_{n+1}} = \sum_{k=0}^{\infty} (-1)^k (\langle \mathbf{b}_i, \mathbf{t} \rangle)^k (\beta_i t_{n+1})^{-1-k}.$$

in t_i, \dots, t_n up to total degree M using the generalized binomial theorem. Applying Lemma 1.2.17 to $H_1 := \prod_{i=1}^{n+d} h_i$ results in the series expansion of

$$\prod_{i=1}^d \frac{e^{\langle \mathbf{a}_s, \mathbf{t} \rangle} e^{\langle \mathbf{r}, \mathbf{t} \rangle}}{-\langle \mathbf{b}_i, \mathbf{t} \rangle - \beta_i t_{n+1}}.$$

up to total degree M in t_1, \dots, t_n and where the power of t_{n+1} at most ranges from $-d(M+1)$ to $-d$.

Let h_{n+d+1} be the series expansion of $e^{\langle \ell_{n+1}, s \rangle t_{n+1}}$ up to degree $d(M+1)$ in t_{n+1} . Next, use Lemma 1.2.17 one last time while treating t_{n+1} as a coefficient and truncating at total degree M to compute $H_2 := H_1 h_{n+d+1}$. Any term where the power of t_{n+1} is not zero can be dropped because $I(P, \ell_1 t_1 + \dots + \ell_{n+1} t_{n+1})$ is holomorphic in t_{n+1} . Repeating this calculation for every simplicial cone results in

$$\sum_{p_1+\dots+p_n \leq M} \left(\int_P \frac{(\langle \ell_1, x \rangle + r_1)^{p_1} \cdots (\langle \ell_n, x \rangle + r_n)^{p_n}}{p_1! \cdots p_n!} dx \right) t_1^{p_1} \cdots t_n^{p_n}.$$

□

2.2.2. Domain: a full dimensional simplex. In [13], a polynomial time algorithm for integrating a product of linear forms was developed. In this section, we will extend the original proof to the slightly more general setting of integrating a product of affine functions.

THEOREM 2.2.3. *Let the dimension d and number of factors n be fixed. Let $\Delta \subset \mathbb{R}^d$ be a full dimensional simplex with vertices s_1, \dots, s_{d+1} , and let $\ell_1, \dots, \ell_n \in \mathbb{R}^d$. Then the value of*

$$\int_{\Delta} \frac{(\langle \ell_1, x \rangle + r_1)^{m_1} \cdots (\langle \ell_n, x \rangle + r_n)^{m_n}}{m_1! \cdots m_n!} dx$$

can be computed in polynomial time in $M := m_1 + \cdots + m_n$ and the usual input size.

PROOF. Similar to the proof of 2.2.2, we instead compute the polynomial

$$\text{sum}_{p_1+\dots+p_n \leq M} \left(\int_{\Delta} \frac{(\langle \ell_1, x \rangle + r_1)^{p_1} \cdots (\langle \ell_n, x \rangle + r_n)^{p_n}}{p_1! \cdots p_n!} dx \right) t_1^{p_1} \cdots t_n^{p_n}.$$

We start with Lemma 8 in [13] and write

$$(2.8) \quad \int_{\Delta} e^{\langle \ell, x \rangle} dx = d! \text{vol}(\Delta) \sum_{k \in \mathbb{N}^{d+1}} \frac{\langle \ell, s_1 \rangle^{k_1} \cdots \langle \ell, s_{d+1} \rangle^{k_{d+1}}}{(|k| + d)!},$$

where $|k| := k_1 + \cdots + k_{d+1}$. Replace ℓ with $\ell_1 t_1 + \cdots + \ell_n t_n$ and multiply both sides by $e^{r_1 t_1 + \cdots + r_n t_n}$ in Equation (2.8). To simplify notation, let $\mathbf{t} = (t_1, \dots, t_n)$, $\mathbf{r} = (r_1, \dots, r_n)$, $\ell_{s_i} = (\langle \ell_1, s_i \rangle, \dots, \langle \ell_n, s_i \rangle)$, then we have

$$(2.9) \quad \int_{\Delta} e^{\langle \ell_1, x \rangle t_1 + \cdots + \langle \ell_n, x \rangle t_n + \langle \mathbf{r}, \mathbf{t} \rangle} dx = d! \text{vol}(\Delta) e^{\langle \mathbf{r}, \mathbf{t} \rangle} \sum_{k \in \mathbb{N}^{d+1}} \frac{\langle \ell_{s_1}, \mathbf{t} \rangle^{k_1} \cdots \langle \ell_{s_{d+1}}, \mathbf{t} \rangle^{k_{d+1}}}{(|k| + d)!}.$$

Notice that the left hand now becomes

$$\int_{\Delta} e^{(\langle \ell_1, x \rangle + r_1)t_1 + \dots + (\langle \ell_n, x \rangle + r_n)t_n} dx = \sum_{(p_1, \dots, p_n) \in \mathbb{N}^n} \left(\int_{\Delta} \frac{(\langle \ell_1, x \rangle + r_1)^{p_1} \dots (\langle \ell_n, x \rangle + r_n)^{p_n}}{p_1! \dots p_n!} dx \right) t_1^{p_1} \dots t_n^{p_n},$$

which contains the desired polynomial. Hence we seek to compute the series expansion of the right hand side of Equation (2.9) up to total degree M in t_1, \dots, t_n .

Let $g_i(t_i)$ be the series expansion of $e^{r_i t_i}$ about $t_i = 0$ up to degree M in t_i for $1 \leq i \leq n$. Using Lemma 1.2.17, let H_1 be the product $d! \text{vol}(\Delta) \cdot g_1(t_1) \dots g_n(t_n)$ truncated at total degree M in t_1, \dots, t_n , which is done in polynomial time in M .

Notice that the sum in Equation (2.9) only needs to run for k such that $k_1 + \dots + k_n \leq M$. This produces $\binom{M+n}{n}$ summands, which is $O(M^n)$ as n is fixed. Let

$$h_k(\mathbf{t}) := \frac{\langle \ell_{s_1}, \mathbf{t} \rangle^{k_1} \dots \langle \ell_{s_{d+1}}, \mathbf{t} \rangle^{k_{d+1}}}{(|k| + d)!},$$

where $|k| \leq M$. The expansion of each $\langle \ell_{s_i}, \mathbf{t} \rangle^{k_i}$ is a homogenous polynomial of degree k_i , which has $\binom{k_i+n-1}{n-1} = O(k_i^{n-1})$ terms. Multiplying everything out in $h_k(\mathbf{t})$ results is at most $O(M^{(n-1)(d+1)})$ terms. Hence $h_k(\mathbf{t})$ can be expanded into a polynomial in polynomial time in M .

Using Lemma 1.2.17 again, the product $H_1 \sum_{k \in \mathbb{N}^n, |k| \leq M} h_k(\mathbf{t})$, truncated at total degree M can be computed in polynomial time. \square

2.2.3. Benefits of Handelman decomposition. In Sections 2.2.3.1, 2.2.3.2, 2.2.3.3, we discuss three benefits of the Handelman decomposition: our algorithms for integrating one Handelman term have reusable computations, the decomposition can have few terms, and it can have sparse LP solutions.

2.2.3.1. *Handelman terms have the same form.* The polynomial time algorithms outlined in Theorems 2.1.3 and 2.1.5 compute the integral of just one power of a linear form, while the algorithms outlined in Theorems 2.2.2 and 2.2.3 compute all the integrals of produces of affine functions up to a given degree. We stress the fact that every term in a Handelman decomposition of a polynomial $f(x)$ is in the same form: $g_1^{\alpha_1} \dots g_n^{\alpha_n}$ where the g_i corresponds to the rows of the polytope's P inequality constraints $b - Ax \geq 0$. The only part that changes between Handelman terms in the powers $\alpha_1, \dots, \alpha_n$. This means, the integral of every Handelman term can be computed via one

series computation from Theorems 2.2.2 and 2.2.3. Hence one big benefit of using the Handelman decomposition over a power of a linear form decomposition, is that the computation in Theorems 2.2.2 and 2.2.3 can be applied to many Handelman terms at once.

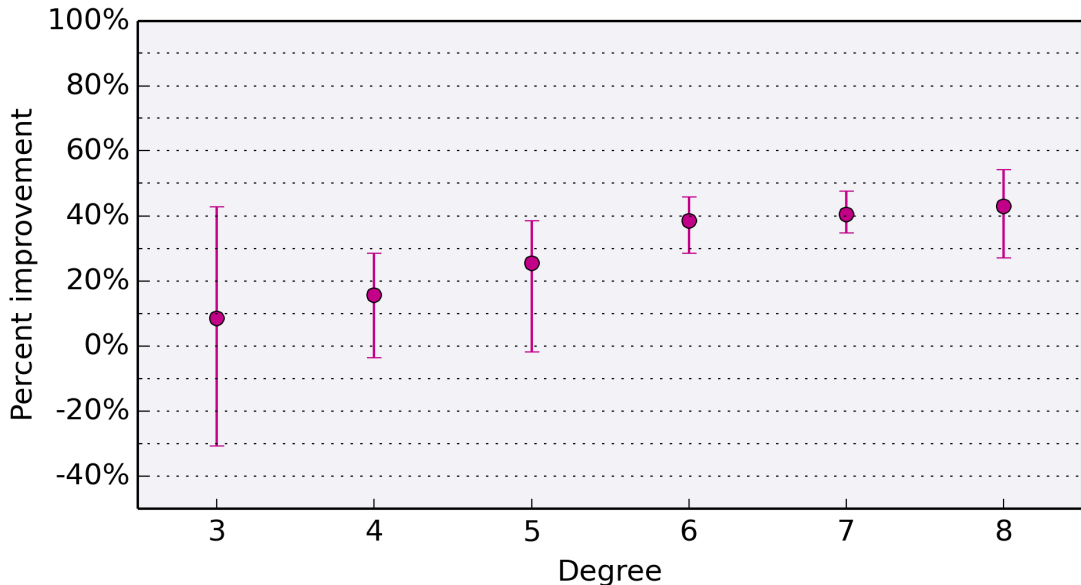
2.2.3.2. Handelman decompositions can have fewer terms. Next we compare between decomposing a random polynomial into a sum of powers of a linear form using Equation (2.1) and the Handelman method. We constructed a set of random polynomials in dimensions 3, 4, and 5 of total degree ranging from 3 to 8. For each dimension and degree pair, five random polynomials were constructed. Each polynomial was 20% dense, meaning, 20% of the coefficients of each polynomial out of the possible $\binom{d+D}{d}$ were nonzero. For the Handelman decomposition, the polytope P was picked to be the box $[-1, 1]^d$, and the objective function enforces a sparse decomposition and minimizes s . Figure 2.6 illustrates how much better the Handelman decomposition can be over the power of linear form formula. The figure plots the average percent change between the number of terms in each method.

For example, looking at the degree 8 polynomials, the Handelman decomposition had about 40% fewer terms than the power of linear forms formula among the 15 test polynomials (five in dimension 3, 4, and 5, each). Among the 15 test polynomials, the best case had about 50% fewer terms while the worst case has about 30% fewer terms.

One interesting fact is that there are one or two examples in degree 3, 4, and 5 where the Handelman decomposition had a few more terms than the power of linear form decomposition (resulting in a negative percent improvement). However, Figure 2.7 reveals that the difference in the number of terms between both methods is small in these dimensions. Hence the benefit of the Handelman decomposition is less important for the low degree polynomials. However, the Handelman decomposition also discovers a lower bound to shift $f(x)$ to make it nonnegative on P .

2.2.3.3. Handelman decompositions can be sparse. Finally, we consider the effect of including a sparse term in the objective function of the linear program in Equation (2.7). Figure 2.8 shows the average percent improvement between the number of linear forms found from our linear program and the number of nonzeros a generic basic feasible solution would have. For example, in degree 8 the Handelman linear program solutions contained about 20% fewer terms than a generic basic feasible solution would have, and the sparsest solution contained 30% fewer terms while the densest

FIGURE 2.6. Percent improvement of the number of terms from a Handelman decomposition versus the number of terms from the power of linear form formula. Bars reflect min and max percent improvements.

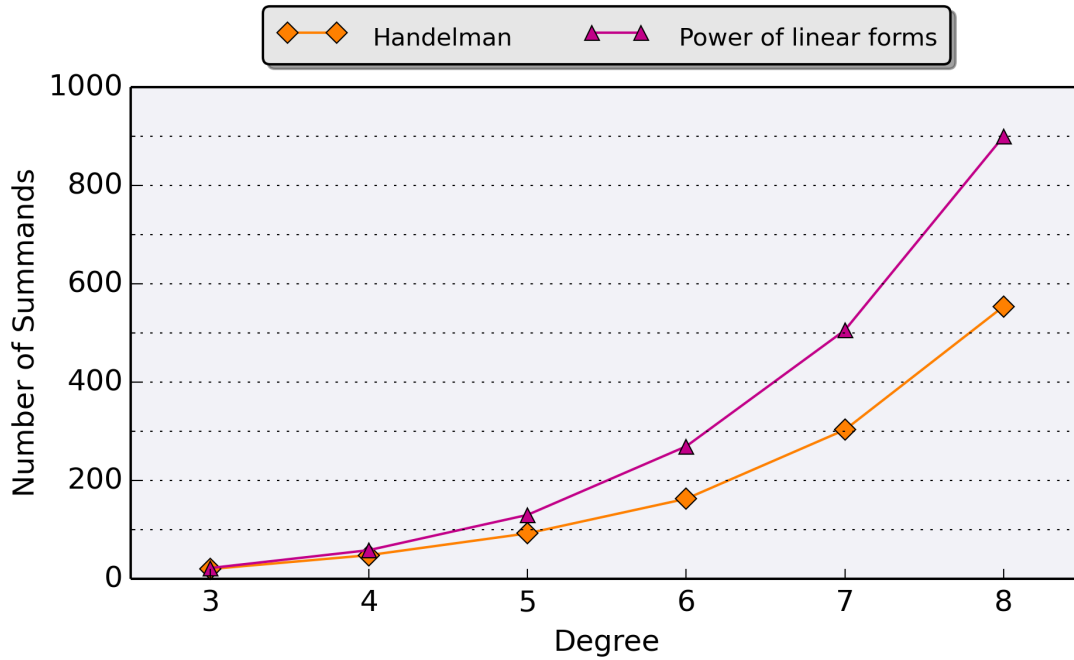


solution had 5% fewer terms than a generic basic solution. Every linear program is degenerate. This shows that it could be worthwhile to build an objective function that controls sparsity. Of course, any objective function that is not just $\min s$ can result in $-s$ being a poor lower bound for f_{\min} .

One troubling fact with searching for a Handelman decomposition of order t on a polytope P with n facets is that a linear program of size $\binom{t+d}{d} \times \binom{t+n}{n}$ needs to be solved. This brute force search quickly becomes impractical for large dimensions or with complicated polytopes. One way to reduce this cost when n is large is to contain P within a larger simpler polytope like a box or simplex, or to decompose P into simpler polytopes. Another idea is to use row and column generation methods for solving the linear program.

Table 2.4 lists the key points made about our two polynomial decomposition methods.

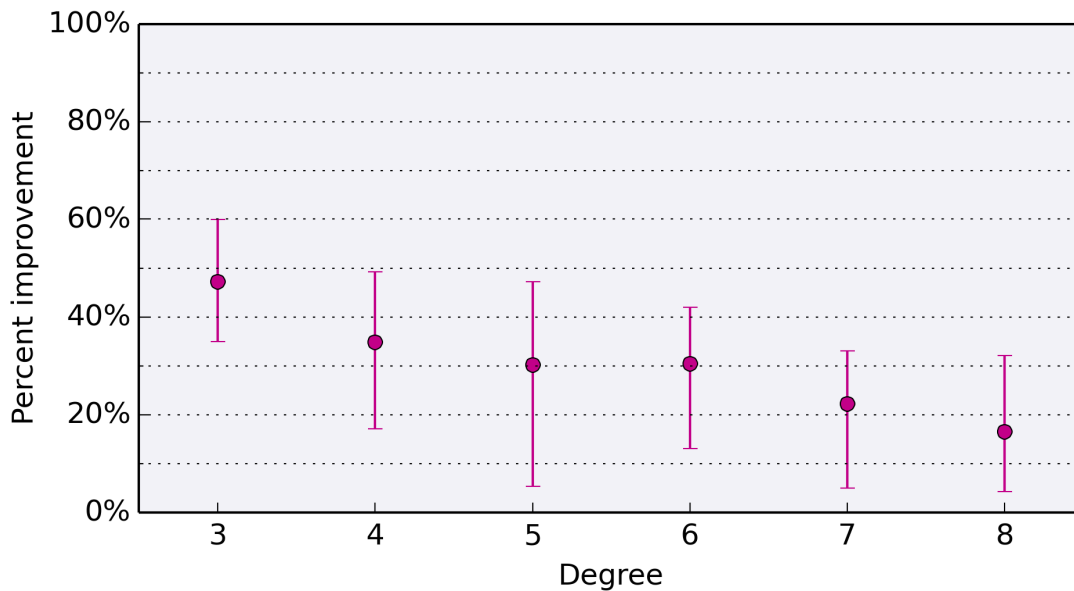
FIGURE 2.7. Average number of terms between the Handelman decomposition and power of linear form decomposition.



Handelman decomposition	Decomposition using Equation (2.1)
<ul style="list-style-type: none"> • harder to find decomposition • fewer terms • domain dependent • only exists for positive polynomials on P, but this can be worked around • s gives lower bound on f_{\min} on P 	<ul style="list-style-type: none"> • easy to find decomposition • many terms • domain independent • works on any polynomial

TABLE 2.4. Comparison between two polynomial decompositions

FIGURE 2.8. Percent improvement of the average number of terms from a Handelman decomposition found by solving a linear program where the objective contains a sparsity term versus the number of nonzeros of a generic basic feasible solution. Bars reflect min and max percent improvements.



CHAPTER 3

Polynomial Optimization

In this chapter, we focus on optimizing a polynomial $f(x)$ over a polytope P . In particular, we explore the discrete and continuous optimization problems:

$$\begin{aligned} \max f(x) \\ x \in P \cap \mathbb{Z}^d, \end{aligned}$$

and

$$\begin{aligned} \max f(x) \\ x \in P. \end{aligned}$$

We denote this maximum by f_{\max} . The exact optimization problems are hard. When the dimension is allowed to vary, approximating the optimal objective value of polynomial programming problems is still hard. See Section 1.3.2 for a review of the complexity for these problems. Hence in this chapter, we develop approximation algorithms for these optimization problems that run in polynomial time when the dimension is fixed.

Our methods are general and do not assume f is convex nor that it has any other special properties. At first, it will be necessary to assume $f(x)$ is nonnegative on P , but this restriction can be resolved. At the heart of our methods is the need to efficiently evaluate (when the dimension is fixed) $\sum_{x \in P \cap \mathbb{Z}^d} f(x)^k$ or $\int_P f(x)^k dx$ for a given $k \in \mathbb{N}$. There are many references in the literature on how to compute these sums and integrals, see [15, 13, 35, 47, 55]. Our focus is on methods that use *generating functions* [19].

When the dimension is fixed, there are many other polynomial time approximation algorithms for polynomial programming. For instance Parrilo [129], building on work by Lasserre [104] and Nesterov [127], developed such methods using sums of squares optimization. These methods were

further developed in [9, 120]. Other methods for polynomial optimization have been developed in [26, 36, 52, 108, 147, 148].

Handelman’s theorem (see Section 2.2) has also been used to optimize a polynomial in [109, 110, 130, 140]. Using Handelman to maximize a polynomial directly would require finding a Handelman decomposition of large degree, which becomes more difficult as degree increases. When we use Handelman’s theorem, it is only for producing a small degree Handelman decomposition of $f(x)$ to use with the polynomial approximation theorems.

Section 3.1 is a overview of [59] for optimizing a polynomial over $P \cap \mathbb{Z}^d$. As a side note, the authors of [60] used the methods in [59] to develop efficient algorithms for optimizing a polynomial over the continuous domain P and a mixed-integer domain $P \cap (\mathbb{R}^{d_1} \times \mathbb{Z}^{d_2})$. Then in Section 3.2, a dedicated algorithm for the continuous optimization problem is developed, which was developed in [53].

3.1. Prior work: integer optimization of polynomials

The *summation method* for optimization uses the elementary relation

$$\max\{s_1, \dots, s_N\} = \lim_{k \rightarrow \infty} \sqrt[k]{s_1^k + \dots + s_N^k}$$

which holds for any finite set $S = \{s_1, \dots, s_N\}$ of nonnegative real numbers. This relation can be viewed as an approximation result for ℓ_k -norms. Let $f(x) \in \mathbb{Q}[x_1, \dots, x_d]$ be a polynomial in d variables that is nonnegative over P , which is a full-dimensional polytope in \mathbb{R}^d . Our goal is to solve the problem

$$(3.1) \quad \begin{aligned} \max f(x) \\ x \in P \\ x_i \in \mathbb{Z}. \end{aligned}$$

This is an NP-hard problem, so instead we seek lower and upper bounds for the maximum. Because f is nonnegative on $P \cap \mathbb{Z}^d$, let $\|f\|_k^k := \sum_{x \in P \cap \mathbb{Z}^d} f(x)^k$, and $\|f\|_\infty = \max_{x \in P \cap \mathbb{Z}^d} f(x)$. Using the above norm-limit idea, we get the bounds

$$\|f\|_k / \sqrt[k]{N} \leq \|f\|_\infty \leq \|f\|_k,$$

where $N := |P \cap \mathbb{Z}^d|$.

EXAMPLE 3.1.1. Let $f(x) = x_1^2 x_2 - x_1 x_2$ with $x_1 \in [1, 3] \cap \mathbb{Z}$ and $x_2 \in [1, 3] \cap \mathbb{Z}$. Then f takes $N = 9$ nonnegative values on its domain: $\{0, 2, 6, 0, 4, 12, 0, 6, 18\}$. Computing the bounds for different k gives:

k	$\ f\ _k / \sqrt[k]{9}$	$\ f\ _k$
10	14.47	18.03
20	16.12	18.00
30	16.72	18.00
40	17.03	18.00

Because f has integer coefficients, for $k = 40$ the bounds $17.03 \leq f_{\max} \leq 18$ implies $f_{\max} = 18$.

This example illustrates that f_{\max} can be approximated by computing $\|f\|_k$. However, to obtain a polynomial time algorithm, enumerating the lattice points in $P \cap \mathbb{Z}^d$ must be avoided. When the domain is a box, $\|f\|_k$ can be computed by first expanding $g(x) := f(x)^k$, and then for each resulting monomial, $cx_1^{m_1} \cdots x_d^{m_d}$, computing $\sum_{x \in P \cap \mathbb{Z}^d} cx_1^{m_1} \cdots x_d^{m_d}$ by repeated application of Bernoulli's formula (which is also sometimes called Faulhaber's formula). The latter is the explicit polynomial in n of degree $p + 1$ for $F(n, p) := \sum_{j=1}^n j^p$, see [46].

EXAMPLE 3.1.2. Let $f(x) = x_1^2 x_2 - x_1 x_2$ with $x_1 \in [-5, 6] \cap \mathbb{Z}$ and $x_2 \in [1, 3] \cap \mathbb{Z}$. Find $\|f\|_1$.

We will compute the sum monomial-by-monomial. The degree of the variables are 1 and 2, so $F(n, 1) = (n^2 + n)/2$ and $F(n, 2) = (2n^3 + 3n^2 + n)/6$. Notice that the domain of x_1 does not start at 1, so we will need to evaluate $F(n, 1)$ and $F(n, 2)$ at different points and subtract or add.

summing the first monomial:

$$\begin{aligned}
 \sum_{x_1=-5}^6 \sum_{x_2=1}^3 x_1^2 x_2 &= \sum_{x_1=-5}^6 x_1^2 \sum_{x_2=1}^3 x_2 \\
 &= (F(5, 2) + F(6, 2))F(3, 1) \\
 &= (55 + 91)6 \\
 &= 876
 \end{aligned}$$

summing the second monomial:

$$\begin{aligned}
 \sum_{x_1=-5}^6 \sum_{x_2=1}^3 -x_1 x_2 &= - \sum_{x_1=-5}^6 x_1 \sum_{x_2=1}^3 x_2 \\
 &= -(-F(5, 1) + F(6, 1))F(3, 1) \\
 &= -(-15 + 21)6 \\
 &= -36
 \end{aligned}$$

Thus, $\|f\|_1 = 876 - 36 = 840$.

A lower and upper bounds for the discrete case are reviewed below.

THEOREM 3.1.3 (Theorem 1.1 in [59]). *Let the number of variables d be fixed. Let $f(x)$ be a polynomial of maximum total degree D with integer coefficients, and let P be a convex rational polytope defined by linear inequalities in d variables. Assume $f(x)$ is nonnegative over P . There is an increasing sequence of lower bounds $\{L_k\}$ and a decreasing sequence of upper bounds $\{U_k\}$ to the optimal value of*

$$\max f(x) \text{ such that } x \in P \cap \mathbb{Z}^d$$

that has the following properties:

(1) *The bounds are given by*

$$L_k := \sqrt[k]{\frac{\sum_{\alpha \in P \cap \mathbb{Z}^d} f(\alpha)^k}{|P \cap \mathbb{Z}^d|}} \leq \max\{f(\alpha) \mid \alpha \in P \cap \mathbb{Z}^d\} \leq \sqrt[k]{\sum_{\alpha \in P \cap \mathbb{Z}^d} f(\alpha)^k} := U_k.$$

(2) L_k and U_k can be computed in time polynomial in k , the input size of P and f , and the total degree D .

(3) The bounds satisfy the following inequality:

$$U_k - L_k \leq f_{\max} \left(\sqrt[k]{|P \cap \mathbb{Z}^d|} - 1 \right).$$

(4) In addition, for $k = (1 + 1/\epsilon) \log(|P \cap \mathbb{Z}^d|)$, L_k is a $(1 - \epsilon)$ -approximation to the optimal value f_{\max} and it can be computed in time polynomial in the input size, the total degree D , and $1/\epsilon$. Similarly, U_k gives a $(1 + \epsilon)$ -approximation to f_{\max} . Moreover, with the same complexity, one can also find a feasible lattice point that approximates an optimal solution with similar quality.

Therefore, computing an approximation for Problem (3.1) via Theorem 3.1.3 requires summing the evaluation of a polynomial over the lattice points of a polytope. In order to compute $\sum_{\alpha \in P \cap \mathbb{Z}^d} f(\alpha)^k$, the authors in [59] suggest computing the expansion $g(x) := f(x)^k$ and then evaluating the generating function for $\sum_{\alpha \in P \cap \mathbb{Z}^d} g(\alpha)z^\alpha$ at $z = 1$ by taking derivatives of the generating function for $\sum_{\alpha \in P \cap \mathbb{Z}^d} g(\alpha)z^\alpha$. They show this can be done in polynomial time when the dimension is fixed; however, is hard to implement. We will illustrate a simpler method that is similar to the ideas of Chapter 2.

To use our generating functions for summing a polynomial over the lattice points of a polytope, the polynomial $g(x) = f(x)^k$ is first decomposed. Again, there are two options, $g(x)$ can be decomposed into a sum of powers of linear forms (via Equation (2.1)) or a sum of products of affine functions (via Handelman's theorem in Section 2.2). Both of these decompositions can be constructed in polynomial time.

What follows is the author's original method for computing the sum of a Handelman term. The method also produces an algorithm for summing a power of a linear form over a polytope by setting $n = 1$ and $r_1 = 0$.

PROPOSITION 3.1.4. *When the dimension d and number of factors n is fixed, the value of*

$$\sum_{x \in P \cap \mathbb{Z}^d} \frac{(\langle \ell_1, x \rangle + r_1)^{m_1} \cdots (\langle \ell_n, x \rangle + r_n)^{m_n}}{m_1! \cdots m_n!}$$

3.1. PRIOR WORK: INTEGER OPTIMIZATION OF POLYNOMIALS

can be computed in polynomial time in $M := \sum_{i=1}^n m_i$ and the size of the input data.

In the proof below, instead of computing the value for a fixed sequence of powers m_1, \dots, m_n , we will compute the polynomial

$$\sum_{p_1 + \dots + p_n \leq M} \left(\sum_{x \in P \cap \mathbb{Z}^d} \frac{\langle \ell_1, x \rangle + r_1^{p_1} \dots \langle \ell_n, x \rangle + r_n^{p_n}}{p_1! \dots p_n!} \right) t_1^{p_1} \dots t_n^{p_n},$$

which includes the desired value as the coefficient of the monomial $t_1^{m_1} \dots t_n^{m_n}$. This is ideal when using a Handelman decomposition because terms in the Handelman decomposition only differs in the exponents m_1, \dots, m_n . When $n = 1$, the extra terms that are computed are unavoidable. The following proof will use a tangent cone decomposition of the polytope P .

PROOF. Because the dimension d is fixed, we can use Barvinok's Algorithm to write down

$$\sum_{x \in P \cap \mathbb{Z}^d} e^{\langle \ell, x \rangle} = \sum_{i \in I} \epsilon_i \frac{e^{\langle \ell, v_i \rangle}}{\prod_{j=1}^d (1 - e^{\langle \ell, u_{ij} \rangle})}$$

where $\epsilon_i \in \{-1, 1\}$, $v_i \in \mathbb{Z}^d$, and $u_{ij} \in \mathbb{Z}^d$, and I is some index set whose size is polynomially bounded in the input size of P . The v_i correspond to the integer point of an unimodular cone and the u_{ij} are the cone's rays. This equality only holds when ℓ is an indeterminate. If ℓ is in \mathbb{Q}^d and orthogonal to some u_{ij} , some of the above fractions are singular. However, the singularity is removed in the sum as the expression is holomorphic in ℓ . See Section 1.2 for a review of these statements.

To work around the possibility that one of the fractions is singular when ℓ is evaluated, we will replace ℓ with $\ell_1 t_1 + \dots + \ell_n t_n + \ell_{n+1} t_{n+1}$ where ℓ_{n+1} has been picked so that $\langle \ell_{n+1}, u_{ij} \rangle \neq 0$ for all u_{ij} . Notice that the set of ℓ_{n+1} that fail this condition have measure zero, and so ℓ_{n+1} can be picked randomly. After doing this, we get

$$\sum_{x \in P \cap \mathbb{Z}^d} e^{\langle \ell_1, x \rangle t_1 + \dots + \langle \ell_{n+1}, x \rangle t_{n+1}} = \sum_{i \in I} \epsilon_i \frac{e^{\langle \ell_1, v_i \rangle t_1 + \dots + \langle \ell_{n+1}, v_i \rangle t_{n+1}}}{\prod_{j=1}^d (1 - e^{\langle \ell_1, u_{ij} \rangle t_1 + \dots + \langle \ell_{n+1}, u_{ij} \rangle t_{n+1}})},$$

where no fraction is singular.

3.1. PRIOR WORK: INTEGER OPTIMIZATION OF POLYNOMIALS

To make the notation cleaner, let $\mathbf{t} = (t_1, \dots, t_n)$, $\mathbf{a}_i = (\langle \ell_1, v_i \rangle, \dots, \langle \ell_n, v_i \rangle)$, $\mathbf{r} = (r_1, \dots, r_n)$, $\mathbf{b}_{ij} = (\langle \ell_1, u_{ij} \rangle, \dots, \langle \ell_n, u_{ij} \rangle)$, $\beta_{ij} := \langle \ell_{n+1}, u_{ij} \rangle$, and $\ell_x = (\langle \ell_1, x \rangle, \dots, \langle \ell_n, x \rangle)$. After multiplying both sides by $e^{\langle \mathbf{r}, \mathbf{t} \rangle}$, we have:

$$(3.2) \quad \sum_{x \in P \cap \mathbb{Z}^d} e^{\langle \ell_x, \mathbf{t} \rangle + \langle \mathbf{r}, \mathbf{t} \rangle + \langle \ell_{n+1}, x \rangle t_{n+1}} = \sum_{i \in I} \epsilon_i \frac{e^{\langle \mathbf{a}_i, \mathbf{t} \rangle} e^{\langle \mathbf{r}, \mathbf{t} \rangle} e^{\langle \ell_{n+1}, v_i \rangle t_{n+1}}}{\prod_{j=1}^d (1 - e^{\langle \mathbf{b}_{ij}, \mathbf{t} \rangle + \beta_{ij} t_{n+1}})}.$$

The left hand side of Equation 3.2 is

$$\sum_{x \in P \cap \mathbb{Z}^d} \prod_{i=1}^n e^{\langle \ell_i, x \rangle t_i + r_i} e^{\langle \ell_{n+1}, x \rangle t_{n+1}}$$

Replacing each exponential function with its Taylor series and expanding the product results in the series expansion in t_1, \dots, t_{n+1} of the left hand side of Equation 3.2. Truncating the series at total degree M contains exactly the desired polynomial plus monomials that have a t_{n+1} factor which can be dropped. Hence the proof is complete once the series expansion of the right hand side of Equation 3.2 can be done in polynomial time. Next write each summand as a product of four terms:

$$(3.3) \quad \frac{e^{\langle \mathbf{a}_i, \mathbf{t} \rangle} e^{\langle \mathbf{r}, \mathbf{t} \rangle} e^{\langle \ell_{n+1}, v_i \rangle t_{n+1}}}{\prod_{j=1}^d (1 - e^{\langle \mathbf{b}_{ij}, \mathbf{t} \rangle + \beta_{ij} t_{n+1}})} = \left(e^{\langle \mathbf{a}_i + \mathbf{r}, \mathbf{t} \rangle} \right) \left(\prod_{j=1}^d \frac{e^{\langle \mathbf{b}_{ij}, \mathbf{t} \rangle + \beta_{ij} t_{n+1}}}{(1 - e^{\langle \mathbf{b}_{ij}, \mathbf{t} \rangle + \beta_{ij} t_{n+1}})} \right) \\ \times \left(\prod_{j=1}^d \frac{1}{e^{\langle \mathbf{b}_{ij}, \mathbf{t} \rangle + \beta_{ij} t_{n+1}}} \right) e^{\langle \ell_{n+1}, v_i \rangle t_{n+1}}.$$

Let h_j be the series expansion of $e^{\langle \ell_j, v_i \rangle + r_j} t_j$ in t_i up to degree M for $1 \leq j \leq n$. Let h_{n+j} be the series expansion of

$$\frac{e^{\langle \mathbf{b}_{ij}, \mathbf{t} \rangle + \beta_{ij} t_{n+1}}}{(1 - e^{\langle \mathbf{b}_{ij}, \mathbf{t} \rangle + \beta_{ij} t_{n+1}})}$$

up to total degree M in t_1, \dots, t_{n+1} for $1 \leq j \leq d$. This can be done in polynomial time as this is the generating function for the Bernoulli numbers, see Lemma 3.1.5. By Lemma 1.2.17, the product $H_1 := \prod_{j=1}^{n+d} h_j$ truncated at total degree M is done in polynomial time in M as n and d are fixed.

3.1. PRIOR WORK: INTEGER OPTIMIZATION OF POLYNOMIALS

Using the generalized binomial theorem we have,

$$\frac{1}{\langle \mathbf{b}_{ij}, \mathbf{t} \rangle + \beta_{ij} t_{n+1}} = \sum_{k=0}^{\infty} (-1)^k (\langle \mathbf{b}_{ij}, \mathbf{t} \rangle)^k (\beta_{ij} t_{n+1})^{-1-k}.$$

Notice that $(\langle \mathbf{b}_{ij}, \mathbf{t} \rangle)^k$ is a polynomial in t_1, \dots, t_n of total degree k . Let h_{n+d+j} represent this sum truncated at $k = M$ for $1 \leq j \leq d$. Note that h_{n+d+j} is a polynomial of total degree M in t_1, \dots, t_n , and the power of t_{n+1} ranges from $-1 - M$ to -1 at most.

Treating t_{n+1} as a coefficient (that is, ignoring its power when computing the degree), we compute the product $H_2 := H_1 \cdot \prod_{j=1}^d h_{n+d+j}$ using Lemma 1.2.17. H_2 is a polynomial in t_1, \dots, t_n of total degree M , and the power of t_{n+1} at most ranges from $-d(M+1)$ to $M-d$.

Finally, let h_{n+2d+1} be the series expansion of $e^{\langle \ell_{n+1}, \mathbf{v}_i \rangle t_{n+1}}$ in t_{n+1} up to degree $d(M+1)$. Using Lemma 1.2.17 to compute $H_3 := H_2 \cdot h_{n+2d+1}$ results in polynomial in of total degree M in t_1, \dots, t_n , and the power of each t_{n+1} is nonnegative.

Dropping terms where the power of t_{n+1} is positive, and repeating the calculation $|I|$ times results in

$$\sum_{p_1 + \dots + p_n \leq M} \left(\sum_{x \in P \cap \mathbb{Z}^d} \frac{\langle (\ell_1, x) + r_1 \rangle^{p_1} \dots \langle (\ell_n, x) + r_n \rangle^{p_n}}{p_1! \dots p_n!} \right) t_1^{p_1} \dots t_n^{p_n}.$$

□

For completeness, we explicitly show how to compute the Bernoulli number generating function.

LEMMA 3.1.5. *Let $\mathbf{t} = (t_1, \dots, t_n)$, and $\mathbf{c} = (c_1, \dots, c_n)$. The series expansion of*

$$\frac{\langle \mathbf{c}, \mathbf{t} \rangle}{1 - e^{\langle \mathbf{c}, \mathbf{t} \rangle}}$$

up to total degree M in t_1, \dots, t_n can be done in polynomial time in M when n is fixed.

PROOF. From [46], we start with

$$\frac{x}{1 - e^{-x}} = \sum_{k=0}^{\infty} B_k \frac{(-x)^k}{k!},$$

where the B_k are the Bernoulli numbers of the first kind.

Then expanding the polynomial

$$-\sum_{k=0}^M B_k \frac{(\langle \mathbf{c}, \mathbf{t} \rangle)^k}{k!}$$

in t_1, \dots, t_n yields the degree M truncation of the series expansion of

$$\frac{\langle \mathbf{c}, \mathbf{t} \rangle}{1 - e^{\langle \mathbf{c}, \mathbf{t} \rangle}}.$$

Because n is fixed, the expansion can be done in polynomial time in M . B_k can be computed in time $O(k^2)$ by the Akiyama–Tanigawa algorithm, which is reproduced in Algorithm 7. \square

Algorithm 7 Akiyama–Tanigawa algorithm for first Bernoulli numbers [90]

Input: k

Output: B_k

Let A be an array of length $k + 1$ with index starting at zero

for i from 0 to k **do**

$A[i] \leftarrow 1/(i + 1)$

for all j from i by -1 to 1 **do**

$A[j - 1] \leftarrow j \cdot (A[j - 1] - A[j])$

end for

end for

if $k = 1$ **then**

return $-A[0]$

end if

return $A[0]$

3.2. Continuous Optimization

This section addresses the problem of approximating the continuous optimization problem

$$(3.4) \quad \begin{aligned} &\max f(x) \\ &x \in P \\ &x_i \in \mathbb{R}, \end{aligned}$$

using the same style of bounded developed in Section 3.1. Theorem 3.2.1 is the continuous analog of Theorem 3.1.3 for optimizing a polynomial f over the continuous domain P . This section is devoted to its proof, and is a highlight of [53].

3.2. CONTINUOUS OPTIMIZATION

We note that Theorem 3.2.1 involves integrating the polynomial $f(x)$. Integral kernel or moment methods produce an approximation to f_{\max} via computing $\int f(x) d\mu_k$ where the measure μ_k usually involves a special subset of nonnegative functions, like sum-of-squares polynomials. Such methods have been developed in [50, 106, 104, 105, 107, 103]. Our method is slightly different as our measure is always the standard Lebesgue measure, while our integrand is $f(x)^k$.

THEOREM 3.2.1. *Let the number of variables d be fixed. Let $f(x)$ be a polynomial of maximum total degree D with rational coefficients, and let P be a full-dimensional convex rational polytope defined by linear inequalities in d variables. Assume $f(x)$ is nonnegative over P . Then there is an increasing sequence of lower bounds $\{L_k\}$ and a decreasing sequence of upper bounds $\{U_k\}$ for $k \geq k_0$ to the optimal value of $\max f(x)$ for $x \in P$ such that the bounds have the following properties:*

(1) For each $k > 0$, the lower bound is given by

$$L_k := \sqrt[k]{\frac{\int_P f(x)^k dx}{\text{vol}(P)}}.$$

(2) Let M be the maximum width of P along the d coordinate directions, $\epsilon' := \frac{d}{d+k}$, and let \mathcal{L} be a Lipschitz constant of f satisfying

$$|f(x) - f(y)| \leq \mathcal{L} \|x - y\|_\infty \text{ for } x, y \in P.$$

Then for all k such that $k \geq k_0$ where $k_0 = \max\{1, d(\frac{f_{\max}}{M\mathcal{L}} - 1)\}$, the upper bound is given by

$$U_k := \left(\frac{\int_P f(x)^k dx}{\text{vol}(P)} \right)^{1/(d+k)} \left(\frac{M\mathcal{L}}{\epsilon'} \right)^{d/(d+k)} \frac{1}{(1 - \epsilon')^{k/(d+k)}}.$$

(3) The bounds L_k and U_k can be computed in time polynomial in k , the input size of P and f .

(4) Let $\epsilon > 0$, and U be an arbitrary initial upper bound for f_{\max} . Then there is a $k \geq k_0$ such that

(a) $U_k - L_k \leq \epsilon f_{\max}$ where k depends polynomially on $1/\epsilon$, linearly in $U/M\mathcal{L}$, and logarithmically on $UM\mathcal{L}$, and

3.2. CONTINUOUS OPTIMIZATION

(b) for this choice of k , L_k is a $(1 - \epsilon)$ -approximation to the optimal value f_{\max} and U_k is a $(1 + \epsilon)$ -approximation to f_{\max} .

PROOF. A polynomial time algorithm for computing $\int_P f(x)^k dx$ is developed in Chapter 2.

We now focus on proving the bounds. The lower bound L_k is immediate. For the upper bound, we take inspiration from the standard proof that $\lim_{p \rightarrow \infty} \|f\|_p = \|f\|_\infty$. Let $\epsilon' > 0$, $P^{\epsilon'} := \{x \in P \mid f(x) \geq (1 - \epsilon')f_{\max}\}$ and $[P^{\epsilon'}]$ denote the characteristic function of $P^{\epsilon'}$. Then we have

$$(1 - \epsilon')f_{\max} \cdot \text{vol}(P^{\epsilon'}) \leq \int_{P^{\epsilon'}} f(x) dx = \int_P f(x)[P^{\epsilon'}] dx \leq \left(\int_P f(x)^k dx \right)^{1/k} \text{vol}(P^{\epsilon'})^{1/q}$$

where the last inequality comes from Hölder's inequality with $\frac{1}{k} + \frac{1}{q} = 1$.

Rearranging the first and last expressions results in

$$\left(\int_P f(x)^k dx \right)^{1/k} \geq (1 - \epsilon')f_{\max} \cdot \text{vol}(P^{\epsilon'})^{1/k}.$$

We now seek a lower bound for $\text{vol}(P^{\epsilon'})$. Because f is a polynomial and P is compact, f has a Lipschitz constant \mathcal{L} ensuring $|f(x) - f(y)| \leq \mathcal{L} \|x - y\|_\infty$ for $x, y \in P$. Let x^* denote an optimal point where $f(x^*) = f_{\max}$ and let

$$B_\infty(x^*, r) := \{x \in \mathbb{R}^d : \|x - x^*\|_\infty \leq r\}$$

be a closed ball of radius r centered at x^* . Then for all x in the ball $B_\infty(x^*, \epsilon' f_{\max}/\mathcal{L})$, $f(x) \geq (1 - \epsilon')f_{\max}$. Therefore,

$$\text{vol}(P^{\epsilon'}) = \text{vol}\{x \in P \mid f(x) \geq (1 - \epsilon')f_{\max}\} \geq \text{vol}\{x \in P \cap B_\infty(x^*, \epsilon' f_{\max}/\mathcal{L})\}.$$

Notice that the ball $B(x^*, \epsilon' f_{\max}/\mathcal{L})$ may not be contained in P , see Figure 3.1a. We need to lower bound the fraction of the ball that intercepts P where x^* could be any point in P . To do this, we will show how a scaled P can be contained in $P^{\epsilon'}$ as in Figure 3.1b. Consider the invertible linear transformation $\Delta : \mathbb{R}^d \rightarrow \mathbb{R}^d$ given by $\Delta x := \delta(x - x^*) + x^*$ where $\delta > 0$ is some unknown scaling term. Notice that this function is simply a scaling about the point x^* that fixes the point x^* . We need to pick δ such that $\Delta P \subseteq P \cap B_\infty(x^*, \epsilon' f_{\max}/\mathcal{L})$.

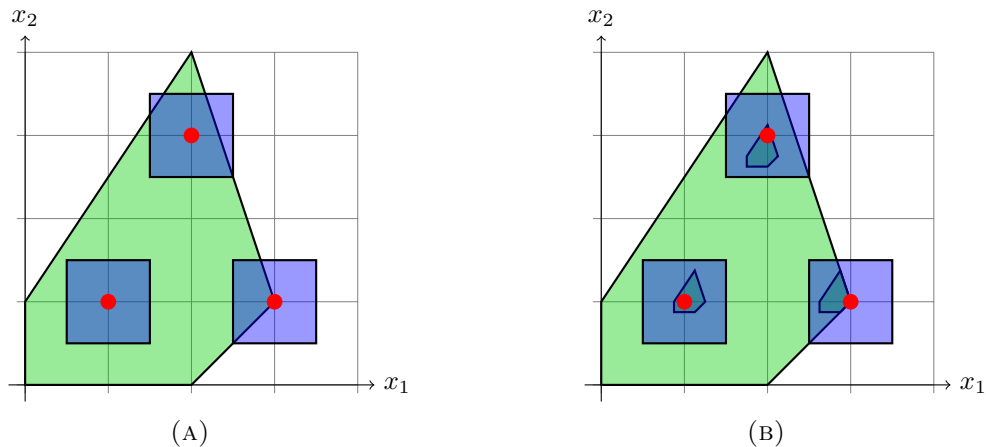


FIGURE 3.1. (A) Pentagon with three possible points x^* that maximize $f(x)$ along with the ℓ_∞ balls $B_\infty(x^*, 1/2)$. It might not be true that the ball intercepts the polytope. (B) However, a scaled pentagon can be contained in the ball and the original polytope.

- If $\Delta P \subseteq B_\infty(x^*, \epsilon' f_{\max}/\mathcal{L})$, then for $x \in P$

$$\begin{aligned} \|\Delta x - x^*\|_\infty &= \|\delta(x - x^*) + x^* - x^*\|_\infty \\ &= \delta \|x - x^*\|_\infty \\ &\leq \frac{\epsilon' f_{\max}}{\mathcal{L}}. \end{aligned}$$

Let M be the maximum width of P along the d coordinate axes, then $0 < \delta \leq \frac{\epsilon' f_{\max}}{M\mathcal{L}}$ is a sufficient condition for $\Delta P \subseteq B_\infty(x^*, \epsilon' f_{\max}/\mathcal{L})$.

- Let $x \in P$, and write x and x^* as a convex combination of the vertices of P . That is, let $x = \sum_{i=1}^N \alpha_i v_i$ and $x^* = \sum_{i=1}^N \beta_i v_i$ where $\sum_{i=1}^N \alpha_i = 1$, $\sum_{i=1}^N \beta_i = 1$, $\alpha_i \geq 0$, and $\beta_i \geq 0$. Then

$$\begin{aligned}\Delta x &= \delta \left(\sum_{i=1}^N \alpha_i v_i - \sum_{i=1}^N \beta_i v_i \right) + \sum_{i=1}^N \beta_i v_i \\ &= \sum_{i=1}^N (\delta \alpha_i + \beta_i - \delta \beta_i) v_i\end{aligned}$$

No matter what δ is, $\sum_{i=1}^N (\delta \alpha_i + \beta_i - \delta \beta_i) = 1$. Forcing $\delta \alpha_i + (1 - \delta) \beta_i \geq 0$ for each i as x and x^* varies over the polytope P is equivalent to $\delta \leq 1$.

Hence, $0 < \delta \leq 1$ a sufficient condition for $\Delta P \subseteq P$.

Therefore, $\text{vol}\{x \in P \cap B_\infty(x^*, \epsilon' f_{\max}/\mathcal{L})\} \geq \text{vol}(\Delta P) = \left(\min\{1, \frac{\epsilon' f_{\max}}{M\mathcal{L}}\} \right)^d \text{vol}(P)$, and finally,

$$\left(\int_P f(x)^k dx \right)^{1/k} \geq (1 - \epsilon') f_{\max} \cdot \text{vol}(P)^{1/k} \left(\min\{1, \frac{\epsilon' f_{\max}}{M\mathcal{L}}\} \right)^{d/k}.$$

As the above inequality is true for all $0 < \epsilon' \leq 1$, we want to pick ϵ' to maximize the function $\phi(\epsilon') := (1 - \epsilon') \left(\min\{1, \frac{\epsilon' f_{\max}}{M\mathcal{L}}\} \right)^{d/k}$. The maximum of $(1 - \epsilon') \left(\frac{\epsilon' f_{\max}}{M\mathcal{L}} \right)^{d/k}$ occurs at $\epsilon' = \frac{d}{d+k}$. Hence the maximum of $\phi(\epsilon')$ occurs at $\epsilon' = \frac{d}{d+k}$ if this is less than $\frac{M\mathcal{L}}{f_{\max}}$. Otherwise if $\epsilon' \geq \frac{M\mathcal{L}}{f_{\max}}$, the maximum of $\phi(\epsilon')$ is at $\epsilon' = \frac{M\mathcal{L}}{f_{\max}}$. Therefore the maximum of $\phi(\epsilon')$ occurs at $\epsilon' = \min\{\frac{d}{d+k}, \frac{M\mathcal{L}}{f_{\max}}\}$. Enforcing $\frac{d}{d+k} \leq \frac{M\mathcal{L}}{f_{\max}}$ is equivalent to $d(\frac{f_{\max}}{M\mathcal{L}} - 1) \leq k$. With this choice of ϵ' and value restriction on k , solving for f_{\max} yields the desired formula for U_k .

The proof of part (4) is completed in the next three lemmas. □

LEMMA 3.2.2. $\frac{1}{\log(1+\epsilon)} \leq 1 + \frac{1}{\epsilon}$ for $0 < \epsilon \leq 1$.

PROOF. It is enough to show that $\phi(\epsilon) := (1 + \frac{1}{\epsilon}) \log(1 + \epsilon) \geq 1$ for $0 < \epsilon \leq 1$. This follows because $\phi(\epsilon)$ is increasing on $0 < \epsilon \leq 1$ and $\lim_{\epsilon \rightarrow 0} \phi(\epsilon) = 1$. □

LEMMA 3.2.3. For every $\delta > 0$, there is a $c_\delta > 0$ such that

$$\frac{\log(z+1)}{z+1} \leq c_\delta (z+1)^{-\frac{1}{1+\delta}}$$

for all $z > 0$.

In particular, if $\delta = 0.1$, then c_δ can be set to 4.05.

3.2. CONTINUOUS OPTIMIZATION

PROOF. Because

$$\lim_{z \rightarrow \infty} \frac{(z+1)^{1-\frac{1}{1+\delta}}}{\log(1+z)} = \infty,$$

there exist a $c > 0$ and $z_0 \geq 0$ such that $\log(z+1) \leq c(z+1)^{1-\frac{1}{1+\delta}}$ for $z \geq z_0$. As $(z+1)^{1-\frac{1}{1+\delta}}$ is positive for $z \geq 0$, there exist a sufficiently large constant, c_δ , such that $\log(z+1) \leq c_\delta(z+1)^{1-\frac{1}{1+\delta}}$ for $z \geq 0$.

Now let $\delta = 0.1$. We show the minimum of $\phi(z) := 4.05(z+1)^{1/11} - \log(z+1)$ is positive. Notice that $\phi(0) > 0$, and $\lim_{z \rightarrow \infty} \phi(z) = \infty$. The only zero of $\phi'(z)$ occurs at $z^* = \left(\frac{11}{4.05}\right)^{11} - 1$. Finally, $\phi(z^*) > 0$. □

LEMMA 3.2.4. *Let $\epsilon > 0$, and U be an arbitrary initial upper bound for f_{\max} . Then there is a $k \geq 1$ such that $U_k - L_k \leq \epsilon f_{\max}$ where k depends polynomially on $1/\epsilon$, linearly in $U/M\mathcal{L}$, and logarithmically on $UM\mathcal{L}$. Moreover, for this choice of k , L_k is a $(1-\epsilon)$ -approximation to the optimal value f_{\max} and U_k is a $(1+\epsilon)$ -approximation to f_{\max} .*

PROOF. Let

$$k = \left\lceil \max \left\{ d \left(\frac{U}{M\mathcal{L}} - 1 \right), \frac{d}{(\epsilon+1)^{1/3}-1}, 3d \log(UM\mathcal{L}) \left(1 + \frac{1}{\epsilon} \right), O \left(\left(1 + \frac{1}{\epsilon} \right)^{1+\delta} \right) \right\} \right\rceil,$$

where the last term is understood to mean for every $\delta > 0$, there exist a $c_\delta > 0$ so that k should be larger than $d \left((3c_\delta)^{1+\delta} \left(1 + \frac{1}{\epsilon} \right)^{1+\delta} - 1 \right)$. In particular, if $\delta = 0.1$, then c_δ could be 4.05.

The first term ensures the formula for U_k holds because

$$k \geq d \left(\frac{U}{M\mathcal{L}} - 1 \right) \geq d \left(\frac{f_{\max}}{M\mathcal{L}} - 1 \right).$$

In terms of a algorithmic implementation, other upper bounds for $d \left(\frac{f_{\max}}{M\mathcal{L}} - 1 \right)$ can be used; for instance, because $f_{\max} - f_{\min} \leq M\mathcal{L}$, $d \left(\frac{f_{\max}}{M\mathcal{L}} - 1 \right) \leq \frac{df_{\min}}{M\mathcal{L}} \leq \frac{df(x_0)}{M\mathcal{L}}$ where x_0 is any point in the domain.

Notice that $\frac{1}{(\epsilon+1)^{1/3}-1} = \frac{1}{\epsilon} + 1 + O(\epsilon)$, so k is bounded by a polynomial in $1/\epsilon$. We proceed with an “ $\epsilon/3$ ” argument.

Because $k \geq \frac{d}{(\epsilon+1)^{1/3}-1}$, after rearranging we have

$$(\epsilon + 1)^{1/3} \geq \frac{d}{k} + 1 = \frac{d+k}{k}.$$

Using the logarithm produces the bounds

$$(3.5) \quad \frac{\log(\epsilon + 1)}{3} \geq \log\left(\frac{d+k}{k}\right) \geq \frac{k}{d+k} \log\left(\frac{d+k}{k}\right).$$

Next, because $k \geq 3d \log(UM\mathcal{L}) \left(1 + \frac{1}{\epsilon}\right)$, we can rearrange this to

$$k \geq 3d \log(UM\mathcal{L}) \left(1 + \frac{1}{\epsilon}\right) \geq \frac{3d \log(UM\mathcal{L})}{\log(\epsilon + 1)} \geq \frac{d[\log(UM\mathcal{L}) - \log(\epsilon + 1)/3]}{\log(\epsilon + 1)/3}$$

where the second inequality comes from Lemma 3.2.2, and the third inequality comes from the fact that $\log(\epsilon + 1) > 0$. After further rearranging of the first and last expressions, we get

$$(3.6) \quad \frac{\log(\epsilon + 1)}{3} \geq \frac{d}{d+k} \log(UM\mathcal{L}).$$

Finally, fix $\delta > 0$, then because $k \geq d \left((3c_\delta)^{1+\delta} \left(1 + \frac{1}{\epsilon}\right)^{1+\delta} - 1 \right)$, rearranging terms results in

$$\frac{k}{d} + 1 \geq (3c_\delta)^{1+\delta} \left(1 + \frac{1}{\epsilon}\right)^{1+\delta}.$$

Then Lemma 3.2.2 implies

$$\frac{k}{d} + 1 \geq \frac{(3c_\delta)^{1+\delta}}{\log(1 + \epsilon)^{1+\delta}},$$

and after solving for the log term gives

$$\frac{\log(1 + \epsilon)}{3} \geq \frac{c_\delta}{\left(\frac{k}{d} + 1\right)^{\frac{1}{1+\delta}}}.$$

Then Lemma 3.2.3 with $z = k/d$ yields

$$(3.7) \quad \frac{\log(1 + \epsilon)}{3} \geq \frac{\log\left(1 + \frac{k}{d}\right)}{1 + \frac{k}{d}} = \frac{d}{d+k} \log\left(\frac{d+k}{d}\right).$$

Using Equations (3.5), (3.6), and (3.7) results in the inequality

$$\begin{aligned} \log(\epsilon + 1) &\geq \frac{d}{d+k} \log\left(\frac{d+k}{d}\right) + \frac{d}{d+k} \log(UM\mathcal{L}) + \frac{k}{d+k} \log\left(\frac{d+k}{k}\right) \\ &= \frac{d}{d+k} \log\left(\frac{UM\mathcal{L}(d+k)}{d}\right) + \frac{k}{d+k} \log\left(\frac{d+k}{k}\right), \end{aligned}$$

which implies

$$\epsilon \geq U^{\frac{d}{d+k}} \left(\frac{M\mathcal{L}(d+k)}{d}\right)^{\frac{d}{d+k}} \left(\frac{d+k}{k}\right)^{\frac{k}{d+k}} - 1.$$

Finally, because $\frac{1}{d+k} - \frac{1}{k} = \frac{1}{k} \cdot \frac{d}{d+k}$ we have that

$$\begin{aligned} U_k - L_k &= \left(\left(\frac{\int_P f^k dx}{\text{vol}(P)} \right)^{\frac{1}{d+k}} \left(\frac{M\mathcal{L}}{\epsilon'} \right)^{\frac{d}{d+k}} \left(\frac{1}{1-\epsilon'} \right)^{\frac{k}{d+k}} \right) - \left(\frac{\int_P f^k dx}{\text{vol}(P)} \right)^{1/k} \\ &= \left(\frac{\int_P f^k dx}{\text{vol}(P)} \right)^{1/k} \left(\left(\frac{\int_P f^k dx}{\text{vol}(P)} \right)^{\frac{1}{d+k} - \frac{1}{k}} \left(\frac{M\mathcal{L}}{\frac{d}{d+k}} \right)^{\frac{d}{d+k}} \left(\frac{1}{1-d/(d+k)} \right)^{\frac{k}{d+k}} - 1 \right) \\ &\leq f_{\max} \left(\left(\frac{\int_P f^k dx}{\text{vol}(P)} \right)^{\frac{1}{d+k} - \frac{1}{k}} \left(\frac{M\mathcal{L}}{\frac{d}{d+k}} \right)^{\frac{d}{d+k}} \left(\frac{1}{1-d/(d+k)} \right)^{\frac{k}{d+k}} - 1 \right) \\ &\leq f_{\max} \left(U^{\frac{d}{d+k}} \left(\frac{M\mathcal{L}(d+k)}{d} \right)^{\frac{d}{d+k}} \left(\frac{d+k}{k} \right)^{\frac{k}{d+k}} - 1 \right) \\ &\leq f_{\max} \cdot \epsilon. \end{aligned}$$

L_k is a $(1 - \epsilon)$ -approximation to f_{\max} because

$$f_{\max} \leq U_k = L_k + (U_k - L_k) \leq L_k + \epsilon f_{\max}$$

and U_k is a $(1 + \epsilon)$ -approximation to f_{\max} because

$$U_k - \epsilon f_{\max} \leq U_k + (L_k - U_k) = L_k \leq f_{\max}.$$

□

An important input to our approximation bounds is a Lipschitz constant \mathcal{L} satisfying $|f(x) - f(y)| \leq \mathcal{L} \|x - y\|_\infty$ for all $x, y \in P$. One natural way to compute this constant is by maximizing $\|\nabla f(x)\|_1$ on P . However this is a difficult problem in general. Instead, one can compute a potentially larger constant by following the next lemma, which produces a Lipschitz constant of polynomial size and in linear time.

LEMMA 3.2.5 (Lemma 11 in [60]). *Let f be a polynomial in d variables with maximum total degree D . Let c denote the largest absolute value of a coefficient of f . Then there exists a Lipschitz constant \mathcal{L} such that $|f(x) - f(y)| \leq \mathcal{L} \|x - y\|_\infty$ for all $|x_i|, |y_i| \leq M$. The constant \mathcal{L} is $O(D^{d+1}cM^D)$, and is computable in linear time in the number of monomials of f .*

Before closing this section, we remark that Theorem 3.2.1 could also be applied for global maximization. If a polynomial has a global maximum, then there is a $M > 0$ such that the maximum is contained in the box $P := [-M, M]^d$. If M can be computed or estimated, this reduces the unbounded problem to maximizing $f(x)$ over P .

3.2.1. An example. We now illustrate our bounds on an example. Let $f(x) = x_1^2 x_2 - x_1 x_2$ with $x_1 \in [1, 3]$ and $x_2 \in [1, 3]$. Note that $f(x)$ is nonnegative on its domain $P = [1, 3]^2$.

For the Lipschitz constant, we could easily maximize $\|\nabla f(x)\|_1$ on P which for this problem is 21. However let us use the bound produced by Lemma 3.2.5 which gives $\mathcal{L} = 33$.

Using our new bounds from Theorem 3.2.1, we have $L_k \leq f_{\max} \leq U_k$ where

$$L_k := \left(\frac{\int_P f(x)^k dx}{\text{vol}(P)} \right)^{1/k}$$

and

$$U_k := \left(\frac{\int_P f(x)^k dx}{\text{vol}(P)} \right)^{1/(d+k)} \left(\frac{M\mathcal{L}}{\epsilon'} \right)^{d/(d+k)} \frac{1}{(1 - \epsilon')^{k/(d+k)}}.$$

Here, $M = 2$, $\epsilon' = \frac{2}{2+k}$, and $\mathcal{L} = 33$. Then for different values of k , the bounds are:

k	L_k	U_k
10	11.07	23.40
20	13.22	20.75
30	14.27	19.84
40	14.91	19.38

Next we want to apply Lemma 3.2.4 when $\epsilon = 0.1$. Using $U = 19.38$, we see that k has to be at least

$$k = \lceil \max\{-1.4, 62.0, 472.2, 434.1\} \rceil$$

to guarantee that $U_k - L_k \leq f_{\max} \cdot \epsilon = 1.8$. However for this example $k = 126$ suffices: $U_{126} - L_{126} = 1.7$.

The integration of $f(x)^k$ can easily be done with the fundamental theorem of calculus because the domain is a box. For general rational full-dimensional polytopes, any method in Chapter 2 can be used.

3.2.2. Summary of the algorithm. Notice that both Theorem 3.1.3 and 3.2.1 require the polynomial $f(x)$ to be nonnegative on the domain P . A shift, $s \in \mathbb{R}$, could be added to $f(x)$ so that $f(x) + s$ is nonnegative on P . We see that any s such that $s \geq -f_{\min}$ will work.

To find such a shift s , we could follow the suggestion in [60] and use linear programming to find the range of each variable x_i and compute $f(x) \geq -rCM^D = -s$, where r is the number of monomials of $f(x)$, C is the largest absolute value of each coefficient in $f(x)$, D is the total degree of $f(x)$, and M is the largest bound on the variables. Another way is to compute a Handelman decomposition for $f(x)$ on P .

Algorithm 8 gives the final connection between optimizing a polynomial, computing integrals, and the Handelman decomposition.

THEOREM 3.2.6. *Fix the dimension d and the number of facets n in P . If $f(x)$ has a Handelman decomposition of order bounded by D , then Algorithm 8 runs in time polynomial in k , D , and the input size of f and P .*

PROOF. Because $f(x)$ had a Handelman decomposition of order bounded by D , let $t = D$. The linear program that is solved has a matrix with dimension at most $O(D^d) \times O(D^n)$. Expanding

3.2. CONTINUOUS OPTIMIZATION

Algorithm 8 Computing $\int_P (f(x) + s)^k dx$ via Handelman for Theorem 3.2.1

Input: A polynomial $f(x) \in \mathbb{Q}[x_1, \dots, x_d]$ of degree D , polytope P , and k .

Output: s such that $f(x) + s \geq 0$ on P , and $\int_P (f(x) + s)^k dx$.

- (1) Let $t \leftarrow D$
 - (2) Find $s \in \mathbb{R}$ and $c_\alpha \geq 0$ such that $f(x) + s = \sum_{|\alpha| \leq t} c_\alpha g^\alpha$ by solving a linear program
 - (3) Expand $h(x) := (\sum_{|\alpha| \leq t} c_\alpha g^\alpha)^k$ to get a new sum of products of affine functions
 - (4) Integrate each Handelman monomial in $h(x)$ by the methods in Section 2.2
-

$(\sum_{|\alpha| \leq t} c_\alpha g^\alpha)^k$ has at most $\binom{kD+n}{n} = O((kD)^n)$ Handelman terms. Finally, each term can be integrated in time polynomial in kD . □

Notice that Steps (2) and (3) in Algorithm 8 can be swapped, resulting in the same time complexity. For example, $h(x) := (f(x) + s)^k$ could first be expanded, and then a Handelman decomposition could be found for $h(x)$.

CHAPTER 4

Top coefficients of the Ehrhart polynomial for knapsack polytopes

This chapter is mostly a highlight of [12]. Let $\alpha = [\alpha_1, \alpha_2, \dots, \alpha_N, \alpha_{N+1}]$ be a sequence of positive integers. If t is a non-negative integer, we denote by $E(\alpha; t)$ the number of solutions in non-negative integers of the equation

$$\sum_{i=1}^{N+1} \alpha_i x_i = t.$$

In other words, $E(\alpha; t)$ is the same as the number of partitions of the number t using the parts $\alpha_1, \alpha_2, \dots, \alpha_N, \alpha_{N+1}$ (with repetitions allowed).

We will use the notation $f(a_1, \dots, a_n; x_1, \dots, x_m)$ to stress that we will think of the a_i as parameters to the function f while the x_i are the important variables. The combinatorial function $E(\alpha; t)$ was called by J. Sylvester the *denumerant*. The denumerant $E(\alpha; t)$ has a beautiful structure: it has been known since the times of Cayley and Sylvester that $E(\alpha; t)$ is in fact a *quasi-polynomial*, i.e., it can be written in the form $E(\alpha; t) = \sum_{i=0}^N E_i(t)t^i$, where $E_i(t)$ is a periodic function of t . In other words, there exists a positive integer Q such that for t in the coset $q + Q\mathbb{Z}$, the function $E(\alpha; t)$ coincides with a polynomial function of t . This chapter presents an algorithm to compute individual coefficients of this function and explores their periodicity. Sylvester and Cayley first showed that the coefficients $E_i(t)$ are periodic functions having period equal to the least common multiple of $\alpha_1, \dots, \alpha_{d+1}$ (see [22, 27] and references therein). In 1943, E. T. Bell gave a simpler proof and remarked that the period Q is in the worst case given by the least common multiple of the α_i , but in general it can be smaller. A classical observation that goes back to I. Schur is that when the list α consist of relatively prime numbers, then asymptotically

$$E(\alpha; t) \approx \frac{t^N}{N! \alpha_1 \alpha_2 \cdots \alpha_{N+1}} \quad \text{as the number } t \rightarrow \infty.$$

EXAMPLE 4.0.7. Let $\alpha = [6, 2, 3]$. Then on each of the cosets $q + 6\mathbb{Z}$, the function $E(\alpha; t)$ coincides with a polynomial $E^{[q]}(t)$. Here are the corresponding polynomials.

$$\begin{aligned} E^{[0]}(t) &= \frac{1}{72}t^2 + \frac{1}{4}t + 1, & E^{[1]}(t) &= \frac{1}{72}t^2 + \frac{1}{18}t - \frac{5}{72}, \\ E^{[2]}(t) &= \frac{1}{72}t^2 + \frac{7}{36}t + \frac{5}{9}, & E^{[3]}(t) &= \frac{1}{72}t^2 + \frac{1}{6}t + \frac{3}{8}, \\ E^{[4]}(t) &= \frac{1}{72}t^2 + \frac{5}{36}t + \frac{2}{9}, & E^{[5]}(t) &= \frac{1}{72}t^2 + \frac{1}{9}t + \frac{7}{72}. \end{aligned}$$

Then the number of nonnegative solutions in $x \in \mathbb{Z}^3$ to $6x_1 + 2x_2 + 3x_3 = 10$ is given by

$$E^{[10 \bmod 6]}(10) = E^{[4]}(10) = 3.$$

It is interesting to note that the coefficients of the polynomial $E^{[t \bmod 6]}(t)$ may not be integer, but the evaluation will always be integer as they count integer solutions to an equation. Also, the coefficient of the highest degree (the t^N term) is constant. In other examples, more t^m terms could be constant.

Naturally, the function $E(\alpha; t)$ is equal to 0 if t does not belong to the lattice $\sum_{i=1}^{N+1} \mathbb{Z}\alpha_i \subset \mathbb{Z}$ generated by the integers α_i . Note that if g is the greatest common divisor of the α_i (which can be computed in polynomial time), and $\alpha/g = [\frac{\alpha_1}{g}, \frac{\alpha_2}{g}, \dots, \frac{\alpha_{N+1}}{g}]$ the formula $E(\alpha; gt) = E(\alpha/g, t)$ holds, hence we assume that the numbers α_i span \mathbb{Z} without changing the complexity of the problem. In other words, we assume that the greatest common divisor of the α_i is equal to 1. With this assumption, there is a large enough integer F such that for any $t \geq F$, $E(\alpha)(t) > 0$ and there is a largest t for which $E(\alpha; t) = 0$.

The focus of this chapter is on developing the polynomial time algorithm that is stated in Theorem 4.0.8.

THEOREM 4.0.8. *Given any fixed integer k , there is a polynomial time algorithm to compute the highest $k + 1$ degree terms of the quasi-polynomial $E(\alpha; t)$, that is*

$$\text{Top}_k E(\alpha; t) = \sum_{i=0}^k E_{N-i}(t)t^{N-i}.$$

The coefficients are recovered as step polynomial functions of t .

As noted in Section 1.4, computing $E(\boldsymbol{\alpha}; t)$ for a given t , is $\#P$ -hard, and computing the polynomial $E^{[q]}(t)$ is NP-hard. Despite this difficulty, when $N + 1$ is fixed, the entire quasi-polynomial $E(\boldsymbol{\alpha}; t)$ can be computed in polynomial time [21, 91]. The above theorem instead allows $N + 1$ to vary but fixes k , computing just the top k terms of the quasi-polynomial $E(\boldsymbol{\alpha}; t)$ in polynomial time.

Note that the number Q of cosets for $E(\boldsymbol{\alpha}; t)$ can be exponential in the binary encoding size of the problem, and thus it is impossible to list, in polynomial time, the polynomials $E^{[q]}(t)$ for all the cosets $q + Q\mathbb{Z}$. That is why to obtain a polynomial time algorithm, the output is presented in the format of *step polynomials*, which we define next.

- (1) Let $\{s\} := s - \lfloor s \rfloor \in [0, 1)$ for $s \in \mathbb{R}$, where $\lfloor s \rfloor$ denotes the largest integer smaller or equal to s . The function $\{s + 1\} = \{s\}$ is a periodic function of s modulo 1.
- (2) If r is rational with denominator q , the function $T \mapsto \{rT\}$ is a function of $T \in \mathbb{R}$ periodic modulo q . A function of the form $T \mapsto \sum_i c_i \{r_i T\}$ will be called a *(rational) step linear function*. If all the r_i have a common denominator q , this function is periodic modulo q .
- (3) Then consider the algebra generated over \mathbb{Q} by such functions on \mathbb{R} . An element ϕ of this algebra can be written (not in a unique way) as

$$\phi(T) = \sum_{l=1}^L c_l \prod_{j=1}^{J_l} \{r_{l,j} T\}^{n_{l,j}}.$$

Such a function $\phi(T)$ will be called a *(rational) step polynomial*.

- (4) We will say that the step polynomial ϕ is of *degree* (at most) u if $\sum_j n_{l,j} \leq u$ for each index l occurring in the formula for ϕ . As a side note, this notion of degree only induces a filtration, not a grading, on the algebra of step polynomials, because there exist polynomial relations between step linear functions and therefore several step-polynomial formulas with different degrees may represent the same function. We will say that ϕ is of *period* q if all the rational numbers r_j have common denominator q .

In Example 4.0.7, instead of the $Q = 6$ polynomials $E^{[0]}(t), \dots, E^{[5]}(t)$ that we wrote down, we could write a single closed formula, where the coefficients of powers of t are step polynomials in t :

$$\frac{1}{72} t^2 + \left(\frac{1}{4} - \frac{\{-\frac{t}{3}\}}{6} - \frac{\{\frac{t}{2}\}}{6} \right) t + \left(1 - \frac{3}{2} \{-\frac{t}{3}\} - \frac{3}{2} \{\frac{t}{2}\} + \frac{1}{2} (\{-\frac{t}{3}\})^2 + \{-\frac{t}{3}\} \{\frac{t}{2}\} + \frac{1}{2} (\{\frac{t}{2}\})^2 \right).$$

For larger Q , one can see that this step polynomial representation is much more economical than writing the individual polynomials for each of the cosets of the period Q .

4.1. The residue formula for $E(\boldsymbol{\alpha}; t)$

Let us begin fixing some notation. If $\phi(z) dz$ is a meromorphic one form on \mathbb{C} , with a pole at $z = \zeta$, we write

$$\text{Res}_{z=\zeta} \phi(z) dz = \frac{1}{2\pi i} \int_{C_\zeta} \phi(z) dz,$$

where C_ζ is a small circle around the pole ζ . If $\phi(z) = \sum_{k \geq k_0} \phi_k z^k$ is a Laurent series in z , we denote by $\text{res}_{z=0}$ the coefficient of z^{-1} of $\phi(z)$. Cauchy's formula implies that $\text{res}_{z=0} \phi(z) = \text{Res}_{z=0} \phi(z) dz$.

Let $\boldsymbol{\alpha} = [\alpha_1, \alpha_2, \dots, \alpha_{N+1}]$ be a list of integers. Define

$$F(\boldsymbol{\alpha}; z) := \frac{1}{\prod_{i=1}^{N+1} (1 - z^{\alpha_i})}.$$

Denote by $\mathcal{P} = \bigcup_{i=1}^{N+1} \{ \zeta \in \mathbb{C} : \zeta^{\alpha_i} = 1 \}$ the set of poles of the meromorphic function $F(\boldsymbol{\alpha})$ and by $p(\zeta)$ the order of the pole ζ for $\zeta \in \mathcal{P}$.

Note that because the α_i have greatest common divisor 1, we have $\zeta = 1$ as a pole of order $N + 1$, and the other poles have order strictly smaller.

THEOREM 4.1.1 (Theorem 2.1 in [12]). *Let $\boldsymbol{\alpha} = [\alpha_1, \alpha_2, \dots, \alpha_{N+1}]$ be a list of integers with greatest common divisor equal to 1, and let*

$$F(\boldsymbol{\alpha}; z) := \frac{1}{\prod_{i=1}^{N+1} (1 - z^{\alpha_i})}.$$

If t is a non-negative integer, then

$$(4.1) \quad E(\boldsymbol{\alpha}; t) = - \sum_{\zeta \in \mathcal{P}} \text{Res}_{z=\zeta} z^{-t-1} F(\boldsymbol{\alpha}; z) dz$$

and the ζ -term of this sum is a quasi-polynomial function of t with degree less than or equal to $p(\zeta) - 1$.

4.1.1. Poles of high and low order. Given an integer $0 \leq k \leq N$, we partition the set of poles \mathcal{P} in two disjoint sets according to the order of the pole:

$$\mathcal{P}_{>N-k} = \{ \zeta : p(\zeta) \geq N + 1 - k \}, \quad \mathcal{P}_{\leq N-k} = \{ \zeta : p(\zeta) \leq N - k \}.$$

EXAMPLE 4.1.2.

- (1) Let $\boldsymbol{\alpha} = [98, 59, 44, 100]$, so $N = 3$, and let $k = 1$. Then $\mathcal{P}_{>N-k}$ consists of poles of order greater than 2. Of course $\zeta = 1$ is a pole of order 4. Note that $\zeta = -1$ is a pole of order 3. So $\mathcal{P}_{>N-k} = \{ \zeta : \zeta^2 = 1 \}$.
- (2) Let $\boldsymbol{\alpha} = [6, 2, 2, 3, 3]$, so $N = 4$, and let $k = 2$. Let $\zeta_6 = e^{2\pi i/6}$ be a primitive 6th root of unity. Then $\zeta_6^6 = 1$ is a pole of order 5, ζ_6 and ζ_6^5 are poles of order 1, and $\zeta_6^2, \zeta_6^3 = -1, \zeta_6^4$ are poles of order 3. Thus $\mathcal{P}_{>N-k} = \mathcal{P}_{>2}$ is the union of $\{ \zeta : \zeta^2 = 1 \} = \{-1, 1\}$ and $\{ \zeta : \zeta^3 = 1 \} = \{\zeta_6^2, \zeta_6^4, \zeta_6^6 = 1\}$.

According to the disjoint decomposition $\mathcal{P} = \mathcal{P}_{\leq N-k} \cup \mathcal{P}_{>N-k}$, we write

$$E_{\mathcal{P}_{>N-k}}(t) = - \sum_{\zeta \in \mathcal{P}_{>N-k}} \operatorname{Res}_{z=\zeta} z^{-t-1} F(\boldsymbol{\alpha}; z) \, dz$$

and

$$E_{\mathcal{P}_{\leq N-k}}(t) = - \sum_{\zeta \in \mathcal{P}_{\leq N-k}} \operatorname{Res}_{z=\zeta} z^{-t-1} F(\boldsymbol{\alpha}; z) \, dz.$$

The following proposition is a direct consequence of Theorem 4.1.1.

PROPOSITION 4.1.3. *We have*

$$E(\boldsymbol{\alpha}; t) = E_{\mathcal{P}_{>N-k}}(t) + E_{\mathcal{P}_{\leq N-k}}(t),$$

where the function $E_{\mathcal{P}_{\leq N-k}}(t)$ is a quasi-polynomial function in the variable t of degree strictly less than $N - k$.

Thus for the purpose of computing $\text{Top}_k E(\boldsymbol{\alpha}; t)$ it is sufficient to compute the function $E_{\mathcal{P}_{>N-k}}(t)$. Notice that in order to compute $E_{\mathcal{P}_{>N-k}}(t)$, we need to compute a residue for every $\zeta \in \mathcal{P}_{>N-k}$. It turns out many of these residue calculations can be grouped together. We will do this by looking at a poset structure of $\mathcal{P}_{>N-k}$ and by using generating functions. We discuss this in the next two sections.

4.2. Using the poset structure of the α_i

We first rewrite our set $\mathcal{P}_{>N-k}$. Note that if ζ is a pole of order $\geq p$, this means that there exist at least p elements α_i in the list $\boldsymbol{\alpha}$ so that $\zeta^{\alpha_i} = 1$. But if $\zeta^{\alpha_i} = 1$ for a set $I \subseteq \{1, \dots, N+1\}$ of indices i , this is equivalent to the fact that $\zeta^f = 1$, for f the greatest common divisor of the elements $\alpha_i, i \in I$.

Now let $\mathcal{I}_{>N-k}$ be the set of subsets of $\{1, \dots, N+1\}$ of cardinality greater than $N-k$. Note that when k is fixed, the cardinality of $\mathcal{I}_{>N-k}$ is a polynomial function of N . For each subset $I \in \mathcal{I}_{>N-k}$, define f_I to be the greatest common divisor of the corresponding sublist $\alpha_i, i \in I$. Let $\mathcal{G}_{>N-k}(\boldsymbol{\alpha}) = \{f_I : I \in \mathcal{I}_{>N-k}\}$ be the set of integers so obtained and let $G(f) \subset \mathbb{C}^\times$ be the group of f -th roots of unity,

$$G(f) = \{\zeta \in \mathbb{C} : \zeta^f = 1\}.$$

The set $\{G(f) : f \in \mathcal{G}_{>N-k}(\boldsymbol{\alpha})\}$ forms a poset $\tilde{P}_{>N-k}$ (partially ordered set) with respect to reverse inclusion. That is, $G(f_i) \preceq_{\tilde{P}_{>N-k}} G(f_j)$ if $G(f_j) \subseteq G(f_i)$ (the i and j become swapped). Notice $G(f_j) \subseteq G(f_i) \Leftrightarrow f_j$ divides f_i . Even if $\tilde{P}_{>N-k}$ has a unique minimal element, we add an element $\hat{0}$ such that $\hat{0} \preceq G(f)$ and call this new poset $P_{>N-k}$.

In terms of the group $G(f)$ we have thus $\mathcal{P}_{>N-k} = \bigcup_{f \in \mathcal{G}_{>N-k}(\boldsymbol{\alpha})} G(f)$. This is, of course, not a disjoint union, but using the inclusion–exclusion principle, we can write the indicator function of the set $\mathcal{P}_{>N-k}$ as a linear combination of indicator functions of the sets $G(f)$:

$$[\mathcal{P}_{>N-k}] = \sum_{f \in \mathcal{G}_{>N-k}(\boldsymbol{\alpha})} \mu_{>N-k}(f)[G(f)],$$

4.2. USING THE POSET STRUCTURE OF THE α_I

where $\mu_{>N-k}(f) := -\mu'_{>N-k}(\hat{0}, G(f))$ and $\mu'_{>N-k}(x, y)$ is the standard Möbius function for the poset $P_{>N-k}$:

$$\begin{aligned}\mu'_{>N-k}(s, s) &= 1 && \forall s \in P_{>N-k}, \\ \mu'_{>N-k}(s, u) &= - \sum_{s \preceq t \prec u} \mu'_{>N-k}(s, t) && \forall s \prec u \text{ in } P_{>N-k}.\end{aligned}$$

For simplicity, $\mu_{>N-k}$ will be called the *Möbius function* for the poset $P_{>N-k}$ and will be denoted simply by $\mu(f)$. We also have the relationship

$$\begin{aligned}\mu(f) &= -\mu'_{>N-k}(\hat{0}, G(f)) \\ &= 1 + \sum_{\hat{0} \prec G(t) \prec G(f)} \mu'_{>N-k}(\hat{0}, G(t)) \\ &= 1 - \sum_{\hat{0} \prec G(t) \prec G(f)} -\mu'_{>N-k}(\hat{0}, G(t)) \\ &= 1 - \sum_{\hat{0} \prec G(t) \prec G(f)} \mu(t).\end{aligned}$$

EXAMPLE 4.2.1 (Example 4.1.2, continued).

- (1) Here we have $\mathcal{I}_{>N-k} = \mathcal{I}_{>2} = \{\{1, 2, 3\}, \{1, 2, 4\}, \{1, 3, 4\}, \{2, 3, 4\}, \{1, 2, 3, 4\}\}$ and $\mathcal{G}_{>N-k}(\alpha) = \{1, 1, 2, 1, 1\} = \{1, 2\}$. Accordingly, $\mathcal{P}_{>N-k} = G(1) \cup G(2)$. The poset $P_{>2}$ is

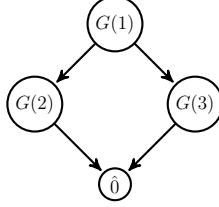


The arrows denote subsets, that is $G(1) \subset G(2)$ and $\hat{0}$ can be identified with the unit circle. The Möbius function μ is simply given by $\mu(1) = 0$, $\mu(2) = 1$, and so $[\mathcal{P}_{>N-k}] = [G(2)]$.

- (2) Now $\mathcal{I}_{>N-k} = \mathcal{I}_{>2} = \{\{1, 2, 3\}, \{1, 2, 4\}, \dots, \{3, 4, 5\}, \{1, 2, 3, 4\}, \{1, 2, 3, 5\}, \{1, 2, 4, 5\}, \{1, 3, 4, 5\}, \{2, 3, 4, 5\}, \{1, 2, 3, 4, 5\}\}$ and thus $\mathcal{G}_{>N-k}(\alpha) = \{2, 3, 1, 1\} = \{1, 2, 3\}$. Hence

4.2. USING THE POSET STRUCTURE OF THE α_I

$\mathcal{P}_{>N-k} = G(1) \cup G(2) \cup G(3) = \{1\} \cup \{-1, 1\} \cup \{\zeta_3, \zeta_3^2, 1\}$, where $\zeta_3 = e^{2\pi i/3}$ is a primitive 3rd root of unity.



The Möbius function μ is then $\mu(3) = 1$, $\mu(2) = 1$, $\mu(1) = -1$, and thus $[\mathcal{P}_{>N-k}] = -[G(1)] + [G(2)] + [G(3)]$.

THEOREM 4.2.2. *Given a list $\alpha = [\alpha_1, \dots, \alpha_{N+1}]$ and a fixed integer k , then the values for the Möbius function for the poset $\mathcal{P}_{>N-k}$ can be computed in polynomial time.*

PROOF. First find the greatest common divisor of all sublists of the list α with size greater than $N - k$. Let V be the set of integers obtained from all such greatest common divisors. We note that each node of the poset $\mathcal{P}_{>N-k}$ is a group of roots of unity $G(v)$. But it is labeled by a non-negative integer v .

Construct an array M of size $|V|$ to keep the value of the Möbius function. Initialize M to hold the Möbius values of infinity: $M[v] \leftarrow \infty$ for all $v \in V$. Then call Algorithm 9 below with $\text{findMöbius}(1, V, M)$.

Algorithm 9 terminates because the number of nodes v with $M[v] = \infty$ decreases to zero in each iteration. To show correctness, consider a node v in the poset \mathcal{P}_{N-k} . If v covers $\hat{0}$, then we must have $M[v] = 1$ as there is no other $G(w)$ with $G(f) \subset G(w)$. Else if v does not cover $\hat{0}$, we set $M[v]$ to be 1 minus the sum $\sum_{w: v|w} M[w]$ which guarantees that the poles in $G(v)$ are only counted once because $\sum_{w: v|w} M[w]$ is how many times $G(v)$ is a subset of another element that has already been counted.

The number of sublists of α considered is $\binom{N}{1} + \binom{N}{2} + \dots + \binom{N}{k} = O(N^k)$, which is a polynomial for k fixed. For each sublist, the greatest common divisor of a set of integers is computed in polynomial time. Hence $|V| = O(N^k)$. Notice that lines 4 to 14 of Algorithm 9 are executed at most $O(|V|)$ times as once a $M[v]$ value is computed, it is never recomputed. The number of

Algorithm 9 findMöbius(n, V, M)

Input: n : the label of node $G(n)$ in the poset $\tilde{P}_{>N-k}$
Input: V : list of numbers in the poset $\tilde{P}_{>N-k}$
Input: M : array of current Möbius values computed for $P_{>N-k}$
Output: updates the array M of Möbius values

- 1: **if** $M[n] < \infty$ **then**
- 2: **return**
- 3: **end if**
- 4: $L \leftarrow \{v \in V : n \mid v\} \setminus \{n\}$
- 5: **if** $L = \emptyset$ **then**
- 6: $M[n] \leftarrow 1$
- 7: **return**
- 8: **end if**
- 9: $M[n] \leftarrow 0$
- 10: **for all** $v \in L$ **do**
- 11: findMöbius(v, L, M)
- 12: $M[n] \leftarrow M[n] + M[v]$
- 13: **end for**
- 14: $M[n] \leftarrow 1 - M[n]$

additions on line 12 is $O(|V|^2)$ while the number of divisions on line 4 is also $O(|V|^2)$. Hence this algorithm finds the Möbius function in $O(|V|^2) = O(N^{2k})$ time where k is fixed. \square

Let us define for any positive integer f

$$E(\boldsymbol{\alpha}, f; t) = - \sum_{\zeta: \zeta^f=1} \text{Res}_{z=\zeta} z^{-t-1} F(\boldsymbol{\alpha}; z) dz.$$

PROPOSITION 4.2.3. *Let k be a fixed integer, then*

$$(4.2) \quad E_{\mathcal{P}_{>N-k}}(t) = \sum_{f \in \mathcal{G}_{>N-k}(\boldsymbol{\alpha})} \mu(f) E(\boldsymbol{\alpha}, f; t).$$

4.2.1. Partial summary so far. As a partial summary, for a fixed integer k , our original goal is to compute

$$\text{Top}_k E(\boldsymbol{\alpha}; t) = \sum_{i=0}^k E_{N-i}(t) t^{N-i},$$

in polynomial time where $E_{N-i}(t)$ are step polynomials. So far we have shown that this is equal to $E_{\mathcal{P}_{>N-k}}(t)$, which in turn is equal to $E_{\mathcal{P}_{>N-k}}(t) = \sum_{f \in \mathcal{G}_{>N-k}(\boldsymbol{\alpha})} \mu(f) E(\boldsymbol{\alpha}, f; t)$. The set $\mathcal{G}_{>N-k}(\boldsymbol{\alpha})$

and the values $\mu(f)$ for $f \in \mathcal{G}_{>N-k}(\boldsymbol{\alpha})$ can be computed in polynomial time in the input size of $\boldsymbol{\alpha}$ when k is fixed. The next section illustrates how to compute $E(\boldsymbol{\alpha}, f; t)$ efficiently.

4.3. Polyhedral reinterpretation of the generating function $E(\boldsymbol{\alpha}, f; t)$

To complete the proof of Theorem 4.0.8 we need only to prove the following proposition.

PROPOSITION 4.3.1. *For any integer $f \in \mathcal{G}_{>N-k}(\boldsymbol{\alpha})$, the coefficient functions of the quasi-polynomial function $E(\boldsymbol{\alpha}, f; t)$ and hence $E_{\mathcal{P}_{>N-k}}(t)$ are computed in polynomial time as step polynomials of t .*

By Proposition 4.2.3 we know we need to compute the value of $E(\boldsymbol{\alpha}, f; t)$. Our goal now is to demonstrate that this function can be thought of as the generating function of the lattice points inside a convex cone. This is a key point to guarantee good computational bounds. Before we can do that we review some preliminaries on generating functions of cones. We recall the notion of generating functions of cones; see also [14].

4.3.1. Review of exponential summation with real shift \mathbf{s} . We will define a *lattice* as the subgroup of all linear combinations of a basis of \mathbb{R}^r with integer coefficients. This material is similar to Section 1.2, but for a general lattice Λ instead of just \mathbb{Z}^r .

Let $V = \mathbb{R}^r$ provided with a lattice Λ , and let V^* denote the dual space. A (*rational*) *simplicial cone* $\mathbf{c} = \mathbb{R}_{\geq 0}\mathbf{w}_1 + \cdots + \mathbb{R}_{\geq 0}\mathbf{w}_r$ is a cone generated by r linearly independent vectors $\mathbf{w}_1, \dots, \mathbf{w}_r$ of Λ . We consider the semi-rational affine cone $\mathbf{s} + \mathbf{c}$, $\mathbf{s} \in V$. Let $\boldsymbol{\xi} \in V^*$ be a dual vector such that $\langle \boldsymbol{\xi}, \mathbf{w}_i \rangle < 0$, $1 \leq i \leq r$. Then the sum

$$S(\mathbf{s} + \mathbf{c}, \Lambda; \boldsymbol{\xi}) = \sum_{\mathbf{n} \in (\mathbf{s} + \mathbf{c}) \cap \Lambda} e^{\langle \boldsymbol{\xi}, \mathbf{n} \rangle}$$

is summable and defines an analytic function of $\boldsymbol{\xi}$. It is well known that this function extends to a meromorphic function of $\boldsymbol{\xi} \in V_{\mathbb{C}}^*$. We still denote this meromorphic extension by $S(\mathbf{s} + \mathbf{c}, \Lambda; \boldsymbol{\xi})$.

EXAMPLE 4.3.2. Let $V = \mathbb{R}$ with lattice \mathbb{Z} , $\mathbf{c} = \mathbb{R}_{\geq 0}$, and $s \in \mathbb{R}$. Then

$$S(s + \mathbb{R}_{\geq 0}, \mathbb{Z}; \xi) = \sum_{n \geq s} e^{n\xi} = e^{\lceil s \rceil \xi} \frac{1}{1 - e^{\xi}}.$$

Using the function $\{x\} = x - \lfloor x \rfloor$, we find $\lceil s \rceil = s + \{-s\}$ and can write

$$(4.3) \quad e^{-s\xi} S(s + \mathbb{R}_{\geq 0}, \mathbb{Z}; \xi) = \frac{e^{\{-s\}\xi}}{1 - e^{\xi}}.$$

Recall the following result:

THEOREM 4.3.3. *Consider the semi-rational affine cone $\mathbf{s} + \mathbf{c}$ and the lattice Λ . The series $S(\mathbf{s} + \mathbf{c}, \Lambda; \boldsymbol{\xi})$ is a meromorphic function of $\boldsymbol{\xi}$ such that $\prod_{i=1}^r \langle \boldsymbol{\xi}, \mathbf{w}_i \rangle \cdot S(\mathbf{s} + \mathbf{c}, \Lambda; \boldsymbol{\xi})$ is holomorphic in a neighborhood of $\mathbf{0}$.*

Let $\mathbf{t} \in \Lambda$. Consider the translated cone $\mathbf{t} + \mathbf{s} + \mathbf{c}$ of $\mathbf{s} + \mathbf{c}$ by \mathbf{t} . Then we have the covariance formula

$$(4.4) \quad S(\mathbf{t} + \mathbf{s} + \mathbf{c}, \Lambda; \boldsymbol{\xi}) = e^{\langle \boldsymbol{\xi}, \mathbf{t} \rangle} S(\mathbf{s} + \mathbf{c}, \Lambda; \boldsymbol{\xi}).$$

Because of this formula, it is convenient to introduce the following function.

DEFINITION 4.3.4. Define the function

$$M(\mathbf{s}, \mathbf{c}, \Lambda; \boldsymbol{\xi}) := e^{-\langle \boldsymbol{\xi}, \mathbf{s} \rangle} S(\mathbf{s} + \mathbf{c}, \Lambda; \boldsymbol{\xi}).$$

Thus the function $\mathbf{s} \mapsto M(\mathbf{s}, \mathbf{c}, \Lambda; \boldsymbol{\xi})$ is a function of $\mathbf{s} \in V/\Lambda$ (a periodic function of \mathbf{s}) whose values are meromorphic functions of $\boldsymbol{\xi}$. It is interesting to introduce this modified function since, as seen in Equation (4.3) in Example 4.3.2, its dependence in \mathbf{s} is via step linear functions of \mathbf{s} .

There is a very special and important case when the function $M(\mathbf{s}, \mathbf{c}, \Lambda; \boldsymbol{\xi}) = e^{-\langle \boldsymbol{\xi}, \mathbf{s} \rangle} S(\mathbf{s} + \mathbf{c}, \Lambda; \boldsymbol{\xi})$ is easy to write down. A *unimodular* cone, is a cone \mathbf{u} whose primitive generators $\mathbf{g}_i^{\mathbf{u}}$ form a basis of the lattice Λ . We introduce the following notation.

DEFINITION 4.3.5. Let \mathbf{u} be a unimodular cone with primitive generators $\mathbf{g}_i^{\mathbf{u}}$ and let $\mathbf{s} \in V$. Then, write $\mathbf{s} = \sum_i s_i \mathbf{g}_i^{\mathbf{u}}$, with $s_i \in \mathbb{R}$, and define

$$\{-\mathbf{s}\}_{\mathbf{u}} = \sum_i \{-s_i\} \mathbf{g}_i^{\mathbf{u}}.$$

Thus $\mathbf{s} + \{-\mathbf{s}\}_u = \sum_i [s_i] \mathbf{g}_i^u$. Note that if $\mathbf{t} \in \Lambda$, then $\{-(\mathbf{s} + \mathbf{t})\}_u = \{-\mathbf{s}\}_u$. Thus, $\mathbf{s} \mapsto \{-\mathbf{s}\}_u$ is a function on V/Λ with value in V . For any $\boldsymbol{\xi} \in V^*$, we then find

$$S(\mathbf{s} + \mathbf{u}, \Lambda; \boldsymbol{\xi}) = e^{\langle \boldsymbol{\xi}, \mathbf{s} \rangle} e^{\langle \boldsymbol{\xi}, \{-\mathbf{s}\}_u \rangle} \frac{1}{\prod_j (1 - e^{\langle \boldsymbol{\xi}, \mathbf{g}_j^u \rangle})}$$

and thus

$$(4.5) \quad M(\mathbf{s}, \mathbf{u}, \Lambda; \boldsymbol{\xi}) = e^{\langle \boldsymbol{\xi}, \{-\mathbf{s}\}_u \rangle} \frac{1}{\prod_j (1 - e^{\langle \boldsymbol{\xi}, \mathbf{g}_j^u \rangle})}.$$

For a general cone \mathbf{c} , we can decompose its indicator function $[\mathbf{c}]$ as a signed sum of indicator functions of unimodular cones, $\sum_u \epsilon_u [\mathbf{u}]$, modulo indicator functions of cones containing lines. As shown by Barvinok (see [17] for the original source and [19] for a great new exposition), if the dimension r of V is fixed, this decomposition can be computed in polynomial time. Then we can write

$$S(\mathbf{s} + \mathbf{c}, \Lambda; \boldsymbol{\xi}) = \sum_u \epsilon_u S(\mathbf{s} + \mathbf{u}, \Lambda; \boldsymbol{\xi}).$$

Thus we obtain, using Formula (4.5),

$$(4.6) \quad M(\mathbf{s}, \mathbf{c}, \Lambda; \boldsymbol{\xi}) = \sum_u \epsilon_u e^{\langle \boldsymbol{\xi}, \{-\mathbf{s}\}_u \rangle} \frac{1}{\prod_j (1 - e^{\langle \boldsymbol{\xi}, \mathbf{g}_j^u \rangle})}.$$

Here \mathbf{u} runs through all the unimodular cones occurring in the decomposition of \mathbf{c} , and the $\mathbf{g}_j^u \in \Lambda$ are the corresponding generators of the unimodular cone \mathbf{u} .

REMARK 4.3.6. For computing explicit examples, it is convenient to make a change of variables that leads to computations in the standard lattice \mathbb{Z}^r . Let B be the matrix whose columns are the generators of the lattice Λ ; then $\Lambda = B\mathbb{Z}^r$.

$$\begin{aligned} M(\mathbf{s}, \mathbf{c}, \Lambda; \boldsymbol{\xi}) &= e^{-\langle \boldsymbol{\xi}, \mathbf{s} \rangle} \sum_{\mathbf{n} \in (\mathbf{s} + \mathbf{c}) \cap B\mathbb{Z}^r} e^{\langle \boldsymbol{\xi}, \mathbf{n} \rangle} \\ &= e^{-\langle B^\top \boldsymbol{\xi}, B^{-1} \mathbf{s} \rangle} \sum_{\mathbf{x} \in B^{-1}(\mathbf{s} + \mathbf{c}) \cap \mathbb{Z}^r} e^{\langle B^\top \boldsymbol{\xi}, \mathbf{x} \rangle} = M(B^{-1} \mathbf{s}, B^{-1} \mathbf{c}, \mathbb{Z}^r; B^\top \boldsymbol{\xi}). \end{aligned}$$

4.3.2. Rewriting $E(\boldsymbol{\alpha}, f; t)$. Currently, we have

$$\begin{aligned} \text{Top}_k E(\boldsymbol{\alpha}; t) &= E_{\mathcal{P}_{>N-k}}(t) = \sum_{i=0}^k E_{N-i}(t)t^{N-i} \\ &= \sum_{f \in \mathcal{G}_{>N-k}(\boldsymbol{\alpha})} \mu(f) E(\boldsymbol{\alpha}, f; t) \\ &= \sum_{f \in \mathcal{G}_{>N-k}(\boldsymbol{\alpha})} \mu(f) \left(- \sum_{\zeta: \zeta^f=1} \text{Res}_{z=\zeta} z^{-t-1} F(\boldsymbol{\alpha}; z) \right). \end{aligned}$$

In the next few sections, $E(\boldsymbol{\alpha}, f; t)$ will be rewritten in terms of lattice points of simplicial cones. This will require some suitable manipulation of the initial form of $E(\boldsymbol{\alpha}, f; t)$.

To start with, we want to write the Ehrhart polynomial $\sum_{i=0}^k E_{N-i}(t)t^{N-i}$ as a function of two variables t and T : $\sum_{i=0}^k E_{N-i}(T)t^{N-i}$. That is, we use T to denote the variable of the periodic coefficients and t to be the variable of the polynomial. To do this, define the function

$$\mathcal{E}(\boldsymbol{\alpha}, f; t, T) = - \text{res}_{z=\zeta} z^{-t-1} \zeta^t \sum_{\zeta: \zeta^f=1} \frac{\zeta^{-T}}{\prod_{i=1}^{N+1} (1 - z^{\alpha_i})}.$$

Notice that the T variable is periodic modulo f . By evaluating at $T = t$, we obtain

$$(4.7) \quad E(\boldsymbol{\alpha}, f; t) = \mathcal{E}(\boldsymbol{\alpha}, f; t, T)|_{T=t}.$$

It will be helpful to perform a change of variables and let $z = \zeta e^x$, then changing coordinates in residue and computing $dz = z dx$ we have that

$$\mathcal{E}(\boldsymbol{\alpha}, f; t, T) = - \text{res}_{x=0} e^{-tx} \sum_{\zeta: \zeta^f=1} \frac{\zeta^{-T}}{\prod_{i=1}^{N+1} (1 - \zeta^{\alpha_i} e^{\alpha_i x})}.$$

DEFINITION 4.3.7. Let k be fixed. For $f \in \mathcal{G}_{>N-k}(\boldsymbol{\alpha})$, define

$$\mathcal{F}(\boldsymbol{\alpha}, f, T; x) := \sum_{\zeta: \zeta^f=1} \frac{\zeta^{-T}}{\prod_{i=1}^{N+1} (1 - \zeta^{\alpha_i} e^{\alpha_i x})},$$

and

$$E_i(f; T) := - \text{res}_{x=0} \frac{(-x)^i}{i!} \mathcal{F}(\boldsymbol{\alpha}, f, T; x).$$

Then

$$\mathcal{E}(\boldsymbol{\alpha}, f; t, T) = -\operatorname{res}_{x=0} e^{-tx} \mathcal{F}(\boldsymbol{\alpha}, f, T; x).$$

The dependence in T of $\mathcal{F}(\boldsymbol{\alpha}, f, T; x)$ is through ζ^T . As $\zeta^f = 1$, the function $\mathcal{F}(\boldsymbol{\alpha}, f, T; x)$ is a periodic function of T modulo f whose values are meromorphic functions of x . Since the pole in x is of order at most $N + 1$, we can rewrite $\mathcal{E}(\boldsymbol{\alpha}, f; t, T)$ in terms of $E_i(f; T)$ and prove:

THEOREM 4.3.8. *Let k be fixed. Then for $f \in \mathcal{G}_{>N-k}(\boldsymbol{\alpha})$ we can write*

$$\mathcal{E}(\boldsymbol{\alpha}, f; t, T) = \sum_{i=0}^N t^i E_i(f; T)$$

with $E_i(f; T)$ a step polynomial of degree less than or equal to $N - i$ and periodic of T modulo f . This step polynomial can be computed in polynomial time.

It is now clear that once we have proved Theorem 4.3.8, then the proof of Theorem 4.0.8 will follow. Writing everything out, for m such that $0 \leq m \leq N$, the coefficient of t^m in the Ehrhart quasi-polynomial is given by

$$(4.8) \quad E_m(T) = -\operatorname{res}_{x=0} \frac{(-x)^m}{m!} \sum_{f \in \mathcal{G}_{>m}(\boldsymbol{\alpha})} \mu(f) \sum_{\zeta: \zeta^f=1} \frac{\zeta^{-T}}{\prod_i (1 - \zeta^{\alpha_i} e^{\alpha_i x})}.$$

As an example, we see that E_N is indeed independent of T because $\mathcal{G}_{>N}(\boldsymbol{\alpha}) = \{1\}$; thus E_N is a constant. We now concentrate on writing the function $\mathcal{F}(\boldsymbol{\alpha}, f, T; x)$ more explicitly.

DEFINITION 4.3.9. For a list $\boldsymbol{\alpha}$ and integers f and T , define meromorphic functions of $x \in \mathbb{C}$ by:

$$\mathcal{B}(\boldsymbol{\alpha}, f; x) := \frac{1}{\prod_{i: f|\alpha_i} (1 - e^{\alpha_i x})},$$

$$\mathcal{S}(\boldsymbol{\alpha}, f, T; x) := \sum_{\zeta: \zeta^f=1} \frac{\zeta^{-T}}{\prod_{i: f \nmid \alpha_i} (1 - \zeta^{\alpha_i} e^{\alpha_i x})}.$$

Thus we have

$$\mathcal{F}(\boldsymbol{\alpha}, f, T; x) = \mathcal{B}(\boldsymbol{\alpha}, f; x) \mathcal{S}(\boldsymbol{\alpha}, f, T; x),$$

and

$$\begin{aligned} \sum_{i=0}^k E_{N-i}(T)t^{N-i} &= \sum_{f \in \mathcal{G}_{>N-k}(\boldsymbol{\alpha})} \mu(f) \mathcal{E}(\boldsymbol{\alpha}, f; t, T) \\ &= \sum_{f \in \mathcal{G}_{>N-k}(\boldsymbol{\alpha})} \mu(f) \left(-\operatorname{res}_{x=0} e^{-tx} \mathcal{B}(\boldsymbol{\alpha}, f; x) \cdot \mathcal{S}(\boldsymbol{\alpha}, f, T; x) \right). \end{aligned}$$

To compute the residue, we need to compute the series expansion about $x = 0$. This can be done by multiplying the series expansions of e^{-tx} , $\mathcal{B}(\boldsymbol{\alpha}, f; x)$, and $\mathcal{S}(\boldsymbol{\alpha}, f, T; x)$. The series expansion of $\mathcal{B}(\boldsymbol{\alpha}, f; x)$ is easy to do because it is related to the Bernoulli numbers, see Remark 4.3.10. We do not want to work with $\mathcal{S}(\boldsymbol{\alpha}, f, T; x)$ in its current form because it contains (possibly irrational) roots of unity.

In the next section, the expression we obtained will allow us to compute $\mathcal{F}(\boldsymbol{\alpha}, f, T)$ by relating $\mathcal{S}(\boldsymbol{\alpha}, f, T)$ to a generating function of a cone. This cone will have fixed dimension when k is fixed.

REMARK 4.3.10. Let x and ϵ be two variables, and $a, b \in \mathbb{R}$. In particular, a or b could be zero, but not at the same time. Then the Laurent series expansion of $\frac{1}{1 - e^{ax+b\epsilon}}$ can be computed using the generating function for the Bernoulli numbers. Note that

$$\frac{1}{1 - e^{ax+b\epsilon}} = \frac{ax + b\epsilon}{1 - e^{ax+b\epsilon}} \times \frac{1}{(ax + b\epsilon)}.$$

The series expansion of the first term in the product can be done using Lemma 3.1.5. If $a \neq 0$, the second term can be expanded using the Binomial theorem:

$$\frac{1}{(ax + b\epsilon)} = \sum_{i=0}^{\infty} (ax)^{-1-k} (b\epsilon)^k$$

4.3.3. $\mathcal{S}(\boldsymbol{\alpha}, f, T; x)$ as the generating function of a cone in fixed dimension. To this end, let f be an integer from $\mathcal{G}_{>N-k}(\boldsymbol{\alpha})$. By definition, f is the greatest common divisor of a sublist of $\boldsymbol{\alpha}$. Thus the greatest common divisor of f and the elements of $\boldsymbol{\alpha}$ which are *not* a multiple of f is still equal to 1. Let $J = J(\boldsymbol{\alpha}, f)$ be the set of indices $i \in \{1, \dots, N+1\}$ such that α_i is indivisible by f , i.e., $f \nmid \alpha_i$. Note that f by definition is the greatest common divisor of all except at most k of the integers α_j . Let r denote the cardinality of J ; then $r \leq k$. Let $V_J = \mathbb{R}^J$ and let V_J^* denote the dual space. We will use the standard basis of \mathbb{R}^J , and we denote by $\mathbb{R}_{\geq 0}^J$ the standard

cone of elements in \mathbb{R}^J having non-negative coordinates. We also define the sublist $\boldsymbol{\alpha}_J = [\alpha_i]_{i \in J}$ of elements of $\boldsymbol{\alpha}$ indivisible by f and view it as a vector in V_J^* via the standard basis.

DEFINITION 4.3.11. For an integer T , define the meromorphic function of $\boldsymbol{\xi} \in V_J^*$,

$$Q(\boldsymbol{\alpha}, f, T; \boldsymbol{\xi}) := \sum_{\zeta: \zeta^f=1} \frac{\zeta^{-T}}{\prod_{j \in J(\boldsymbol{\alpha}, f)} (1 - \zeta^{\alpha_j} e^{\xi_j})}.$$

REMARK 4.3.12. Observe that $Q(\boldsymbol{\alpha}, f, T)$ can be restricted at $\boldsymbol{\xi} = \boldsymbol{\alpha}_J x$, for $x \in \mathbb{C}$ generic, to give $\mathcal{S}(\boldsymbol{\alpha}, f, T; x)$.

We find that $Q(\boldsymbol{\alpha}, f, T; \boldsymbol{\xi})$ is the discrete generating function of an affine shift of the standard cone $\mathbb{R}_{\geq 0}^J$ relative to a certain lattice in V_J which we define as:

$$(4.9) \quad \Lambda(\boldsymbol{\alpha}, f) := \left\{ \mathbf{y} \in \mathbb{Z}^J : \langle \boldsymbol{\alpha}_J, \mathbf{y} \rangle = \sum_{j \in J} y_j \alpha_j \in \mathbb{Z}f \right\}.$$

Consider the map $\phi: \mathbb{Z}^J \rightarrow \mathbb{Z}/\mathbb{Z}f$, $\mathbf{y} \mapsto \langle \boldsymbol{\alpha}, \mathbf{y} \rangle + \mathbb{Z}f$. Its kernel is the lattice $\Lambda(\boldsymbol{\alpha}, f)$. Because the greatest common divisor of f and the elements of $\boldsymbol{\alpha}_J$ is 1, by Bezout's theorem there exist $s_0 \in \mathbb{Z}$ and $\mathbf{s} \in \mathbb{Z}^J$ such that $1 = \sum_{i \in J} s_i \alpha_i + s_0 f$. Therefore, the map ϕ is surjective, and therefore the index $|\mathbb{Z}^J : \Lambda(\boldsymbol{\alpha}, f)|$ equals f .

THEOREM 4.3.13. Let $\boldsymbol{\alpha} = [\alpha_1, \dots, \alpha_{N+1}]$ be a list of positive integers and f be the greatest common divisor of a sublist of $\boldsymbol{\alpha}$. Let $J = J(\boldsymbol{\alpha}, f) = \{i : f \nmid \alpha_i\}$. Let $s_0 \in \mathbb{Z}$ and $\mathbf{s} \in \mathbb{Z}^J$ such that $1 = \sum_{i \in J} s_i \alpha_i + s_0 f$ using Bezout's theorem. Consider $\mathbf{s} = (s_i)_{i \in J}$ as an element of $V_J = \mathbb{R}^J$. Let T be an integer, and $\boldsymbol{\xi} = (\xi_i)_{i \in J} \in V_J^*$ with $\xi_i < 0$. Then

$$Q(\boldsymbol{\alpha}, f, T; \boldsymbol{\xi}) = f e^{\langle \boldsymbol{\xi}, T\mathbf{s} \rangle} \sum_{\mathbf{n} \in (-T\mathbf{s} + \mathbb{R}_{\geq 0}^J) \cap \Lambda(\boldsymbol{\alpha}, f)} e^{\langle \boldsymbol{\xi}, \mathbf{n} \rangle}$$

REMARK 4.3.14. The function $Q(\boldsymbol{\alpha}, f, T; \boldsymbol{\xi})$ is a function of T periodic modulo f . Since $f\mathbb{Z}^J$ is contained in $\Lambda(\boldsymbol{\alpha}, f)$, the element $f\mathbf{s}$ is in the lattice $\Lambda(\boldsymbol{\alpha}, f)$, and we see that the right hand side is also a periodic function of T modulo f .

PROOF OF THEOREM 4.3.13. Consider $\boldsymbol{\xi} \in V_J^*$ with $\xi_j < 0$. Then we can write the equality

$$\frac{1}{\prod_{j \in J} (1 - \zeta^{\alpha_j} e^{\xi_j})} = \prod_{j \in J} \sum_{n_j=0}^{\infty} \zeta^{n_j \alpha_j} e^{n_j \xi_j}.$$

So

$$Q(\boldsymbol{\alpha}, f, T; \boldsymbol{\xi}) = \sum_{\mathbf{n} \in \mathbb{Z}_{\geq 0}^J} \left(\sum_{\zeta: \zeta^f=1} \zeta^{\sum_j n_j \alpha_j - T} \right) e^{\sum_{j \in J} n_j \xi_j}.$$

We note that $\sum_{\zeta: \zeta^f=1} \zeta^m$ is zero except if $m \in \mathbb{Z}f$, when this sum is equal to f . Then we obtain that $Q(\boldsymbol{\alpha}, f, T)$ is the sum over $\mathbf{n} \in \mathbb{Z}_{\geq 0}^J$ such that $\sum_j n_j \alpha_j - T \in \mathbb{Z}f$. The equality $1 = \sum_{j \in J} s_j \alpha_j + s_0 f$ implies that $T \equiv \sum_j t s_j \alpha_j$ modulo f , and the condition $\sum_j n_j \alpha_j - T \in \mathbb{Z}f$ is equivalent to the condition $\sum_j (n_j - T s_j) \alpha_j \in \mathbb{Z}f$.

We see that the point $\mathbf{n} - T\mathbf{s}$ is in the lattice $\Lambda(\boldsymbol{\alpha}, f)$ as well as in the cone $-T\mathbf{s} + \mathbb{R}_{\geq 0}^J$ (as $n_j \geq 0$). Thus the claim. \square

By definition of the meromorphic functions $S(-T\mathbf{s} + \mathbb{R}_{\geq 0}^J, \Lambda(\boldsymbol{\alpha}, f); \boldsymbol{\xi})$ and $M(-T\mathbf{s}, \mathbb{R}_{\geq 0}^J, \Lambda(\boldsymbol{\alpha}, f); \boldsymbol{\xi})$, we obtain the following equality.

COROLLARY 4.3.15.

$$Q(\boldsymbol{\alpha}, f, T; \boldsymbol{\xi}) = f M(-T\mathbf{s}, \mathbb{R}_{\geq 0}^J, \Lambda(\boldsymbol{\alpha}, f); \boldsymbol{\xi}).$$

Using Remark 4.3.12 we thus obtain by restriction to $\boldsymbol{\xi} = \boldsymbol{\alpha}_J x$ the following equality.

COROLLARY 4.3.16.

$$\mathcal{F}(\boldsymbol{\alpha}, f, T; x) = f M(-T\mathbf{s}, \mathbb{R}_{\geq 0}^J, \Lambda(\boldsymbol{\alpha}, f); \boldsymbol{\alpha}_J x) \prod_{j: f|\alpha_j} \frac{1}{1 - e^{\alpha_j x}}.$$

4.3.4. Unimodular decomposition in the dual space. The cone $\mathbb{R}_{\geq 0}^J$ is in general not unimodular with respect to the lattice $\Lambda(\boldsymbol{\alpha}, f)$. By decomposing $\mathbb{R}_{\geq 0}^J$ in cones \mathbf{u} that are unimodular with respect to $\Lambda(\boldsymbol{\alpha}, f)$, modulo cones containing lines, we can write

$$M(-T\mathbf{s}, \mathbb{R}_{\geq 0}^J, \Lambda(\boldsymbol{\alpha}, f)) = \sum_{\mathbf{u}} \epsilon_{\mathbf{u}} M(-T\mathbf{s}, \mathbf{u}, \Lambda),$$

where $\epsilon_u \in \{\pm 1\}$. This decomposition can be computed using Barvinok’s algorithm in polynomial time for fixed k because the dimension $|J|$ is at most k .

REMARK 4.3.17. For this particular cone and lattice, this decomposition modulo cones containing lines is best done using the “dual” variant of Barvinok’s algorithm, as introduced in [20]. This is in contrast to the “primal” variant described in [34, 100]; see also [16] for an exposition of Brion–Vergne decomposition and its relation to both decompositions. To explain this, let us determine the index of the cone $\mathbb{R}_{\geq 0}^J$ in the lattice $\Lambda = \Lambda(\boldsymbol{\alpha}, f)$; the worst-case complexity of the signed cone decomposition is bounded by a polynomial in the logarithm of this index.

Let B be a matrix whose columns form a basis of Λ , so $\Lambda = B\mathbb{Z}^J$. Then $|\mathbb{Z}^J : \Lambda| = |\det B| = f$. By Remark 4.3.6, we find

$$M(-T\mathbf{s}, \mathbb{R}_{\geq 0}^J, \Lambda; \boldsymbol{\xi}) = M(-TB^{-1}\mathbf{s}, B^{-1}\mathbb{R}_{\geq 0}^J, \mathbb{Z}^J; B^\top \boldsymbol{\xi}).$$

Let \mathfrak{c} denote the cone $B^{-1}\mathbb{R}_{\geq 0}^J$, which is generated by the columns of B^{-1} . Since B^{-1} is not integer in general, we find generators of \mathfrak{c} that are primitive vectors of \mathbb{Z}^J by scaling each of the columns by an integer. Certainly $|\det B|B^{-1}$ is an integer matrix, and thus we find that the index of the cone \mathfrak{c} is bounded above by f^{r-1} . We can easily determine the exact index as follows. For each $i \in J$, the generator \mathbf{e}_i of the original cone $\mathbb{R}_{\geq 0}^J$ needs to be scaled so as to lie in the lattice Λ . The smallest multiplier $y_i \in \mathbb{Z}_{>0}$ such that $\langle \boldsymbol{\alpha}_J, y_i \mathbf{e}_i \rangle \in \mathbb{Z}f$ is $y_i = \text{lcm}(\alpha_i, f)/\alpha_i$. Thus the index of $\mathbb{R}_{\geq 0}^J$ in \mathbb{Z}^J is the product of the y_i , and finally the index of $\mathbb{R}_{\geq 0}^J$ in Λ is

$$\frac{1}{|\mathbb{Z}^r : \Lambda|} \prod_{i \in J} \frac{\text{lcm}(\alpha_i, f)}{\alpha_i} = \frac{1}{f} \prod_{i \in J} \frac{\text{lcm}(\alpha_i, f)}{\alpha_i}.$$

Instead we consider the dual cone, $\mathfrak{c}^\circ = \{ \boldsymbol{\eta} \in V_J^* : \langle \boldsymbol{\eta}, \mathbf{y} \rangle \geq 0 \text{ for } \mathbf{y} \in \mathfrak{c} \}$. We have $\mathfrak{c}^\circ = B^\top \mathbb{R}_{\geq 0}^J$. Then the index of the dual cone \mathfrak{c}° equals $|\det B^\top| = f$, which is much smaller than f^{r-1} .

Following [63], we now compute a decomposition of \mathfrak{c}° in cones \mathfrak{u}° that are unimodular with respect to \mathbb{Z}^J , modulo lower-dimensional cones,

$$[\mathfrak{c}^\circ] \equiv \sum_{\mathfrak{u}} \epsilon_{\mathfrak{u}} [\mathfrak{u}^\circ] \quad (\text{modulo lower-dimensional cones}).$$

Then the desired decomposition follows:

$$[c] \equiv \sum_{\mathbf{u}} \epsilon_{\mathbf{u}}[\mathbf{u}] \quad (\text{modulo cones with lines}).$$

Because of the better bound on the index of the cone on the dual side, the worst-case complexity of the signed decomposition algorithm is reduced. This is confirmed by computational experiments.

REMARK 4.3.18. Although we know that the meromorphic function $M(-T\mathbf{s}, \mathbb{R}_{\geq 0}^J, \Lambda(\boldsymbol{\alpha}, f); \boldsymbol{\xi})$ restricts via $\boldsymbol{\xi} = \boldsymbol{\alpha}_J x$ to a meromorphic function of a single variable x , it may happen that the individual functions $M(-T\mathbf{s}, \mathbf{u}, \Lambda(\boldsymbol{\alpha}, f); \boldsymbol{\xi})$ do not restrict. In other words, the line $\boldsymbol{\alpha}_J x$ may be entirely contained in the set of poles. If this is the case, we can compute (in polynomial time) a regular vector $\boldsymbol{\beta} \in \mathbb{Q}^J$ so that, for $\epsilon \neq 0$, the deformed vector $(\boldsymbol{\alpha}_J + \epsilon\boldsymbol{\beta})x$ is not a pole of any of the functions $M(-T\mathbf{s}, \mathbf{u}, \Lambda(\boldsymbol{\alpha}, f); \boldsymbol{\xi})$ occurring. We then consider the meromorphic functions $\epsilon \mapsto M(-T\mathbf{s}, \mathbf{u}, \Lambda(\boldsymbol{\alpha}, f); (\boldsymbol{\alpha}_J + \epsilon\boldsymbol{\beta})x)$ and their Laurent expansions at $\epsilon = 0$ in the variable ϵ . We then add the constant terms of these expansions (multiplied by $\epsilon_{\mathbf{u}}$). This is the value of $M(-T\mathbf{s}, \mathbb{R}_{\geq 0}^J, \Lambda(\boldsymbol{\alpha}, f); \boldsymbol{\xi})$ at the point $\boldsymbol{\xi} = \boldsymbol{\alpha}_J x$.

4.3.5. The periodic dependence in T . Now let us analyze the dependence in T of the functions $M(-T\mathbf{s}, \mathbf{u}, \Lambda(\boldsymbol{\alpha}, f))$, where \mathbf{u} is a unimodular cone. Let the generators be $\mathbf{g}_i^{\mathbf{u}}$, so the elements $\mathbf{g}_i^{\mathbf{u}}$ form a basis of the lattice $\Lambda(\boldsymbol{\alpha}, f)$. Recall that the lattice $f\mathbb{Z}^r$ is contained in $\Lambda(\boldsymbol{\alpha}, f)$. Thus as $\mathbf{s} \in \mathbb{Z}^r$, we have $\mathbf{s} = \sum_i s_i \mathbf{g}_i^{\mathbf{u}}$ with $f s_i \in \mathbb{Z}$ and hence $\{-T\mathbf{s}\}_{\mathbf{u}} = \sum_i \{-T s_i\} \mathbf{g}_i^{\mathbf{u}}$ with $\{-T s_i\}$ a function of T periodic modulo f .

Thus the function $T \mapsto \{-T\mathbf{s}\}_{\mathbf{u}}$ is a step linear function, modulo f , with value in V . We then write

$$M(-T\mathbf{s}, \mathbf{u}, \Lambda(\boldsymbol{\alpha}, f); \boldsymbol{\xi}) = e^{\langle \boldsymbol{\xi}, \{-T\mathbf{s}\}_{\mathbf{u}} \rangle} \prod_{j=1}^r \frac{1}{1 - e^{\langle \boldsymbol{\xi}, \mathbf{g}_j \rangle}}.$$

Recall that by Corollary 4.3.16,

$$\mathcal{F}(\boldsymbol{\alpha}, f, T; x) = f M(-T\mathbf{s}, \mathbb{R}_{\geq 0}^J, \Lambda(\boldsymbol{\alpha}, f); \boldsymbol{\alpha}_J x) \prod_{j: f|\alpha_j} \frac{1}{1 - e^{\alpha_j x}}.$$

Thus this is a meromorphic function of the variable x of the form:

$$\sum_{\mathbf{u}} e^{l_{\mathbf{u}}(T)x} \frac{h(x)}{x^{N+1}},$$

where $h(x)$ is holomorphic in x and $l_{\mathbf{u}}(T)$ is a step linear function of T , modulo f . Thus to compute

$$E_i(f; T) = \operatorname{res}_{x=0} \frac{(-x)^i}{i!} \mathcal{F}(\boldsymbol{\alpha}, f, T; x)$$

we only have to expand the function $x \mapsto e^{l_{\mathbf{u}}(T)x}$ up to the power x^{N-i} . This expansion can be done in polynomial time. We thus see that, as stated in Theorem 4.3.8, $E_i(f; T)$ is a step polynomial of degree less than or equal to $N - i$, which is periodic of T modulo f . This completes the proof of Theorem 4.3.8 and thus the proof of Theorem 4.0.8.

4.4. Periodicity of coefficients

By Schur's result, it is clear that the coefficient $E_N(t)$ of the highest degree term is just an explicit constant. Our analysis of the high-order poles of the generating function associated to $E(\boldsymbol{\alpha}; t)$ allows us to decide what is the highest-degree coefficient of $E(\boldsymbol{\alpha}; t)$ that is not a constant function of t (we will also say that the coefficient is *strictly periodic*).

THEOREM 4.4.1. *Given a list of non-negative integer numbers $\boldsymbol{\alpha} = [\alpha_1, \dots, \alpha_{N+1}]$, let ℓ be the greatest integer for which there exists a sublist $\boldsymbol{\alpha}_J$ with $|J| = \ell$, such that its greatest common divisor is not 1. Then for $k \geq \ell$ the coefficient of degree k is a constant while the coefficient of degree $\ell - 1$ of the quasi-polynomial $E(\boldsymbol{\alpha}; t)$ is strictly periodic. Moreover, if the numbers α_i are given with their prime factorization, then detecting ℓ can be done in polynomial time.*

EXAMPLE 4.4.2. We apply the theorem above to investigate the question of periodicity of the denumerant coefficients in the case of the classical partition problem $E([1, 2, 3, \dots, m]; t)$. It is well known that this coincides with the classical problem of finding the number of partitions of the integer t into at most m parts, usually denoted $p_m(t)$ (see [8]). In this case, Theorem 4.4.1 predicts indeed that the highest-degree coefficient of the partition function $p_m(t)$ which is non-constant is the coefficient of the term of degree $\lceil m/2 \rceil$. This follows from the theorem because the even numbers in the set $\{1, 2, 3, \dots, m\}$ form the largest sublist with gcd two.

4.4. PERIODICITY OF COEFFICIENTS

Now that we have the main algorithmic result we can prove some consequences to the description of the periodicity of the coefficients. In this section, we determine the largest i with a non-constant coefficient $E_i(t)$ and we give a polynomial time algorithm for computing it. This will complete the proof of Theorem 4.4.1.

THEOREM 4.4.3. *Given as input a list of integers $\alpha = [\alpha_1, \dots, \alpha_{N+1}]$ with their prime factorization $\alpha_i = p_1^{a_{i1}} p_2^{a_{i2}} \dots p_n^{a_{in}}$, there is a polynomial time algorithm to find all of the largest sublists where the greatest common divisor is not one. Moreover, if ℓ denotes the size of the largest sublists with greatest common divisor different from one, then (1) there are polynomially many such sublists, (2) the poset $\tilde{P}_{>\ell-1}$ is a fan (a poset with a maximal element and adjacent atoms), and (3) the Möbius function for $P_{>\ell-1}$ is $\mu(f) = 1$ if $G(f) \neq G(1)$ and $\mu(1) = 1 - (|\mathcal{G}_{>\ell-1}(\alpha)| - 1)$.*

PROOF. Consider the matrix $A = [a_{ij}]$. Let c_{i_1}, \dots, c_{i_k} be column indices of A that denote the columns that contain the largest number of non-zero elements among the columns. Let $\alpha^{(c_{i_j})}$ be the sublist of α that corresponds to the rows of A where column c_{i_j} has a non-zero entry. Each $\alpha^{(c_{i_j})}$ has greatest common divisor different from one. If ℓ is the size of the largest sublist of α with greatest common divisor different from one, then there are ℓ many α_i 's that share a common prime. Hence each column c_{i_1} of A has ℓ many non-zero elements. Then each $\alpha^{(c_{i_j})}$ is a largest sublist where the greatest common divisor is not one. Note that more than one column index c_i might produce the same sublist $\alpha^{(c_{i_j})}$. The construction of A , counting the non-zero elements of each column, and forming the sublist indexed by each c_{i_j} can be done in polynomial time in the input size.

To show the poset $\tilde{P}_{>\ell-1}$ is a fan, let $\mathcal{G} = \{1, f_1, \dots, f_m\}$ be the set of greatest common divisors of sublists of size $> \ell - 1$. Each f_i corresponds to a greatest common divisor of a sublist $\alpha^{(i)}$ of α with size ℓ . We cannot have $f_i \mid f_j$ for $i \neq j$ because if $f_i \mid f_j$, then f_i is also the greatest common divisor of $\alpha^{(i)} \cup \alpha^{(j)}$, a contradiction to the maximality of ℓ . Then the Möbius function is $\mu(f_i) = 1$, and $\mu(1) = 1 - m$.

As an aside, $\gcd(f_i, f_j) = 1$ for all $f_i \neq f_j$ as if $\gcd(f_i, f_j) \neq 1$, then we can take the union of the sublist that produced f_i and f_j thereby giving a larger sublist with greatest common divisor not equal to one, a contradiction. \square

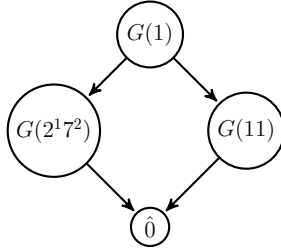
4.4. PERIODICITY OF COEFFICIENTS

EXAMPLE 4.4.4. $[2^2 7^4 41^1, 2^1 7^2 11^1, 11^4, 17^3]$ gives the matrix

$$\begin{pmatrix} 2 & 4 & 0 & 0 & 1 \\ 1 & 2 & 1 & 0 & 0 \\ 0 & 0 & 4 & 0 & 0 \\ 0 & 0 & 0 & 3 & 0 \end{pmatrix}$$

where the columns are the powers of the primes indexed by $(2, 7, 11, 17, 41)$. We see the largest sublists that have gcd not equal to one are $[2^2 7^4 41^1, 2^1 7^2 11^1]$ and $[2^1 7^2 11^1, 11^4]$. Then $\mathcal{G} = \{1, 2^1 7^2, 11\}$.

The poset $P_{>1}$ is



and $\mu(1) = -1$, $\mu(11) = \mu(2^1 7^2) = 1$.

PROOF OF THEOREM 4.4.1. Let ℓ be the greatest integer for which there exists a sublist α_J with $|J| = \ell$, such that its gcd f is not 1. Then for $m \geq \ell$ the coefficient of degree m , $E_m(T)$, is constant because in Equation (4.8), $\mathcal{G}_{>m}(\alpha) = \{1\}$. Hence $E_m(T)$ does not depend on T . We now focus on $E_{\ell-1}(T)$. To simplify Equation (4.8), we first compute the $\mu(f)$ values.

LEMMA 4.4.5. *For ℓ as in Theorem 4.4.1, the poset $\mathcal{G}_{>\ell-1}(\alpha)$ is a fan, with one maximal element 1 and adjacent elements f which are pairwise coprime. In particular, $\mu(f) = 1$ for $f \neq 1$.*

PROOF. Let $\alpha_{J_1}, \alpha_{J_2}$ be two sublists of length ℓ with gcd's $f_1 \neq f_2$ both not equal to 1. If f_1 and f_2 had a nontrivial common divisor d , then the list $\alpha_{J_1 \cup J_2}$ would have a gcd not equal to 1, in contradiction with its length being strictly greater than ℓ . \square

Next we recall a fact about Fourier series and use it to show that each term in the summation over $f \in \mathcal{G}_{>\ell-1}(\alpha)$ in Equation (4.8) has smallest period equal to f .

4.4. PERIODICITY OF COEFFICIENTS

LEMMA 4.4.6. *Let f be a positive integer and let $\phi(t)$ be a periodic function on $\mathbb{Z}/f\mathbb{Z}$ with Fourier expansion*

$$\phi(t) = \sum_{n=0}^{f-1} c_n e^{2i\pi nt/f}.$$

If $c_n \neq 0$ for some n which is coprime to f then $\phi(t)$ has smallest period equal to f .

PROOF. Assume $\phi(t)$ has period m with $f = qm$ and $q > 1$. We write its Fourier series as a function of period m .

$$\phi(t) = \sum_{j=0}^{m-1} c'_j e^{2i\pi jt/m} = \sum_{j=0}^{m-1} c'_j e^{2i\pi(jq)t/f}.$$

By uniqueness of the Fourier coefficients, we have $c_n = 0$ if n is not a multiple of q (and $c_{qj} = c'_j$).

We claim that if n is coprime to f , then n is not a multiple of q . This is true by considering the contrapositive.

Hence, $c_n = 0$ if n is coprime to f , a contradiction. \square

Theorem 4.4.1 is thus the consequence of the following lemma.

LEMMA 4.4.7. *Let $f \in \mathcal{G}_{>\ell-1}(\boldsymbol{\alpha})$. The term in the summation over f in (4.8) has smallest period f as a function of T .*

PROOF. For $f = 1$, the statement is clear. Assume $f \neq 1$. We observe that the f -term in (4.8) is a periodic function (of period f) which is given as the sum of its Fourier expansion and is written as $\sum_{n=0}^{f-1} c_n e^{-2i\pi nT/f}$ where

$$c_n = -\operatorname{res}_{x=0} \frac{(-x)^{\ell-1}}{(\ell-1)! \prod_j (1 - e^{-2i\pi n\alpha_j/f} e^{\alpha_j x})}.$$

Consider a coefficient for which n is coprime to f . We decompose the product according to whether f divides α_j or not. The crucial observation is that there are exactly ℓ indices j such that f divides α_j , because of the maximality assumption on ℓ . Therefore $x = 0$ is a simple pole and the residue is readily computed. We obtain

$$c_n = \frac{(-1)^{\ell-1}}{(\ell-1)!} \cdot \frac{1}{\prod_{j:f \nmid \alpha_j} (1 - e^{2i\pi n\alpha_j/f})} \cdot \frac{1}{\prod_{j:f|\alpha_j} \alpha_j}.$$

Thus $c_n \neq 0$ for an n coprime with f . By Lemma 4.4.6, each f -term has minimal period f . \square

As the various numbers f in $\mathcal{G}_{>\ell-1}(\boldsymbol{\alpha})$ different from 1 are pairwise coprime and the corresponding terms have minimal period f , $E_{\ell-1}(T)$ has minimal period $\prod_{f \in \mathcal{G}_{>\ell-1}(\boldsymbol{\alpha})} f > 1$. This completes the proof of Theorem 4.4.1. \square

4.5. Summary of the algorithm to compute top coefficients

In this section, we give a detailed outline of the main algorithm. Given a sequence of integers $\boldsymbol{\alpha}$ of length $N + 1$, we wish to compute the top $k + 1$ coefficients of the quasi-polynomial $E(\boldsymbol{\alpha}; t) = \sum_{i=0}^N E_i(t)t^i$ of degree N . Note that $\boldsymbol{\alpha}$ is not a set and is allowed to have repeated numbers. Recall that

$$E(\boldsymbol{\alpha}; t) = \sum_{i=0}^N E_i(t)t^i$$

where $E_i(t)$ is a periodic function of t modulo some period q_i . We assume that greatest common divisor of the list $\boldsymbol{\alpha}$ is 1.

- (1) For every subsequence of $\boldsymbol{\alpha}$ of length greater than $N - k$, compute the greatest common divisor. Assign these values to the set $\mathcal{G}_{>N-k}(\boldsymbol{\alpha})$ (ignoring duplicates). Note that $1 \in \mathcal{G}_{>N-k}(\boldsymbol{\alpha})$.
- (2) For each $f \in \mathcal{G}_{>N-k}(\boldsymbol{\alpha})$, compute $\mu(f)$ by Theorem 4.2.2.

Recall some notation

- $J = J(\boldsymbol{\alpha}, f) = \{i \in \{1, \dots, N + 1\} : f \nmid \alpha_i\}$, and $\boldsymbol{\alpha}_J = [\alpha_i]_{i \in J}$
- $s_0 \in \mathbb{Z}$ and $\mathbf{s} \in \mathbb{Z}^J$ such that $1 = \sum_{i \in J} s_i \alpha_i + s_0 f$ (as a superscript, we mean $\mathbb{Z}^J = \mathbb{Z}^{|J|}$),
- $\Lambda(\boldsymbol{\alpha}, f) := \left\{ \mathbf{y} \in \mathbb{Z}^J : \langle \boldsymbol{\alpha}_J, \mathbf{y} \rangle = \sum_{j \in J} y_j \alpha_j \in \mathbb{Z}f \right\}$.

Then we seek to compute

$$\begin{aligned} \sum_{i=0}^k E_{N-i}(T)t^{N-i} &= \sum_{f \in \mathcal{G}_{>N-k}(\boldsymbol{\alpha})} \mu(f) \mathcal{E}(\boldsymbol{\alpha}, f; t, T) \\ &= \sum_{f \in \mathcal{G}_{>N-k}(\boldsymbol{\alpha})} \mu(f) \left(-\text{Res}_{x=0} e^{-tx} \mathcal{F}(\boldsymbol{\alpha}, f, T; x) \right) \\ &= \sum_{f \in \mathcal{G}_{>N-k}(\boldsymbol{\alpha})} \mu(f) \left(-\text{Res}_{x=0} e^{-tx} \cdot f \cdot M(-T\mathbf{s}, \mathbb{R}_{\geq 0}^J, \Lambda(\boldsymbol{\alpha}, f); \boldsymbol{\alpha}_J x) \cdot \prod_{j: f|\alpha_j} \frac{1}{1 - e^{\alpha_j x}} \right). \end{aligned}$$

We return to the algorithm by describing how to compute the term in the big parentheses above for every fixed f value.

- (3) To compute $s \in \mathbb{Z}^J$, let A be the $(|J| + 1) \times 1$ matrix given by $A = (\alpha_J, f)^T$. Compute the Hermite Normal Form of A [143]. Let $H \in \mathbb{Z}^{|J|+1 \times 1}$ be the Hermite Normal Form of A , and let $U \in \mathbb{Z}^{|J|+1 \times |J|+1}$ be a unimodular matrix such that $UA = H$. Note that H will have the form $H = (1, 0, \dots, 0)^T$. If $u := (u_1, \dots, u_{|J|}, u_{|J|+1})$ denotes the first row of U , then $u \cdot A = 1$. So $\mathbf{s} \in \mathbb{Z}^J$ is the first $|J|$ elements of u .
- (4) To compute a basis for $\Lambda(\alpha, f)$, we again use the Hermite Normal Form. Let A be the column matrix of α_J . Let $H \in \mathbb{Z}^{J \times 1}$, and $U \in \mathbb{Z}^{J \times J}$ be the Hermite Normal Form of A and unimodular matrix U , respectively, such that $UA = H$. H will have the form $H = (h, 0, 0, \dots, 0)^T$, where h is the smallest positive integer that can be written as an integer combination of α_J . To make sure h is a multiple of f , scale the first row of U by $\frac{f}{\gcd(h, g)}$. Let \tilde{U} be this scaled U matrix. Then $\hat{U}A = (\text{lcm}(h, f), 0, \dots, 0)^T$, where lcm is the lowest common multiple, and so the rows of \tilde{U} form a basis for $\Lambda(\alpha, f)$. Let $B = \tilde{U}^T$, then $\Lambda(\alpha, f) = B\mathbb{Z}^J$.
- (5) Let B be the matrix whose columns are the generators of the lattice Λ as in the last step. Then $B^{-1}\mathbb{R}_{\geq 0}^J$ is the $|J|$ -dimensional cone in \mathbb{R}^J generated by the nonnegative combinations of the columns of B^{-1} . Using Barvinok's *dual* algorithm [17, 19, 20, 34], the cone $B^{-1}\mathbb{R}_{\geq 0}^J$ can be written as a signed sum of unimodular cones. Let U_B be the set of resulting unimodular cones and $\epsilon_u \in \{-1, 1\}$ for each $u \in U_B$. Also, for $\mathbf{u} \in U_B$, let g_i^u be the corresponding rays of the cone \mathbf{u} for $i = 1, \dots, |J|$. Then

$$\begin{aligned}
 M(-T\mathbf{s}, \mathbb{R}_{\geq 0}^J, \Lambda(\alpha, f); \alpha_J x) &= M(-TB^{-1}\mathbf{s}, B^{-1}\mathbb{R}_{\geq 0}^J, \mathbb{Z}^J; B^T \alpha_J x) \\
 &= \sum_{\mathbf{u} \in U_B} \epsilon_u M(-TB^{-1}\mathbf{s}, \mathbf{u}, \mathbb{Z}^J; B^T \alpha_J x) \\
 &= \sum_{\mathbf{u} \in U_B} \epsilon_u e^{\langle B^T \alpha_J x, \{TB^{-1}\mathbf{s}\}_{\mathbf{u}} \rangle} \frac{1}{\prod_j (1 - e^{\langle B^T \alpha_J x, \mathbf{g}_j^{\mathbf{u}} \rangle})}.
 \end{aligned}$$

To compute $\{TB^{-1}\mathbf{s}\}_{\mathbf{u}}$, write $B^{-1}\mathbf{s}$ in the basis given by the rays of cone \mathbf{u} : $B^{-1}\mathbf{s} = \gamma_1 g_1^{\mathbf{u}} + \dots + \gamma_{|J|} g_{|J|}^{\mathbf{u}}$. Then $\{TB^{-1}\mathbf{s}\}_{\mathbf{u}}$ is the vector $(\{\gamma_1 T\}, \dots, \{\gamma_{|J|} T\})$. Note that T is a symbolic

variable, so every calculation involving the function $\{x\}$ must be done symbolically in some data structure.

Although $M(-T\mathbf{s}, \mathbb{R}_{\geq 0}^J, \Lambda(\boldsymbol{\alpha}, f); \boldsymbol{\alpha}_J x)$ is well defined at $\boldsymbol{\alpha}_J x$, it may happen that $\langle B^T \boldsymbol{\alpha}_J x, \mathbf{g}_j^u \rangle = 0$ for some rays \mathbf{g}_j^u at some cone \mathbf{u} . That is, one of the cones could be singular at $\boldsymbol{\alpha}_J x$. To fix this, as noted in Remark 4.3.18, we replace $\boldsymbol{\alpha}_J$ with $\boldsymbol{\alpha}_J + \epsilon \beta$ such that $\langle B^T \beta x, \mathbf{g}_j^u \rangle \neq 0$. The set of β that fail this condition has measure zero, so β can be picked randomly. After computing the limit as ϵ goes to zero, the new variable ϵ is eliminated. To compute the limit, it is enough to find the series expansion of ϵ . Positive powers of ϵ in the series can be ignored because they will vanish in the limit, while negative powers of ϵ can also be dropped because they are guaranteed to cancel out in the summation over U_B . Hence it is enough to compute the series expansion in ϵ and only keep the coefficient of ϵ^0 . Then finally,

$$M(-T\mathbf{s}, \mathbb{R}_{\geq 0}^J, \Lambda(\boldsymbol{\alpha}, f); \boldsymbol{\alpha}_J x) = \sum_{\mathbf{u} \in U_B} \epsilon_{\mathbf{u}} \operatorname{Res}_{\epsilon=0} \frac{1}{\epsilon} e^{\langle B^T(\boldsymbol{\alpha}_J + \beta \cdot \epsilon)x, \{TB^{-1}\mathbf{s}\}_{\mathbf{u}} \rangle} \frac{1}{\prod_j (1 - e^{\langle B^T(\boldsymbol{\alpha}_J + \beta \cdot \epsilon)x, \mathbf{g}_j^u \rangle})}$$

(6) The series expansion of

$$f \cdot \left(\sum_{\mathbf{u} \in U_B} \epsilon_{\mathbf{u}} \operatorname{Res}_{\epsilon=0} \frac{1}{\epsilon} e^{\langle B^T(\boldsymbol{\alpha}_J + \beta \cdot \epsilon)x, \{TB^{-1}\mathbf{s}\}_{\mathbf{u}} \rangle} \frac{1}{\prod_j (1 - e^{\langle B^T(\boldsymbol{\alpha}_J + \beta \cdot \epsilon)x, \mathbf{g}_j^u \rangle})} \right) \prod_{j: f|\alpha_j} \frac{1}{1 - e^{\alpha_j x}}$$

can be computed by first finding the Laurent series expansion at $x = 0$ and at $\epsilon = 0$ of each of the terms

- $e^{\langle B^T \boldsymbol{\alpha}_J x, \{TB^{-1}\mathbf{s}\}_{\mathbf{u}} \rangle}$,
- $e^{\langle B^T \beta \cdot \epsilon x, \{TB^{-1}\mathbf{s}\}_{\mathbf{u}} \rangle}$,
- $\frac{1}{1 - e^{\langle B^T(\boldsymbol{\alpha}_J + \beta \cdot \epsilon)x, \mathbf{g}_j^u \rangle}}$, and
- $\frac{1}{1 - e^{\alpha_j x}}$,

by using the Taylor expansion of e^x and Remark 4.3.10, and then by multiplying each series together. This Laurent series starts at x^{-N-1} , and so the coefficient of x^{-N-1+i} in this Laurent series contributes to $E_{N-i}(T)$ (after being multiplied by $\mu(f) \cdot \frac{(-1)^i}{i!}$). Therefore it is enough to compute at most the first k terms of any partial Laurent series.

4.6. Experiments

This chapter closes with an extensive collection of computational experiments (Section 4.6). We constructed a dataset of over 760 knapsacks and show our new algorithm is the fastest available method for computing the top k terms in the Ehrhart quasi-polynomial. Our implementation of the new algorithm is made available as a part of the free software `LattE integrale` [54], version 1.7.2.¹

We first wrote a preliminary implementation of our algorithm in `Maple`, which we call *M-Knapsack* in the following. Later we developed a faster implementation in C++, which is referred to as *LattE Knapsack* in the following (we use the term knapsack to refer to the Diophantine problem $\alpha_1x_1 + \alpha_2x_2 + \dots + \alpha_Nx_N + \alpha_{N+1}x_{N+1} = t$). Both implementations are released as part of the software package `LattE integrale` [54], version 1.7.2.²

We report on two different benchmarks tests:

- (1) We test the performance of the implementations *M-Knapsack*³ and *LattE Knapsack*⁴, and also the implementation of the algorithm from [14], which refer to as *LattE Top-Ehrhart*⁵, on a collection of over 750 knapsacks. The latter algorithm can compute the weighted Ehrhart quasi-polynomials for simplicial polytopes, and hence it is more general than the algorithm we present in this chapter, but this is the only other available algorithm for computing coefficients directly. Note that the implementations of the *M-Knapsack* algorithm and the main computational part of the *LattE Top-Ehrhart* algorithm are in `Maple`, making comparisons between the two easier.
- (2) Next, we run our algorithms on a few knapsacks that have been studied in the literature. We chose these examples because some of these problems are considered difficult in the literature. We also present a comparison with other available software that can also

¹Available under the GNU General Public License at <https://www.math.ucdavis.edu/~latte/>.

²Available under the GNU General Public License at <https://www.math.ucdavis.edu/~latte/>. The `Maple` code *M-Knapsack* is also available separately at <https://www.math.ucdavis.edu/~latte/software/packages/maple/>.

³`Maple` usage: `coeff_Nminus_knapsack(<knapsack list>, t, <k value>)`.

⁴Command line usage: `dest/bin/top-ehrhart-knapsack -f <knapsack file> -o <output file> -k <k value>`.

⁵Command line usage: `dest/bin/integrate --valuation=top-ehrhart --top-ehrhart-save=<output file> --num-coefficients=<k value> <LattE style knapsack file>`.

compute information of the denominator $E_\alpha(t)$: the codes *CTEuclid6* [156] and *pSn* [145].⁶

These codes use mathematical ideas that are different from those used in this chapter.

All computations were performed on a 64-bit Ubuntu machine with 64 GB of RAM and eight Dual Core AMD Opteron 880 processors.

4.6.1. *M-Knapsack vs. LattE Knapsack vs. LattE Top-Ehrhart.* Here we compare our two implementations with the *LattE Top-Ehrhart* algorithm from [14]. We constructed a test set of 768 knapsacks. For each $3 \leq d \leq 50$, we constructed four families of knapsacks:

random-3: Five random knapsacks in dimension $d - 1$ where $a_1 = 1$ and the other coefficients,

a_2, \dots, a_d , are 3-digit random numbers picked uniformly

random-15: Similar to the previous case, but with a 15-digit random number

repeat: Five knapsacks in dimension $d - 1$ where $\alpha_1 = 1$ and all the other α_i 's are the same 3-digit random number. These produce few poles and have a simple poset structure. These are among the simplest knapsacks that produce periodic coefficients.

partition: One knapsack in the form $\alpha_i = i$ for $1 \leq i \leq d$.

For each knapsack, we successively compute the highest degree terms of the quasi-polynomial, with a time limit of 200 CPU seconds for each coefficient. Once a term takes longer than 200 seconds to compute, we skip the remaining terms, as they are harder to compute than the previous ones. We then count the maximum number of terms of the quasi-polynomial, starting from the highest degree term (which would, of course, be trivial to compute), that can be computed subject to these time limits. Figures 4.1, 4.2, 4.3, 4.4 show these maximum numbers of terms for the random-3, random-15, repeat, and partition knapsacks, respectively. For example, in Figure 4.1, for each of the five random 3-digit knapsacks in ambient dimension 50, the *LattE Knapsack* method computed at most 6 terms of an Ehrhart polynomial, the *M-Knapsack* computed at most four terms, and the *LattE Top-Ehrhart* method computed at most the trivially computable highest degree term.

In each knapsack family, we see that each algorithm has a “peak” dimension where after it, the number of terms that can be computed subject to the time limit quickly decreases; for the *LattE*

⁶Both codes can be downloaded from the locations indicated in the respective papers. Maple scripts that correspond to our tests of these codes are available at <https://www.math.ucdavis.edu/~latte/software/denominatorSupplemental/>.

Knapsack method, this is around dimension 25 in each knapsack family. In each family, there is a clear order to which algorithm can compute the most: *LattE Knapsack* computes the most coefficients, while the *LattE Top-Ehrhart* method computes the least number of terms. In Figure 4.3, the simple poset structure helps every method to compute more terms, but the two `Maple` scripts seem to benefit more than the *LattE Knapsack* method.

Figure 4.4 demonstrates the power of the *LattE* implementation. Note that a knapsack of this particular form in dimension d does not start to have periodic terms until around $d/2$. Thus even though half of the coefficients are only constants we see that the *M-Knapsack* code cannot compute past a few periodic term in dimension 10–15 while the *LattE Knapsack* method is able to compute the entire polynomial.

In Figure 4.5 we plot the average speedup ratio between the *M-Knapsack* and *LattE Top-Ehrhart* implementations along with the maximum and minimum speedup ratios (we wrote both algorithms in `Maple`). The ratios are given by the time it takes *LattE Top-Ehrhart* to compute a term, divided by the time it takes *M-Knapsack* to compute the same term, where both times are between 0 and 200 seconds. For example, among all the terms computed in dimension 15 from random 15-digit knapsacks, the average speedup between the two methods was 8000, the maximum ratio was 20000, and the minimum ratio was 200. We see that in dimensions 3–10, there are a few terms for which the *LattE Top-Ehrhart* method was faster than the *M-Knapsack* method, but this only occurs for the highest degree terms. Also, after dimension 25, there is little variance in the ratios because the *LattE Top-Ehrhart* method is only computing the trivial highest term. Similar results hold for the other knapsack families, and so their plots are omitted.

4.6.2. Other examples. Next we focus on ten problems listed in Table 4.1. Some of these selected problems have been studied before in the literature [2, 61, 155, 156]. Table 4.2 shows the time in seconds to compute the entire denominator using the *M-Knapsack*, *LattE Knapsack* and *LattE Top-Ehrhart* codes with two other algorithms: *CTEuclid6* and *pSn*.

The *CTEuclid6* algorithm [156] computes the lattice point count of a polytope, and supersedes an earlier algorithm in [155].⁷ Instead of using Barvinok’s algorithm to construct unimodular cones, the main idea used by the *CTEuclid6* algorithm to find the constant term in the generating

⁷Maple usage: `CTEuclid(F(α; x)/xb, t, [x]);` where $b = \alpha_1 + \dots + \alpha_{N+1}$.

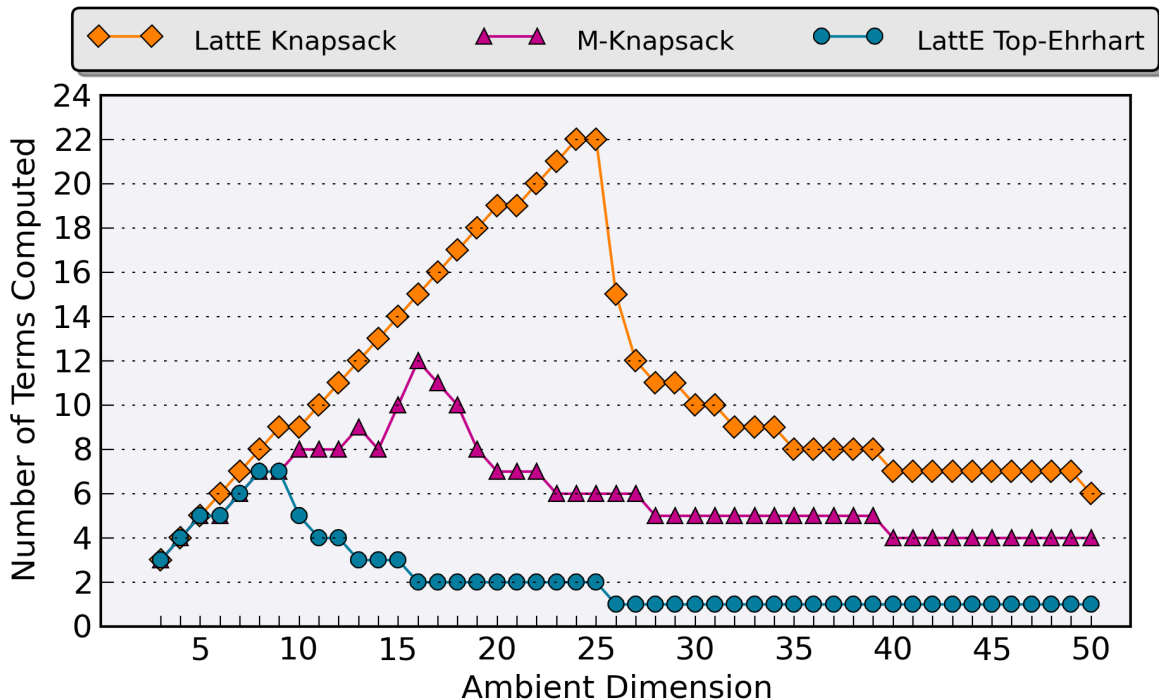


FIGURE 4.1. Random 3-digit knapsacks: Maximum number of coefficients each algorithm can compute where each coefficient takes less than 200 seconds.

function $F(\alpha; z)$ relies on recursively computing partial fraction decompositions to construct the series. Notice that the *CTEuclid6* method only computes the number of integer points in one dilation of a polytope and not the full Ehrhart polynomial. We can estimate how long it would take to find the Ehrhart polynomial using an interpolation method by computing the time it takes to find one lattice point count times the periodicity of the polynomial and degree. Hence, in Table 4.2, column “one point” refers to the running time of finding one lattice point count, while column “estimate” is an estimate for how long it would take to find the Ehrhart polynomial by interpolation. We see that the *CTEuclid6* algorithm is fast for finding the number of integer points in a knapsack, but this would lead to a slow method for finding the Ehrhart polynomial.

The *pSn* algorithm of [145] computes the entire denumerant by using a partial fraction decomposition based method.⁸ More precisely the quasi-polynomials are represented as a function $f(t)$ given by q polynomials $f^{[1]}(t), f^{[2]}(t), \dots, f^{[q]}(t)$ such that $f(t) = f^{[i]}(t)$ when $t \equiv i \pmod{q}$. To

⁸Maple usage: `QPStoTrunc(pSn(knapsack list),n,j),n)`; where j is the smallest value in $\{100, 200, 500, 1000, 2000, 3000\}$ that produces an answer.

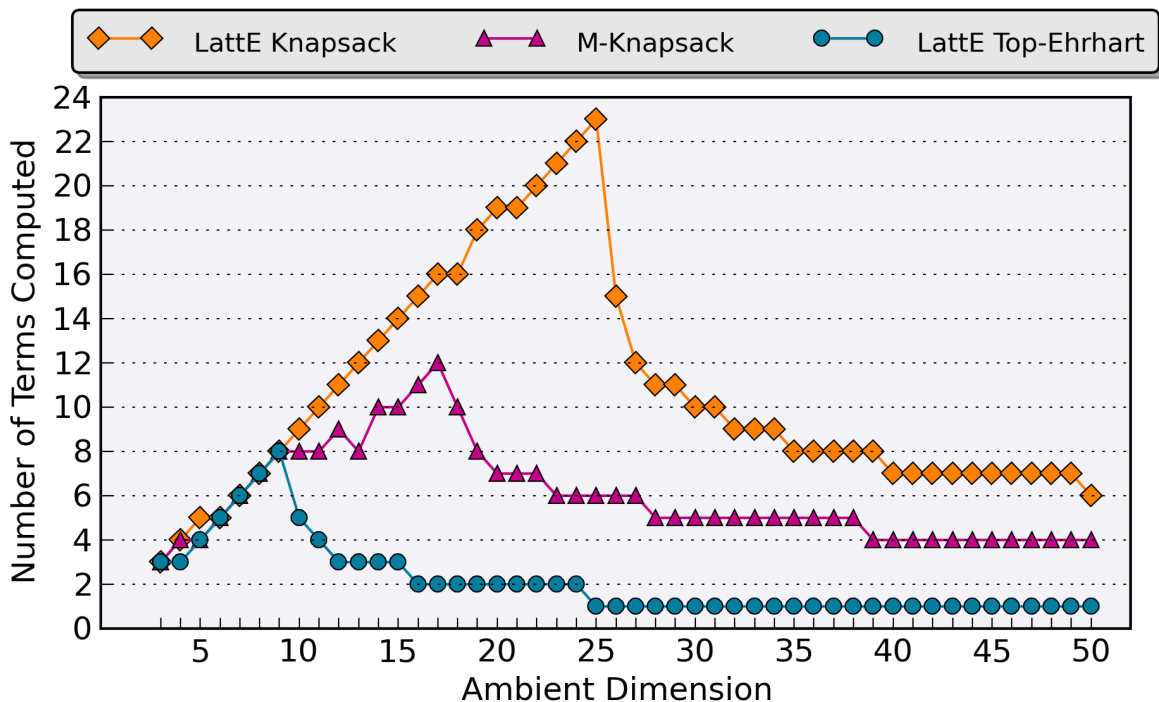


FIGURE 4.2. Random 15-digit knapsacks: Maximum number of coefficients each algorithm can compute where each coefficient takes less than 200 seconds.

find the coefficients of the $f^{[i]}$ their method finds the first few terms of the Maclaurin expansion of the partial fraction decomposition to find enough evaluations of those polynomials and then recovers the coefficients of each the $f^{[i]}$ as a result of solving a linear system. This algorithm goes back to Cayley and it was implemented in `Maple`. Looking at Table 4.2, we see that the pSn method is competitive with *LattE Knapsack* for knapsacks 1, 2, \dots , 6, and beats *LattE Knapsack* in knapsack 10. However, the pSn method is highly sensitive to the number of digits in the knapsack coefficients, unlike our *M-Knapsack* and *LattE Knapsack* methods. For example, the knapsacks [1, 2, 4, 6, 8] takes 0.320 seconds to find the full Ehrhart polynomial, [1, 20, 40, 60, 80] takes 5.520 seconds, and [1, 200, 600, 900, 400] takes 247.939 seconds. Similar results hold for other three-digit knapsacks in dimension four. However, the partition knapsack [1, 2, 3, \dots , 50] only takes 102.7 seconds. Finally, comparing the two `Maple` scripts, the *LattE Top-Ehrhart* method outperforms the *M-Knapsack* method.

Table 4.2 ignores one of the main features of our algorithm: that it can compute just the top k terms of the Ehrhart polynomial. In Table 4.3, we time the computation for finding the top

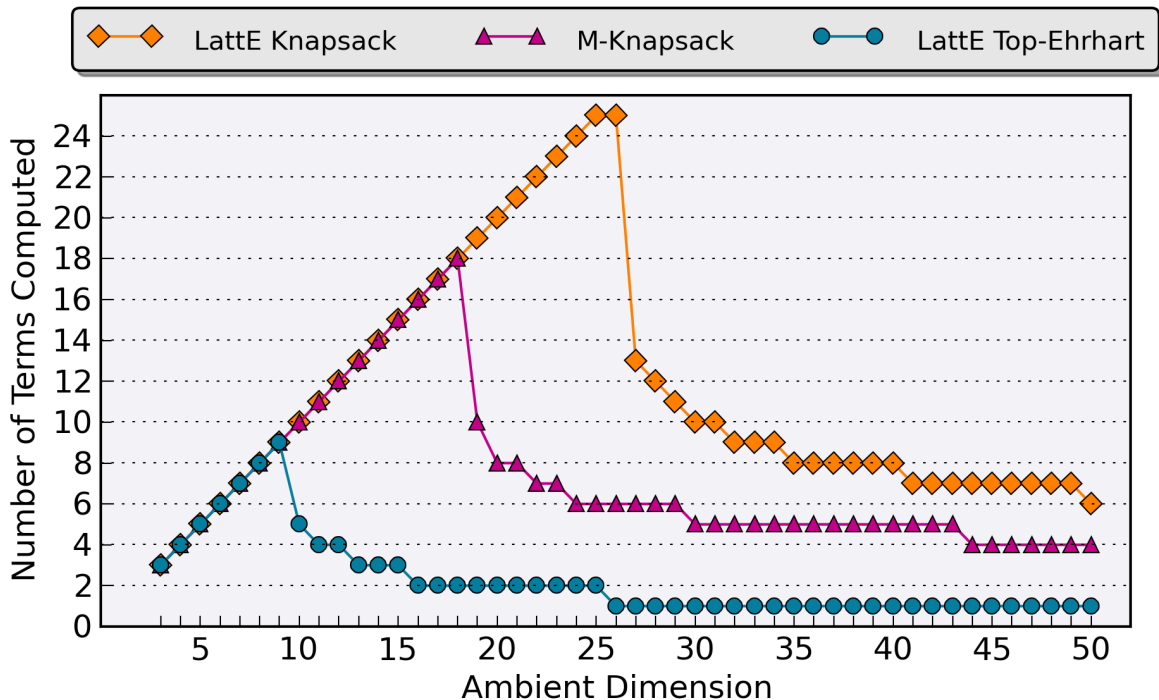


FIGURE 4.3. Repeat knapsacks: Maximum number of coefficients each algorithm can compute where each coefficient takes less than 200 seconds.

three and four terms of the Ehrhart polynomial on the knapsacks in Table 4.1. We immediately see that our *LattE Knapsack* method takes less than one thousandth of a second in each example. Comparing the two *Maple* scripts, *M-Knapsack* greatly outperforms *LattE Top-Ehrhart*. Hence, for a fixed k , the *LattE Knapsack* is the fastest method.

In summary, the *LattE Knapsack* is the fastest method for computing the top k terms of the Ehrhart polynomial. The *LattE Knapsack* method can also compute the full Ehrhart polynomial in a reasonable amount of time up to around dimension 25, and the number of digits in each knapsack coefficient does not significantly alter performance. However, if the coefficients each have one or two digits, the *pSn* method is faster, even in large dimensions.

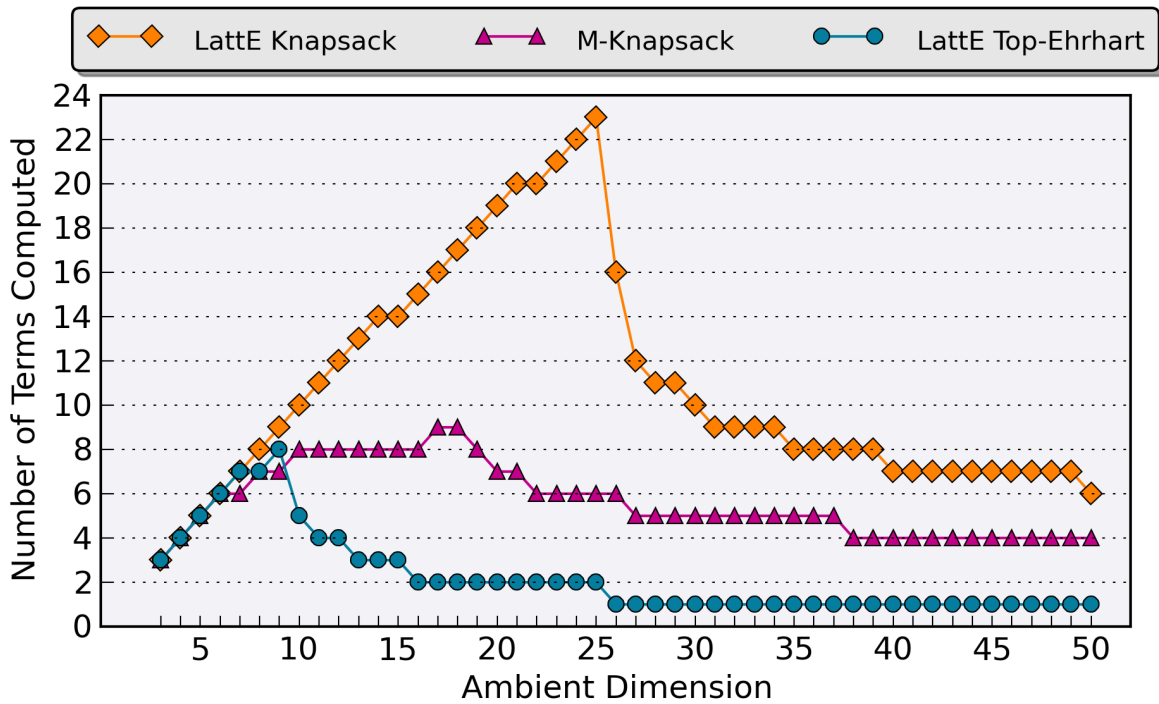


FIGURE 4.4. Partition knapsacks: Maximum number of coefficients each algorithm can compute where each coefficient takes less than 200 seconds.

TABLE 4.1. Ten selected instances

Problem	Data
#1	[8, 12, 11]
#2	[5, 13, 2, 8, 3]
#3	[5, 3, 1, 4, 2]
#4	[9, 11, 14, 5, 12]
#5	[9, 10, 17, 5, 2]
#6	[1, 2, 3, 4, 5, 6]
#7	[12223, 12224, 36674, 61119, 85569]
#8	[12137, 24269, 36405, 36407, 48545, 60683]
#9	[20601, 40429, 40429, 45415, 53725, 61919, 64470, 69340, 78539, 95043]
#10	[5, 10, 10, 2, 8, 20, 15, 2, 9, 9, 7, 4, 12, 13, 19]

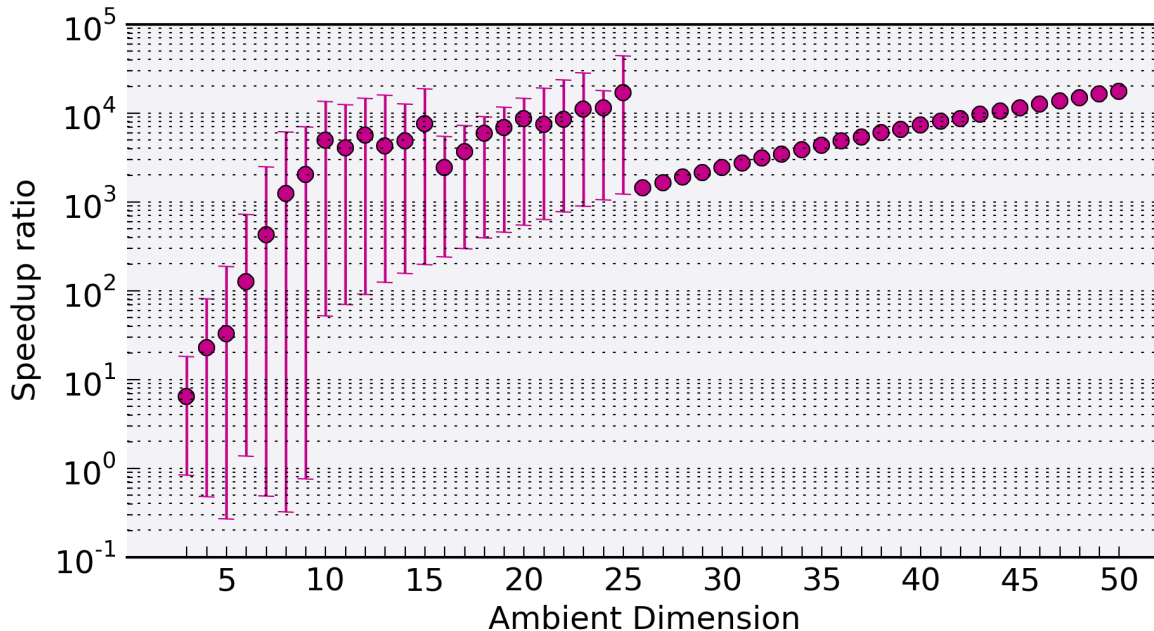


FIGURE 4.5. Average speedup ratio (dots) between the *M-Knapsack* and *LattE Top-Ehrhart* codes along with maximum and minimum speedup ratio bounds (vertical lines) for the random 15-digit knapsacks.

TABLE 4.2. Computation times in seconds for finding the full Ehrhart polynomial using five different methods.

	<i>LattE Knapsack</i>	<i>M-Knapsack</i>	<i>LattE Top-Ehrhart</i>	<i>CTEuclid6</i>		
				One point	estimate	<i>pSn</i>
#1	0	0.316	0.160	0.004	3.168	0.328
#2	0.03	5.984	2.208	0.048	347.4	0.292
#3	0.02	4.564	0.148	0.031	9.60	0.212
#4	0.08	18.317	3.884	0.112	7761.6	0.496
#5	0.06	15.200	3.588	0.096	734.4	0.392
#6	0.11	37.974	8.068	0.088	31.68	0.336
#7	0.19	43.006	8.424	0.436	9.466e+20	>30min
#8	1.14	1110.857	184.663	2.120	8.530e+20	>30min
#9	>30min	>30min	>30min	>30min	>30min	>30min
#10	>30min	>30min	>30min	142.792	1.333e+9	2.336

4.6. EXPERIMENTS

TABLE 4.3. Computation times in seconds for finding the top three and four terms of the Ehrhart polynomial

	Top 3 coefficients			Top 4 coefficients		
	<i>LattE</i> <i>Knapsack</i>	<i>M-Knapsack</i>	<i>LattE</i> <i>Top-Ehrhart</i>	<i>LattE</i> <i>Knapsack</i>	<i>M-Knapsack</i>	<i>LattE</i> <i>Top-Ehrhart</i>
#1	0	0.305	0.128	–	–	–
#2	0	0.004	0.768	0	0.096	1.356
#3	0	0.004	0.788	0	0.080	1.308
#4	0	0.003	0.792	0	0.124	1.368
#5	0	0.004	0.784	0	0.176	1.424
#6	0	0.004	1.660	0	0.088	2.976
#7	0	0.004	0.836	0	0.272	1.652
#8	0	0.068	1.828	0	0.112	3.544
#9	0	0.004	18.437	0	0.016	59.527
#10	0	0.012	142.104	0	0.044	822.187

CHAPTER 5

MILP heuristic for finding feasible solutions

In this chapter, we describe the author’s 2014 summer internship project at SAS Institute where he developed a Mixed-Integer Linear Programming (MILP) heuristic for finding feasible solutions to MILP problems. The focus of this chapter is to describe a data structure for finding a feasible solution to a system of set partition constraints. We use this data structure to find feasible solutions to more general MILP problems. See Section 1.5 for a short background on mixed integer linear programming.

5.1. Motivation

A set partitioning constraint is a linear equality constraint that only includes binary variables and every coefficient, including the constant, is one (e.g., $x_1 + x_2 = 1$, $x_i \in \{0, 1\}$). Despite having a very specific form, set partitioning constraints have very useful modeling power and often play an important role in MILP problems. There are many examples where these constraints play a role [11, 73, 74, 121, 152]. This section gives a quick introduction via one example.

5.1.1. Example. Consider the following motivating example. Suppose you are responsible for scheduling fabrication jobs to machines in a job shop. Assume the following.

- (1) There are N jobs and M machines, each with slightly different characteristics.
- (2) A job can only be processed on one machine. Once a job has started on a machine, it cannot be preempted or paused.
- (3) Each job $i \in N$ takes $t_i \in \mathbb{R}$ hours to complete.
- (4) No machine is allowed to work for more than 8 hours in a day to give time for maintenance.
- (5) Job i has a production cost of c_{ij} if processed on machine $j \in M$.

5.1. MOTIVATION

- (6) Each machine j has a fixed start up expense of c_j . Meaning, if at least one job is assigned to machine j , c_j must be paid as an expense. If no job is assigned to machine j , then there is no expense.

We give one mathematical encoding of the problem. Let us encode on which machine a job is scheduled by a binary variable:

$$x_{ij} := \begin{cases} 1 & \text{if job } i \text{ is scheduled on machine } j \\ 0 & \text{else.} \end{cases}$$

Then requirement (2) above can be encoded in the constraints

$$\sum_j x_{ij} = 1 \text{ for each job } i.$$

Notice that this produces $|N|$ set partitioning constraints. Requirement (4) can be encoded as

$$\sum_i t_i x_{ij} \leq 8 \text{ for each machine } j.$$

Let us introduce another set of binary variables to model the fixed start up expense:

$$y_j := \begin{cases} 1 & \text{if machine } j \text{ is used} \\ 0 & \text{else.} \end{cases}$$

To force y_j to be 1 when at least one job is scheduled on machine j can be done with $|M| \cdot |N|$ constraints:

$$x_{ij} \leq y_j \text{ for each } i \text{ and } j.$$

Finally, the total expense is then the sum of two terms: the production expenses c_{ij} and set-up expenses c_j . We need to minimize

$$\sum_j c_j y_j + \sum_{ij} c_{ij} x_{ij}.$$

This example shows two important properties that a lot of MILP problems have. First, notice that the number of set partitioning constraints ($\sum_j x_{ij} = 1$) is small compared to the total number of constraints in the problem. However, these are the “most important” because once the x_{ij} have

been fixed, they force values for everything (or almost everything in the general case). Second, once the x_{ij} have been set, their feasibility can be easily checked.

We will use these two properties to form the basis of a MILP heuristic in Section 5.3. The focus of this chapter will be generating feasible solutions to the set partitioning constraints.

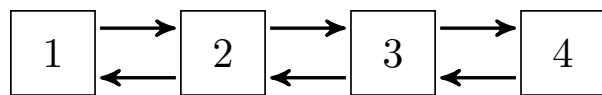
5.1.2. MIPLIB. One of the most publicized benchmarks is the MIPLIB 2010 benchmark set [95]. This set contains 361 MILP problem instances sorted into three groups: 1) 220 easy problems that can be solved within one hour using any commercial MILP solver, 2) 59 hard problems that cannot be solved within an hour, and 3) 82 currently unsolved problems. The benchmark contains real-world problems from both industry and academia.

Out of the benchmark, 133 or 37% of the problems contain set partitioning constraints. So the MILP heuristic that will be described in this chapter is usable by over a third of the problems in the MIPLIB set! Said differently, it is worth it to develop a heuristic for this special problem structure as it is extremely common.

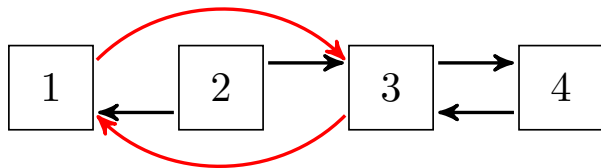
5.2. Dancing Links

In this section we review the *Dancing Links algorithm* as described in [94]. The algorithm finds a feasible solution to a system of set partition equations by running an exhaustive enumeration over the binary variables. The key feature of the algorithm is a data structure for doing two things: 1) propagating new variable fixings when a variable has been set, 2) bookkeeping everything so that the decision to set a variable to a given value can be undone.

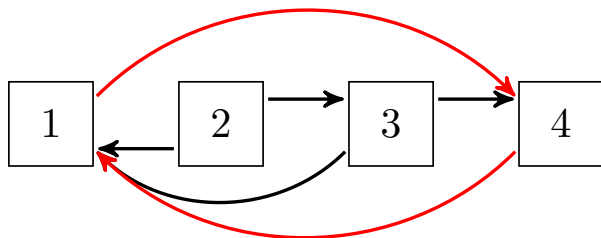
The key idea that makes propagating the implications of setting a variable to a value, and being able to undo all the implications quickly lies in a doubly linked list, a standard data structure [48]. Consider the linked list in Figure 5.1a. The squares in the figures are the nodes in the linked list, and arrows denote who a node points to in the list. Let $L[2]$ denotes what node two points to on the left, and let $R[2]$ denote what node two points to on the right, then it is easy to remove node two from the list. All we have to do is set $R[L[2]] \leftarrow R[2]$ and $L[R[2]] \leftarrow L[2]$ to produce Figure 5.1b. If we were really deleting node two, we should also remove what it is pointing to and delete it. Instead, lets leave node two alone; meaning, we want node two to keep pointing to its old neighbors. If we wanted to insert node two, it would be easy, as node two points to the nodes for



(A) State of initial of the doubly linked list.



(B) After removing node 2. Notice that node 2 points to its old neighbors.



(C) After removing node 3. Reading the list forward or backward results in only seeing nodes 1 and 4.

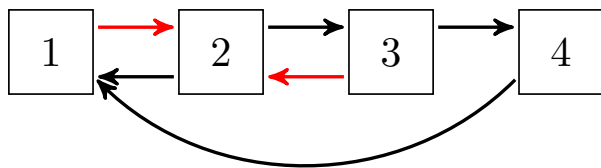
(D) Inserting node 2 in, before inserting node 3 back in. Reading the list forwards results in $\{1, 2, 3, 4\}$. Reading the list backwards results in $\{1, 4\}$.

FIGURE 5.1. The problem with not using first-out last-in ordering.

which we have to update their pointers. This is the genius behind the dancing links algorithm. It is easy to remove a node by simply updating a set of pointers, and if we want to quickly undo this, the deleted node remembers which nodes to update.

One side affect of this double link structure is that deleted nodes cannot be reinserted in any order, they must be removed and then inserted in a first-out last-in order. If we first remove node two and then node three, we must add node three back in before adding node two. Figure 5.1 illustrates how the linked list can become corrupted if this order is not kept. Donald Knuth used this idea to develop a data structure that could quickly backtrack in solving the set partitioning problem via brute-force enumeration in [94].

Next we will illustrate his data structure and algorithm on an example.

$$(A) \quad 1 = x_2 + x_4$$

$$(B) \quad 1 = x_3 + x_5$$

$$(C) \quad 1 = x_1 + x_3$$

$$(D) \quad 1 = x_1 + x_2 + x_3$$

Before describing the data structure behind dancing links, let's see how a brute force search for a solution can be performed. Let's assume $x_2 = 1$ and see if a solution is possible. The equations become

$$(A) \quad 1 = 1 + x_4$$

$$(B) \quad 1 = x_3 + x_5$$

$$(C) \quad 1 = x_1 + x_3$$

$$(D) \quad 1 = x_1 + 1 + x_3.$$

This implies that $x_2 = x_3 = x_4 = 0$. Inserting these values produces a contradiction in equation (C),

$$(A) \quad 1 = 1 + 0$$

$$(B) \quad 1 = 0 + x_5$$

$$(C) \quad 1 = 0 + 0$$

$$(D) \quad 1 = 0 + 1 + 0.$$

We see that the assumption $x_2 = 1$ produces a contradiction, and so if a solution to this system, x_2 must equal zero. The data structure in the dancing links algorithm will easily keep track of which variables are assigned values, propagate variable implications, and undo things when contradictions are produced.

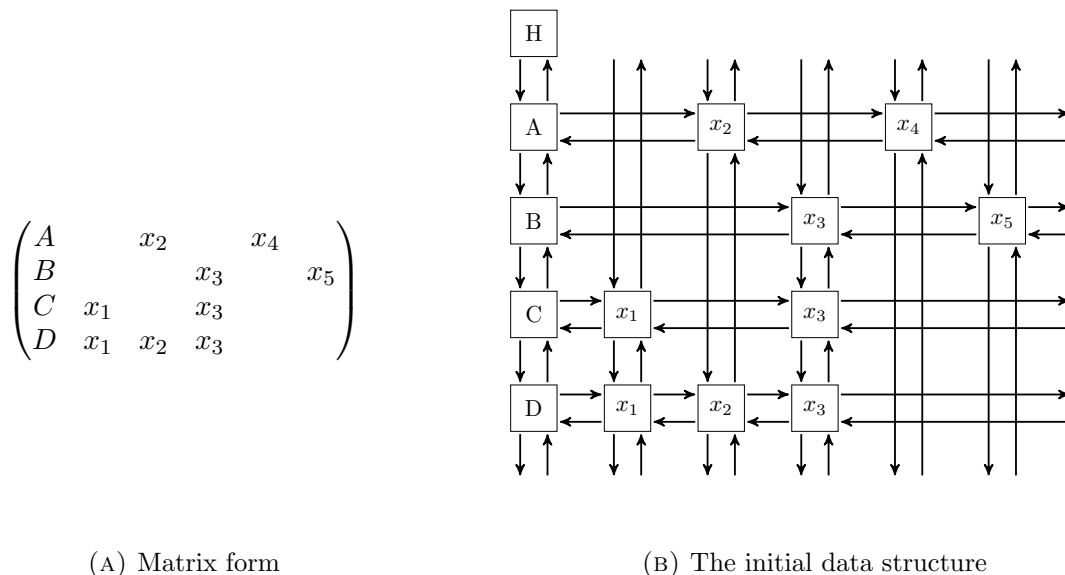


FIGURE 5.2. The initial state of the dancing links data structure

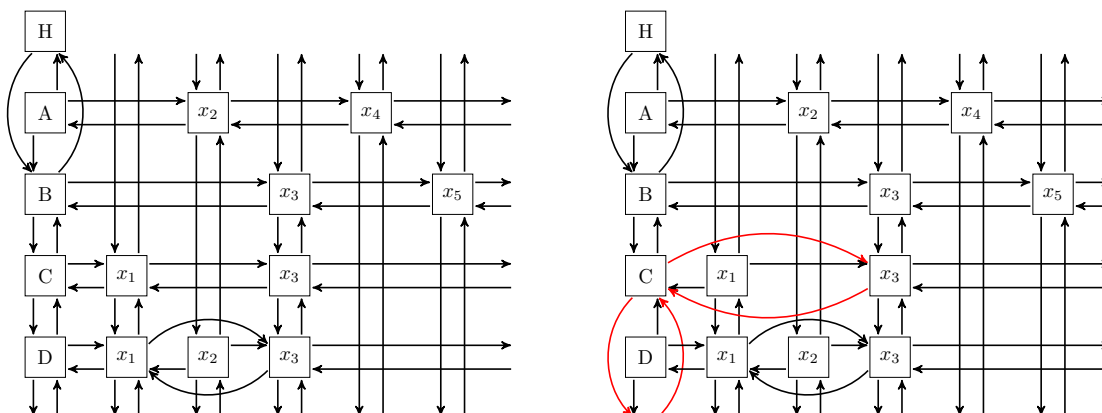
We now collect the original equations into the rows of a matrix, and because the constant term is always one, it can be ignored, see Figure 5.2a. We then associate a doubly linked circular list to each column and row of the matrix, see Figure 5.2b. The first column contains row-headings for each row. The first data node in the header column is a special “root” like object that is the starting point for any list iteration. Each data node n will have five arrays of pointers associated with it: $L[n], R[n], U[n], D[n], H[n]$. These correspond to a node’s left, right, up, and down neighbors in the linked list structures. $H[n]$ is a pointer back to a node in the header row (not illustrated in Figure 5.2b). The root header object does not have a left or right linked list attached to it. Also, every header row node does not use the $H[n]$ pointer.

The outline of the method is given in Algorithm 10. We now illustrate the workings of the algorithm on our example. We start by calling procedure `SEARCH`. First, let us pick row A to process. The first thing we do is run procedure `COVER` on the row. This procedure has the job of removing x_2 and x_4 from the list. By this, we mean it will be impossible to start at the root node and iterate over the list at reach a x_2 or x_4 node. See Figure 5.3a. The outer for-loop then loops over the variables in the A row and iteratively attempts to assign them to 1. When a node (variable) is assigned to one, it is recorded by inserting it into the solution stack S , so at any point S will contain which variables are nonzero. It is important that S is a stack of nodes in the linked

Algorithm 10 Dancing Links Algorithm

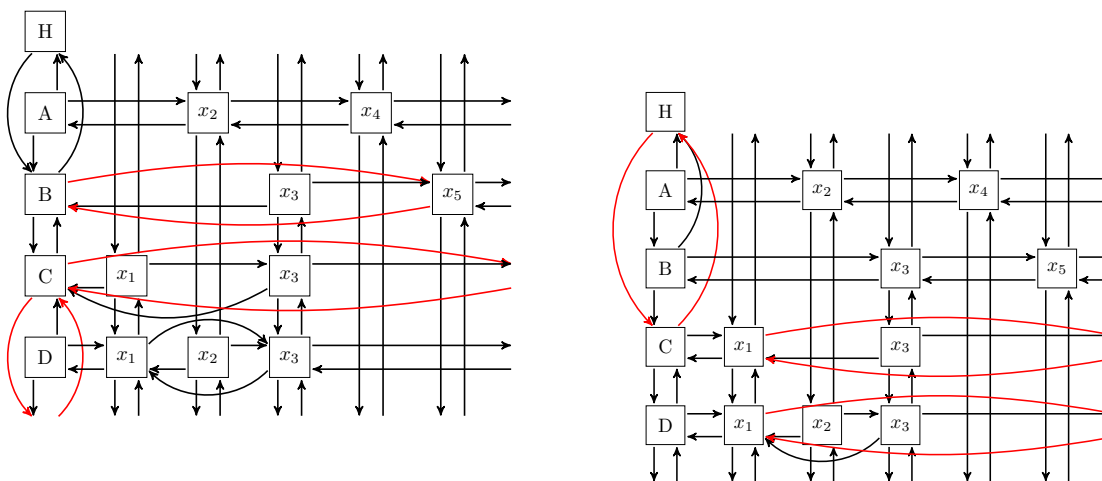
Procedure **SEARCH**Let H be the root node.Let S be a stack of nodes that are nonnegative.If $D[H] = H$, print the current solution from stack S and stop.Pick a row r to process (say $r \leftarrow D[H]$)Run procedure **COVER**(r).**for** $n \leftarrow R[r], R[R[r]], \dots$, while $n \neq r$ **do** $S.PUSH(n)$ **for** $j \leftarrow U[n], U[U[n]], \dots$, while $j \neq n$ **do** Run procedure **COVER**($H[j]$). **end for** Run procedure **SEARCH** $n \leftarrow S.POP()$, $r \leftarrow H[n]$ {Search failed, undo last step} **for** $j \leftarrow D[n], D[D[n]], \dots$, while $j \neq n$ **do** Run procedure **UNCOVER**($H[j]$). **end for** **end for**Run procedure **UNCOVER**(r) and stop.Procedure **COVER**(n) $D[U[n]] \leftarrow D[n]$, and $U[D[n]] \leftarrow U[n]$.**for** $i \leftarrow R[n], R[R[n]], \dots$, while $i \neq n$ **do** **for** $j \leftarrow U[i], U[U[i]], \dots$, while $j \neq i$ **do** $L[R[j]] \leftarrow L[j]$, and $R[L[j]] \leftarrow R[j]$ **end for****end for**

list structure, and not just a stack of which variables are one. This allows us to POP a node from S and know what variable it represents, and what row it came from. At this point we add row A 's x_2 node to the solution stack S . The first inner for-loop then loops over the rows that have an x_2 and calls the **COVER** procedure on them. This has the effect of propagating the implications of setting $x_2 = 1$, in that row D is removed (because it is satisfied) and variables x_1 and x_3 have been removed (set to zero). The first step in covering row D is to remove the x_1 node, see Figure 5.3b. The second step in covering row D is to remove the x_3 node, see Figure 5.4a. Next we finally enter our first recursive call to **SEARCH**. Upon doing so we should pick row C to process next. We immediately see that row C has no nodes left, and hence our current variable assignment $x_2 = 1$ leads to an infeasible system.



(A) After running the cover procedure on row A. Will first pick $x_2 = 1$. (B) Propagating $x_2 = 1$: Cover row D. Step one is to remove x_1 from the list.

FIGURE 5.3. Selecting $x_2 = 1$.



(A) Propagating $x_2 = 1$: Cover row D. Step two is to remove x_3 from the list. This produces the contradiction in row C.

(B) After covering row B.

FIGURE 5.4. Getting a contradiction and undoing it.

We continue stepping in the algorithm to see how it handles this. First, COVER is called on row C which only has the effect of removing itself from the home column. The outer for-loop does not perform any iterations as $R[C] = C$. The UNCOVER procedure is not reproduced here, but it has the task of undoing what the COVER procedure does. Hence UNCOVER on row C just puts it back into the first column's list. The second call to SEARCH now terminates and returns control to the

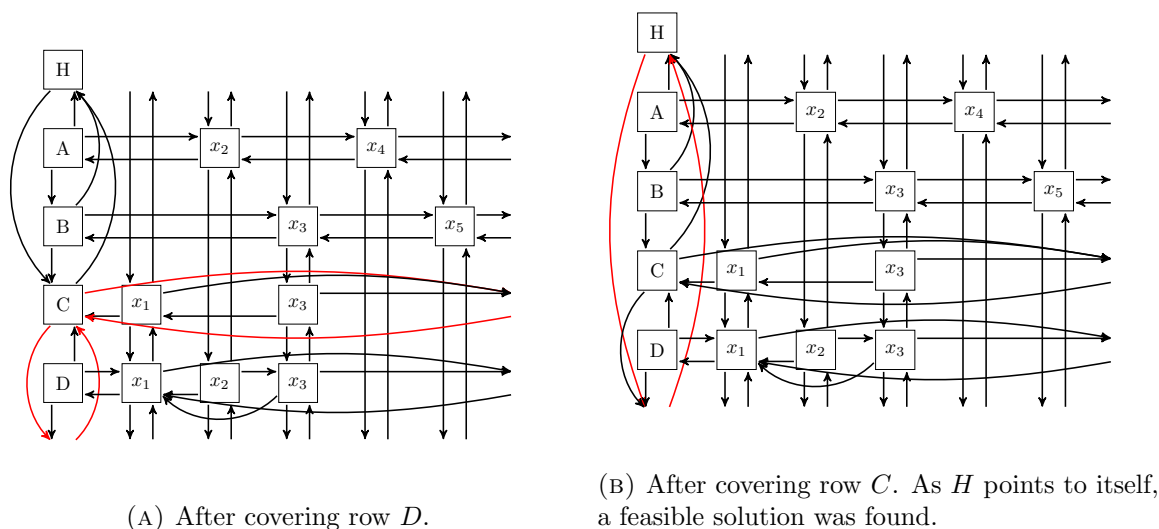


FIGURE 5.5. The final state

first **SEARCH** call. Node A 's x_2 is removed from the stack S . **UNCOVER** is called on row D and the data structure is put back into the initial state after **COVER** was called on row A (see Figure 5.3a). Node A 's x_4 is then set to one and inserted in S . It appears in no other row, so no additional **COVER** operations are done. Then **SEARCH** is called again (the recursive tree is at depth one now). Let us pick row B to process, and start by calling **COVER** on row B , see Figure 5.4b. The first element in the row is selected and $x_3 = 1$, and B 's x_3 is inserted in S . As x_3 appears in rows C and D , **COVER** is also called on those rows, see Figure 5.5. This concludes the bound propagation of $x_3 = 1$, and **SEARCH** is recursively called again. However, the linked list starting at the root only contains the root, and so this procedure terminates. The state of the stack S contains x_4 and x_3 , implying a solution of $x_4 = x_3 = 1$ with the other variables set to zero.

There are no restrictions on how to pick the next row to process, other than it has to be one obtainable from the root's linked list. One could select a row randomly, or by selecting the row with the fewest (or largest) number of variables left. There are many ways a row could be given a priority. For example, a row's priority could be a function of how many of its variables appear in other rows.

Lastly, if these figures were placed in a movie, it would be clear why this algorithm is called dancing links! See [94] for a full description of the **UNCOVER** procedure.

5.3. How to use dancing links

There are a few ways dancing links can be applied in the solution process; for example, as a heuristic for finding a feasible point to a MILP problem. Even within this area, there are a few ways of doing this. Our approach will be to use dancing links to get a partial feasible solution and create a new MILP to build the fully feasible solution.

Consider the MILP

$$\begin{aligned} \min \quad & c_1^T x + c_2^T y \\ & Ax + By \leq b \\ & Cy = \mathbf{1} \\ & y_i \in \{0, 1\} \\ & x_i \in \mathbb{Z} \text{ for } i \in I \end{aligned}$$

where we explicitly write the set partition constraints in the form $Cy = \mathbf{1}$, and $\mathbf{1}$ is a vector of all ones.

The strategy behind our heuristic is to apply dancing links to $Cy = \mathbf{1}$. If dancing links shows that $Cy = \mathbf{1}$ is infeasible, then the original MILP must be infeasible. Otherwise, we have that $Cy^0 = \mathbf{1}$ and $y_i^0 \in \{0, 1\}$. We can create a new MILP by plugging in the values for the y variable and solve the smaller problem

$$\begin{aligned} \min \quad & c_1^T x \\ & Ax \leq b - By^0 \\ & x_i \in \mathbb{Z} \text{ for } i \in I. \end{aligned}$$

This then produces a feasible point to the original problem. The idea is that by fixing the y variable, the new problem is very easy to solve. If this is not the case, then creating a sub-MILP problem has no benefits.

TABLE 5.1. Impact of using dancing links in a sub-MILP heuristic

	Number of problems	Percent of problems
size of benchmark	184	
new feasible points	35	19%
better feasible points	13	7%

Extending the partial feasible solution y^0 to a feasible solution to the original problem can be done in many different ways. The above idea was to create a smaller MILP problem to find a x^0 solution to go with y^0 . Extending the partial feasible solutions to fully feasible solutions are generally referred to as “repair” heuristics in the literature, and so dancing links can be paired with many repair heuristics.

5.4. Results

One main contribution of the author’s internship was implementing the above strategy as a heuristic plugin to the SAS/OR MILP solver. Table 5.1 illustrates the impact the heuristic had on a benchmark set. The benchmark used contained 184 problems, where each problem contained set partition constraints and the SAS solver called the heuristic at least once on each of them. Of these 184 problems, the sub-MILP heuristic was able to find feasible points to 35 of these, so the heuristic was successful on 19% of the problems. The feasible point that was found was the best feasible point in the solution process at the time to 13 problems. Said differently, on 13 or 7% of the problems, the heuristic was responsible for producing new global primal bounds.

The dancing links data structure produces a decent MILP heuristic that takes advantage of the role set partitioning constraints play in many problems. A nice feature of the data structure is that it can be extended to work with more general constraints.

It is easy to extend dancing links to also work with set packing constraints (e.g., $x_1 + x_2 \leq 1$, x_i binary). For example, these rows could simply be added to the dancing links data structure. Every row could be given a priority based on their type, and when picking a new row to process, the priority could be taken into account. If set partition constraints correspond to a high priority and set packing constraints correspond to a low priority, then when a low priority row is processed, all the set partition constraints are satisfied and a feasible solution is obtained.

CHAPTER 6

Application in distance geometry for neuro-immune communication

This chapter explains the mathematical tools used to study the neuro-immune interaction in the spleen during inflammation. See Section 1.6 for a fuller description of the medical problem. There are two kinds of objects in the spleen we are interested in: $CD4^+ChAT^+$ T-cells (henceforth referred to as just T-cells) and nervous-system filaments. The main question was, how does the distribution of these two objects change as the spleen responds to inflammation? That is, are T-cells found closer to nerve cells during inflammation, or is there no relationship between the location of these two types of cells in the spleen?

To research this question, my collaborators at the University of California, Davis, School of Veterinary Medicine have imaged the spleen of 18 mice, some of which suffer from inflammation. Advanced imaging technology is used to map the location of each cell type. However, the resulting image is extremely noisy. The software tool Imaris [30] is used to construct the true location of the T-cells and nerve filaments. Despite being a powerful tool, using Imaris to clean the imaging data is a labor- and time-intensive task. However, it is possible to write **MATLAB** [123] scripts that can interface with Imaris data sets. To help clean the data, we have written **MATLAB** scripts that take Imaris data, clean it up by reducing the noise, and return it to Imaris. Section 6.1 explains some of the methods we have developed to speed up the data cleaning steps.

After the data is cleaned, the central task was to study the distribution of T-cells and nerve cells. Our approach was to use cluster analysis to determine if there are differences during inflammation. Section 6.2 is devoted to this process.

All code from this project can be found in the appendix.

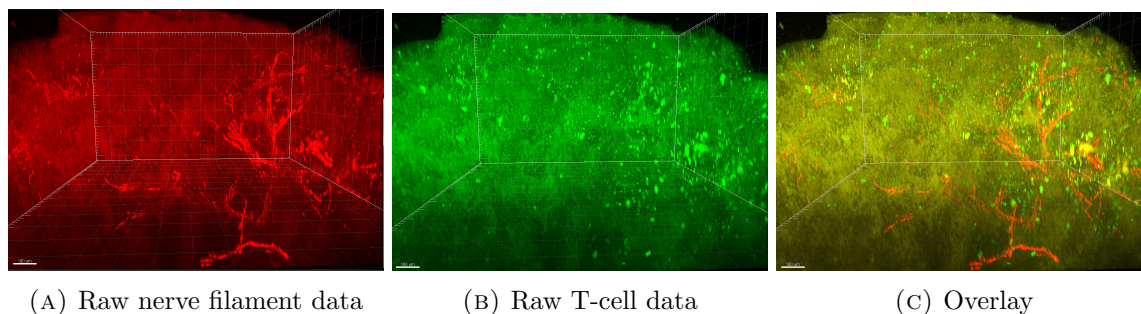


FIGURE 6.1. Raw microscope data

6.1. Cleaning the data

The initial data contains pixel information from the microscope. Each image is layered, creating a three dimensional array of pixel information called *voxels*. The spleen is stained and the voxel values contain an intensity value of how much dye was detected by the microscope. Larger intensity values are associated with T-cells and nerve cells. Figure 6.1 shows the raw voxel information. An immediate observation is that the imaging data is extremely noisy. Consider the raw nerve cell data. We can see a few regions of bright red lines or strings. These correspond to true nerve filaments. There is also a cloud of low intensity red points everywhere. These low intensity points mark other cells we are not interested in, and also contains imaging noise. The low intensity points must be filtered out. Likewise, the bright green areas are the T-cells we are interested in, while the low intensity cloud of points are noise representing other cell types.

In Figure 6.2, we show how to use Imaris to remove the noise from the red nerve filaments, and how the filaments are modeled as a triangulated surface. That is, Figure 6.2a contains about 2000 different surfaces, where each surface is a two dimensional triangulated mesh. The T-cell data is simply modeled as a collection of spheres in Figure 6.2b, and we refer to these spheres as *spots*. Going from Figure 6.1 to Figure 6.2 is an extremely time-consuming process. In this section we describe the process of cleaning the data and how we applied mathematical tools to speed the process up.

6.1.1. Step 1: the boundary. The boundary of the spleen produces imaging artifacts. Figure 6.3a shows a slice of the spleen in the original voxel data. There is a band of data near the boundary of the spleen where the voxel data looks fuzzy. This results in many false positives for

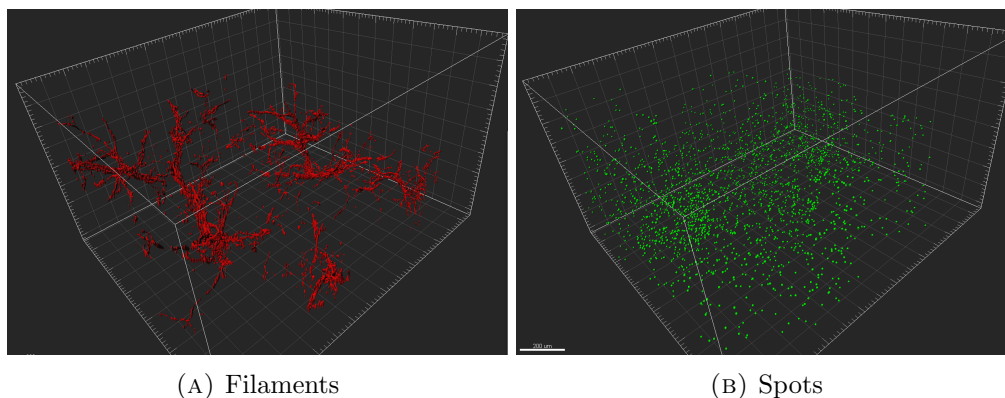


FIGURE 6.2. Clean data model

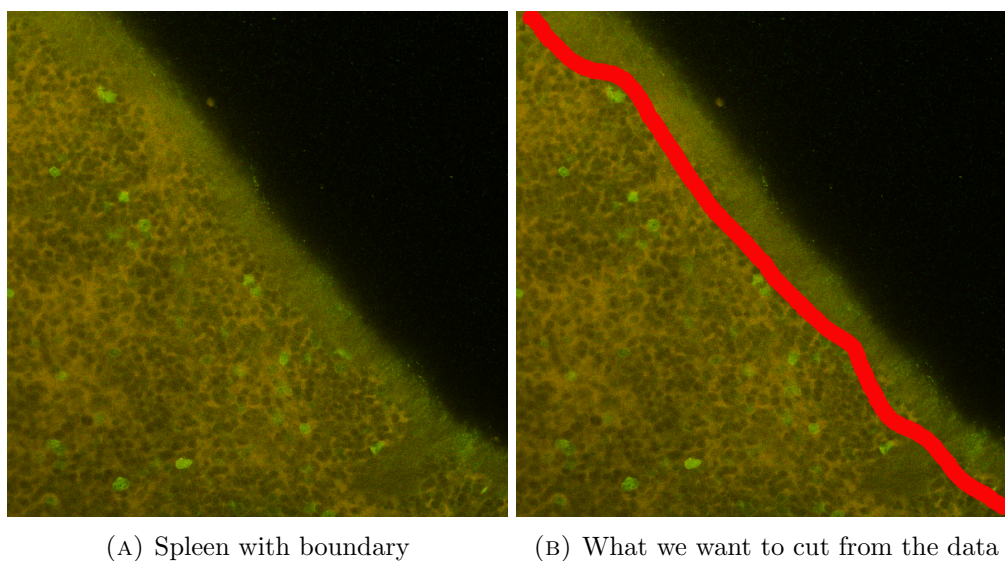
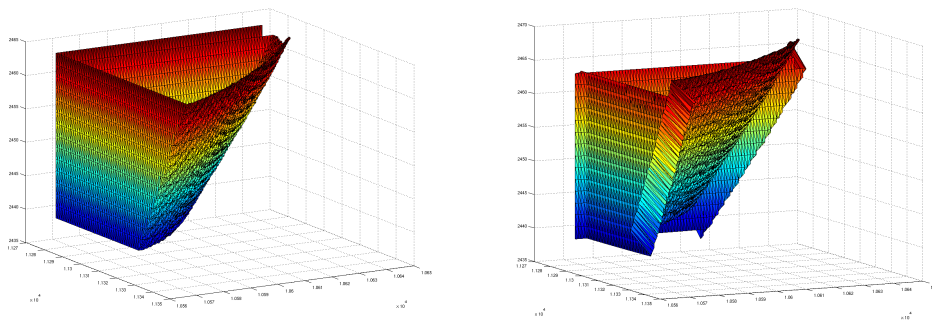


FIGURE 6.3. Boundary of the spleen

T-cells and nerve filaments from the raw microscope data. If this band of noise is not removed from the data set, Imaris will later identify these areas as having unrealistically many T-cells and nerve filaments. Therefore, the first step in processing the image data is to remove the boundary from the raw voxel data set. Before joining the project, the researchers in the veterinary school were manually erasing the noisy boundary from each slice of the image. That is, if a spleen contained 2000 image slices, a human would manually edit 2000 images by erasing the boundary. This was a highly repetitive and time-consuming task.



(A) Partial view of triangulated boundary (B) Naive shrinking of the boundary

FIGURE 6.4. Triangular mesh of spleen boundary

To do this automatically, our approach was to build a surface using Imaris that is a triangular mesh representing the boundary of the spleen. Imaris has the capability to filter a data set based on whether it is inside of some surface. The boundary surface can be shifted inward by a small distance, and then Imaris can be used to filter data that now lies on the outside of the smaller surface. This would remove the boundary of the spleen. Figure 6.4a is a partial view of the triangulated surface representing the boundary of the surface. Notice that this mesh has some flat sides representing the face where the spleen was cut by a scalpel. Also, the full surface is essentially a deformed sphere, without any holes. Hence the problem was to take a polygonal mesh, and offset it by a small negative distance. In the computational geometry community, this problem is related to computing *straight skeletons* [5], and many excellent software packages exist for this kind of computation such as the Computational Geometry Algorithms Library [38]. See also [41, 116, 117]. The difficulty in computing mesh offsets is that the topology of the mesh can change. For example, when shrinking a surface, two edges might intersect, requiring finding a new set of vertices and triangles to describe the shifted mesh. Instead of proceeding further, we experimented with the naive approach of just shifting each vertex in the negative direction of its vertex normal vector. A vertex normal vector is the average of the normals at each facet the vertex is adjacent to. This simple approach is incorrect, as it does not work at sharp angles, see Figure 6.4b. However, we were able to easily remove the noisy spleen boundary in Imaris with this approach. This is a rare example when the *correct* (and more sophisticated) method was not the best way to solve a problem!

6.1.2. Step 2: making Imaris spots from voxel data. The task now is to go from the voxel data in Figure 6.1b to Imaris spots in Figure 6.2b. Imaris constructs spots by looking at the voxel data and identifying a spot as a collection of voxels of high intensity. The threshold of when a voxel intensity is part of a spot is a user-defined constant in Imaris. This leads to a major problem: Imaris cannot be used to make spots for the entire spleen at once. This is because the average intensity values change throughout the spleen. The optimal thresholding value is a local value and changes throughout the spleen. If the Imaris constructs spots for the entire spleen at once, some regions will have too many spots, while other regions would appear not to contain T-cells. Looking at the raw data, we can see how Imaris is wrong in this case. Hence the spleen must be divided into smaller boxes, the spot-making function in Imaris must be used on each small box, and a unique threshold parameter must be assigned to each box. Speeding up this process is difficult. One thought was to write a MATLAB extension that divides the spleen volume into smaller boxes, runs the Imaris spot making function on each box, and then sets the correct threshold value by also analyzing the raw data. After contacting Imaris, we discovered that each step is not supported. Because of these limitations, a human must divide up the spleen into smaller regions and apply the spot making function. This would not be a problem if we only needed to subdivide the spleen into a few boxes. But because of our dataset's size, we needed to subdivide the spleen into a few hundred boxes! Figure 6.5 shows the steps involved in using Imaris to make the spots in each subdivision. In total four menus must be clicked through before the spots are made, and for each menu, the user has to enter a command and click the next button. Figure 6.5c, or menu 2, is where the box boundary is modified, and Figure 6.5d is where the key spot parameter is modified. It is this parameter that must be set by the expert on each subdivision.

To reduce the necessary repetition, we sought to automatically divide the spleen into smaller boxes and run the Imaris spot making function on each box with the default value that Imaris produces on each box. The default value that Imaris uses on each small box is different for each box and is better than running the spot making function on the entire spleen at once, but a human might still need to modify the value. Hence our solution was to automatically build the spots on each box with the default value Imaris uses for each box. A human can then do a second pass through the set of boxes and modify the spot parameter on each box as necessary.

6.1. CLEANING THE DATA

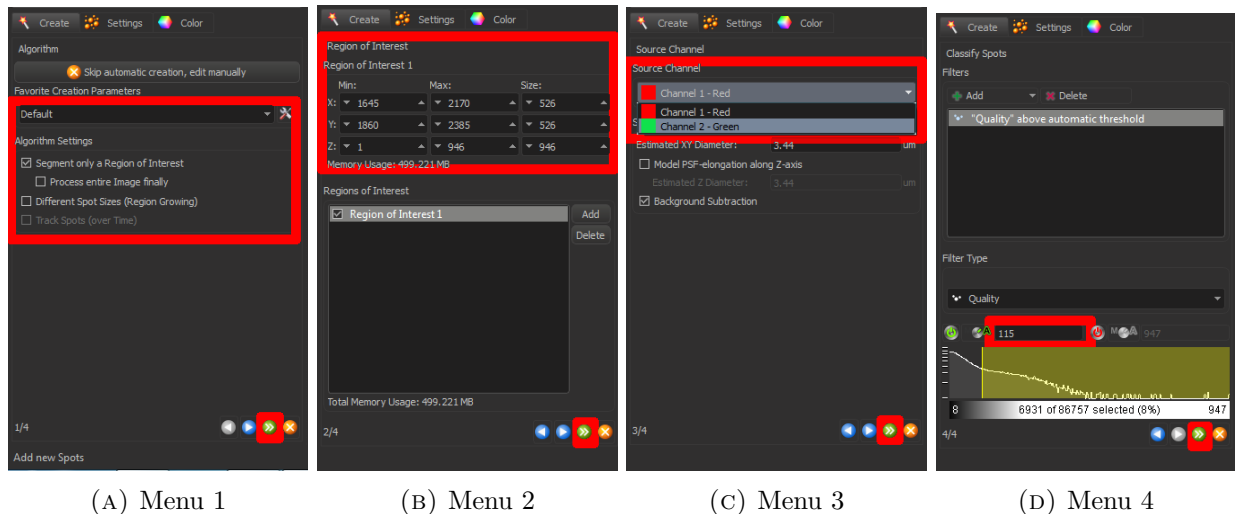


FIGURE 6.5. Sequence of menus for making spots

To automatically make the spots, we wrote a script using AutoIt [118], which is a tool popular in IT administration for programming mouse and keyboard input. With this script, we automatically click through all the menus to build a few hundred boxes containing spots. Using this tool may not be an application of data science, but it is very important in reducing time spent cleaning the data. The AutoIt script allowed the researchers to better spend their time and improved their work flow.

Dividing the spleen into smaller boxes and building spots in each box produces one problem. The same spot can be identified twice. For example, let B_1, B_2 be boxes defined by

$$B_1 = \{x \in \mathbb{R}^3 \mid 0 \leq x_1 \leq 1, 0 \leq x_2 \leq 1, 0 \leq x_3 \leq 1\},$$

$$B_2 = \{x \in \mathbb{R}^3 \mid 1 \leq x_1 \leq 2, 0 \leq x_2 \leq 1, 0 \leq x_3 \leq 1\},$$

and note that they have a common intersection. It is possible that a spot with center $(.9, 0, 0)$ and radius 0.2 is produced in B_1 . Notice that this spot produced by Imaris is allowed to extend past its box boundary! Moreover, Imaris could produce a spot with center $(1.1, 0, 0)$ and radius 0.2 in B_2 . This means the spots overlap, or that two different T-cells are in the same location, an impossibility. Therefore “almost duplicate” spots can be created. To remove these, we simply compute the nearest neighbor of each spot, and if two spots intercept, we keep just one of the spots. The nearest neighbor calculation is very similar to what is described in Section 6.2.1.

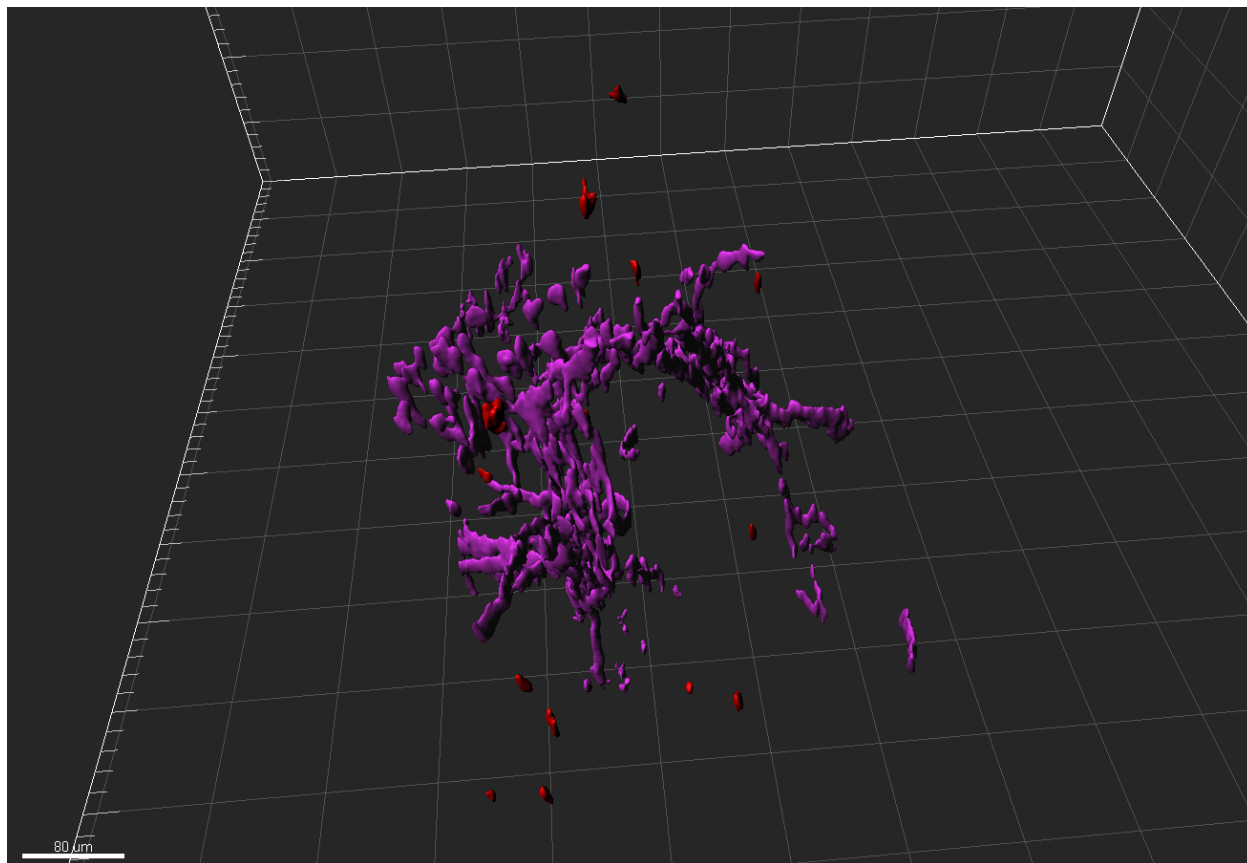


FIGURE 6.6. Red surfaces are noise, purple surfaces are true filament models

6.1.3. Step 3: making Imaris filament surfaces from voxel data. The process of going from voxel data in 6.1a to the Imaris surfaces in Figure 6.2a starts with applying the same techniques as for the spots. The spleen is subdivided, and the Imaris function that builds the surfaces from the voxel data is applied on each box. AutoIt can again be applied to speed things up. One difference is that duplicate surfaces are not produced by Imaris.

But there is one key difference: sometimes Imaris will identify noise as being true filaments. Sometimes we cannot modify Imaris parameters on a box that keep all the true filaments while deleting all the noise. Often there are small surfaces, in regions isolated from the other larger filaments, that Imaris identifies as filaments. The problem is illustrated in Figure 6.6. The purple area is a collection of surfaces that model the true nerve filaments. The isolated red surfaces are noise. They are not clearly connected to a larger filament, nor do they seem to be connected by a line, which would also imply they form a filament.

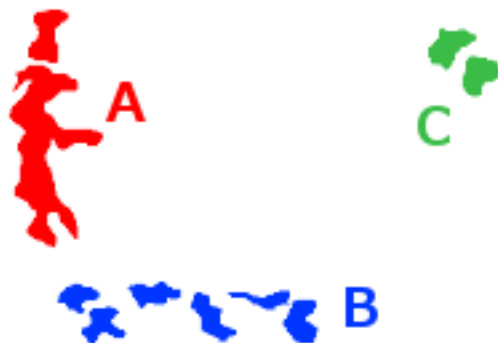


FIGURE 6.7. We remove cluster C

Our strategy for removing the noise is to compute the closest neighbors for each surface. If a surface contains a large volume, or is near such a surface, we keep it. We also keep surfaces that form a large group. Figure 6.7 illustrates in dimension two what kind of surfaces we want to identify. We keep both surfaces in the red C cluster because one surface is large, and the other is near to a large surface. We keep all the surfaces in the blue B cluster because their group size is large. The green surfaces in cluster C are removed from everything, has a small total volume, and is a small group. Therefore the goal is to remove the surfaces in the C cluster.

To implement this heuristic, we compute the distance between any two surfaces. Using this, we compute an agglomerative hierarchical clustering [119]. This creates a cluster tree where each surface starts off in its own cluster and forms the leaf nodes of the tree. Pairs of clusters are merged as one moves up the hierarchy. The height at which two clusters are merged in the tree represents the minimum distance between the two clusters. We cut the tree at height $20\mu\text{m}$, meaning that if two surfaces are further than $20\mu\text{m}$, then they are not merged together. The value $20\mu\text{m}$ was selected as it produced visually appropriate clusters.

For each resulting cluster of surfaces, we perform two heuristics on them. First, we compute the volume of each surface in a cluster. We then keep the largest clusters that account for 90% of the total volume. In the example figure, this may mean that only cluster A would pass in Figure 6.7. The clusters that fail this test contain only small surfaces. We then apply the second heuristic on these small clusters, which is simply thresholding the number of surfaces in a cluster. In Figure 6.7 this means cluster B is kept while cluster C is removed.

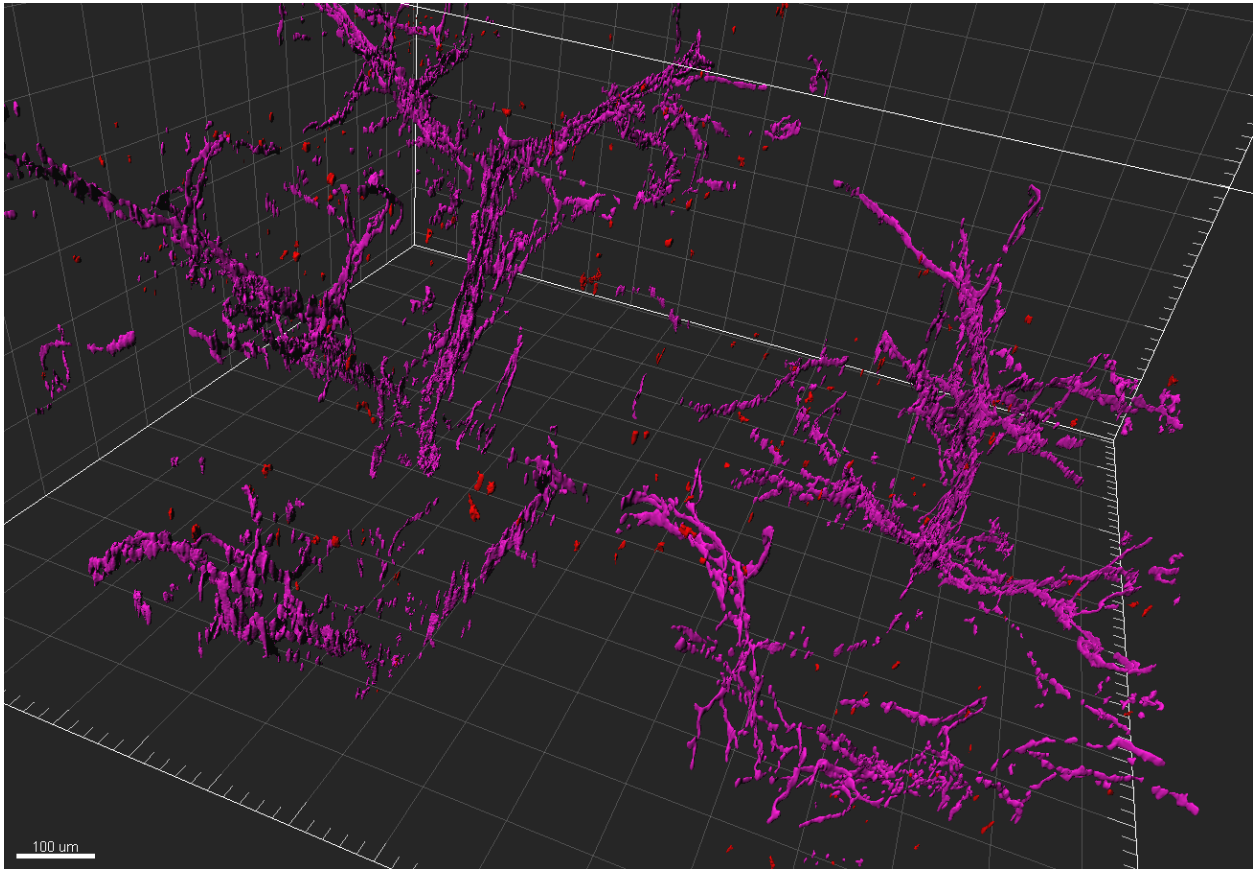


FIGURE 6.8. Red surfaces are noise, purple surfaces are true filament models

Figure 6.8 shows the result of this strategy on about 1600 surfaces, composing the filaments for the entire spleen. Originally, every surface is marked red. Our algorithm returns the surfaces to keep. The purple surfaces are the cleaned filament model, and the red surfaces are classified as noise and deleted.

6.2. Cluster analysis

The previous section described how we cleaned the data. Now we address the central research question: how does the distribution of spots and filaments change under inflammation? Figure 6.9 shows a zoomed in overlay after cleaning the data in Figures 6.2a and 6.2b. We highlighted two regions in blue boxes. In the lower right box, we see that there are green spots really close to the red filaments. This suggest the T-cells and nerve cells are closely interacting, and potentially connecting. However, as the upper left box shows, many spots are not close to *any* filament. To

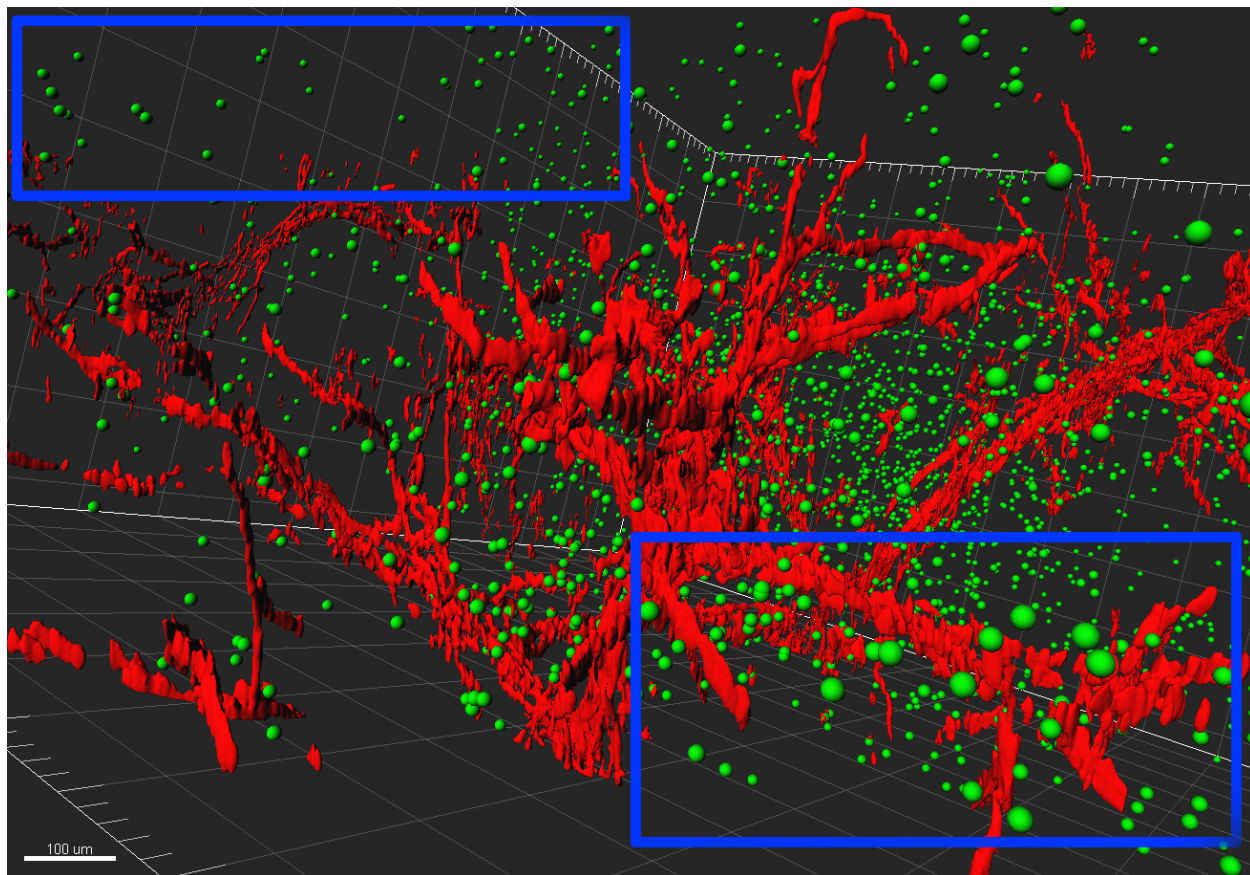


FIGURE 6.9. Zoomed in overlay of spots and filaments

study the distribution of these two sets, we computed the distance from each spot to its closest point on a filament. For each spleen sample, we know if it came from a mouse with inflammation or not. Using the distribution of distance values between the spots and filaments, together with the inflammation label, we sought a pattern in the distance distributions. At the time of writing, work on this project was not completed. In the next sections, we describe the steps we *will* perform in exploring how the distance distributions changes under inflammation.

6.2.1. Step 1: computing nearest neighbour. Each surface in Imaris is a triangulated mesh containing vertices and triangles. Because the mesh is very fine, we approximate computing the nearest distance from a spot to a filament by instead computing for each spot, the closest distance from a spot's center to a red vertex. This is a classic nearest neighbor calculation on two point sets: for each green point, find its nearest neighbor among the red points.

Before joining this project, the author’s collaborators were using a `MATLAB` extension from the vendor’s website for computing these distance values. The algorithm employed took $O(rg)$ time where r is the number of red vertices from the filaments, and g is the number of green spots. The script was similar to Algorithm 11. As r is in the order of tens of millions, and g is in the order of tens of thousands, this took many hours to compute. For a moderately sized spleen, this resulted in 6+ hours of computational time to find these distances. Worse, sometimes things would crash and a day would be wasted. Again, the software tools are a shared resource, and so it could essentially take a few days to compute these distances! We immediately replaced the $O(rg)$ algorithm with a $O(g \log(r))$ average time algorithm using `MATLAB`’s nearest neighbor functions. The result was a $35x$ computing time decrease. The 6-hour computation was reduced to 10 minutes. Because this improvement was so large, we next describe the core data structure behind `MATLAB`’s nearest neighbor search function.

Algorithm 11 The initial algorithm from the Imaris website for computing the nearest distance between two point sets

Input: Set of spot centers $S \subset \mathbb{R}^3$, set of vertices $V \subset \mathbb{R}^3$

Output: For each $s_i \in S$, the minimum distance $d_i \in \mathbb{R}$ to a vertex in V

for all $s_i \in S$ **do**

$d_i \leftarrow \infty$

for all $v \in V$ **do**

$d_i \leftarrow \min(d_i, \|s_i - v\|)$

end for

end for

return d_i for $i = 1, 2, \dots, |S|$

At the heart of `MATLAB`’s nearest neighbor function, `knnsearch`, is a kd-tree. A kd-tree is a binary tree where the leaf nodes are buckets containing points in \mathbb{R}^k and each non-leaf node contains a coordinate index i and a split value v_i . The left subtree of a non-leaf node contains points $x \in \mathbb{R}^k$ for which $x_i \leq v_i$ and the right subtree contains points where $x_i > v_i$. The non-leaf nodes implicitly define a splitting hyperplanes that are perpendicular to one axis. Figure 6.10 shows a kd-tree with the points $(2, 9, 1)$, $(6, 1, 1)$, $(9, 3, 1)$, $(13, 1, 2)$, $(17, 2, 2)$, $(7, 1, 10)$, $(9, 2, 12)$, $(12, 3, 14)$, $(15, 1, 11)$, $(7, 8, 1)$, $(6, 7, 3)$, $(6, 5, 5)$, $(7, 5, 5)$, and $(7, 6, 5)$. Imagine inserting a new point, $(6, 5, 3)$ into the tree. The search process starts at the root. The root node says that points where the first coordinate is less than or equal to five are in the left child while points where the first coordinate is larger

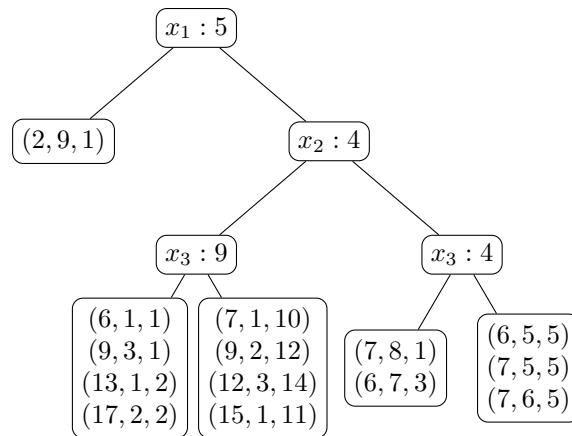


FIGURE 6.10. Example kd-tree

than five are in the right child. Because $6 > 5$, the right child is explored. The node $x_2 : 4$ tests the second coordinate of the point $(6, 5, 3)$. The right child is taken and we arrive at node $x_3 : 4$. The third coordinate is tested and the left child is taken. At this point, the node is simply a list of points, and the new point is appended to this list. Searching for a point is a similar process. Leaf nodes can be split if their size becomes too large. For example, if we impose a limit of four on the leaf nodes and the point $(9, 1, 10)$ is inserted, the right child of the node $x_3 : 9$ will have to be split. The test coordinates can be cycled, and the new node could just test the first coordinate. For a complete description of a kd-tree and how they are used for computing the nearest neighbor, see [49, 78].

6.2.2. Step 2: dimensionality reduction. Let g be the number of spots in the data set, then the nearest neighbor calculation produces g distance numbers. We compute a histogram of these distance numbers with N bins. Computing the histograms of the nearest neighbor distance for each spleen allows us to study how the distribution of T-cells and nerve cells changes with inflammation. Figure 6.11 shows one such histogram with $N = 100$. The horizontal axis show the ranges of each bin, and the vertical axis is the frequency. Two observations are obvious. First, there is a large spike at the first bin, meaning there are many spots that are really close to a nerve filament. Second, most spots are not close to a nerve filament. This histogram is from a healthy spleen. At the time of writing, the data processing has not been finished for the other spleens,

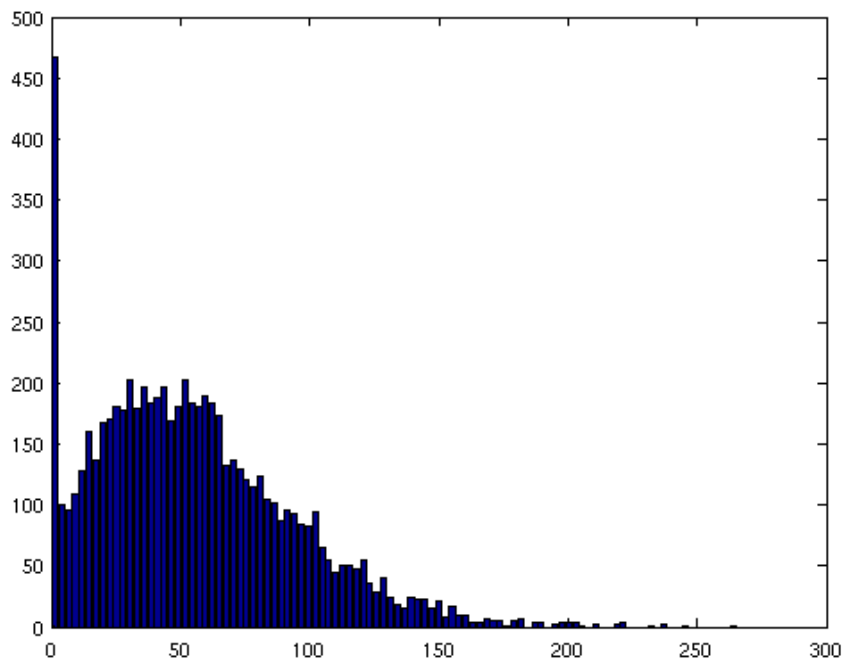


FIGURE 6.11. Histogram of nearest neighbor distances for a small spleen sample

but it was hypothesized that the mass of the histogram would shift to the left for spleens with inflammation.

Quantifying the difference between histograms with 100 bins is not easily done. Our approach was to encode the histogram into one vector $h \in \mathbb{R}^N$ where h_i is the count in bin i . When we process all 18 spleens, we will have 18 histogram vectors h^1, \dots, h^{18} in \mathbb{R}^N . Using the inflammation data, it would be trivial to cluster 18 points in a large dimensional space into two sets. To better analyze the 18 histograms, we first used dimensionality reduction techniques to map the \mathbb{R}^N data into a low dimensional space such as \mathbb{R}^2 .

Principal component analysis (PCA) [89] is a general technique for exploring the structure of data. It takes a set of points in \mathbb{R}^N in the standard basis, and computes a new orthogonal basis. In the new basis, each coordinate is uncorrelated with the other coordinates. The first coordinate has the largest possible variance, and accounts for as much of the variability in the data as possible. The i^{th} basis gives the direction that contains the largest variance in the data under the constraint that it is orthogonal to the preceding directions. PCA is often used to visualize a high-dimensional

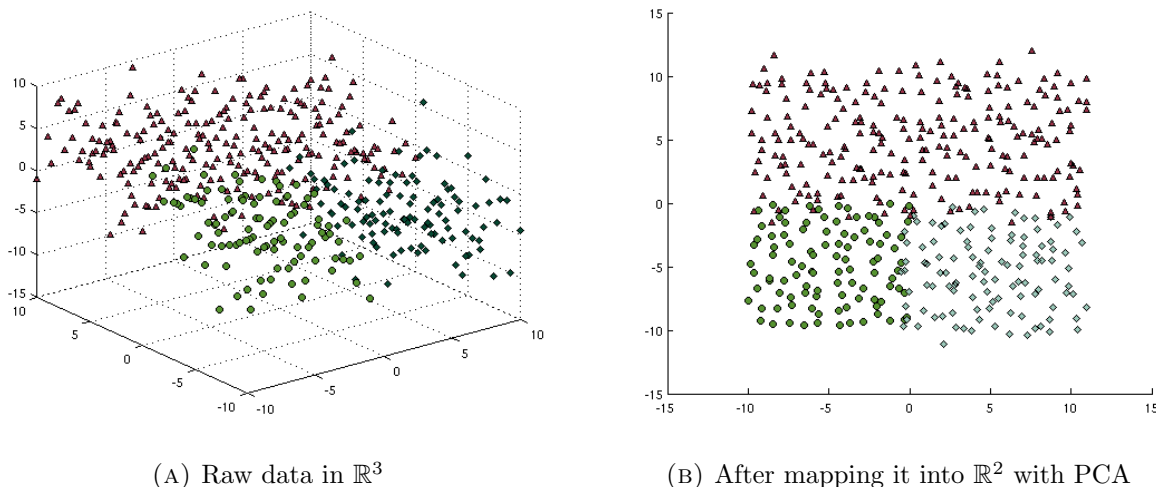


FIGURE 6.12. Example of using PCA for visualization

data set by first writing each point in the new basis, and then truncating the coordinates in each point. That is, for each data point, only the first few coordinates are kept. As an example, Figure 6.12a shows three different types of points in \mathbb{R}^3 . It is difficult to see how these points are related. Figure 6.12b plots the same points after running PCA and keeping the leading two components. It is now easy to see that these three point types are clusterable. This illustrates the two main uses for PCA: visualizing high-dimensional data, and as a preprocessing step for a clustering algorithm.

We now briefly mention one way to compute the PCA representation. Let $\hat{H} \in \mathbb{R}^{18 \times N}$ be a matrix containing the 18 spleen histogram vectors. PCA is a linear model, and each column of \hat{H} should have zero mean. Let $\bar{h} = \frac{1}{18} \sum_{i=1}^{18} h^i$ be the average spleen histogram vectors, and define $H \in \mathbb{R}^{18 \times N}$ as the matrix formed by subtracting \bar{h} from each row of \hat{H} .

Singular value decomposition (SVD) on H produces matrices $U \in \mathbb{R}^{18 \times 18}$, $\Sigma \in \mathbb{R}^{18 \times N}$ and $V \in \mathbb{R}^{N \times N}$ such that $H = U\Sigma V^T$, where U and V are orthogonal matrices, and Σ is diagonal matrix with non-negative real numbers on the diagonal [151]. The histogram data in the new basis is given by the rows of HV . Let $1 \leq r \leq \min(18, N)$, and let U_r be the first r columns U , V_r be the first r columns of V , and Σ_r be the upper left r by r submatrix. If H has full rank, it can be shown that $U_r \Sigma_r V_r^T$ is the best rank r approximation to H under the Frobenius norm. The histogram data in the new basis after keeping the largest r components is given by the rows of HV_r . Hence V_r encodes a map from histogram vectors in \mathbb{R}^N into \mathbb{R}^r . It was our belief that $r = 2$ or $r = 3$ would

suffice for a nice mapping where the spleens labeled with inflammation are clearly grouped in the new space.

Finally, there are many models for dimensionality reduction other than PCA. In particular, factor analysis [44], projection pursuit [87], independent component analysis [88], neural networks [86], and random projection methods [92, 96] have been used for dimensionality reduction. See for example [71, 113]. These methods could also be explored.

The author's impact in this collaboration was twofold. First, significant improvements to how the veterinary researchers clean and model their data was made. These improvements came about by recognizing classic problems from data science and geometry, and knowing how to implement more efficient algorithms to solve them. Second, we explored classic dimensionality reduction and clustering tools to automatically identify which spleens are connected to inflammation. Any result on how the distribution of T-cells and nervous cells is affected by inflammation can lead future researchers to better understand this interaction.

APPENDIX A

Computer source code

A.1. Codes for integrating a polynomial over a polytope and for computing the top coefficients of the Ehrhart polynomial

The source code for many of the algorithms covered in Sections 2 and 4 are online in the software package `LattE integrale` [54]. All code is available under the GNU General Public License at

<https://www.math.ucdavis.edu/~latte/>.

The `LattE integrale 1.7.3` bundle contains all software dependencies to run `LattE`. Within the bundle, the folder “latte-int-1.7.3” contains the core `LattE` code. The algorithms from Section 2 can be found in two folders:

“latte-int-1.7.3/code/latte/integration” and “latte-int-1.7.3/code/latte/valuation”.

Algorithms from Section 4 are in the folder “latte-int-1.7.3/code/latte/top-knapsack”. Refer to the manual for examples of integrating a polynomial over a polytope, and for computing Ehrhart polynomials.

It must also be noted that `LattE` can also compute other things not covered in this thesis. These include counting the number of integer points in a polytope, and computing Ehrhart quasi-polynomials for integer and rational polytopes.

A.2. Codes for cleaning and processing the spleen data

This section contains the `MATLAB` scripts used within `Imaris` [30] and other source code from Section 6.

A.2.1. Code for processing the boundary of the spleen. This `MATLAB` file is for processing the noisy boundary of the spleen from Section 6.1.1 by shifting a triangular mesh inward.

```
1 % Shrink a surface by its normals.
```

A.2. CODES FOR CLEANING AND PROCESSING THE SPLEEN DATA

```
2 %
3 %
4 % Installation :
5 % - Copy this file into the XTensions folder
6 % - You will find this function in the Image Processing menu
7 %
8 % <CustomTools>
9 %   <Menu>
10 %     <Submenu name="Spots Functions">
11 %       <Item name="shrink" icon="Matlab" tooltip="shrink">
12 %         <Command>MatlabXT::XTshrink(%i)</Command>
13 %       </Item>
14 %     </Submenu>
15 %   </Menu>
16 % <SurpassTab>
17 %   <SurpassComponent name="bpSpots">
18 %     <Item name="shrink" icon="Matlab" tooltip="shrink">
19 %       <Command>MatlabXT::XTshrink(%i)</Command>
20 %     </Item>
21 %   </SurpassComponent>
22 %   <SurpassComponent name="bpSurfaces">
23 %     <Item name="shrink" icon="Matlab" tooltip="shrink">
24 %       <Command>MatlabXT::XTshrink(%i)</Command>
25 %     </Item>
26 %   </SurpassComponent>
27 % </SurpassTab>
28 % </CustomTools>
```

```
29 %
30 % Description:
31 % Translate each vertex by its normal vector
32
33 function XTshrink(aImarisApplicationID)
34     % connect to Imaris interface
35     if ~isa(aImarisApplicationID, 'Imaris.IApplicationPrxHelper')
36         javaaddpath ImarisLib.jar
37         vImarisLib = ImarisLib;
38         if ischar(aImarisApplicationID)
39             aImarisApplicationID = round(str2double(
40                 aImarisApplicationID));
41         end
42         vImarisApplication = vImarisLib.GetApplication(
43             aImarisApplicationID);
44     else
45         vImarisApplication = aImarisApplicationID;
46     end
47     % get the spots
48     vSurfaces = vImarisApplication.GetFactory.ToSurfaces(
49         vImarisApplication.GetSurpassSelection);
50
51     if ~vImarisApplication.GetFactory.IsSurfaces(vSurfaces)
52         msgbox('Please select a surfaces object!');
53     end
54     return;
```



```
53
54     getData = true;
55     while getData == true
56         prompt = {'Distance to move each point:',};
57         dlg_title = 'Distance';
58         num_lines = 1;
59         defaultans = {'10',};
60         answer = inputdlg(prompt, dlg_title, num_lines, defaultans);
61         scaleFactor = str2double(answer{1});
62         if isnan(scaleFactor)
63             disp('Incorrect input');
64         else
65             getData = false;
66         end
67     end
68
69     vNumberOfSurfaces = 0;
70     vParentGroup = vSurfaces.GetParent;
71     vResult = vImarisApplication.GetFactory.CreateSurfaces;
72     vEdges = [];
73     vSelection = [];
74     vSinglesCount = 0;
75     isNewWrite = 1;
76     vNumberOfChildren = vParentGroup.GetNumberOfChildren;
77
78     for vChildIndex = 1:vNumberOfChildren
79         vObjects = vParentGroup.GetChild(vChildIndex - 1);
```

```
80     if vImarisApplication.GetFactory.IsSurfaces(vObjects)
81         vSurface = vImarisApplication.GetFactory.ToSurfaces(
            vObjects);
82         vSize = vSurface.GetNumberOfSurfaces;
83
84         for vIndex = 1:vSize
85             vTimeIndex = vSurface.GetTimeIndex(vIndex - 1);
86             vVertices = vSurface.GetVertices(vIndex - 1);
87             vTriangles = vSurface.GetTriangles(vIndex - 1);
88             vNormals = vSurface.GetNormals(vIndex - 1);
89             vVertices = updateVertices(vVertices, vNormals,
                scaleFactor);
90             vResult.AddSurface(vVertices, vTriangles, vNormals,
                vTimeIndex);
91         end
92
93         vSurface.SetVisible(false);
94         vNumberOfSurfaces = vNumberOfSurfaces + 1;
95         vSinglesCount = vSinglesCount + vSize;
96     end
97 end
98
99 % copy metadata from selected surfaces
100 vRGBA = vSurfaces.GetColorRGBA;
101 vResult.SetColorRGBA(vRGBA);
102 vResult.SetName(sprintf('scaled surface %f', scaleFactor));
103 vParentGroup.AddChild(vResult, -1);
```

```
104 end
105
106
107 function [newVertices] = updateVertices(vertices, normals, scaleFactor)
108     %make sure the normals are of unit length
109     normals = bsxfun(@times, normals, 1./sqrt(sum(normals.^2, 2)));
110     newVertices = vertices - scaleFactor * normals;
111 end
```

A.2.2. Code for processing the filament surfaces. This MATLAB file is for removing noisy filament surfaces from Section 6.1.3.

```
1 % Remove noisy surfaces
2 %
3 %
4 % Installation:
5 % - Copy this file into the XTensions folder
6 % - You will find this function in the Image Processing menu
7 %
8 % <CustomTools>
9 % <Menu>
10 % <Submenu name="Spots Functions">
11 % <Item name="FilterFilaments" icon="Matlab" tooltip="
    FilterFilaments.">
12 % <Command>MatlabXT::XTFilterFilaments(%i)</Command>
13 % </Item>
14 % </Submenu>
15 % </Menu>
16 % <SurpassTab>
```

A.2. CODES FOR CLEANING AND PROCESSING THE SPLEEN DATA

```
17 % <SurpassComponent name="bpSpots">
18 % <Item name="FilterFilaments" icon="Matlab" tooltip="
    FilterFilaments.">
19 % <Command>MatlabXT::XTFilterFilaments(%i)</Command>
20 % </Item>
21 % </SurpassComponent>
22 % <SurpassComponent name="bpSurfaces">
23 % <Item name="FilterFilaments" icon="Matlab" tooltip="
    FilterFilaments.">
24 % <Command>MatlabXT::XTFilterFilaments(%i)</Command>
25 % </Item>
26 % </SurpassComponent>
27 % </SurpassTab>
28 % </CustomTools>
29 %
30 % Description:
31 % Filters noise from filament surface data.
32
33 function XTFilterFilaments(aImarisApplicationID)
34 % global parameters for easy editing
35 global gp_SMALL_VOLUME_THRESHOLD;
36 global gp_CLUSTER_CUTOFF;
37 global gp_VOLUME_PERCENT_TEST;
38 global gp_CLUSTER_CONNECTIVITY_TEST;
39
40 % delete any surface with less than this 'volume'
41 gp_SMALL_VOLUME_THRESHOLD = 300;
```

```

42
43     % in micro meters.
44     gp_CLUSTER_CUTOFF = 20;
45
46     % larger percent = more clusters kept
47     gp_VOLUME_PERCENT_TEST = 0.95;
48
49     % number of surfaces in a cluster to keep.
50     gp_CLUSTER_CONNECTIVITY_TEST = 3;
51
52     % connect to Imaris interface
53     if ~isa(aImarisApplicationID, 'Imaris.IApplicationPrxHelper')
54         javaaddpath ImarisLib.jar
55         vImarisLib = ImarisLib;
56         if ischar(aImarisApplicationID)
57             aImarisApplicationID = round(str2double(
58                 aImarisApplicationID));
59         end
60         vImarisApplication = vImarisLib.GetApplication(
61             aImarisApplicationID);
62     else
63         vImarisApplication = aImarisApplicationID;
64     end
65     vSurface = vImarisApplication.GetFactory.ToSurfaces(
66         vImarisApplication.GetSurpassSelection);

```

```
66     if ~vImarisApplication.GetFactory.IsSurfaces(vSurface)
67         msgbox('Please select a surfaces object!');
68         return;
69     end
70
71     vSurface.SetVisible(false);
72     vResult = vImarisApplication.GetFactory.CreateSurfaces;
73
74     vSize = vSurface.GetNumberOfSurfaces;
75     allVolume = zeros(vSize, 2);
76
77     fprintf('Computing volume proxy for %d surfaces...', vSize);
78     for vIndex = 1:vSize
79         vVertices = vSurface.GetVertices(vIndex - 1);
80         vTriangles = vSurface.GetTriangles(vIndex - 1);
81         volume_proxy = 0.5 * size(vVertices, 1) + 0.5*size(vTriangles,
82             1);
83
84         allVolume(vIndex, 1) = vIndex;
85         allVolume(vIndex, 2) = volume_proxy;
86     end
87
88     fprintf('done.\n');
89
90     %Filter the really small surfaces out right now.
91     bigVolumeIndex = allVolume(:, 2) > gp_SMALL_VOLUME_THRESHOLD;
92     deletedSurfaces = allVolume(~bigVolumeIndex, 1);
93     allVolume = allVolume(bigVolumeIndex, :);
```

```
92
93 %sort the rows of allVolume with the smallest volume first.
94 [~, sortIndex] = sort(allVolume(:, 2));
95 allVolume = allVolume(sortIndex, :);
96
97 numSurfaces = size(allVolume, 1);
98
99 % partition the surfaces into a 'keep' and 'delete' set.
100 rng(654364);
101 [surfIDKeep, surfIDDelete] = FilterSurfaces_(vSurface, allVolume);
102
103 % insert the surfaces to keep into vResult
104 fprintf('Removing surfaces %s...', sprintf('%d, ', [surfIDDelete,
105     deletedSurfaces ]));
106 for vIndex = surfIDKeep
107     vTimeIndex = vSurface.GetTimeIndex(vIndex - 1);
108     vVertices = vSurface.GetVertices(vIndex - 1);
109     vTriangles = vSurface.GetTriangles(vIndex - 1);
110     vNormals = vSurface.GetNormals(vIndex - 1);
111     vResult.AddSurface(vVertices, vTriangles, vNormals, vTimeIndex)
112     ;
113     pause(0.01); %try to prevent matlab from saying 'not responding
114     ,
115
116 end
117 fprintf('done.\n');
118
119 vRGBA = vSurface.GetColorRGBA;
```

```
116     vResult.SetColorRGBA(vRGBA);
117     vResult.SetName(sprintf('Filtered Surface of %s', char(vSurface.
        GetName())));
118     vParentGroup = vSurface.GetParent;
119     vParentGroup.AddChild(vResult, -1);
120 end
121
122
123 function [surfIDKeep, surfIDDelete] = FilterSurfaces_(vSurface,
    allVolume)
124     % Partitions the surface ids in the first column of allVolume into
        two
125     % row vectors (surfIDKeep, surfIDDelete).
126     % parameters
127     %   vSurface: Imaris surface object, contains surfaces
128     %   allVolume: n x 2 matrix. Cols are surface-id, volume.
129
130     global gp_CLUSTER_CUTOFF;
131
132     surfNumbers = allVolume(:, 1)';
133
134     z = getLinkage_(vSurface, surfNumbers);
135     %figure()
136     %dendrogram(z, 0)
137     %title('Dendrogram of input surfaces')
138
139
```



```
140 % other interesting things that can be done with z
141 % http://www.mathworks.com/help/stats/cophenet.html
142 % http://www.mathworks.com/help/stats/inconsistent.html
143 % http://www.mathworks.com/help/stats/cluster.html
144 % http://www.mathworks.com/help/stats/silhouette.html
145 %Tdist = cluster(z, 'cutoff', .5, 'criterion', 'inconsistent');
146 fprintf('Clustering surfaces ... ');
147 Tdist = cluster(z, 'cutoff', gp.CLUSTER_CUTOFF, 'criterion', '
        distance');
148 fprintf('done.\n');
149
150 % cluster makes new cluster/surface id's.
151 % surface surfNumbers(i) is now part of cluster Tdist(i)
152 assert( length(surfNumbers) == length(Tdist));
153
154 % Apply two test to keep surfaces.
155 % 1) First keep, the largest clusters so that we keep x% of the
        total
156 % volume.
157 [surfNKeep, surfNDelet] = filterClustersByVolume_(allVolume,
        surfNumbers, Tdist);
158 % 2) Of the reject surfaces from test 1, keep thsoe that contain
        many
159 % surfaces
160 [surfNDeletKeep, surfNDeletDelete] = filterClustersByConnectivity_(
        allVolume, surfNDelet, surfNumbers, Tdist);
161
```

```
162     surfIDKeep = [surfNKeep, surfNDeletKeep];
163     surfIDDelete = surfNDeletDelete;
164 end
165
166
167 function [z] = getLinkage_(vSurface, surfNumbers)
168     %calls Matlab's linkage function.
169
170     n = length(surfNumbers);
171     D = zeros(n,n);
172
173     for i = 2:n
174         verticesSetI = vSurface.GetVertices(surfNumbers(i) - 1);
175         verticesSetI = sampleVertices_(verticesSetI);
176         for j = 1:(i-1)
177
178             verticesSetJ = vSurface.GetVertices(surfNumbers(j) - 1);
179             D(i,j) = min(pdist2(verticesSetI, verticesSetJ, 'euclidean'
180                 , 'Smallest', 1));
181
182         end
183         fprintf('Finished distance for index %d/%d\n', i, n);
184         pause(0.01); %try to prevent matlab from saying 'not responding
185             ,
186     end
187
188     Y = squareform(D);
189     fprintf('Computing linkage ...');
```

```
187     z=linkage(Y, 'single');
188     fprintf('done.\n');
189 end
190
191
192 function newVertices = sampleVertices_(oldVertices)
193     %Sample surfaces if more than 500 points.
194
195     N = size(oldVertices, 1);
196     if N <= 500
197         newVertices = oldVertices;
198         return;
199     end
200
201     numSample = round(max(500, 0.10 * N));
202     numSample = min(numSample, 4000);
203     newVertices = oldVertices(randsample(1:N,numSample),:);
204 end
205
206
207 function [surfNKeep, surfNDelete] = filterClustersByVolume_(volumes,
    oldClusterID, newClusterID)
208     % Partitions oldClusterID into two sets, surfaces we will keep, and
209     % surfaces we can delete. This is done by keeping newClusterID's
        that
210     % account for the largest X% of the data.
211     % Parameters:
```

A.2. CODES FOR CLEANING AND PROCESSING THE SPLEEN DATA

```
212 % volumes: n x 2 matrix. 1st column=old surface id, 2nd column=  
    volume  
213 % oldClusterID, newClusterID: each are length n arrays.  
214 % oldClusterID(i) is mapped into newClusterID(i)  
215  
216 assert( length(oldClusterID) == length(newClusterID));  
217  
218 % First, find the volume the new clusters contain by adding the  
    volumes  
219 % of the corresponding original surface ids  
220 uniqueClusters = unique(newClusterID(:));  
221  
222 % 1st column=newClusterID, 2nd column=total volume of surfaces in  
    this  
223 % new cluster  
224 newVolumes = zeros(length(uniqueClusters), 2);  
225  
226 for i = 1:length(uniqueClusters)  
227     volumesToAdd = oldClusterID(newClusterID == uniqueClusters(i));  
228     idv = ismember(volumes(:, 1), volumesToAdd);  
229     newVolumes(i, 1) = uniqueClusters(i);  
230     newVolumes(i, 2) = sum(volumes(idv, 2));  
231  
232 end  
233  
234 %clusters2Keep is a list of newClusterID's to keep.  
235
```

A.2. CODES FOR CLEANING AND PROCESSING THE SPLEEN DATA

```
236 %select surfaces with p% of the volume
237 % larger percent = more clusters kept
238 global gp-VOLUME_PERCENT_TEST;
239 p = gp-VOLUME_PERCENT_TEST;
240 sortedVolumes = sort(newVolumes(:, 2));
241 cumulativeSortedSum = cumsum(sortedVolumes);
242 cumulativeSortedSumPercent = cumulativeSortedSum/
    cumulativeSortedSum(end);
243
244 %find the first index where cumulativeSortedSumPercent < (1-p)
245 [~, cutOffIndex] = min(cumulativeSortedSumPercent < (1-p));
246 clusters2Keep = newVolumes(newVolumes(:, 2) >= sortedVolumes(
    cutOffIndex), 1);
247
248 % clusters2Keep is a list of newClusterID's to keep, so map these
    ids
249 % into oldClusterID's.
250
251 surfNKeep = [];
252 surfNDelete = [];
253 for i =1:length(oldClusterID)
254     if any( clusters2Keep == newClusterID(i))
255         surfNKeep = [surfNKeep, oldClusterID(i)];
256     else
257         surfNDelete = [surfNDelete, oldClusterID(i)];
258     end
259 end
```

```
260 end
261
262 function [surfNKeep, surfNDelete] = filterClustersByConnectivity_(
    volumes, surfN, oldClusterID, newClusterID)
263     % Partitions surfN into two lits of surfaces to keep or delete
264     % Parameters
265     % surfN: list of surface id's to partition. Id's are in the old
266     % numbering.
267     % oldClusterID(i) maps to newClusterID(i)
268
269     global gp_CLUSTER_CONNECTIVITY_TEST;
270
271     assert( length(oldClusterID) == length(newClusterID) );
272     surfNDelete = [];
273     maybe = [];
274
275     %delete any small-cluster surfaces
276     for i = 1:length(surfN)
277         oldIndex = find(oldClusterID == surfN(i));
278         newID = newClusterID(oldIndex);
279         numClusters = sum(newClusterID == newID);
280
281         if numClusters >= gp_CLUSTER_CONNECTIVITY_TEST
282             maybe = [maybe, surfN(i)];
283         else
284             surfNDelete = [surfNDelete, surfN(i)];
285     end
```

```
286     end
287
288     %todo: add other heristics , like checking if the surface is part of
           a
289     %larger "line" of clusters forming a filament.
290     surfNKeep = maybe;
291 end
```

A.2.3. Code for computing nearest neighbors. This MATLAB file is used in Section 6.2.1

```
1 % Read in two files (spots and vertices), and write a file of nearest
2 % neighbor distances
3
4
5 vertexFileName = 'path/RedPoints.csv';
6 spotFileName = 'path/GreenPoints.csv';
7 distanceFileName = 'output_distance_file.csv';
8
9
10 bucketSize = 10000;
11
12
13 vertices = csvread(vertexFileName);
14 spots = csvread(spotFileName);
15
16
17 fprintf('Building nearest neighbor tree...');
18 tic;
19 knn = createns(vertices, 'BucketSize', bucketSize);
```

```
20 t = toc;
21 fprintf('done. Time was %g seconds\n', t);
22
23 fprintf('Searching over spots... ');
24 tic;
25 %no need to record the vertex id of the nearest neighbor.
26 [~, nearestDistance] = knnsearch(knn, spots);
27 t = toc;
28 fprintf('done. Time was %g seconds\n', t);
29
30 fprintf('Saving distance values... ');
31 tic;
32 csvwrite(distanceFileName, nearestDistance);
33 t = toc;
34 fprintf('done. Time was %g seconds\n', t);
```


Bibliography

- [1] 4ti2 team. 4ti2—a software package for algebraic, geometric and combinatorial problems on linear spaces. Available from URL www.4ti2.de.
- [2] Karen Aardal and Arjen K. Lenstra. Hard equality constrained integer knapsacks. *Math. Oper. Res.*, 29(3):724–738, 2004.
- [3] Geir Agnarsson. On the Sylvester denumerants for general restricted partitions. In *Proceedings of the Thirty-third Southeastern International Conference on Combinatorics, Graph Theory and Computing (Boca Raton, FL, 2002)*, volume 154, pages 49–60, 2002.
- [4] Luigi Agnati, Giuseppina Leo, Alessio Zanardi, Susanna Genedani, Alicia Rivera, Kjell Fuxe, and Diego Guidolin. Volume transmission and wiring transmission from cellular to molecular networks: history and perspectives. *Acta Physiologica*, 187(1-2):329–344, 2006.
- [5] Oswin Aichholzer, Franz Aurenhammer, David Alberts, and Bernd Gärtner. *A novel type of skeleton for polygons*. Springer, 1996.
- [6] James Alexander and André Hirschowitz. Polynomial interpolation in several variables. *J. Algebraic Geom.*, 4:201–222, 1995.
- [7] Ulf Andersson and Kevin Tracey. A new approach to rheumatoid arthritis: treating inflammation with computerized nerve stimulation. In *Cerebrum: the Dana forum on brain science*, volume 2012. Dana Foundation, 2012.
- [8] George Andrews. *The theory of partitions*. Cambridge Mathematical Library. Cambridge University Press, Cambridge, 1998. Reprint of the 1976 original.
- [9] Miguel Anjos and Jean Lasserre. *Handbook on Semidefinite, Conic and Polynomial Optimization*. International Series in Operations Research & Management Science. Springer US, 2011.
- [10] David Avis. A revised implementation of the reverse search vertex enumeration algorithm. In *Polytopescombinatorics and computation*, pages 177–198. Springer, 2000.
- [11] Egon Balas and Manfred Padberg. Set partitioning: A survey. *SIAM Review*, 18(4):710–760, 1976.
- [12] Velleda Baldoni, Nicole Berline, Jesús De Loera, Brandon Dutra, Matthias Köppe, and Michèle Vergne. Coefficients of Sylvester’s denumerant. *INTEGERS, Electronic Journal of Combinatorial Number Theory*, 15(A11):1–32, 2015.
- [13] Velleda Baldoni, Nicole Berline, Jesús De Loera, Matthias Köppe, and Michèle Vergne. How to integrate a polynomial over a simplex. *Mathematics of Computation*, 80(273):297–325, 2011.
- [14] Velleda Baldoni, Nicole Berline, Jesús De Loera, Matthias Köppe, and Michèle Vergne. Computation of the highest coefficients of weighted Ehrhart quasi-polynomials of rational polyhedra. *Foundations of Computational Mathematics*, 12:435–469, 2012.
- [15] Velleda Baldoni, Nicole Berline, Jesús A. De Loera, Matthias Köppe, and Michèle Vergne. Computation of the highest coefficients of weighted Ehrhart quasi-polynomials of rational polyhedra. *Foundations of Computational Mathematics*, 12(4):435–469, 2011.
- [16] Velleda Baldoni, Nicole Berline, Matthias Köppe, and Michèle Vergne. Intermediate sums on polyhedra: Computation and real Ehrhart theory. *Mathematika*, 59(1):1–22, September 2013.
- [17] Alexander Barvinok. Polynomial time algorithm for counting integral points in polyhedra when the dimension is fixed. *Mathematics of Operations Research*, 19:769–779, 1994.
- [18] Alexander Barvinok. Computing the Ehrhart quasi-polynomial of a rational simplex. *Math. Comp.*, 75(255):1449–1466, 2006.
- [19] Alexander Barvinok. *Integer Points in Polyhedra*. Zürich Lectures in Advanced Mathematics. European Mathematical Society (EMS), Zürich, Switzerland, 2008.
- [20] Alexander Barvinok and James Pommersheim. An algorithmic theory of lattice points in polyhedra. In Louis J. Billera, Anders Björner, Curtis Greene, Rodica E. Simion, and Richard P. Stanley, editors, *New Perspectives*

-
- in Algebraic Combinatorics*, volume 38 of *Math. Sci. Res. Inst. Publ.*, pages 91–147. Cambridge Univ. Press, Cambridge, 1999.
- [21] Alexander Barvinok and Kevin Woods. Short rational generating functions for lattice point problems. *J. Amer. Math. Soc.*, 16(4):957–979 (electronic), 2003.
- [22] Matthias Beck, Ira Gessel, and Takao Komatsu. The polynomial part of a restricted partition function related to the Frobenius problem. *Electron. J. Combin.*, 8(1):Note 7, 5 pp. (electronic), 2001.
- [23] Matthias Beck, Christian Haase, and Frank Sottile. (formulas of brion, lawrence, and varchenko on rational generating functions for cones). *The Mathematical Intelligencer*, 31(1):9–17, 2009.
- [24] Matthias Beck and Sinai Robins. *Computing the continuous discretely: integer-point enumeration in polyhedra*. Undergraduate Texts in Mathematics. Springer, 2007.
- [25] Matthias Beck and Frank Sottile. Irrational proofs for three theorems of Stanley. *European Journal of Combinatorics*, 28(1):403–409, 2007.
- [26] Sönke Behrends, Ruth Hübner, and Anita Schöbel. Norm Bounds and Underestimators for Unconstrained Polynomial Integer Minimization. *ArXiv e-prints*, February 2015.
- [27] Eric Bell. Interpolated denumerants and Lambert series. *Amer. J. Math.*, 65:382–386, 1943.
- [28] Mihir Bellare and Phillip Rogaway. The complexity of approximating a nonlinear program. *Math. Program.*, 69(3):429–441, September 1995.
- [29] Timo Berthold. Primal heuristics for mixed integer programs. Master’s thesis, Technische Universität Berlin, 2006.
- [30] Bitplane. Imaris 8.1. Badenerstrasse 682, CH-8048 Zurich, Switzerland. <http://www.bitplane.com/imaris/imaris>.
- [31] Maria Chiara Brambilla and Giorgio Ottaviani. On the Alexander–Hirschowitz theorem. e-print arXiv:math.AG/0701409v2, 2007.
- [32] C.J. Brianchon. Théorème nouveau sur les polyèdres. *École Polytechnique*, 15:317–319, 1837.
- [33] Michel Brion. Points entiers dans les polyèdres convexes. *Ann. Sci. École Norm. Sup.*, 21(4):653–663, 1988.
- [34] Michel Brion and Michèle Vergne. Residue formulae, vector partition functions and lattice points in rational polytopes. *J. Amer. Math. Soc.*, 10(4):797–833, 1997.
- [35] Manuel Bronstein. *Symbolic Integration I: Transcendental Functions*. Algorithms and Combinatorics. Springer, 2005.
- [36] Christoph Buchheim and Claudia D’Ambrosio. Box-constrained mixed-integer polynomial optimization using separable underestimators. In Jon Lee and Jens Vygen, editors, *Integer Programming and Combinatorial Optimization*, volume 8494 of *Lecture Notes in Computer Science*, pages 198–209. Springer International Publishing, 2014.
- [37] Benno Büeler, Andreas Enge, and Komei Fukuda. Exact volume computation for polytopes: A practical study. In Gil Kalai and Günter M. Ziegler, editors, *Polytopes – Combinatorics and Computation*, volume 29 of *DMV-Seminars*, Basel, 2000. Birkhäuser Verlag.
- [38] Fernando Cacciola. 2D straight skeleton and polygon offsetting. In *CGAL User and Reference Manual*. CGAL Editorial Board, 4.7 edition, 2015.
- [39] Enrico Carlini, Maria Catalisano, and Anthony Geramita. The solution to the Waring problem for monomials and the sum of coprime monomials. *Journal of Algebra*, 370(0):5 – 14, 2012.
- [40] Mari Castle, Victoria Powers, and Bruce Reznick. A quantitative Pólya’s Theorem with zeros. *Journal of Symbolic Computation*, 44(9):1285 – 1290, 2009. *Effective Methods in Algebraic Geometry*.
- [41] Yong Chen, Hongqing Wang, David W Rosen, and Jarek Rossignac. A point-based offsetting method of polygonal meshes. *ASME Journal of Computing and Information Science in Engineering*, 2005.
- [42] Kwanghun Chung and Karl Deisseroth. Clarity for mapping the nervous system. *Nature methods*, 10(6):508–513, 2013.
- [43] Kwanghun Chung, Jenelle Wallace, Sung-Yon Kim, Sandhiya Kalyanasundaram, Aaron Andalman, Thomas Davidson, Julie Mirzabekov, Kelly Zalocusky, Joanna Mattis, Aleksandra Denisin, et al. Structural and molecular interrogation of intact biological systems. *Nature*, 497(7449):332–337, 2013.
- [44] Andrew Comrey and Howard Lee. *A first course in factor analysis*. Psychology Press, 2013.
- [45] Louis Comtet. *Advanced combinatorics*. D. Reidel Publishing Co., Dordrecht, enlarged edition, 1974. The art of finite and infinite expansions.
- [46] John Conway and Richard Corman. *The Book of Numbers*. Springer Science & Business Media, 1996.
- [47] Ronald Cools and Ann Haegemans. Algorithm 824: CUBPACK: a package for automatic cubature; framework description. *ACM Trans. Math. Software*, 29(3):287–296, 2003.

-
- [48] Thomas Cormen, Charles Leiserson, Ronald Rivest, and Clifford Stein. *Introduction to algorithms third edition*. The MIT Press, 2009.
- [49] Mark de Berg. *Computational Geometry: Algorithms and Applications*. Springer, 2008.
- [50] Etienne de Klerk, Jean Lasserre, Monique Laurent, and Zhao Sun. Bound-constrained polynomial optimization using only elementary calculations. *ArXiv e-prints*, July 2015.
- [51] Etienne de Klerk and Monique Laurent. Error bounds for some semidefinite programming approaches to polynomial minimization on the hypercube. *SIAM Journal on Optimization*, 20(6):3104–3120, 2010.
- [52] Etienne de Klerk, Monique Laurent, and Pablo Parrilo. A PTAS for the minimization of polynomials of fixed degree over the simplex. *Theoretical Computer Science*, 361(23):210 – 225, 2006. Approximation and Online Algorithms.
- [53] Jesús De Loera, Brandon Dutra, and Matthias Köppe. Approximating the maximum of a polynomial over a polytope using Handelman’s decomposition and continuous generating functions, 2016. Draft Paper.
- [54] Jesús De Loera, Brandon Dutra, Matthias Köppe, Stanislav Moreinis, Gregory Pinto, and Jianqiu Wu. A users guide for latte integrale v1.5. Available from URL <http://www.math.ucdavis.edu/~latte/>, 2011.
- [55] Jesús De Loera, Brandon Dutra, Matthias Köppe, Stanislav Moreinis, Gregory Pinto, and Jianqiu Wu. Software for exact integration of polynomials over polyhedra. *ACM Commun. Comput. Algebra*, 45(3/4):169–172, January 2012.
- [56] Jesús De Loera, Brandon Dutra, Matthias Köppe, Stanislav Moreinis, Gregory Pinto, and Jianqiu Wu. Software for exact integration of polynomials over polyhedra: online supplement. Available from URL <http://www.math.ucdavis.edu/~latte/theory/SoftwareExactIntegrationPolynomialsPolyhedraOnlineSupplement.pdf>, 2012.
- [57] Jesús De Loera, David Haws, Raymond Hemmecke, Peter Huggins, Jeremiah Tauzer, and Ruriko Yoshida. LatTE, version 1.2. Available from URL <http://www.math.ucdavis.edu/~latte/>, 2005.
- [58] Jesús De Loera, Raymond Hemmecke, and Matthias Köppe. *Algebraic and Geometric Ideas in the Theory of Discrete Optimization*. MOS-SIAM Series on Optimization. Society for Industrial and Applied Mathematics, 2013.
- [59] Jesús De Loera, Raymond Hemmecke, Matthias Köppe, and Robert Weismantel. Integer polynomial optimization in fixed dimension. *Mathematics of Operations Research*, 31(1):147–153, 2006.
- [60] Jesús De Loera, Raymond Hemmecke, Matthias Köppe, and Robert Weismantel. FPTAS for optimizing polynomials over the mixed-integer points of polytopes in fixed dimension. *Mathematical Programming, Series A*, 118:273–290, 2008.
- [61] Jesús De Loera, Raymond Hemmecke, Jeremiah Tauzer, and Ruriko Yoshida. Effective lattice point counting in rational convex polytopes. *Journal of Symbolic Computation*, 38(4):1273–1302, 2004.
- [62] Jesús De Loera, Joerg Rambau, and Francisco Santos. *Triangulations: Structures for Algorithms and Applications*, volume 25 of *Algorithms and Computation in Mathematics*. Springer, 1st edition, 2010.
- [63] Martin Dyer and Ravi Kannan. On Barvinok’s algorithm for counting lattice points in fixed dimension. *Mathematics of Operations Research*, 22:545–549, 1997.
- [64] Eugene Ehrhart. Geometrie diophantienne-sur les polyedres rationnels homothetiques an dimensions. *Comptes rendus de l’Académie des sciences*, 254(4):616, 1962.
- [65] Eugene Ehrhart. *Polynômes arithmétiques et méthode des polyèdres en combinatoire*. Birkhäuser Verlag, Basel, 1977. International Series of Numerical Mathematics, Vol. 35.
- [66] David Einstein, Daniel Lichtblau, Adam Strzebonski, and Stan Wagon. Frobenius numbers by lattice point enumeration. *Integers*, 7:A15, 63, 2007.
- [67] Michael Elad. *Sparse and Redundant Representations: From Theory to Applications in Signal and Image Processing*. Springer New York, 2010.
- [68] Kristoffer Famm, Brian Litt, Kevin Tracey, Edward Boyden, and Moncef Slaoui. Drug discovery: a jump-start for electroceuticals. *Nature*, 496(7444):159–161, 2013.
- [69] David Felten, Suzanne Felten, Denise Bellinger, Sonia Carlson, Kurt Ackerman, Kelley Madden, John Olschowki, and Shmuel Livnat. Noradrenergic sympathetic neural interactions with the immune system: structure and function. *Immunological reviews*, 100(1):225–260, 1987.
- [70] Matteo Fischetti and Andrea Lodi. *Heuristics in Mixed Integer Programming*. John Wiley Sons, Inc., 2010.
- [71] Imola Fodor. A survey of dimension reduction techniques, 2002.
- [72] Komei Fukuda. *cddlib*, version 094a. Available from URL http://www.cs.mcgill.ca/~fukuda/soft/cdd_home/cdd.html, 2005.

-
- [73] Robert Garfinkel and George Nemhauser. The set-partitioning problem: Set covering with equality constraints. *Operations Research*, 17(5):848–856, 1969.
- [74] Robert Garfinkel and George Nemhauser. *Integer programming*, volume 4. Wiley New York, 1972.
- [75] Mickaël Gastineau and Jacques Laskar. Development of TRIP: Fast sparse multivariate polynomial multiplication using burst tries. In Vassil Alexandrov, Geert van Albada, Peter Sloot, and Jack Dongarra, editors, *Computational Science – ICCS 2006*, volume 3992 of *Lecture Notes in Computer Science*, pages 446–453. Springer Berlin / Heidelberg, 2006.
- [76] Ewgenij Gawrilow and Michael Joswig. polymake: a framework for analyzing convex polytopes. In Gil Kalai and Günter M. Ziegler, editors, *Polytopes — Combinatorics and Computation*, pages 43–74. Birkhäuser, 2000.
- [77] GMP, version 4.1.4, the GNU multiple precision arithmetic library. Available from URL <http://www.swox.com/gmp/>, 2004.
- [78] Jacob Goodman and Joseph O’Rourke, editors. *Handbook of discrete and computational geometry*. CRC Press, Inc., Boca Raton, FL, USA, 1997.
- [79] Jørgen Gram. Om rumvinklerne i et polyeder. *Tidsskrift for Math*, 3(4):161–163, 1871.
- [80] Ignacio Grossmann. Review of nonlinear mixed-integer and disjunctive programming techniques. *Optimization and Engineering*, 3(3):227–252, 2002.
- [81] Christelle Guéret, Christian Prins, Marc Sevaux, and Susanne Heipcke. *Applications of Optimization with Xpress-MP*. Dash Optimization Limited, 2002.
- [82] David Handelman. Representing polynomials by positive linear functions on compact convex polyhedra. *Pacific J. Math.*, 132(1):35–62, 1988.
- [83] Johan Håstad. Some optimal inapproximability results. In *Journal of the ACM*, pages 1–10, 1999.
- [84] Raymond Hemmecke, Akimichi Takemura, and Ruriko Yoshida. Computing holes in semi-groups and its application to transportation problems. *Contributions to Discrete Mathematics*, 4:81–91, 2009.
- [85] Peter Henrici. *Applied and computational complex analysis. Vol. 1*. Wiley Classics Library. John Wiley & Sons Inc., New York, 1988. Power series—integration—conformal mapping—location of zeros, Reprint of the 1974 original, A Wiley-Interscience Publication.
- [86] Geoffrey Hinton and Ruslan Salakhutdinov. Reducing the dimensionality of data with neural networks. *Science*, 313(5786):504–507, 2006.
- [87] Peter Huber. Projection pursuit. *The annals of Statistics*, pages 435–475, 1985.
- [88] Aapo Hyvärinen, Juha Karhunen, and Erkki Oja. *Independent component analysis*, volume 46. John Wiley & Sons, 2004.
- [89] Ian Jolliffe. *Principal Component Analysis*. Springer, 2002.
- [90] Masanobu Kaneko. The Akiyama–Tanigawa algorithm for Bernoulli numbers. *Journal of Integer Sequences*, 3(00.2.9):1–7, 2000.
- [91] Ravi Kannan. Lattice translates of a polytope and the Frobenius problem. *Combinatorica*, 12(2):161–177, 1992.
- [92] Samuel Kaski. Dimensionality reduction by random mapping: Fast similarity computation for clustering. In *Neural Networks Proceedings, 1998. IEEE World Congress on Computational Intelligence. The 1998 IEEE International Joint Conference on*, volume 1, pages 413–418. IEEE, 1998.
- [93] Hans Kellerer, Ulrich Pferschy, and David Pisinger. *Knapsack problems*. Springer-Verlag, Berlin, 2004.
- [94] Donald Knuth. Dancing links. In Jim Davies, editor, *Millennial perspectives in computer science : proceedings of the 1999 Oxford-Microsoft Symposium in honour of Professor Sir Antony Hoare*, pages 187–214. Palgrave, Houndmills, Basingstoke, Hampshire, 2000.
- [95] Thorsten Koch, Tobias Achterberg, Erling Andersen, Oliver Bastert, Timo Berthold, Robert Bixby, Emilie Danna, Gerald Gamrath, Ambros Gleixner, Stefan Heinz, Andrea Lodi, Hans Mittelmann, Ted Ralphs, Domenico Salvagnin, Daniel Steffy, and Kati Wolter. MIPLIB 2010. *Mathematical Programming Computation*, 3(2):103–163, 2011.
- [96] Teuvo Kohonen, Samuel Kaski, Krista Lagus, Jarkko Salojärvi, Jukka Honkela, Vesa Paatero, and Antti Saarela. Self organization of a massive document collection. *Neural Networks, IEEE Transactions on*, 11(3):574–585, 2000.
- [97] Matthias Köppe. A primal Barvinok algorithm based on irrational decompositions. *SIAM Journal on Discrete Mathematics*, 21(1):220–236, 2007.
- [98] Matthias Köppe. LattE macchiato, version 1.2-mk-0.9.3, an improved version of De Loera et al.’s LattE program for counting integer points in polyhedra with variants of Barvinok’s algorithm. Available from URL <http://www.math.ucdavis.edu/~mkoeppel/latte/>, 2008.

-
- [99] Matthias Köppe. On the complexity of nonlinear mixed-integer optimization. In Jon Lee and Sven Leyffer, editors, *Mixed Integer Nonlinear Programming*, volume 154 of *The IMA Volumes in Mathematics and its Applications*, pages 533–557. Springer New York, 2012.
- [100] Matthias Köppe and Sven Verdoolaege. Computing parametric rational generating functions with a primal Barvinok algorithm. *The Electronic Journal of Combinatorics*, 15:1–19, 2008. #R16.
- [101] Jean-Louis Krivine. Quelques propriétés des préordres dans les anneaux commutatifs unitaires. *Comptes Rendus de l'Académie des Sciences de Paris*, 258:3417–3418, 1964.
- [102] Jean Lasserre. An analytical expression and an algorithm for the volume of a convex polyhedron in \mathbb{R}^n . *Journal of Optimization Theory and Applications*, 39(3):363–377, 1983.
- [103] Jean Lasserre. Optimisation globale et thorie des moments. *Comptes Rendus de l'Académie des Sciences - Series I - Mathematics*, 331(11):929 – 934, 2000.
- [104] Jean Lasserre. Global optimization with polynomials and the problem of moments. *SIAM Journal on Optimization*, 11:796–817, 2001.
- [105] Jean Lasserre. Semidefinite programming vs. lp relaxations for polynomial programming. *Mathematics of operations research*, 27(2):347–360, 2002.
- [106] Jean Lasserre. *Moments, Positive Polynomials and Their Applications*. Imperial College Press Optimization. Imperial College Press, 2009.
- [107] Jean Lasserre. A new look at nonnegativity on closed sets and polynomial optimization. *SIAM Journal on Optimization*, 21(3):864–885, 2011.
- [108] Jean Lasserre and Tung Phan Thanh. Convex underestimators of polynomials. *Journal of Global Optimization*, 56(1):1–25, 2013.
- [109] Monique Laurent. Sums of squares, moment matrices and optimization over polynomials. In *Emerging applications of algebraic geometry*, pages 157–270. Springer, 2009.
- [110] Monique Laurent and Zhao Sun. Handelmans hierarchy for the maximum stable set problem. *Journal of Global Optimization*, 60(3):393–423, 2014.
- [111] Jim Lawrence. Rational-function-valued valuations on polyhedra. In *Discrete and computational geometry (New Brunswick, NJ, 1989/1990)*, volume 6 of *DIMACS Ser. Discrete Math. Theoret. Comput. Sci.*, pages 199–208. Amer. Math. Soc., Providence, RI, 1991.
- [112] Carl Lee. Regular triangulations of convex polytopes. In P. Gritzmann and B. Sturmfels, editors, *Applied Geometry and Discrete Mathematics: The Victor*, pages 443–456. American Mathematical Society, Providence, RI, 1991.
- [113] John Lee and Michel Verleysen. *Nonlinear dimensionality reduction*. Springer Science & Business Media, 2007.
- [114] Eva Linke. Rational Ehrhart quasi-polynomials. *Journal of Combinatorial Theory, Series A*, 118(7):1966–1978, 2011.
- [115] Petr Lisoněk. Denumerants and their approximations. *J. Combin. Math. Combin. Comput.*, 18:225–232, 1995.
- [116] Shengjun Liu and Charlie CL Wang. Fast intersection-free offset surface generation from freeform models with triangular meshes. *Automation Science and Engineering, IEEE Transactions on*, 8(2):347–360, 2011.
- [117] Yang Liu and Wenping Wang. On vertex offsets of polyhedral surfaces. *Proc. of Advances in Architectural Geometry*, pages 61–64, 2008.
- [118] AutoIt Consulting Ltd. Autoit v3.3.14.2. <https://www.autoitscript.com/site/>.
- [119] Oded Maimon and Lior Rokach. *Data mining and knowledge discovery handbook*, volume 2. Springer, 2005.
- [120] Murray Marshall. *Positive Polynomials and Sums of Squares*. Mathematical surveys and monographs. American Mathematical Society, 2008.
- [121] Roy Marsten and Fred Shepardson. Exact solution of crew scheduling problems using the set partitioning model: recent successful applications. *Networks*, 11(2):165–177, 1981.
- [122] Silvano Martello and Paolo Toth. *Knapsack problems*. Wiley-Interscience Series in Discrete Mathematics and Optimization. John Wiley & Sons Ltd., Chichester, 1990. Algorithms and computer implementations.
- [123] MATLAB. *version 8.6.0 (R2015b)*. The MathWorks Inc., Natick, Massachusetts, 2015.
- [124] Christine Metz and Kevin Tracey. It takes nerve to dampen inflammation. *Nature immunology*, 6(8):756–757, 2005.
- [125] Theodore Motzkin and Ernst Straus. Maxima for graphs and a new proof of a theorem of Turán. *Canadian Journal of Mathematics*, 17:533–540, 1965.
- [126] Arnaud Muller, Victory Joseph, Paul Slesinger, and David Kleinfeld. Cell-based reporters reveal in vivo dynamics of dopamine and norepinephrine release in murine cortex. *nature methods*, 11(12):1245–1252, 2014.

-
- [127] Yurii Nesterov. Squared functional systems and optimization problems. In Hans Frenk, Kees Roos, Tamás Terlaky, and Shuzhong Zhang, editors, *High Performance Optimization*, volume 33 of *Applied Optimization*, pages 405–440. Springer US, 2000.
- [128] Quoc-Thang Nguyen, Lee Schroeder, Marco Mank, Arnaud Muller, Palmer Taylor, Oliver Griesbeck, and David Kleinfeld. An in vivo biosensor for neurotransmitter release and in situ receptor activity. *Nature neuroscience*, 13(1):127–132, 2010.
- [129] Pablo Parrilo. Semidefinite programming relaxations for semialgebraic problems. *Mathematical Programming*, 96(2):293–320, 2003.
- [130] Pablo Parrilo and Bernd Sturmfels. Minimizing polynomial functions. In Saugata Basu and Laureano Gonzalez-Vega, editors, *Algorithmic and Quantitative Real Algebraic Geometry*, volume 60 of *DIMACS Series in Discrete Mathematics and Theoretical Computer Science*, pages 83–99. AMS, 2003.
- [131] Valentin Pavlov and Kevin Tracey. The vagus nerve and the inflammatory reflex linking immunity and metabolism. *Nature Reviews Endocrinology*, 8(12):743–754, 2012.
- [132] Julian Pfeifle and Jörg Rambau. Computing triangulations using oriented matroids. In Michael Joswig and Nobuki Takayama, editors, *Algebra, Geometry, and Software Systems*, pages 49–75. Springer, 2003.
- [133] Aleksandr Pukhlikov and Askold Khovanskii. The Riemann-Roch theorem for integrals and sums of quasipolynomials on virtual polytopes. *Algebra i analiz*, 4(4):188–216, 1992.
- [134] Joerg Rambau. Topcom. Available from URL <http://www.rambau.wm.uni-bayreuth.de/TOPCOM/>.
- [135] Joerg Rambau. *TOPCOM: Triangulations of Point Configurations and Oriented Matroids*. Konrad-Zuse-Zentrum für Informationstechnik Berlin. ZIB, 2002.
- [136] Jorge Ramírez Alfonsín. *The Diophantine Frobenius problem*, volume 30 of *Oxford Lecture Series in Mathematics and its Applications*. Oxford University Press, Oxford, 2005.
- [137] John Riordan. *An introduction to combinatorial analysis*. Dover Publications Inc., Mineola, NY, 2002. Reprint of the 1958 original [Wiley, New York; MR0096594 (20 #3077)].
- [138] Mauricio Rosas-Ballina, Peder Olofsson, Mahendar Ochani, Sergio Valdés-Ferrer, Yaakov Levine, Colin Reardon, Michael Tusche, Valentin Pavlov, Ulf Andersson, Sangeeta Chavan, et al. Acetylcholine-synthesizing t cells relay neural signals in a vagus nerve circuit. *Science*, 334(6052):98–101, 2011.
- [139] Sage. *Sage Mathematics Software (Version 6.10)*, 2016. Available from URL <http://www.sagemath.org>.
- [140] Sriram Sankaranarayanan, Xin Chen, and Erika Abraham. Lyapunov function synthesis using handelmann representations. In *The 9th IFAC Symposium on Nonlinear Control Systems*, pages 576–581, 2013.
- [141] Martin Sarter, Vinay Parikh, and Matthew Howe. Phasic acetylcholine release and the volume transmission hypothesis: time to move on. *Nature Reviews Neuroscience*, 10(5):383–390, 2009.
- [142] Alexander Schrijver. *Combinatorial Optimization: Polyhedra and Efficiency*. Springer, 2003.
- [143] Alexander Schrijver. *Theory of linear and integer programming*. John Wiley & Sons, Inc., New York, NY, USA, 1986.
- [144] Victor Shoup. NTL, a library for doing number theory. Available from URL <http://www.shoup.net/ntl/>, 2005.
- [145] Andrew Sills and Doron Zeilberger. Formulæ for the number of partitions of n into at most m parts (using the quasi-polynomial ansatz). *Adv. in Appl. Math.*, 48:640–645, 2012.
- [146] Richard P. Stanley. *Enumerative Combinatorics*, volume I. Cambridge, 1997.
- [147] Mohit Tawarmalani. and Nikolaos Sahinidis. *Convexification and Global Optimization in Continuous and Mixed-Integer Nonlinear Programming: Theory, Algorithms, Software, and Applications*. Nonconvex Optimization and Its Applications. Springer, 2002.
- [148] Mohit Tawarmalani and Nikolaos Sahinidis. A polyhedral branch-and-cut approach to global optimization. *Mathematical Programming*, 103:225–249, 2005.
- [149] Jean-Nicolas Tournier and Anne Hellmann. Neuro-immune connections: evidence for a neuro-immunological synapse. *Trends in immunology*, 24(3):114–115, 2003.
- [150] Hsing-Chen Tsai, Feng Zhang, Antoine Adamantidis, Garret Stuber, Antonello Bonci, Luis De Lecea, and Karl Deisseroth. Phasic firing in dopaminergic neurons is sufficient for behavioral conditioning. *Science*, 324(5930):1080–1084, 2009.
- [151] Henk van der Vorst and Paul Van Dooren. *Parallel algorithms for numerical linear algebra*, volume 1. Elsevier, 2014.
- [152] Rao Vemuganti. Applications of set covering, set packing and set partitioning models: A survey. In *Handbook of combinatorial optimization*, pages 573–746. Springer, 1999.
- [153] Sven Verdoolaege. [barvinok](http://freshmeat.net/projects/barvinok/). Available from URL <http://freshmeat.net/projects/barvinok/>, 2007.
- [154] Leonard Wapner. *The Pea and the Sun: A Mathematical Paradox*. Ak Peters Series. Taylor & Francis, 2005.

-
- [155] Guoce Xin. A fast algorithm for MacMahon's partition analysis. *Electr. J. Comb.*, 11(1), 2004.
- [156] Guoce Xin. A Euclid style algorithm for MacMahon partition analysis. e-print <http://arxiv.org/abs/1208.6074>, 2012.
- [157] Günter Ziegler. *Lectures on Polytopes*. Number 152 in Graduate texts in Mathematics. Springer, New York, 1995.